Control of redox homeostasis: environmental and genetic regulation of oxidative protein damage in *Schizosaccharomyces pombe*

Sarela García Santamarina

TESI DOCTORAL UPF / ANY 2013

DIRECTOR DE LA TESI

Dra. Elena Hidalgo Hernando
Departament Ciències Experimentals i de la Salut

Á miña família.

Biologically, life is not maintenance or restoration of equilibrium
but is essentially maintenance of disequilibrium,
as the doctrine of the organism as open system reveals.
Reaching equilibrium means death and consequent decay.
Ludwig von Bertalanffy
Passage in General Systems Theory (1968)

Agradecementos

Bueno, después de 5 años ha llegado el momento de depositar el resultado de tanto trabajo en un pequeño volumen de 250 páginas... como ha podido caber?....Pues seguramente debido a que en esos 5 años hay muchas cosas, vivencias que no tienen cabida en una evaluación académica, pero que requieren ser mencionadas, aunque sea sólo en dos hojas.

En primer lugar quiero agradecerte, Elena, la oportunidad que me brindaste para realizar la tesis en este laboratorio. Siempre me hablas de gente que marca tendencia en el campo de la bioquímica redox, sin embargo, creo que eres tú quién marcas tendencia en éste campo, cualquier laboratorio del mundo me resulta pequeño cuando lo comparo con éste. Muchas gracias por lo que me has enseñado y por preocuparte por mi presente y por mi futuro. Gracias a José por estar siempre ahi dispuesto a resolver las dudas de una química poco genetista y por mostrar siempre una sonrisa.

Gracias a todos mis compañeros de laboratorio. Quiero empezar por Sue, me has dado mucho estos años, me has enseñado filosofía de vida, siempre sonriendo (bueno, creo que una vez te oí decir un taco un poco enfadada...mmmm no se, no se, esa actitud...). Gracias a Nati y a Tsvety, mis nuevas hermanas, mis damas de honor, mis cuidadoras, tantas meriendas me has dado, Nati, para envidia de muchos..., tu honestidad baby, no es fácil de encontrar, os llevaré siempre conmigo (más concretamente en mi dedo anular)...Gracias Isa por ser siempre tan positiva y transmitírmelo, por enseñarme protocolo y sociabilizarme...y por el último aliento de ayuda.... Gracias Blanquita por tu dulzura, por tu sentido de la vida, por enseñarme que correr es más que un deporte. Itzel, nunca olvidaré tus risas en el fondo del laboratorio, las echamos de menos...Os quiero...Gracias Mercè por bajar cuestas tan empinadas conmigo, a veces bajar es más difícil que subir..., quién lo diría! Gracias Esther, hemos hecho un equipo ganador, ahora tu eres el relevo, confio en ti más que en nadie!! Gracias Iva Diva! soy tu fan, iré a todos tus conciertos, me ha encantado escucharte!! Gracias Patri, por enseñarme la pregunta más mágica y salvadora: qué tal el viaje? no sabes cuántas veces la he usado ya...y por el último aliento de ayuda...Gracias Isa A por darme los buenos días, por confiar en que siempre hay un momento de fiesta juuusto cuando no estás cerca. Gracias Ángel por hablarme tanto a partir de las 6, taantas diluciones de spots que he tenido que repetir... no tienen precio! Gracias Jorge polo teu carácter galego, non sabes o que era o labo sin ti...ninguén dicindo La Virgen! un bueno chavales no mellor momento,... gracias polos momentos Miguelín...os echaré de menos...Gracias Ali por taantos tiramisús, cómo has podido abandonarnos a nuestra suerte? Gracias Míriam por tu pasión, en la vida, en el trabajo,...Gracias Deib por todo lo que nos hemos reído,...ya hace tiempo que os echo de menos...Gracias a presentes Javi, Alba, Laura y a pasados Alberto, Mónica, Iván, Dani, Paula, Rosa, Marina,... me falta alguien?? Muchísmias gracias a Chelo, Mari, Montse, Enri, por conservar vuestro buen humor ante montañas y montañas de cacharros...Gracias Rafa por conseguir que el laboratorio funcione siempre, en serio, no sabes cuánto estrés nos has evitado...Gracias a cualquier posas que en algún momento he

molestado para pedirle cualquier cosa...tener buenos vecinos no tiene precio...

To Henrik, thank you for giving me the opportunity to work with you. Your interest in the project, your ideas, your improvements...these can not be paid!

Kashif, siempre tan diferente y especial, algún dia conseguiremos nuestro gran negocio, Jose motivador, energético y positivo, me han encantado todos nuestros momentos montaña, Jordi en el fuego y en la nieve, Oriol tranquilo, Pere genio y figura, Lucía sonriente, Eva transparente, Emre dulce turco...

Y el premio gordo! Gracias Ahmed por taaaaaaaanta paciencia, taaaaaaaantos tuppers, por cuidarme cuando fue fácil y sobre todo cuando te lo puse difícil, por aguantarme en mis 'mejores' momentos, por lo que hemos pasado y por nuestro futuro. Gracias a tus amigos Albert y Marc, por enseñarme otras maneras de ver la vida.

Á miña familia, ós que dedico esta tesis, a papá e a Pilar, que tanto luitastes por nos, tanto sacrificio, esforzo...non creo que haxa maneira de agradecelo suficiente, pero sabede que como pouco somos conscientes delo, á nova família María e a nova família Xes, gracias por Adán e por Xan, son tan divers! a Roque e Marita, por esperarme tantas veces na Coruña, a Tocho, Roque, Menani, Cibrán, Duarte, polos productos do horto, pola tortilla de patacas, polas patacas sin tortilla, polos chourizos, por seguir mantendo en Samartín un fogar ó que volver, especialmente apréciase desde lonxe, a Mónica por estar sempre, a pesar das miñas largas ausencias, sabes que somos irmás, a Felipe e Ana, e especialmente a Sandra, por enseñarme que nunca hai que deixar de luitar...

Abstract

Proteins are among the main targets of reactive oxygen species reactivity. Reversible oxidation of specific cysteines in proteins by hydrogen peroxide (H_2O_2) is a mechanism for triggering signalling pathways, such as antioxidant responses in microbial systems. However, H_2O_2 can be transformed to the more reactive hydroxyl radical ($OH^{\cdot}$) species, responsible of formation of protein carbonyls, which constitute classical marks of oxidative damage.

Along this thesis we studied these two different oxidative modifications in proteins. We developed protocols for studying cysteine oxidations at the proteome level, and used them to characterize redox-sensitive cysteines upon H_2O_2 and in the absence of the thioredoxin system. We also tried protocols for the identification of protein carbonyls and established that ubiquitination tags carbonylated proteins prior to their degradation. Finally, we also identified the peroxiredoxin Tpx1 and catalase as the main H_2O_2 scavengers in *S. pombe* and discovered free methionine as a primary barrier in the defence against H_2O_2 stress.

Resum

Les proteïnes són uns dels primers objectius de la reactivitat de les espècies reactives d'oxigen. L'oxidació reversible de cisteïnes en proteïnes per peròxid d'hidrogen (H_2O_2) és un mecanisme d'activació de rutes de senyalització. L'H_2O_2 també es pot transformar en radicals hidroxil, més reactius i causants de la formació de grups carbonil en proteïnes. Durant aquesta tesis, hem estudiat aquests dos tipus de modificació en proteïnes. Hem desenvolupat protocols per a estudiar oxidacions de cisteïnes per H_2O_2 i en absència del sistema tioredoxina. També hem provat protocols per a identificar grups carbonil en proteïnes i hem establert que la ubiquitinació marca les proteïnes carbonilades abans de la seva degradació. Per últim, hem identificat la peroxiredoxina Tpx1 i la catalasa com els primers detoxificants d'H_2O_2 en *S. pombe*, i hem descobert que la metionina és una primera barrera en la defensa de l'estrès per H_2O_2.

Contents

Chapter 1

INTRODUCTION

Introduction

1.1 Reactive oxygen species and oxidative stress

When living organisms first appeared on Earth, they lived under an atmosphere rich in N_2 and CO_2 but scarce on O_2, they were anaerobes. As atmospheric O_2 rose, largely due to the evolution of cyanobacteria photosynthesis (over 2.2 billion years ago), many anaerobic organisms died (nowadays strict anaerobes are restricted to anoxic microenvironments), in spite of other newly appearing organisms, which were able to evolve antioxidant defences and were therefore, better fitted to survive under the new oxidant environment [1].

Reactive oxygen species (ROS) refer to a variety of molecules and free radicals (species with one unpaired electron) derived from O_2. Molecular oxygen is itself a stable di-radical, with parallel spins. This is important in terms of reactivity, because it means that organic molecules with spin-paired electrons (the vast majority of organic molecules) cannot transfer more than one electron at a time to O_2. Hence, although thermodynamically favourable, O_2 cannot efficiently oxidise biomolecules such as amino acids and nucleic acids. However, it is readily reduced by unpaired electrons from transition metals and organic radicals yielding relatively stable intermediates [2]. Thus, one-electron reduction of oxygen produces superoxide anion ($O_2^{-\cdot}$), the precursor of many ROS. $O_2^{-\cdot}$ dismutation, either spontaneously or catalysed by superoxide dismutase (see below, section 1.1.3.1), yields hydrogen peroxide (H_2O_2), a non-radical species with a weak oxygen-oxygen bond. In turn, H_2O_2 can be partially reduced to hydroxyl radical ($OH^{\cdot}$), one of the strongest oxidants in nature, or fully reduced to water [3].

ROS inside cells are produced as normal by-products of oxygen metabolism. Antioxidant molecules or enzymes keep them at steady-state concentrations. Small fluctuations of this normal concentrations may play roles in intracellular signalling [4], however, uncontrolled increases lead to free radical-mediated chain reactions that indiscriminately target proteins [5], lipids [6], and DNA [7]. The latter deleterious processes, resulting from the imbalance between excessive ROS production or limited antioxidant defences, is defined as **oxidative stress** [3].

Superoxide anion, $O_2^{-\cdot}$ $O_2^{-\cdot}$ is produced at a rate of 5 μM/s, reaching steady state concentrations of $\sim 10^{-10}$ M [8]. It reacts at a rate that is almost diffusion-limited (half-life of 10^{-6} s) with iron from iron-sulphur (Fe-S) clusters. Nevertheless, due to its inability to diffuse through membranes (it is a charged molecule) and to its instability (dismutation), $O_2^{-\cdot}$ does not react as easily with other intracellular compounds. Additionally, $O_2^{-\cdot}$ can react with other radical species, such as nitric oxide ($NO^{\cdot}$) to yield peroxynitrite ($ONOO^-$).

This is a powerful oxidizing and nitrating agent which can directly damage proteins, lipids, and DNA. Moreover, it can undergo homolytic fission to give $OH^{\cdot}$ and nitrogen dioxide ($NO_2^{\cdot}$) radicals, or react with CO_2 to yield carbonate radical ($CO_3^{-\cdot}$) and $NO_2^{\cdot}$. In all cases, these $O_2^{-\cdot}$-derived species are radicals which are, in turn, powerful oxidants [1]. $NO^{\cdot}$ derived oxidants are known as reactive nitrogen species (RNS).

Hydrogen peroxide, H_2O_2 H_2O_2 toxicity is mainly due to its reduction to $OH^{\cdot}$. In general, it reacts slowly with Fe-S clusters, and very slowly with both low molecular weight thiols and thiols in proteins. However, its reactivity towards protein thiols can significantly increase depending on the protein environment. This property, together with the relatively stable H_2O_2 steady-state concentrations ($\sim 10^{-7}$ M), half-life ($\sim$ 1 ms) and ability to diffuse through membranes make H_2O_2 one of the ROS more fitted for signalling.

Hydroxyl radical, $OH^{\cdot}$ $OH^{\cdot}$ has high indiscriminate reactivity, which limits its diffusion to sites of production (half-life 10^{-9} s) [4]. In biological systems, it is mainly generated through the ferrous ion (Fe^{2+}) catalysed reduction of H_2O_2, commonly known as Fenton reaction (equation 1.1).

$$H_2O_2 + Fe^{2+} \rightarrow OH^{\cdot} + OH^{-} + Fe^{3+} \qquad \text{Fenton Reaction} \tag{1.1}$$

ROS reactivity depends on the nature of the considered species. Thus, the oxidizing strength of radicals is better ranked on the basis of their one-electron reducing potential. This is due to the low activating energy of radical reactions. However, for two-electron oxidants, reduction potentials determine the strength of the oxidant, but in this case, kinetic considerations are more important in determining their reactivity (see **table 1.1**) [9].

One electron		**Two electron**	
Radical	Reduction potential (V), pH 7	**Oxidant**	Rate constant (M^{-1} s^{-1}) with GSH
$OH^{\cdot}$, H^+/H_2O	2.31	HOCl	3 x 10^7
$CO_3^{-\cdot}$	1.78	$ONOO^-$	700
$RO^{\cdot}$	1.6	Chloramines	100-700
$NO_2^{\cdot}$	1.04	H_2O_2	0.9
$O_2^{-\cdot}/2H^+/H_2O_2$	0.94		
$PhO^{\cdot}$, H^+/PhOH	0.9		
$Cys^{\cdot}/CysS^-$	0.92		
$ROO^{\cdot}$, H^+/ROOH	0.77-1.44		
NO	0.8		

Table 1.1: Relative reactivities of selected one-electron and two-electron oxidants. Adapted from [9].

1.1.1 ROS sources in the cell

Although ROS can form part of environmental insults, they can also arise from side reactions of normal aerobic metabolism. Important contributions include proteins from the plasma membrane, such as NADPH oxidases [10], peroxisomal fatty acid degradation in the β-oxidation pathway [11], or oxidative protein folding in the ER [12]. However, the vast majority of cellular ROS ($\sim 90\%$) can be traced back to the mitochondria.

Mitochondria are in charge of producing the majority of cellular ATP. The electrochemical proton gradient across the mitochondrial inner membrane provides the necessary energy for ATP synthesis. This gradient, known as proton motive force, is composed of a pH component (ΔpH) and an electrical component, the mitochondrial membrane potential ($\Delta\Psi$), and it is generated by the enzymes of the electron transport chain as they pump protons from the mitochondrial matrix to the inter-membrane space. The released energy as the electrons are passed from carriers in complex I, with high potential energy, through carriers in complex III to carriers in complex IV, with lower potential energy, is profited by the mitochondria for proton pumping. Pairs of electrons enter the chain from reduced substrates at complex I, complex II and other dehydrogenases, and reduce O_2 to water at complex IV. Nevertheless, in certain sites in the chain, the electrons must pass one by one to carriers such as Fe-S centres or to flavins or quinones, which have stable one-electron reduced intermediates. These single electrons may occasionally directly react with O_2, resulting in ${O_2}^{-\cdot}$ formation [13].

The electron flow through the mitochondrial electron transport chain is described in **figure 1.1**. NADH, which is generated by dehydrogenases of the Krebs cycle, is first oxidized at complex I. Electrons from NADH are then transferred to the first mobile electron acceptor, the oxidized coenzyme *Q*, as the energy is dissipated by proton-pumping. Alternatively, coenzyme *Q* can also accept electrons donated by $FADH_2$ from complex II, bypassing complex I and one proton pumping site. Then, coenzyme *Q* donates its electrons to cytochrome *b* in complex III, in a closely potential energy neutral process. In complex III, electrons are donated to cytochrome *c1*, with the dissipative ejection of protons. Next, cytochrome *c1* transfers electrons to the second mobile element in the cytochrome chain, cytochrome *c*. The latter, in turn, reduces cytochrome oxidase (COX) in complex IV, which ultimately reduces molecular oxygen to form water, concomitantly with a final proton pumping to dissipate energy. In this form, the cytochrome chain transforms the redox energy from NADH and $FADH_2$ into a $\Delta\Psi$ across the inner mitochondrial membrane.

In complex I, the primary source of ${O_2}^{-\cdot}$ appears to be one of the Fe-S clusters and in complex III, most of the ${O_2}^{-\cdot}$ appears to be formed as a result of ubisemiquinone autooxidation (reviewed in [14]).

Yeast mitochondria (*Saccharomyces cerevisiae* and *Schizosaccharomyces pombe*) lack complex I. Instead they have single-peptide NADH dehydrogenases, which are rotenone-insensitive and do not pump protons [15]. In *S. cerevisiae* NADH generated in the

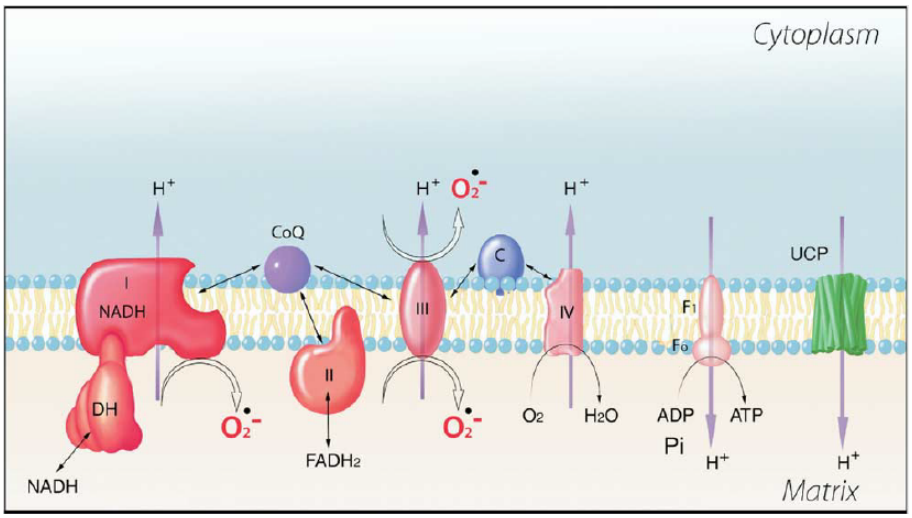

Figure 1.1: ROS generation in the mitochondria. The major $O_2^{-\cdot}$ generators are indicated as sites I and III. The different complexes of oxidative phosphorylation are colour coded regarding the E_{ox} for reducing O_2, with red (dehydrogenases and complex I) having the highest potential and pink (complex IV) the lowest potential. The family of uncoupling proteins (UCP), in green, reduces the overall mitochondrial membrane potential ($\Delta\Psi$). This results in a lower E_{ox} in complexes I and III and in a reduced ROS generation. Reprinted from [14].

mitochondrial matrix is oxidised by internal NADH dehydrogenase or Ndi1. Additionally, this organism harbors two external NADH dehydrogenases (Nde1 and Nde2), still without a clarified role [16] [17] [18].

Mitochondrial ROS production may be modulated by different mechanisms. Thus, the rate of $O_2^{-\cdot}$ formation increases if the electron flow slows down, by increasing the concentration of electron donors, or alternatively by increasing the oxygen concentration. For instance, proton ejection ceases if there is no ADP, this creates an excess of protons which causes electron flow to slow down and a more reduced respiratory chain, therefore producing more $O_2^{-\cdot}$. Also, $O_2^{-\cdot}$ formation can be increased by inhibiting complex I (rotenone) or by inhibiting complex III (antimycin), due to full reduction of those carriers upstream from the site of inhibition.

A large increase in ROS formation can be seen in a condition known as reverse electron flow. This consists in adding succinate (a complex II substrate) in the presence of a complex III inhibitor, thereby generating a reverse flow of electrons from complex II to complex I (reviewed in [3] [14]).

Other important physiological regulators of the electron transport chain are the family of uncoupling proteins (UCPs). Uncoupling protein 1 (UCP1) diverts energy from ATP synthesis to thermogenesis in the mitochondria of brown adipose tissue by catalysing a regulated leak of protons across the inner membrane [19]. UCPs cause a mild uncoupling in response to oxidants, leading to a diminished proton motive force, which reduces both

$\Delta\Psi$ and ROS production. Thus, uncoupling has been proposed as an important feedback circuit to reduce ROS levels when there is an excess of $O_2^{-\cdot}$ production. Importantly, $O_2^{-\cdot}$ may also directly activate UCPs [19].

1.1.2 ROS damage to biomolecules

1.1.2.1 Lipid peroxidation

Lipid peroxidation comprises a series of chain reactions that are started by the abstraction of a hydrogen atom in an poly-unsaturated fatty acyl (PUFA) chain, yielding a carbon centred radical. This process is commonly initiated by $O_2^{-\cdot}$, $OH^{\cdot}$ and transition metals. Then, in an aerobic environment, oxygen will be added to the carbon radical to produce a lipid peroxyl radical, $LOO^{\cdot}$. Once formed, $LOO^{\cdot}$ can further propagate the peroxidation chain reaction by abstracting an hydrogen atom from other vicinal unsaturated fatty acid resulting lipid hydroperoxide (LOOH). This can easily decompose in other species including lipid alkoxyl radicals ($LO^{\cdot}$), and the carbonyl derivatives alkanals, alkenals, hydroxyalkenals, glyoxal, and aldehydes (e.g. malonyldialdehyde, MDE) [20].

Among lipids, membrane phospholipids are major targets of ROS, since O_2 and its derivatives are more soluble in lipid membrane bilayers than in solution. Peroxidized membranes become rigid, lose selective permeability, and under harsh oxidizing conditions, lose integrity. Importantly, due to the lower susceptibility of monosaturated or saturated fatty acids to ROS, membrane composition is a key determinant on its susceptibility to oxidative damage [21].

The carbonyl compounds derived from LOOH have long half-lives (minutes) and can migrate with relative ease through hydrophobic membranes and the hydrophilic cytoplasmic media, extending their damaging effects on target sites both within and outside membranes. These carbonyl compounds, and possibly their peroxide precursors, react with nucleophilic groups in proteins forming a variety of adducts and cross-links collectively named advanced lipoxidation end products (ALEs) [22].

Lipid peroxidation-derived end products ('enals') can also react at the exocyclic amino groups of deoxyguanosine, deoxyadenosine, and deoxycytosine to form various alkylated products. Some common enals that cause DNA damage are MDE, acrolein, and 4-hydroxynonenal (HNE), among others. The most common adducts arising from enals are exocyclic adducts such as etheno adducts, and MDE-deoxyguanosine. These DNA damage markers are mutagenic and carcinogenic, with powerful effects on signal transduction pathways [22].

Thus, cumulative effects of lipid peroxidation are implicated in various pathological conditions including atherosclerosis, hemolytic anemias, ischemia-reperfusion injuries and others. However, there are some protective mechanisms which can relief lipid peroxidation

toxicity. Cytoplasmic released lipid hydroperoxides are metabolized by glutathione peroxidases (Gpx), which act on H_2O_2 and also on free fatty acid hydroperoxides, reducing them to fatty acid alcohols. Additionally, a phospholipid hydroperoxide glutathione peroxidase (PHGPX) was described in mammalian tissues. This enzyme resulted able to act on peroxidized fatty acid chains still esterified to membrane lipids resulting in an important antioxidant defence for membranes *in situ* [23].

Membrane lipid remodelling is other important mechanism for removing peroxidized lipids. Phospholipase A_2 acts at the second carbon group of the phospholipid glycerol backbone to generate a free fatty acid and a lysophospholipid, preferentially hydrolizing fatty acids from oxidized liposomes [24]. Moreover, the newly formed lysophospholipids are substrates for reacylation reactions (readdition of fatty acids to the second carbon group position), which regenerate intact phospholipids [20].

1.1.2.2 DNA damage

Hydroxyl radical, $OH^{\cdot}$, is the main ROS reacting with nucleic acids. Specially, DNA may be particularly prone to iron-catalysed oxidation, since Fe^{2+} directly binds to the phosphodiester backbone, subsequently catalysing $OH^{\cdot}$ radical generation [25]. The types of DNA damage can be grouped into strand breaks (single and double), sister chromatid exchange, DNA-DNA and DNA-protein cross-links and base modifications. Among bases, the more frequent modifications are the non-bulky 8-oxoguanine and formamidopyrimidine, and the bulky cyclpurine and etheno adducts. These leads to ring saturation, ring opening, ring contraction, and hydroxylation, resulting in loss of aromacity and planarity, provoking local distortions in the double helix. Morevoer, depending on the type and the extent of the damage, the altered bases can be found either attached to or dissociated from the DNA molecule to generate apurinic/apyrimidinic (AP) sites [20].

Additionally, the phosphodiester backbone may also be a ROS target. Oxidation of the sugar and phosphate moieties may result in strand breaks. If the radical attacks the 3' or the 5' ends (i.e. non-3'-OH or non-5'-PO_4) they are no longer DNA polymerase substrates, and must be removed before any repair can occur [20].

Oxidative modifications to the nucleic acid polymers were shown to alter transcription, translation, DNA replication, to give raise to mutations and eventually to cell senescence and death. Even in physiological conditions DNA damage is estimated to be as high as 1 base modification per 130,000 bases in nuclear DNA. Damage to mitochondrial DNA is even higher, with a rate of 1 base modification per 8,000 bases [20]. Due to the extent and importance of these types of modifications, it is crucial the presence of cellular repair processes in terms of limiting mutagenesis, cytostasis and cytotoxicity.

Base lesions from oxidative DNA damage are repaired mainly, but not exclusively, by two different activities. The first one, base-excision repair (BER), uses a specific

glycosylase followed by abasic site priming, gap filling and DNA ligation, these three activities being common irrespectively of the identity of the glycosylase. The second one, nucleotide excision repair (NER), is more complex and involves the removal of a lesion-containing oligonucleotide. This consists of multiple lesion recognition and incision proteins, DNA re-synthesis and ligation [7].

BER can be further divided in two main pathways, short-patch/single nucleotide replacement BER or long-patch BER, depending on whether there is a monofunctional glycosylase simply removing the base lesion or a bi-functional glycosilase removing the base lesion and generating a nick using a subsequent AP-lyase activity [7] [26].

1.1.2.3 Protein oxidation

ROS oxidation of proteins leads to amino acid residue modifications, cleavage of peptide bonds, and formation of covalent protein-protein cross-linked derivatives. Side chain amino acid oxidation may result in reversible or irreversible modifications. Reversible modifications include some types of cysteine (Cys) and methionine (Met) oxidation. Specific enzymatic activities are involved in their repair (reduction), and these enzymatic redox cycling processes may be profited by cells for signalling processes. However, most of the oxidative modification of proteins results in their definitive damage, leading to loss-of-function and protein degradation. It may happen that the accumulation of oxidative damaged proteins overcomes the proteolytic cellular capabilities, therefore accumulating in the form of toxic aggregates. The latter are associated with neurodegenerative diseases and ageing. It is still a matter of debate whether these toxic modifications are involved in cell signalling or not, since they do not accomplish the reversibility principle required for cell signalling events.

One of the main purposes of this thesis is the study of the reversible and irreversible protein modifications.

Reversible oxidative modifications, their redox cycling and their involvement in cell signalling are introduced in more detail in section 1.2. On another hand, irreversible protein modifications are described below, and section 1.3 is dedicated to introduce protein quality control systems involved in the degradation of damaged and misfolded proteins, including those damaged by oxidative stress.

Peptide bond cleavage Oxidative attack of the polypeptide backbone is initiated by $OH^{\cdot}$ abstracting a hydrogen atom from the α-CH(R)- group of an amino acid residue to form a carbon-centred radical. The carbon-centred radical rapidly reacts with O_2 to form an alkylperoxyl radical intermediate, which can give rise first to an alkylhydroperoxide, then to an alkoxyl radical and finally to a hydroxyl protein derivative. The previously mentioned intermediate radicals generated may undergo side reactions with other amino acid residues

in the same or in different protein molecules to generate new carbon-centred radicals, capable of undergoing similar reactions. Additionally, alkoxyl radicals are the starting point for peptide bond cleavages by either the diamide or the α-amidation pathways. If the cleavage is through the diamide pathway, the resulting N-terminal portion of the protein will possess a diamide structure whereas the C-terminal portion will possess an isocyanate structure. If the cleavage is through the α-amidation pathway, the peptide fragment obtained from the N-terminal portion will possess an amide group, whereas the N-terminal amino acid residue derived from the C-terminal portion of the protein will exist as an N-α-ketoacyl derivative. Upon acid hydrolysis, the peptide fragments obtained by the diamide pathway will yield CO_2, NH_3 and a free carboxylic acid, whereas hydrolisis of the fragment obtained by the α-amidation pathway will yield NH_3 and a free α-ketocarboxylic acid. Finally, peptide bond cleavage can also occur as a result of ROS attack of glutamyl, aspartyl and prolyl side chains (reviewed in [27] and references herein).

Cross-linking reactions Protein-protein cross-linked derivatives promoted by ROS can be formed by different mechanisms. Thus, thiol oxidation to a disulphide may form protein cross-links; also the interaction of the aldehyde group of an HNE-protein adduct, or of the carbonyl group of a glycated protein, or of MDE and of the carbonyl group produced in the oxidation of an amino acid residue side chain with the ε-NH_2 group of a lysine residue on other protein results in protein cross-linking. Finally, protein-protein cross-links can be formed by the interaction of carbon centred radicals between two different protein molecules. Importantly, the formation of cross-linked complexes may have important implications in the accumulation of oxidized proteins, as occurs in ageing and some diseases, as these are often resistant to proteolytic degradation and even they may inhibit the capacity of some proteases to degrade the oxidized forms of other proteins [28].

Oxidation of amino acid side chains One or the most reactive groups of amino acid side chains are thiols from Cys. Both one-electron and two-electron oxidants are able to react with thiols (-SH), although yielding different products. Two electron oxidants generate a sulphenic acid (-SOH) as the initial product. Sulphenic acid is highly reactive, its stability being influenced by the availability of a proximal thiol group with which it condenses to form a disulphide bond, or by the availability of a proximal nitrogen to form a sulphenamide or, in the presence of more oxidant, it may further become oxidised to sulphinic (-SO_2H) or sulphonic (-SO_3H) acids (**figure 1.2**). One electron oxidation produces the thyl radical. Thiyl radicals readily react with the thiolate anion, which ultimately results in disulphide bond formation. However, it also yields $O_2^{-\cdot}$ which may amplify in this way the oxidant response. Alternatively, under low O_2 conditions, it reacts with ascorbate to give ascorbyl radicals [4] [29].

The oxidized forms -SOH, disulphide bond (-SS-), sulphenamide, and occasionally -SO_2H, together with methionine sulphoxide (Met-O, see below), are the only ROS-driven

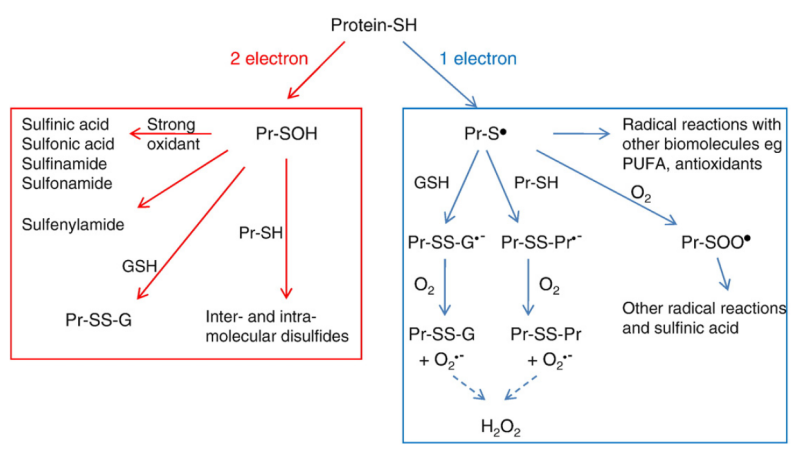

Figure 1.2: Pathways for one electron and two electron oxidation of protein thiols. Left-hand pathway, two-electron oxidation of a protein thiol (Pr-SH) initially yields sulphenic acid (Pr-SOH) which is a transient intermediate that undergoes a series of secondary reactions. It can form mixed disulphides with GSH (Pr-SS-G); vicinal thiols favour the formation of intra-molecular disulphides; inter-molecular disulphides can form between proteins; strong oxidants can generate the higher oxidation products, including sulphinic and sulphonic acids. Right-hand pathway, one-electron oxidants (radicals and transition metals) yield the thyil radical (Pr-S$^{\cdot}$). In aerobiosis its most favoured reaction is with a thiolate anion (from a protein or GSH) to give the disulphide anion radical and generating $O_2^{-\cdot}$, which amplifies the oxidative burst. Alternatively, the thiyl radical can propagate radical reactions or be quenched by scavengers. Reprinted from [29]

protein modifications that can be repaired in cells thanks to specific cellular activities.

Met residues of proteins are also sensitive to oxidation by virtually all kinds of ROS. Mild oxidising conditions convert Met to methionine sulphoxide (Met-O) derivatives. Most biological systems contain methionine sulphoxide reductases (Msrs), which are able to convert Met-O back to Met. In section 1.2.6.2 there is a summary of the functions of Msrs and their relevance regarding the possible role of Met oxidation/reduction as a built-in ROS scavenger.

Aromatic amino acid residues are also highly susceptible to ROS attack. Thus, tryptophan residues are readily oxidized to formylkynurenine, to kynurenine and to various hydroxy derivatives, phenylalanine and tyrosine residues yield a number of hydroxy derivatives, and finally, histidine residues are converted to 2-oxohistidine, asparagine and aspartic acid residues (see **table 1.2**).

Protein carbonylation Oxidation of some amino acid residues (lysine, arginine and proline residues, **table 1.2**) leads to formation of carbonyl derivatives. Additionally, carbonyl derivatives in proteins are produced as a consequence of oxidative cleavage of the peptide backbone via the α-amidation pathway or cleavage associated with the oxidation of glutamyl residues. Likewise, carbonyl derivatives can also be formed as a consequence of secondary reactions of some amino acid side chains with lipid oxidation products, such

Amino Acids	Oxidation products
Tryptophan	2-, 4-, 5-, 6-, and 7-Hydroxytryptophan, nitrotryptophan, kynurenine, 3-hydroxykynurinine formylkynurinine
Phenylalanine	2,3-Dihydroxyphenylalanine, 2-,3-, and 4-hydroxypenylalanine
Tyrosine	3,4-Dihydroxyphenylalanine, tyrosine-tyrosine cross-linkages, Tyr-O-Tyr, cross-linked nitrotirosine
Histidine	2-Oxohistidine, asparagine, aspartic acid
Arginine	Glutamic semialdehyde
Lysine	α-Aminoadipid semialdehyde
Proline	2-Pyrrolidone, 4- and 5-hydroxyproline pyroglutamic acid, glutamic semialdehyde
Threonine	2-Amino-3-ketobutyric acid
Glutamyl	Oxalic acid, pyruvic acid

Table 1.2: Oxidation products of protein side chain amino acids. Adapted from [27].

as HNE, or with reducing sugars or their oxidation products (see **figure 1.3**). Thus, HNE reacts by a mechanism of Michael addition with either the ε-NH_2 of lysine, the imidazole moiety of histidine or the thiol group of Cys residues. Similarly, reaction of one of the two aldehyde groups of MDE, with the ε-amino group of lysine leads to formation of Schiff base adducts possessing an aldehydic function [30].

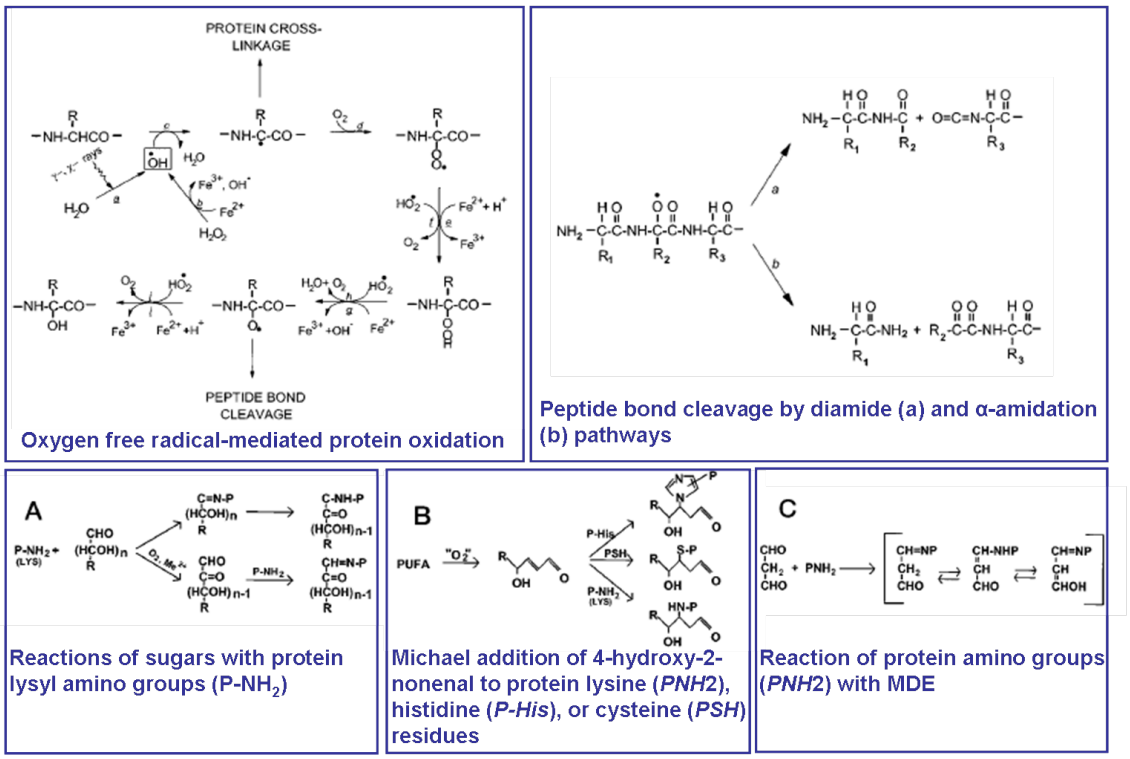

Figure 1.3: Pathways for protein carbonylation. See text for details. Reprinted from [27]

Accumulation of oxidized proteins The intracellular level of oxidized proteins reflects the balance between the rate of protein oxidation and the rate of protein degradation

or protein repair. ROS concentrations are key in this regard, therefore the intracellular concentration of enzymatic and non enzymatic antioxidants also determines protein carbonylation levels. For example, the $O_2^{-\cdot}$ generated as a consequence of the cellular aerobic metabolism is readily converted to H_2O_2 either spontaneously or by the action of superoxide dismutase. This H_2O_2, together with H_2O_2 produced by various oxidases, is readily degraded by thiol peroxidases, glutathione peroxidases, other thiol-specific antioxidants and catalase. However, if the concentrations of these H_2O_2-scavenging activities becomes limiting, H_2O_2 can undergo metal ion-catalyzed cleavage by the Fenton reaction generating the more toxic $OH^{\cdot}$. This reaction is in turn dependent upon the availability of iron and copper, which is determined by the concentrations of metal-binding proteins, and of multiple factors such as iron responsive transcription factors, as well as factors that influence the binding or the release of metal ions from these binding proteins. Other divalent cations (Mg^{2+}, Mn^{2+} and Zn^{2+}) may compete with Fe^{2+} or Cu^{+} for binding to metal binding sites on proteins, and thereby preventing site-specific generation of $OH^{\cdot}$, which is probably the most important mechanism of protein damage.

Degradation of those oxidative damaged proteins that cannot be repaired is an important issue regarding accumulation of oxidized proteins. Thus, the rate of protein degradation is dependent upon many variables, including the concentrations of proteases that preferentially degrade oxidized proteins and numerous factors (inhibitors, activators and regulatory proteins) that affect their proteolytic activities. For instance, oxidized forms of some proteins, mainly cross-linked proteins or proteins modified by glycation or lipid peroxidation products, not only are resistant to proteolysis but also they may inhibit the ability of proteases to degrade the oxidized forms of other proteins [31].

1.1.3 Antioxidant defences

ROS production is continuous in all aerobic organisms. To cope with these intermediate-O_2 species as they are generated, and keep the intracellular redox environment in a reduced state, organisms have evolved a series of antioxidant defence mechanisms, which include both enzymatic and non-enzymatic activities. Catalases, superoxide dismutases (SODs), glutathione peroxidases (Gpxs), and thioredoxin peroxidases or peroxiredoxins (Prxs) are enzymatic activities which directly interact with ROS leading to their decomposition. Also, some non-enzymatic activities, which normally consist of small molecules, can act as free radical scavengers. Some of these are glutathione, ascorbic acid, and vitamin E [32].

Other activities, including the thioredoxin (Trx) and the glutathione/glutaredoxin (GSH/Grx) system, methionine sulphoxide reductase (Msrs) or sulfiredoxin are antioxidants which act by repairing/reversing some types of Cys oxidations (Trx and GSH/Grx systems reduce disulphides and sulphenamides, sulfiredoxin reduces sulphinic acid in peroxiredoxins) or Met oxidations (Msrs).

However, even being present all these detoxifying activities, ROS are not totally detoxified, they are physiologically present at low steady-state concentrations (see section 1.1) able to continuously produce irreversible damages to biomolecules. These damages are even higher in situations of oxidative stress. In the case of proteins, when damages are irreversible (protein carbonylation), these are directed towards degradation pathways. This is explained in section 1.3.

1.1.3.1 Enzymatic detoxifying activities

The Trx and the GSH/Grx system, Prxs and sulfiredoxin, and Msrs are explained in more detail in subsequent sections of this Introduction (sections 1.2.3, 1.2.4, 1.2.6.1, and 1.2.6.2, respectively).

Catalases Catalases are ubiquitous hydrogen peroxidases which dismutate H_2O_2 into O_2 and two water molecules (equation 1.2).

$$2H_2O_2 \rightarrow 2H_2O + O_2 \tag{1.2}$$

Their origin is monophyletic and group into three different families. Two of the protein families are heme enzymes: typical catalases and catalase-peroxidases. Typical catalases comprise the most abundant group found in Eubacteria, Archaeabacteria, Protista, Fungi, Plantae, and Animalia, and they are divided based on having large ($>$ 75 kDa) or small ($<$ 60 kDa) subunits. Catalase-peroxidases are not found in plants and animals and exhibit both catalatic and peroxidatic activities. The third group is a minor bacterial protein family with a dimanganese active site called manganese catalases. Although catalysing the same reaction, the three groups differ significantly in their overall and active-site architecture and the mechanism of reaction [33].

Heme-containing catalases all have in common a two-step mechanism for the H_2O_2 degradation [34]. In the first step, one H_2O_2 oxidises the heme to an oxyferryl species in which one oxidation equivalent is removed from the iron and one from the porphyrin ring to generate a porphyrin cation radical (equation 1.3).

$$Por - Fe^{III} + H_2O_2 \rightarrow Por^{+\cdot} - Fe^{IV} + H_2O \tag{1.3}$$

A second H_2O_2 molecule is utilized as a reductant of the previously generated porphyrin cation radical and the oxyferryl species to regenerate the resting-state enzyme, H_2O and O_2 (equation 1.4).

$$Por^{+\cdot} - Fe^{IV} + H_2O \rightarrow Por - Fe^{III} + H_2O + O_2 \tag{1.4}$$

Catalases do not follow Michaelis-Menten kinetics except at very low concentrations. Small subunit enzymes suffer inactivation at concentrations above 300 to 500 mM H_2O_2. On the other hand, large subunit enzymes are activated by substrate [35], and start to suffer inhibition only above 3 M H_2O_2. Typical K_m range from 38 to 599 mM [34].

Superoxide dismutases (SODs) SODs catalyze the dismutation of $O_2^{-\cdot}$ to H_2O_2 and O_2. This activity was discovered in 1969 by McCord and Fridovich [36], who, for the first time, showed the scavenging of ROS by an enzymatic activity. Depending on their metal co-factor SODs can be classified into four major families. Thus, CuZnSOD type bind both copper and zinc [36], MnSOD types bind manganese, FeSOD types bind iron [37], and NiSOD bind nickel [38].

The SOD-catalysed dismutation of $O_2^{-\cdot}$ is described in the following half-reactions (equations 1.5 and 1.6).

$$M^{(n+1)} - SOD + O_2^{-\cdot} \rightarrow M^{+} - SOD + O_2 \tag{1.5}$$

$$M^{(+)} - SOD + O_2^{-\cdot} + 2H^{+} \rightarrow M^{n+1} - SOD + H_2O_2 \tag{1.6}$$

where if M=Cu n=1; and if M=Mn, Fe, or Ni n=2

Prokaryotes and mitochondria use Fe or MnSOD, whereas, in general, eukaryotic cells contain both a cytoplasmic and a glycosilated extracellular CuZnSOD, and a mitochondrial MnSOD. MnSOD represents the first line of defence against the $O_2^{-\cdot}$ produced as a by-product of oxidative phosphorylation in mitochondria [39].

As an example, exponentially growing *E. coli* cells contain approximately 20 μM of dimeric cytoplasmic SOD, being the amount of enzyme five orders of magnitude more abundant that its substrate (a typical steady-state concentration of *E. coli* $O_2^{-\cdot}$ is ~ 0.1 nM). Yet both the abundance and the catalytic efficiency of SOD, this 0.1 nM concentration of $O_2^{-\cdot}$ inactivates labile [4Fe-4S] enzymes at a rate of 10^6-10^7 M^{-1} s^{-1} (half-life of 30 min) [40].

Glutathione peroxidases Glutathione peroxidases (Gpxs) are considered to provide the main enzymatic defence against oxidative stress by hydroperoxides in eukaryotic cells. They decompose H_2O_2 or other organic hydroperoxides, such as fatty acid hydroperoxides, to water or their conrresponding alcohol, respectively. In this process, two Cys residues of Gpxs are oxidized to a disulphide bond; electrons required for the reduction of the disulphide to the thiol form will be provided by reduced cofactor NADPH, with the mediation of GSH [41]

Importantly, yeast (*S. cerevisiae* or *S. pombe*) do not express any classical Gpx. Rather, Gpxs from yeast are better classified as atypical 2-Cys peroxiredoxins, since they form an intra-molecular disulphide bond in their catalytic cycle, which is reduced by Trx [42] [43]. Moreover, *S. cerevisiae* Gpx3 has a role as a peroxide sensor and activator of the transcription factor Yap1 [44].

1.1.3.2 Non-enzymatic antioxidant molecules

Glutathione is described in section 1.2.4.1. Ascorbic acid and vitamin E are the most abundant hydrosoluble and lyposoluble vitamins, respectively, thus these are the only ones believed to have a role in the antioxidant defence.

Ascorbic acid Ascorbic acid is a hydrosoluble antioxidant, commonly acting as a redox couple with glutathione in many eukaryotes [45]. In yeast, it is not clear if ascorbate functions as an antioxidant, since it is found at very low concentrations [46]. However, yeast cells deleted for *alo1*, a gene encoding D-arabinono-1,4-lactone oxidase, which catalyses the final step in the erythroascorbate biosynthesis (a 5-carbon analogue of ascorbate) are sensitive to H_2O_2 and $O_2^{-\cdot}$ [47] [48].

Vitamin E Vitamin E acts as a lipid-based radical chain breaking molecules with scavenging capacity for free radicals including lipid peroxyl, alkoxyl and $OH^{\cdot}$. Trolox, an analogue soluble model compound for α-tocopherol decreases the levels of H_2O_2 and $O_2^{-\cdot}$ [49].

1.1.4 *In vivo* models of oxidative stress: *Schizosaccharomyces pombe*

As mentioned in section 1.1, oxidative stress is defined as a condition in which there is an imbalance between ROS production and ROS detoxification. Enhanced ROS generation or defects in ROS detoxification may be due to particular situations in the cell (mitochondrial dysfunction, genetic defects in the expression of antioxidant enzymes such as catalase or SOD, increased production by mitochondria, peroxisomes or NADPH oxidases), leading to endogenous oxidative stress. Also, increased ROS exposure from exogenous sources (UV light, environmental pollutants, re-perfusion and others) generate situations of exogenous oxidative stress.

A good model for studying oxidative stress is therefore an organism in which both endogenous and exogenous oxidative stress situations can be reproduced. *S. pombe*, an organism extensively used in the lab as a model organism for molecular biology,

accomplishes several requisites which also make it an appropriate model for studying oxidative stress.

S. pombe is a single-celled free living archiascomycete fungi first described by P. Lindner in 1893 after its isolation from an East African beer. Its name derives from the Swahili word for beer, pombe. *S. pombe* forms a rod-shaped non motile cell that grows by elongation and divides by medial fission.

The genome of *S. pombe* bas been fully sequenced. It is the smallest genome among eukaryotes, with a size of 13.8-Mb distributed among three chromosomes, together with a 20-kb mitochondrial genome. It codes for a maximum of 4,940 predicted protein coding genes (including 11 mitochondrial genes) and 33 pseudogenes. Special characteristics of this yeast are the essential character of its mitochondria (it is a petite-negative yeast, while it is dispensable in *S. cerevisiae*) and the conservation of its genome, since it experienced low genome arrangements in its evolution [50] [51].

Important for studying not only oxidative stress but also other types of intracellular processes and pathways, is the ability of this cell to grow in a haploid state. Therefore, if not essential, genes can be easily deleted by classical techniques of DNA recombination as they are present in the genome in a single copy.

Many are the *S. pombe* genes which deletion may enhance endogenous ROS production or decrease ROS detoxification. Some of them are presented in **table 1.3**. Typical enzymes involved in detoxification of endogenous oxidative stress are the peroxiredoxin Tpx1, which is required for the aerobic growth of *S. pombe* [52], or Sod1 and Sod2, directly involved in $O_2^{-\cdot}$ disumtation. Also, mitochondrial deletion mutants, which produce mitochondrial dysfunction, were shown to be required for the aerobic growth of this organism in respiratory-prone conditions [53]. The transcription factors Pap1, Prr1 and Atf1 are activated upon exogenous oxidative stress (see section 1.1.4.2).

1.1.4.1 Environmental stress

Cells use specific sensory and signalling systems to obtain and transmit information from the environment to adjust cellular metabolism, growth and survival. Stress on cells can be considered as any disturbance of the normal or optimal growth conditions. Unicellular organisms cope with variations in nutrient availability, pH, temperature, osmolarity, ultraviolet radiation, or exposure to several toxic compounds. These have developed systems to sense and adapt to fluctuations in the intensity, concentrations or presence of such variables. Low levels o stress often trigger adaptive responses which result in transient resistance to higher levels of the same stress, and that can also lead to increased resistance (cross-protection) to other types of stresses [54] [55]. This phenomenon of cross-protection suggests that either different stress conditions trigger similar defence mechanisms or that there is a general stress response that can confer a basic level of

	Gene	Location	Product
Transcription factors	*pap1*	Cyt, Nucl	AP-1 like transcription factor
	prr1	Nucl	response regulator
	atf1	Nucl	cyclic-AMP-dependent transcription factor 1
Thioredoxin	*trx1*	Cyt	cytoplasmic thioredoxin
	trx2	Mit	mitochondrial thioredoxin
	trx3 (txl1)	Nucl, Cyt, proteasome	thioredoxin-like I protein
Thioredoxin reductase	*trr1*	Cyt, Nucl	thioredoxin reductase
Peroxiredoxins	*tpx1*	Cyt, Nucl	thioredoxin peroxidase, subfamily Prx1
	bcp	Cyt, Nucl	thioredoxin peroxidase, subfamily BCP
	pmp20	Cyt, Nucl	thioredoxin peroxidase, subfamily PrxV
Glutaredoxin	*grx1*	Cyt, Nucl	glutaredoxin
	grx2	Mit	glutaredoxin
	grx3	ER, Golgi, nucleolus	monothiol glutaredoxin
	grx4	Nucl	glutaredoxin
	grx5	Cyt, Mit, Nucl	monothiol glutaredoxin
Glutathione reductase	*pgr1*	Cyt, Mit	glutathione reductase
Glutathione peroxidase	*gpx1*	Cyt, Mit, Nucl	glutathione peroxidase (thioredoxin dependent)
GSH biosynthesis	*gcs1*	Cyt, Nucl	gamma-glutamylcysteine synthetase
Catalase	*ctt1*	Cyt, Nucl	catalase
Superoxide dismutase	*sod1*	Cyt, Nucl	Cu-Zn superoxide dismutase
	sod2		manganese superoxide dismutase
Chaperone of Sod1	*ccs1*		superoxide dismutase copper chaperone
Methionine sulphoxide reductases	*mxr1/msrA*	Cyt, Nucl	methionine (S)-sulphoxide reductase
	mxr2/msrB	Cyt, Nucl	methionine (R)-sulphoxide reductase
Mitochondrial components	*SPBC26H8.12*	Mit	cytochrome c heme lyase
	SPAC1071.11	Mit	NADH-dependent flavin oxidoreductase
	rip1	Mit	ubiquinol-cytochrome-c reductase complex
	sco1	Mit	chaperone for complex IV assembly
	SPAC1672.04c	Mit	chaperone required for complex IV assembly
	dps1	Mit	required for ubiquinone biosynthesis
	cox6	Mit	heme-A containing chain of cytochrome c oxidase
	coq2, 3, 4, 5, 10	Mit	required for ubiquinone biosynthesis
	SPBC336.13c	Mit	mitochondrial inner membrane peptidase complex
	tom70	Mit	mitochondrial import protein
	ppr4	Mit	mitochonrial translation regulator
	mss1	Mit	modification of mitochondrial tRNAs
	mug178	Mit	mitochondrial ribosomal protein
	mtg1	Mit	mitochondrial GTPase involved in translation
	SPAC1610.02c	Mit	mitochondrial ribosomal protein

Table 1.3: *S. pombe* genes coding for proteins with roles in ROS detoxification and in ROS generation.

protection from environmental changes [54] [55] [56].

Whole genome expression profiles revealed general responses to different types of insults in both the fission yeast and the budding yeast *S. cerevisiae* [54] [55] [56]. This core response is very conserved between these two distantly related species. Induced genes are involved in carbohydrate metabolism, ROS detoxification, protein folding and degradation, vacuolar and mitochondrial functions, autophagy, and metabolite transport. Repressed genes are involved in RNA processing, transcription and translation, and ribosomes and nucleotides biosynthesis, processes generally involved in energy consumption and cellular growth. This response was termed as environmental stress response (ESR) [55] or common environmental response (CER) [54] in *S. cerevisiae*, and as common environmental stress response (CESR) in *S. pombe* [56].

1.1.4.2 Oxidative stress signalling in *S. pombe*

In *S. pombe* the transcriptional response to oxidative stress, induced by H_2O_2, is mediated at least by two transcriptional factors, the AP-1 like Pap1 and the bZIP Atf1 controlled by the mitogen-activated protein kinase (MAPK) Sty1 (**table 1.3**). These act in an intensity-dependent fassion. Pap1 is required for the response to low levels of H_2O_2, inducing an adaptive response, whereas Sty1-Atf1 are more important for the response to high levels of H_2O_2 and triggers a survival response [57] [58] (**figure 1.4**). None of these conserved pathways [59] is required for viability upon aerobiosis, however they are essential for cell survival upon oxidative stress conditions.

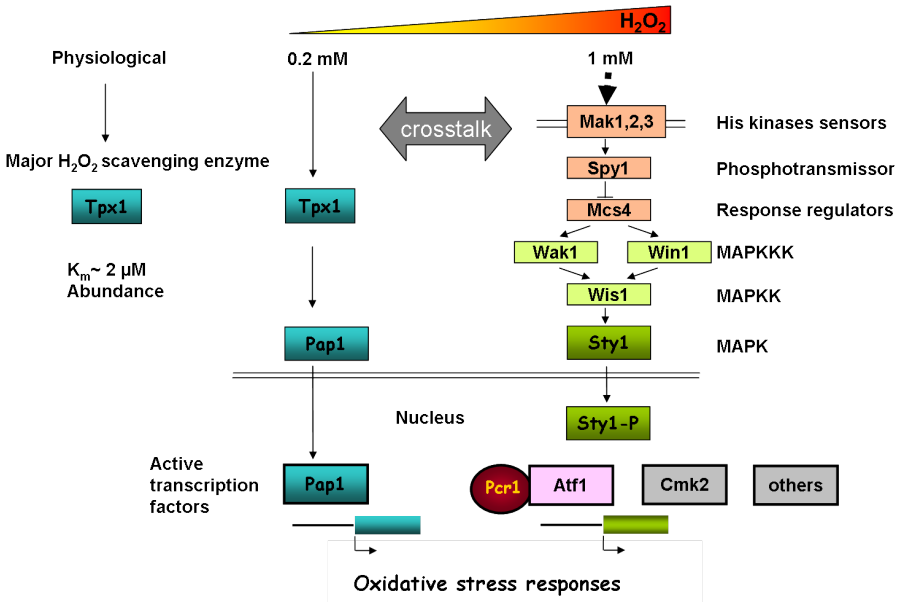

Figure 1.4: *S. pombe* triggers two independent but cross-talking signalling pathways upon oxidative stress depending on the concentration of the insult. The Pap1 pathway is activated upon low doses of H_2O_2 inducing an adaptive response, however the MAPK Sty1 responds to higher doses of H_2O_2 triggering survival responses.

Sty1 pathway The *S. pombe* Sty1 pathway is activated upon different insults including UV light, DNA damaging agents, heavy metals, oxidative stress, heat or osmotic stress [60] [61] [62]. The cascade begins upstream with activation of the histidine kinases Mak1, -2 and -3 [63] [64] [65]. These kinases activate the phosphotransmitter Spy1/Mpr1 [66] [67], which in turn controls the response regulator Mcs4 [62] [68]. Mcs4 then activates the upstream components of the MAPK module, the MAPKKKs Wak1 (also known as Wis4 or Wik1) and Win1 [69] [70]. These in turn activate the MAPK kinase Wis1 [71] [62] [72]. Activated Wis1 dually phosphorylates Sty1 on neighboring threonine and tyrosine residues [71] [73] [72] [74]. The basal activity of the pathway and its inactivation after

stress are regulated by tyrosine and serine-threonine phosphatases, such as Pyp1 and Pyp2 and Ptc1 to -4 [75] [76] [77]. This cascade is homologous to the HOG1 MAPK pathway in *S. cerevisiae* and to the mammalian c-Jun NH_2-terminal kinase (JNK) and p38 activated protein kinase cascade pathways [78].

Upon stress-mediated phosphorylation, Sty1 accumulates in the nucleus [79] [80], where it activates a complex transcriptional program of stress defense mechanisms [56]. Thus, in the response to four out of five types of stress stimuli, Sty1 is required for the transcriptional regulation of a large set of genes that constitute the CESR genes [56]. For the majority of these genes, regulation is also dependent on the transcription factor Atf1; and although several Sty1 substrates have been identified, the main one seems to be Atf1 [73] [81] [74].

One of the genes which is highly up-regulated in a Sty1- and Atf1-dependent manner upon oxidative stress is *ctt1* (**table 1.3**) which encodes for the only *S. pombe* catalase protein.

Pap1 pathway The *S. pombe* Pap1 pathway (homologue of c-Jun in mammals and Yap1 in *S. cerevisiae*) is triggered by low doses of H_2O_2. Pap1 is regulated by sub-cellular localization; before stress it is inactive in the cytosol, whereas after stress it becomes nuclear and active. Pap1 has a double nuclear import signal (NLS), which is recognized by Imp1 (importin-α) and a nuclear export signal (NES) Crm1-(exportin) dependent. The Crm1-dependent export of Pap1 prevails over the import, and therefore the transcription factor displays cytosolic localization prior to stress imposition. Pre-existing Pap1 accumulates in the nucleus upon oxidative treatments, as a consequence of inhibition of Crm1 dependent Pap1 nuclear export [82] [83].

Pap1 contains two clusters of three and four Cys residues each. One is located at the centre of the protein (n-CRD), with four Cys residues, and the second at the carboxy-terminal region (c-CRD), with three Cys residues, where the NES is also located. Conditions suspected to alter the intracellular redox state of Pap1 Cys residues, such as H_2O_2, diamide, diethylmaleate (DEM), heavy metals, and a variety of toxic drugs, induce the expression of Pap1-dependent genes [82].

In the case of low doses of H_2O_2, at least one intra-molecular disulphide bond is formed in Pap1 between two distant Cys residues, one from the n-CRD (Cys278) and the other one from the c-CRD (Cys 501 or Cys 532). This disulphide bond causes a conformational change, which impairs the access of Crm1, leading to its dissociation from the Crm1-Hba1 nuclear export machinery, and therefore to its nuclear accumulation (**figure 1.5**) [83] [84] [58].

Oxidation and nuclear accumulation of Pap1 induces more than 2-fold a subset of more than 50 genes [85]. There are two types of responses triggered by low H_2O_2 doses, adaptation to oxidative stress and tolerance to toxic drugs [86]. Some of the genes activated

by the Pap1 pathway, including *caf5* (coding for an efflux pump), *obr1* (coding for an ubiquitin-like protein) or *SPCC663.08c* (coding for a dehydrogenase), only require nuclear Pap1 for their activation. However, another subset of genes, including those coding for Ctt1, Srx1 or Trr1 (**table 1.3**), require nuclear and oxidized Pap1 to form an heterodimer with the constitutively nuclear transcription factor Prr1.

Importantly, H_2O_2 is not directly oxidizing Pap1, this process is mediated by the peroxiredoxin Tpx1 (**figure 1.5**). This is described in more detail in section 1.2.6.1. Also, it was proposed that the Trx system is involved in keeping reduced Pap1 in the absence of stress and in restoring oxidized and active Pap1 to its basal state (**figure 1.5**), as *S. pombe* mutants deleted for *trr1* have constitutive oxidized and nuclear Pap1 [58]. Curiously, *trr1* is one of the genes whose transcription is dependent on Pap1, allowing a negative feedback regulation of the pathway.

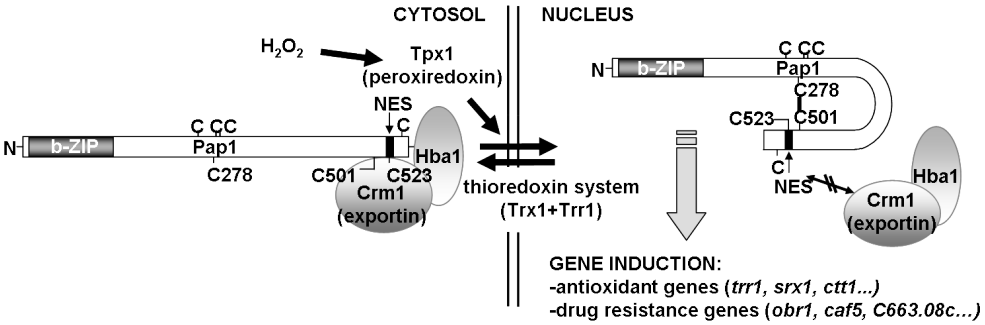

Figure 1.5: Schematic representation of Pap1-transcription activation by H_2O_2. Upon H_2O_2, Tpx1 mediates the formation of at least one disulphide bond between the c-CRD and the n-CRD in Pap1. This produces a conformational change in Pap1, which hinders the NES to the exportin Crm1 and its co-factor Hba1. Nuclear accumulation of Pap1 triggers the transcription of both antioxidant and drug resistance genes. Important Pap1-Cys residues are indicated.

1.2 Regulation of cellular thiol-redox homeostasis

Cys in proteins and low molecular weight thiols have important roles in the cellular biochemistry. First, thiols in proteins are able to stabilize protein structures by forming disulphide bonds or by coordinating transition metal ions. Second, while many protein oxidative modifications are irreversible, most thiol modifications that involve sulphur in low oxidation states are reversible. Thus, disulphide bonds, mixed disulphides with glutathione, and sulphenic acids can be either directly or indirectly reduced by the thioredoxin (Trx) or the glutathione/glutaredoxin (GSH/Grx) systems. As a result, these reversible thiol modifications are used as regulatory switches in redox sensitive proteins, including oxidative stress transcription factors such as the mentioned above Pap1 or the *S. cerevisiae* Yap1 (Pap1 homologue), and others.

1.2.1 Kinetic and thermodynamic aspects of thiol-disulphide redox exchanges

Life is based on different and regulated systems of electron flow, consisting on transferring electrons from an electron donor (reducer) to an electron acceptor (oxidant). One of the ways by which organisms carry electrons from electron donors to final acceptors is through reversible thiol-disulphide redox exchanges. Thiol-disulphide redox pathways are involved in many functions including normal metabolism, responses to stress (mainly H_2O_2 related) or protein folding [87].

In the case of aerobic metabolism, the net, two-electron oxidation of two thiols to a disulphide is ultimately linked to the reduction of oxygen (equation 1.7). The opposite, the reverse reaction, occurs at the expense of reducing equivalents, normally provided by nicotinamide dinucleotides (NADH or NADPH) (equation 1.8).

$$2R-SH \rightleftharpoons R-SS-R+2e^{-}+2H^{+} \tag{1.7}$$

$$RSSR+NADPH+H^{+} \rightleftharpoons NADP^{+}+2R-SH \tag{1.8}$$

Moreover, thiol-disulphide exchange reactions can also transfer reducing equivalents between two thiol-disulphide pairs (equation 1.9) [88].

$$R-SH+RSSR' \rightleftharpoons RSSR+R'SH \tag{1.9}$$

Inside cells, different compartments have different reducing conditions. Thus, nucleus and cytoplasm are considered to be reducing environments, attributed to the expression of the potent thiol-dependent redox buffers, Trx and the GSH/Grx systems, with yield and overall redox potential close to -250 mV, whereas the endoplasmic reticulum (ER), the mitochondrial inter-membrane space (IMS), or the periplasm in prokaryotes are considered to be more oxidizing. Thus, the ER and the IMS possess specific systems to catalyze disulphide formation to mediate polypeptide folding and/or protein activity. Likewise, the bacterial periplasm harbors the DsbA-D system to introduce and isomerize disulphides in this compartment.

Cys in proteins are usually found in the reduced thiol state, in cytosol and nucleus, and in the oxidized disulphide state in the ER, the IMS or in the periplasm. Nevertheless, some catalytic processes yield protein-disulphides in cytoplasmic or nuclear proteins and protein-thiols exist in the ER, the IMS or the periplasm, in spite of being oxidizing environments. How does this happen? The interconversion of thiols and disulphides is a reversible oxidation-reduction process, not only linked to the availability of appropriate electron donors and acceptors, with suitable redox potentials (thermodynamics of the reaction), but also linked to kinetic barriers. Thus, even if a thiol-disulphide exchange is thermodinamically favoured, it will only take place if the transition energy (E_a, **figure 1.6**) to form the transition state complex (TS, **figure 1.6**) can be overcome.

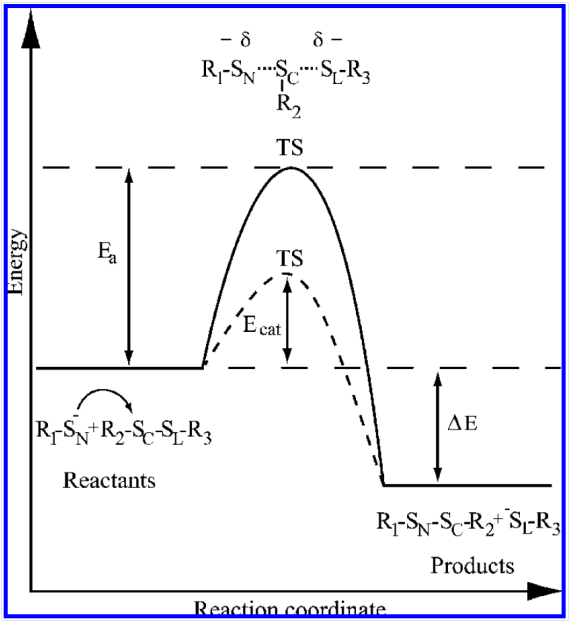

Figure 1.6: Energy diagram of a thiol-disulphide exchange reaction. A thiolate anion nucleophylically attacks on a disulphide to form a transition state (TS) between the nucleophilic thiol (SN), the central thiol (SC), and the leaving thiol (SL). The energy barrier between the reactants and the transition state (TS) is the activation energy (E_a) of the reaction. E_a decreases by the action of catalysts (E_{cat}). The difference in potential energy between reactants and products is denoted as ΔE. Adapted from [89]

1.2.1.1 Thermodynamics of thiol-disulphide exchange

Thiol-disulphide exchange reactions involve a thiolate anion attacking by a nucleophilic substitution type 2 mechanim (SN_2) on a disulphide, resulting in an exchange of the covalent disulphide bond. The deprotonation state of the thiol yields information about reactivity, being the equilibrium constant for deprotonation directly linked to the pK_a value of the thiol (equations 1.10 to 1.12).

$$PSH \rightleftharpoons PS^- + H^+ \tag{1.10}$$

$$K_{eq} = K_a = \frac{[PS^-]_{eq}[H^+]_{eq}}{[PSH]} \tag{1.11}$$

$$pK_a = -logK_a \tag{1.12}$$

Considering the reaction for the thiol-disulphide exchange between a protein thiol and glutathione disulphide (GSSG) (equation 1.13); the equilibrium constant is referred to as K_{ox} (equation 1.14), and reflects a dynamic state where forward and reverse reactions take place with equal rates, so that equilibrium concentrations are maintained. Both, the rate

constants of the reaction (k_1 and k_2) and the change in standard Gibbs free energy ($\Delta G^{\circ'}$) of the reaction (equation 1.15) are related with the equilibrium constant. K_{ox} and $\Delta G^{\circ'}$ can be used to predict the direction of the thermodynamically favorable reaction if the concentrations of all involved species are 1M (standard state). In the rest of situations, the mass ratio Q must be calculated (equation 1.16), and the ratio between K_{ox} and Q will give the sign of $\Delta G'$ (equation 1.17) and thus the direction of the thermodynamically favored reaction [89].

$$RSH + GSSG \underset{k_1}{\overset{k_2}{\rightleftharpoons}} RSSG + GSH \tag{1.13}$$

$$K_{eq} = K_{ox} = \frac{[RSSG]_{eq}[GSH]_{eq}}{[RSH]_{eq}[GSSG]_{eq}} = \frac{k_1}{k_2} \tag{1.14}$$

$$\Delta G^{\circ'} = -RT\,ln K_{eq} \tag{1.15}$$

R is the gas constant (8.31 J K^{-1} mol$-$1), T is the temperature (K), $\Delta G^{\circ'}$ is the standard Gibbs free energy (J mol^{-1}) at 1 atm, 298 K and pH 7

$$\Delta G' = \Delta G^{\circ'} + RT\,ln Q \quad \text{where} \quad Q = \frac{[RSSG][GSH]}{[RSH][GSSG]} \tag{1.16}$$

$\Delta G'$ is the Gibbs free energy (J mol^{-1}) at pH 7

$$\Delta G' = RT\,ln\left(\frac{Q}{K_{eq}}\right) \tag{1.17}$$

The change in free energy is also related with the changes in redox potentials ($\Delta E'$), according to the Nernst equation (equation 1.18). For changes to occur in a closed system, $\Delta G'$ must be $<$ than 0. From equation 1.19 it can be seen that positive $\Delta E'$, and thus positive $\Delta E^{\circ'}$, favour thermodynamic changes. $\Delta E^{\circ'}$ reflects the difference of standard reduction potentials (E°). They are calculated relative to H_2, in 1 atm, pH 0, 25°C and 1 M of the compound, and reflect the tendency of a compound to give or take electrons from H_2 [87].

$$\Delta G' = -nF\Delta E' \quad \text{where} \quad \Delta E' = \Delta E^{\circ'} - \frac{RT\,ln Q}{nF} \tag{1.18}$$

n is the number of electrons exchanged in the reaction and F is the Faraday constant

$$\Delta G' = -nF\Delta E^{\circ'} + RT\,ln Q \tag{1.19}$$

1.2.1.2 Kinetics of thiol-disulphide exchange

From a thermodynamic point of view the transfer of electrons from an electron donor (low affinity for electrons) to an acceptor (high affinity for electrons) would produce a negative change in Gibbs free energy (thermodynamically favored). Nevertheless, kinetic barriers can impede the reaction to take place. The rate of protein thiol-disulphide exchange is affected by many factors including pK_a, charge of nearby residues, local electric field, hydrogen-bond interactions, solvation, steric and mechanical strain and others [90] [89].

Influence of pK_a on the thiol-disulphide reaction rate In a thiol-disulphide exchange reaction, the attacking species is a thiolate anion, hence the thiol pK_a and the pH of the solution directly determine the availability of the deprotonated thiol and the reaction rate. Most Cys in proteins have pK_a values around 8.5, being most of them at their neutral protonated state under physiological conditions. Lowering the pK_a of the nucleophilic Cys will increase its thiolate fraction and thus its reactivity. However, decreasing too much the pK_a may also decrease the thiolate nucleophilicity, rendering a larger energy to reach the transition state (E_a, **figure 1.6**). Therefore, the effect of lowering the pK_a on rate enhancement is more significant at pK_a values close to the pH of the solution [90].

For low molecular thiols, the Brønsted equation (equation 1.20) establishes a relationship between reaction rates and pK_a, being the reaction rate a function of the sum of the contribution of each individual thiol pK_a. Therefore, reaction rates are also affected by the pK_a values of the central sulphur atom at the transition state and of the leaving group thiol. Thus, the lower the pK_a of the leaving group the faster the reaction, and in the case of an asymmetrical disulphide, the nucleophilic thiol will attack that one with the lower pK_a [89].

$$logk = \beta_N pK_a^N + \beta_C pK_a^C + \beta_L pK_a^L + D \tag{1.20}$$

k is the rate constant, β are the Brønsted coefficients for the nucleophilic thiol (N), the central thiol (C) and the leaving group thiol (L), D is a constant. β_N has a positive sign (range between 0 and 1) meanwhile β_C and β_L have negative values.

The pK_a can be lowered if the negative charge of the thiolate anion is stabilized. This effect can be produced by positive charged residues or electron-withdrawing groups in the proximity of the Cys residue (ion-pairing interactions). On the contrary, anionic residues in the vicinity cause thiols to behave as weaker acids. Moreover, since negative charges are involved in both the ground state and the transition state of thiol-disulphide exchange reactions, the local electric distribution around the sulphur atom may also influence the reaction rate. For instance, most N-terminal Cys in proteins having a Trx fold (section 1.2.2) are more acidics, in part due to a local electric field created by an α-helix close to the attacking Cys of the fold [90]. Weak interactions with uncharged residues also

affects the stabilization of thiolates. For instance, hydrogen-bond interactions (ion-dipole interactions) differentially stabilize the thiolate, lowering its pK_a, in comparison with the protonated thiol, which is a poor hydrogen-bond acceptor.

Solvation is another factor affecting reaction rates. In water or other protic solvents, the solvation energy affects the nucleophilicity, since it lowers the energy of the ground-state relative to the transition state, causing an increment in the activation energy (**figure 1.6**). As an example, in the highly reactive peroxiredoxins (section 1.2.6.1) water molecules are almost always excluded from the catalytic site [90].

Effects of entropy and strain on thiol-disulphide reaction rates Entropy is a measure of the randomness and disorder in a system, and a gain of entropy helps to drive a reaction. For instance, formation of intra-molecular disulphide bonds is normally associated with less entropy loss than formation of inter-molecular disulphide bonds, and therefore they are more easily made. The reason is that thiols in the same molecule are already linked, whereas for an inter-molecular disulphide bond to form, two molecules have to be linked together, which is associated with loss of translational and rotational degrees of freedom. Any factor placing two Cys together will increase their effective molarity, increasing the reaction rates and the equilibrium constants towards disulphide bond formation. Nevertheless, formation of a disulphide bond also results in strain of the molecule, which is directly connected to the stability of the disulphide. If little or no strain is introduced upon disulphide formation, it will be stable (high K_{ox} values). However, if the disulphide imposes strain on the protein, by making it less flexible, it will be less stable, and the breakage of the disulphide will be associated with a larger gain in entropy (low K_{ox} values) [89].

1.2.2 Catalysis of thiol-disulphide reactions

The main group of enzymes that catalyse thiol-disulphide exchange reactions are a group of oxidoreductases that belong to the Trx family of proteins, which in general share a common structural motif known as the Trx fold. The conserved Trx fold can be found in a variety of functionally different proteins such as thiol-disulphide oxidoreductases, protein disulphide isomerases, disulphide oxidases, glutathione *S*-transferases or thiol dependent peroxidases. Structurally, the Trx fold consists of a central four-stranded β-sheet surrounded by three α-helices. Hallmarks of the Trx fold are a *cis*-proline residue located before the β-sheet three and the CXXC or CXXS active site motif located on the loop connecting β-sheet one and α-helix one (**figure 1.7**). The nature of the two aminoacids between the redox-active Cys determines the standard redox potential of the proteins harbouring the Trx motif, explaining their different role as oxidases, reductases or isomerases [91]. For instance, the strongest reductants, the Trxs (CGPC) have standard redox potentials ranging from -260 to -285 mV. Grxs (CPTC) are less reducing (-198 mV to -233 mV), protein disulphide isomerases (PDI) (CGHC) have intermediate redox values (-147 to -175 mV) and the

strongest oxidants, periplasmic DsbA(s) (they act as thiol oxidases in the protein folding process) (CPHC) have higher standard redox potentials (-90 mV to -110 mV). Mutation of the *Eschericchia coli* Trx CGPC to CGHC increased the redox potential towards that of PDI, accompanied by a 10-fold increase in PDI activity, and the opposite, a mutation of the CGHC motif in PDI to CGPC resulted in a decrease in the redox potential yielding a protein that was more Trx-like. Moreover, replacing CPHC found in DsbAs by CGPC resulted in a Trx-like DsbA and a 1200-fold decrease in K_{eq} for the reaction with GSH (reviewed in [91] and [92]).

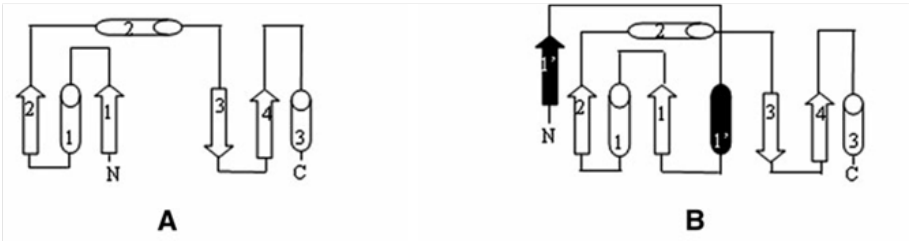

Figure 1.7: Basic thioredoxin fold in glutaredoxins (A) and thioredoxins (B). Reprinted from [91].

1.2.3 The thioredoxin system

1.2.3.1 Thioredoxins

Thioredoxin, the eponymous founder of the Trx family of proteins, is a thiol-disulphide oxidoreductase that was discovered in 1964 as an electron donor for *E. coli* ribonucleotide reductase (RNR), an enzyme required for DNA synthesis [93]. From then onwards, it became clear that Trxs regulate a wide number of processes in eukaryotic and prokaryotic organisms, apart from DNA repair and synthesis, such as antioxidant defence and redox regulation, sulphur metabolism, apoptosis and others, through participation, as an electron donor, in the catalytic cycles of enzymes like peroxiredoxins (Prxs), methionine sulphoxide reductases (Msrs), phosphoadenylyl sulphate (PAPS) reductase or ribonucleotide reductase (RNR) [92] [94].

The reaction catalysed by Trx is a nucleophilic substitution type 2 (SN_2), in which the electrons coming from Trx are shuttled to a substrate protein. As mentioned above, Trx contains at its catalytic centre a CGPC motif. The N-terminal Cys of this motif, with a pK_a ~ 7, is a solvent exposed thiolate that attacks on a disulphide, in the substrate protein, to form an inter-molecular mixed disulphide. This is sequentially and selectively attacked by the thiolate of the C-terminal Cys, which drops its initial pK_a (~ 9) in the mixed disulphide complex, yielding the reduced target protein and oxidized Trx. The new disulphide bond formed on Trx is not a structural disulphide; thus oxidised Trx has to be converted back to the reduced state to keep its biological activity. Enzymes that reduce Trx are Trx reductases

(TrxR) which drive electrons from NADPH to Trx. Trx, together with TrxR and NADPH constitute **the Trx system**, one of the main systems involved in redox homoeostasis inside the cell.

One major role of the Trx system is providing reducing power for proteins involved in the defence to oxidative stress. Thus, in yeast, the Trx system is the primary electron donor of Trx-dependent peroxiredoxins (glutathione-dependent peroxidases are absent in *S. cerevisiae* and in *S. pombe*), it directly reduces Msrs, which revert oxidized Met, both free and in proteins, and it is involved in the reduction of transcription factors, such as Yap1 in *S. cerevisiae* [95] and probably in *S. pombe* Pap1, which regulate a number of oxidative stress-responsive genes.

1.2.3.2 Thioredoxin reductase

TrxR are enzymes that belong to the flavoprotein family of pyridine nucleotide-disulphide oxidoreductases, which also include lipoamide dehydrogenase, glutathione reductase (the prototype member of this family), mercuric reductase and NADH peroxidase. All members are homodimers, except NADH peroxidase, and all are very closely related except NADH peroxidase and TrxR [96]. Each monomer of the enzyme includes a FAD prosthetic group, a NADPH-binding site and an active site containing a redox-active disulphide. In the catalytic mechanism of TrxR, electrons flow from NADPH to the FAD, from reduced FAD to the active site disulphide, and finally, from the nascent active site dithiol to the disulphide of Trx by two sequential thiol-disulphide exchange reactions (**figure 1.8**) [96].

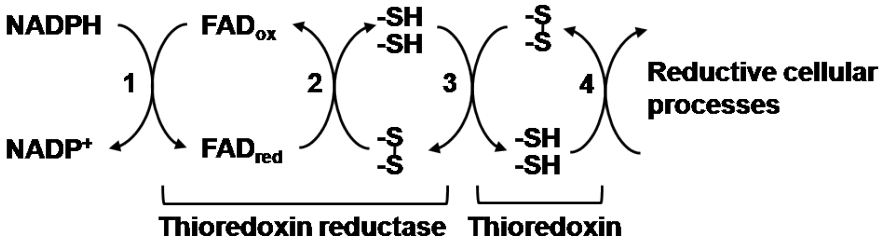

Figure 1.8: Electron flow in *E. coli* thioredoxin reductase catalisis. Reducing equivalents from NADPH are transferred to the flavin cofactor (step 1), then to the enzyme disulphide (Cys135-Cys138) (step 2), next to the disulphide (Cys32-Cys35) of oxidized Trx (step 3), and finally to the oxidized substrate (step 4). Adapted from [97]

One of the TrxR catalytic mechanisms more extensively studied is that of *E. coli* TrxR (*trxB*). This enzyme was first isolated as the electron donor for Trx when reducing RNR [93]. The two thiols that form the active centre disulphide (Cys135 and Cys138) are in the NADPH domain.

Mammalian TrxR, with higher M_r ($\sim$ 55 kDa) (TrxR from prokaryotes, lower eukaryotes and archaea have $M_r \sim 35$ kDa), share higher degree of sequence identity and

mechanistic similarity with glutathione reductase (GSHR) than with *E. coli* TrxR. In glutathione reductase, both the active-site residues, located in the FAD domain, and the bound NADPH, are close to the isoalloxazine ring of FAD, allowing electrons to flow from NADPH to glutathione (GSH) via FAD and the active-site disulphide without conformational changes in the enzyme [98]. Moreover, mammalian TrxR have an additional C-terminal -Cys-SeCys-Gly sequence, not present in glutathione reductases, which, although is not forming part of the active site, is required for catalysis. Differently than low eukaryotes and prokaryotes, which are highly specific for Trx, mammalian TrxR are promiscuos enzymes having a broad number of substrates, including lipoic acid, lipid hydroperoxides, dehydroascorbic acid, tumour supressor protein p53 or vitamin K_3 ([98] and references herein). This broad substrate specifitity has been attributed to the C-terminal SeCys. One of the proposed mechanisms is that the C-terminal end of TrxR is flexible, allowing the -Cys-SeCys-Gly moiety to carry electrons from the conserved active-site Cys residues to the substrate [98].

1.2.3.3 Thioredoxin system in *S. pombe*

***S. pombe* thioredoxins** The *S. pombe* genome codes for three Trxs, Trx1, Trx2, and Trx3 [50].

Trx1 is a 103 aa protein, predicted to be cytoplasmic, sharing a 51% identity and 74% similarity with Trx2 of *S. cerevisiae*. *S. pombe* cells lacking *trx1* are more sensitive than wild type to H_2O_2, cumene hydroperoxide, menadione ($O_2^{-\cdot}$ generator) and paraquat ($O_2^{-\cdot}$ generator). Nevertheless, they resulted more resistant than wild type to diamide, a thiol-oxidizing agent, a phenotype also shared by *S. pombe* cells lacking *trx2*, suggesting either that oxidized Trxs are harmful to cells, or that lack of Trxs prevents induction of stress-responsive genes that protect cells from this stress. *trx1* mRNA is induced upon H_2O_2 treatment (0.2 mM H_2O_2) in a Pap1 dependent manner. According to this, there is a Pap1 recognition sequence within 550 bp from the start codon at the genomic sequence. Similarly than in *S. cerevisiae*, in which double disruption of *trx1* and *trx2* causes constitutive activation of Yap1 [95], *S. pombe trx1* disruption also causes constitutive activation of the Yap1 homologue Pap1. Moreover, not only the basal level of Pap1-dependent genes is up-regulated, but also the transient nature of the activation of Pap1-dependent genes upon oxidative stress is compromised. Since lack of Trx1 does not increase the intracellular ROS amount, it is likely that Trx1 affects the thiol-disulphide status of Pap1, in non-stressed conditions and/or upon stress, as it is also implied from the role of Trxs on *S. cerevisiae* Yap1 redox status [95]. *S. pombe Δtrx1* cells are unable to grow in minimal media without Cys, or any Cys source, such as glutathione, N-acetyl-cysteine or sulfite, and this Cys auxotrophy is not recovered by multicopy expression of *trx2*, *pgr1* (glutathione reductase) or *grx1* (Grx), suggesting the importance of Trx1 as the sole source of electrons for *S. pombe* PAPS reductase (see section 1.2.6.4) [99].

S. pombe Trx2 is a mitochondrial protein of 121 aa. In comparison with Trx1, Trx2 has a minor role in the defence against general oxidative stress, as *Δtrx2 S. pombe* cells are not sensitive to H_2O_2, menadione or cumene hydroperoxide. Nevertheless, they are sensitive to paraquat, a $O_2^{-\cdot}$ generator, and similarly to *Δtrx1* cells, they are resistant to diamide (see above). *trx2* mRNA is slightly increased (2 fold) upon oxidative stress induced by H_2O_2, and this increase is Pap1 dependent [99]. The major role of Trx2 seems to be in mitochondrial functions. Trx2 over-expressed in a *S. pombe* strain conditionally deleted for glutathione reductase (*pgr1*) was able to revert some of the phenotypes caused by down-expression of *pgr1*, such as loss of oxidation-sensitive Fe-S clusters and increased iron concentrations. Nevertheless, Trx2 over-expressed, in the same mutant, with the Cys of its catalytic centre mutated, was unable to restore the phenotypes produced by the conditionally deleted *pgr1*, what suggested that this phenotypical reversion was due to the oxidoreductase activity of Trx2 [100] [101]. Another important mitochondrial function, independent of its oxidoreductase activity, is its role in mitochondrial respiration and the urea cycle. *Δtrx2 S. pombe* cells are unable to grow in non-fermentable carbon sources such as glycerol, and are auxotrophic for both arginine and Cys. Arginine auxotrophy in *Δtrx2* was restored by over-expressing Arg3, which codes for ornithine carbamoyltransferase (OCTase), a mitochondrial enzyme catalyzing the conversion from ornithine to citrulline in the urea cycle. Arg3 was found to directly interact with Trx2 *in vivo*, and the mRNA, protein levels and activity of OCTase resulted strongly dependent on the presence of Trx2. The fact that loss of Trx2 contributed to decreased *arg3* expression, and since the arginine pathway is tightly interlinked with carbon and nitrogen metabolism, it was hypothesized that this pathway communicates mitochondrial function with nuclear gene expression [101].

Trx3 or Txl1 is a protein with two big domains, a N-terminal Trx-like domain, with Trx activity and a C-terminal domain, by which it associates with the 26S proteasome, the latter establishing a link between the proteasome and oxidative stress [102]. This Trx is not very extensively characterized in *S. pombe* and it does not have any known orthologues in *S. cerevisiae*. However, it has mammalian orthologues, although these have reduced oxidoreductase compared with *S. pombe* Txl1. The simpler explanation might be the fact that the active site of the *S. pombe* Txl1 is preceded by a tryptophan residue (WCGPC) whereas in mammals, the tryptophan residue is substituted in the Txl1 protein by a glycine residue (GCGPC). It localizes to cytoplasm and nucleus, its gene deletion yields cells sensitive to *tert*-butil hydroperoxide (*t*BOOH) but not to H_2O_2, although neither its mRNA levels increase nor its over-expression improves growth upon *t*BOOH [103].

***S. pombe* thioredoxin reductase** The *S. pombe* genome codes for a single TrxR protein (Trr1). This was first cloned and sequenced upon a genetic screen searching for mutants able to suppress the growth inhibition triggered by the human tumour-supressor p53, when expressed in this organism [104]. Human tumour-suppressor p53 is a Trx-dependent redox-controlled protein with the ability to activate transcription of other genes that prevent

cells from entering in S phase with damaged DNA. Similar results were obtained in *S. cerevisiae*, where *trr1* deletion inhibited the ability of human p53 to stimulate reporter gene expression. Importantly, this effect was dependent on oxidized Trxs, since deletion of both *S. cerevisiae* Trx genes (*trx1* and *trx2*) suppressed this inhibitory effect caused by the single *trr1* deletion [105].

A different *trr1* mutation, *caf4-83*, was isolated in a screening of mutants conferring a phenotype of caffeine resistance in *S. pombe*. Almost equal phenotypes (caffeine resistance, increased sensitivity to UV radiation, impaired fertility or lengthened cell cycle) were showed with other mutants, *caf1-21*, *caf2-3*, *caf3-89* and *caf5*, suggesting a unique caffeine-tolerance pathway [106]. In fact, *caf3* resulted to be allelic to *pap1*, and *caf3-89* is a mutation in its NES (nuclear export signal). The rest of the mutations were also related with this transcription factor, thus *caf2* resulted allelic to *crm1*, the nuclear exporter of Pap1 and *caf1* was allelic to *hba1*, a cofactor of the Cmr1-driven export of Pap1. All these were loss-of-function mutations which rendered constitutively nuclear and active Pap1. In the cases of *caf3-89*, *caf2-3* due to defective Pap1 export, whereas in the case of *caf4-83* due to constitutively oxidized Pap1. Finally, *caf5* was allelic to an ABC transporter, Caf5, which expression is dependent on Pap1 [107] [108] [58].

Further studies showed that the toxic effects of caffeine were not mediated by direct generation of ROS, although its resistance was directly related with Pap1 activation (no caffeine concentration ranging from 0.05 to 30 mM triggered Pap1 activation) but mainly due to the downstream target of Pap1, the gene coding for the efflux pump Hba2, and in a lesser extent due to Caf5. Thus, cells lacking *trr1* and both *hba2* and *caf5* resulted very sensitive to caffeine, and cells lacking *hba2* resulted almost as sensitive to caffeine as cells lacking *pap1* [109].

S. pombe TrxR Trr1 has a M_r of 34 kDa, it contains the consensus active syte Cys-Ala-Val-Cys and an extra Cys residue at the C-terminal site. From phylogenetic analysis, the *S. pombe* Trr1 is closer to higher eukaryotes than to *S. cerevisiae* TrxR1 or TrxR2. A reporter system fusing 1526 bp upstream of the coding sequence into a promoter-less β-galactosidase gene showed increased synthesis of β-galactosidase upon menadione, mercuric chloride, H_2O_2, aluminium chloride and sodium selenite, being the expression upon menadione and mercuric chloride dependent on the transcription factor Pap1 [110]. Oxidative stress induced *trr1* expression is also dependent on oxidized Pap1 forming an heterodimer with Prr1, a constitutive nuclear transcription factor [86].

1.2.3.4 Functional relevance of Trx system components in thiol homoeostasis

Beckwith and colleagues genetically demonstrated how electrons flow through the Trx system in *E. coli*. They designed a disulphide reporter system taking advantage of the periplasmic enzyme alkaline phosphatase (AP), which became active when folded by intra-molecular disulphide bond formation. If expressed in the cytoplasm, upon removal

of its signal sequence, the protein was not properly folded due to lack of oxidation and remained inactive. However, in a mutational screening, this group found that AP activity was restored in the cytoplasm of cells lacking TrxR (TrxB in *E. coli*) [111]. Later, they showed that deletion of the two *E. coli* cytoplasmic Trxs, *trxA* and *trxC*, completely eliminated the AP activity restored by *trxB* [112]. These results suggested that lack of TrxR promoted protein disulphide bond formation (in this particular case formation of an AP intra-molecular disulphide) due to accumulation of oxidized Trxs. Or, in other words, that blocking the electron flow upstream of Trx in the Trx system, transformed this protein into a thiol oxidation catalyst. This study challenged the classical view of Trxs as main keepers of reduced solvent-exposed Cys, what is partially true, since they keep reduced Cys, both in general Cys-solvent proteins and in the recycling of enzymes which cycle from a thiol to a disulphide form as part of their catalytic cycles, but only when there is an appropriate reducing environment, which in this case means presence of TrxR and reduced cofactor NADPH. According to this, Trx expression with a periplasmic signal sequence, behaved as an oxidant able to replace DsbA in the oxidative protein-folding pathway [113].

1.2.4 Glutathione/glutaredoxin system

The glutathione/glutaredoxin system consists of Grx, glutathione (GSH) and NADPH-dependent glutathione disulphide (GSSG)-reductase (GR).

1.2.4.1 Glutathione

Glutathione (GSH) (γ-glutamyl-cysteinyl-glycine) is a very conserved and abundant low-molecular-weight slulfhydryl compound (up to 10 mM inside cells). GSH can be directly oxidized to GSSG by a two electron process. Upon oxidation, GSSG can be reduced with the help of the dimeric flavoenzyme glutathione reductase (GR) at the expense of NADPH. The GSH/GSSG couple has a very low standard redox potential $E^{o\prime}$ of -240 mV, which together with its high abundance confer to the couple GSH/GSSG the properties of a cellular redox buffer. In fact, it is common to mention the [GSH] to [GSSG] ratio as a measure of the cellular redox potential, although it would be more appropriate to use the Nernst equation (equation 1.21), as it takes into account the stoichiometry of the reaction.

$$E = -240 + \frac{RT}{2F} \ln\frac{GSSG}{GSH^2} \qquad \text{Nernst equation} \tag{1.21}$$

As a redox buffer, it is thought to be one of the major keepers of the cellular thiol-disulphide redox status, it is an electron donor for some enzymes having a catalytic cycle involving a thiol-disulphide step, which is normally mediated by Grxs, it participates in the scavenging of toxic compounds making conjugates with xenobiotics, with the help of GSH-S-transferases (GSTs), it can modulate enzyme activities, for instance by protecting

thiols from over-oxidation in a process known as glutathionylation or it participates in ROS metabolism, either directly of indirectly through glutathione peroxidases ([114] [32] [115] and references therein).

The synthesis of GSH involves two ATP-dependent enzymatic reactions, sequentially catalysed by γ-glutamylcysteine synthetase (Gcs) and glutathione synthetase (Gs). First, Gcs catalyses the formation of γ-glutamylcysteine from glutamate and Cys, being this the rate-limiting step in the *de novo* GSH biosynthesis. This step is regulated both by the availability of Cys and by feed-back competitive inhibition of GSH. Then, Gs catalyses the ATP-dependent formation of GSH from γ-glutamylcysteine and glycine [116].

In *E. coli*, lack of GSH is not essential for aerobic growth, unless deprived of the Trx system. The lethality produced by the lack of the two thiol redox branches is ascribed to a defect on the reduction of a disulphide bond produced in the essential catalytic process of reducing ribonucleotides to deoxyribonucleotides by RNR [117]. Nevertheless, GSH is an essential metabolite by itself in eukaryotes, and for instance, *S. cerevisiae* cells lacking Gcs ($\Delta gsh1$) are aerobically and anaerobically inviable, only growing if GSH is exogenously added. The fact that these cells are anaerobically inviable, suggests that GSH essentiallity is not due to its ROS-protective function. Also, in *S. cerevisiae* and in other eukaryotes, RNR reduction is mainly carried out by the Trx system, the GSH/Grx system having a secondary role. Toledano and co-workers performed studies in this regard, and found that both GSH cellular depletion and toxic amounts of GSH caused major alterations in iron metabolism, without significantly impacting thiol-redox control, except for the effect of high GSH levels blocking oxidative protein folding and secretion. Thus, iron metabolism required very low, but essential amounts of GSH whereas its cytoplasmic thiol-redox function required high amounts of GSH, only needed as a Trx backup. This results suggested a new functional role for GSH, which departed from the classical notion of GSH as a major actor in thiol-redox maintenance, having this an important function of GSH in Fe/S cluster biogenesis [118] [119] [120].

1.2.4.2 Glutaredoxins

Grxs are disulphide oxidoreductases that catalyze GSH-dependent thiol-disulphide exchange reactions. They were first discovered by A. Holmgren as GSH-, GR- and NADPH-coupled alternative electron donors for RNR in *E. coli* mutants lacking Trx [121]. They are small and heat stable proteins with a Trx fold (see section 1.2.2), harbouring the same type of Trx motifs: CXXC or CXXS and a *cis*-Pro residue as Trxs do. Similar to Trx, the N-terminal Cys is solvent exposed and has a low pKa whereas the N-terminal Cys is buried and has a higher pKa. Moreover, a lysine proximal to the active site and a GG-motif at the C-region are other typical Grx features required for GSH binding.

In the enzymatic reduction of Grx substrates, two different but functionally connected reaction mechanisms evolved, the dithiol and the monothiol mechanisms. Similar to Trxs,

Grxs are also able to catalyse the reversible reduction of protein disulphides utilizing the Cys residues of their active site. For the dithiol mechanism, the reaction starts with the N-terminal Cys residue performing a nucleophilic attack on the target disulphide (step 1 in **figure 1.9**). Next, the mixed disulphide intermediate formed between the two proteins is attacked by the second thiolate of the active site (step 2 in **figure 1.9**). The resulting disulphide in the active site is reduced by one molecule of GSH, leading to a mixed disulphide between GSH and the N-terminal active site Cys of the Grx (step 3 in **figure 1.9**). This mixed disulphide is subsequently reduced by a second GSH molecule (step 4 in **figure 1.9**). The monothiol mechanism (deglutathionylation) is followed when disulphides formed between GSH and proteins or small molecular weight compounds need to be reduced. This mechanism only requires the N-terminal Cys residue. In this case, the non-GSH molecule is the best leaving group, whereas GSH forms a mixed disulphide with the N-terminal thiol (step 6 in **figure 1.9**). As described for the dithiol mechansim, this disulphide is reduced by a second molecule of GSH (step 4 in **figure 1.9**). The resulting GSSG is then regenerated by glutathione reductase at the expense of NADPH (step 5 in **figure 1.9**) [115].

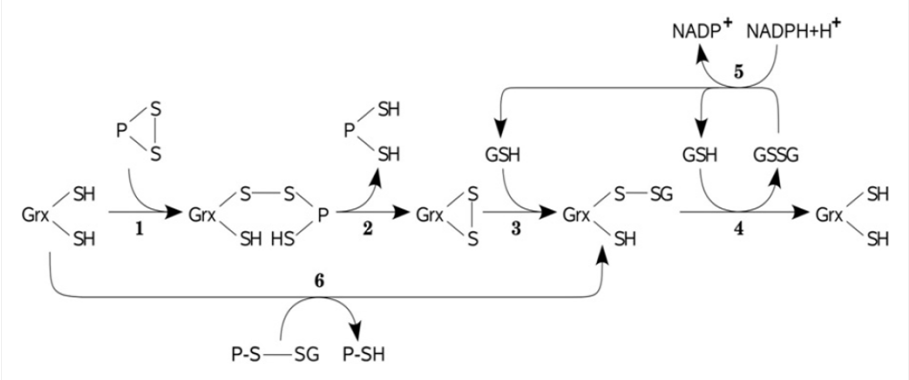

Figure 1.9: Glutaredoxin catalysis. Glutaredoxins catalyse the reversible reduction of protein disulphides utilizing both of their active site Cys residues (reactions 1 to 4). Disulphides between GSH and proteins or low molecular weight compounds are reduced in the monothiol mechanism which only requires the N-terminal active site Cys residue (reactions 6 and 4). In both cases, the GSSG formed in the reaction is reduced by glutathione reductase at the expense of NADPH (reaction 5). Adapted from [115]

Typical dithiol Grxs have a CPYC active site, although some of them, such as the *S. pombe* Grx2, one of the three *Candida albicans* Grxs [122], and also Grx from pig liver [123] and *Vaccinia virus* [124] have the more rare CPFC motif. Human Grx2, instead, contains a CSYC motif, which lowers its dithiol-transferase activity against the standard enzyme substrate β-hydroxyethil disulphide (HEDS), but increases its affinity towards glutathionylated proteins [125] [126]. Monothiol Grxs mostly have a CGFS active site, and they can be classified into two classes: those which harbour a single Grx domain (for instance *S. cerevisiae* Grx5 or *S. pombe* Grx5), and those harbouring an N-terminal Trx domain, including a WAxPC motif, followed by a Grx domain (Trx-Grx class of Grxs) (for instance the nuclear *S. cerevisiae* Grx3 or Grx4 and *S. pombe* Grx4). There are also a

group of monothiol Grxs with some homology to dithiol Grx, which contain a CPxS motif (for instance, CPYS in *S. pombe* Grx3) reminiscent of the dithiol CPYC motif. Many of these proteins contain a N-terminal region suggesting that these proteins are secreted or membrane ancored [122].

Grxs participate as electron donors for proteins such as RNR and PAPS reductase. They are also mediators of the formation and the reduction of mixed disulphides between protein thiols and GSH (glutahionylation), a mechanism which has been proposed for the oxidative stress protection of free thiols in proteins. For instance, upon oxidative stress one of the three isoforms of *S. cerevisiae* glyceraldehyde 3-P dehydrogenase (GAPDH), Tdh3, is glutahionylated, resulting in its reversible inhibition, its activity being restored by the monothiol Grx5 [127] [128]. Grxs are also key players in the cellular iron metabolism, by participating in Fe-S clusters biogenesis and delivery (see Grx5 in section 1.2.4.4), by controlling iron homoeostasis (see Grx4 in section 1.2.4.4), and even some of them are iron containing proteins, such as human Grx2. Grx2 is a Fe-S protein of the Trx fold protein family. It forms a $[2Fe\text{-}2S]^{2+}$ cluster that bridges two Grx2 molecules via two structural Cys residues to form a dimeric holo-Grx2. The [2Fe-2S]-bridged dimer is enzymatically inactive, but GSSG as well as free radicals promote its degradation leading to Grx2 monomerization, and therefore to protein activation. Both GSSG and free radicals are typical oxidative stress conditions, so it was proposed that the Fe-S cluster serves as a redox sensor for Grx2 activation upon oxidative stress [129].

1.2.4.3 Glutathione reductase

Glutathione reductases are enzymes that belong to the flavoprotein family of pyridine nucleotide disulphide oxidoreductases as TrxR. These type of enzymes were already described in section 1.2.3.2 (thioredoxin reductase section).

1.2.4.4 Glutaredoxin system in *S. pombe*

***S. pombe* glutaredoxins** *S. pombe* genome codes for two dithiol Grxs, Grx1 and Grx2, and three monothiol Grxs, Grx3, Grx4 and Grx5 [50].

grx1 and *grx2* genes have four exons and three introns, with additional in-frame start codons, but which code for a single Grx1 of 101 aa and a single Grx2 of 110 aa, respectively. Grx1 harbours a motif CPYC, highly conserved from bacteria to mammals, whereas Grx2 harbours a CPFC motif, rarely found among Grxs, which probably explains the different roles of these proteins in *S. pombe*. Thus, Grx1 is a cytoplasmic protein which accounts for the majority of GSH-dependent oxidoreductase activity of *S. pombe*, and although its deletion is only sensitive to H_2O_2, its expression is induced by H_2O_2, salt, heat shock or stationary phase. Gene induction by H_2O_2 or heat shock is dependent on

Sty1 alone, or on both Atf1 and Pap1 [130]. *grx2* mRNA levels are not induced upon stress (either oxidative, heat or salt), and lack of *grx2* only render cells sligthly sensitive to paraquat. Cells lacking both *grx1* and *grx2* enhance single deletion phenotypes, thus being sensitive to H_2O_2, paraquat and menadione. Cellular localization of Grx2 is also different from Grx1, as Grx2 fused to GFP was found in mitochondria [130] and nucleus [131].

Grx3, Grx4 and Grx5 are monothiol Grxs of 156, 244 and 146 aa respectively. Grx3 is the most distant, it contains a CPYS Grx motif and is localized at the nuclear rim and at the endoplasmic reticulum. Cells lacking *grx3* are not sensitive to oxidants such as H_2O_2, paraquat or diamide, only they are slightly sensitive to cumene hydroperoxide. Grx4 is essential for aerobic growth (it can be isolated under anaerobic conditions), it contains a CGFS Grx motif and a extra N-terminal extension with a Trx domain WAAPCK, which contributes to its nuclear localization. Grx5 also contains a CGFS Grx motif, it is localized in mitochondria, and *Δgrx5* cells are slow growing, sensitive to H_2O_2, paraquat and diamide, unable to grow in non-fermentable carbon sources, display Cys auxotrophy, and these phenotypes are enhanced by a double delete with *grx2*, suggesting some overlapping roles between these two mitochondrial proteins [132].

Grx4 and Grx5 have major roles in iron homeostasis inside the cell. Hence, *Δgrx5* cells are defficient in activities of both mitochondrial and cytoplasmic Fe-S proteins, such as aconitase, succinate dehydrogenase, or sulfite reductase. In fact, Cys auxotrophy was attributed to the lack of activity of sulfite reductase, a Fe-S protein involved in the Cys biosynthetic pathway. Screening of multicopy suppressors of the growth defects of the mutant identified *isa1*, encoding a putative A-type Fe-S scaffold, in addition to *mas5* and *hsc1*, encoding putative chaperones for Fe-S assembly processes. Further search of chaperones and scaffolds complementing cell growh of *Δgrx5* also identified *isa2*. Isa1 and Isa2 physically interacted with Grx5, and their over-expression was able to restore not only the growth defect of *Δgrx5* but also the activities of aconitase, succinate dehydrogenase and sulfite reductase, the latter allowing recovery of Cys prototrophy. On the contrary, Mas5 and Hsc1 over-expression only restored aconitase activity. All these results together suggested a main role of Grx5 in Fe-S clusters delivery for both mitochondrial and cytoplasmic proteins [133]. The *S. cerevisiae* homologue Grx5, is also located at the mitochondrial matrix, its absence activates many genes involved in iron acquisition, provoking an intracellular iron overload [134]. A role in Fe-S clusters maturation was attributed to this protein, either in the transfer of Fe-S clusters to apo-proteins [135] or in the initial assembly of Fe-S clusters into scaffold proteins [136] [122].

The role of Grx4 in *S. pombe* iron homeostasis was characterized in more detail. In this organism, Fep1 and Php4 are the key regulators of iron homeostasis, as they control iron acquisition and iron utilization, respectively. Upon high iron concentrations, Fep1, a GATA type transcription factor, represses the expression of several genes involved in iron uptake (*frp1*, *fio1*, *fip1*, *str1/2/3*, *abc3*, *php4*). However, when the availability of iron is limited, Fep1 fails to act as a repressor resulting in iron uptake. The CCAAT-binding

subunit Php4 downregulates the expression of up to 86 genes involved in iron requiring metabolic pathways, such as the tricarboxylic acid (TCA) cycle, the electron transport chain, and the Fe-S cluster biogenesis machinery, through recognition of the CCAAT-binding complex, which is composed of Php2, Php3, and Php5. The Php2/Php3/Php5 heterotrimer binds CCAAT *cis*-acting elements, whereas Php4 lacks DNA-binding activity. Php4 is responsible for the capability of the Php complex to repress transcription in response to iron starvation. At the same time, *fep1* is regulated by Php4, creating a reciprocal regulatory loop between both iron-responsive sensors ([137] and references herein). Grx4 physically interacts with both iron regulators Fep1 and Php4, in an iron-independent manner (constitutively) through its Trx domain (Cys35 required), and in an iron-dependent manner through its Grx domain (Cys172 required). Thus, under iron-replete conditions, the Grx domain of Grx4 exerts an iron-dependent inhibitory effect on Php4, what leads to Php4 inactivation and up-regulation of iron utilization genes. Moreover, in the transition from low to high iron concentrations, Php4 travelled from the nucleus to the cytosol in a Crm1 and Grx4-dependent processes. On the contrary, under iron-deplete conditions, Grx4 exerts an inhibitory effect on Fep1, which leads to de-repression of Fep1-dependent genes involved in iron acquisition. In this case, the Grx domain of Grx4 associates with the N-terminal region of Fep1, what probably leads to a conformational change and Fep1-chromatin dissociation [138] [139] [137] [140].

Similarly than in *S. pombe*, *S. cerevisiae* Grx3 and Grx4 (Trx-Grx class of Grxs) are required for Aft1-mediated iron regulation. *S. cerevisiae* Aft1 is a transcriptional factor that is activated in iron-deficient cells regulationg iron uptake and homeostasis. Thus, *S. cerevisiae* mutant cells lacking both Grx3 and Grx4 displayed constitutive expression of genes involved in iron homeostasis. To accomplish their role, both Grxs physically interact with Aft1 and the Cys residue of the CGFS sequence in the Grx domain is crucial for such regulation [141] [122].

Glutathione reductase in *S. pombe* *S. pombe* glutathione reductase or Pgr1 is mainly a mitochondrial protein of 465 aa (although it can be also found in the cytosol), that when over-expressed confers cells with some resistance to menadione, but not to oxidative stress by H_2O_2. *pgr1* expression is increased by menadione, cumene hydroperoxide, diamide, osmolarity, heat shock and stationary phase, in a Pap1-dependent manner. Pgr1 is required for the aerobic growth of *S. pombe*, and its deletion was not complemented by increasing GSH or N-acetyl-cysteine levels [142], although over-expression of the mitochondrial protein Trx2 was able to restore some of the phenotypes caused by a conditionally deleted *pgr1*. Cells with low levels of Pgr1 arrested at G1 phase, accumulated GSSG, causing a $\sim$ 50-fold reduction of the GSH/GSSG ratio, had reduced respiration rates (3 to 4 fold), and had almost completely lack of activity of both mitochondrial (aconitase) and cytoplasmic (sulfite reductase) Fe-S cluster proteins, concomitantly with a 7-fold increase in iron concentrations. These results together suggested that the main reason for the growth defect caused by *pgr1* depletion is the lost of oxidation-sensitive Fe-S protein activities in both

mitochondria and cytosol [100].

1.2.5 Overlapping functions of the Trx and GSH/Grx systems

Trx and GSH/Grx systems are key mediators of electron flow. These systems are thermodinamically linked by the ultimate electron donor inside the cell, NADPH (redox potential of -315 mV), and transfer the electrons from this metabolite to their final substrates through gradients in redox potentials. In many cases, Trxs and Grxs can substitute for each other in their enzymatic processes, being largely redundant.

1.2.5.1 *E. coli*

In *E. coli*, the GSH/Grx system is composed of the enzymes required for GSH biosynthesis, coded by *gshA* (rate-limiting) and *gshB*, glutathione reductase coded by *gor*, three dithiol Grxs coded by *grxA*, *grxB* and *grxC*, one monothiol Grx coded by *grxD* and a Grx-like protein coded by *nrdH*, whereas the Trx system is formed by two Trxs coded by *trxA* and *trxC* and one TrxR coded by *trxB* [143]. The only essential member of the previously mentioned genes is *grxD*, coding for Grx4, highly homologue with *Sc*Grx5, which, as mentioned above, has a function related with Fe-S cluster assembly [144] [145]. Grx4 in its reduced form contains three thiols, and treatment with GSSG resulted in glutathionylation and formation of a disulphide. Remarkably, this disulphide of Grx4 was a direct substrate for TrxR, whereas the mixed disulphide was reduced by Grx1.

For the rest of the components of the Trx and GSH/Grx systems, only mutants lacking enzymes of both pathways are not viable, suggesting overlapping roles between them. Thus, double mutants *trxA grxA* or *trxA gshA* on minimal media or in low Cys concentrations are inviable as a consequence of accumulation of PAPS, a toxic metabolite from the sulphate assimilation pathway (see section 1.2.6.4), suggesting that both TrxA and GrxA are required for PAPS reductase reduction. Consistently, this lethal phenotype could be restored by increasing extracellular sulphate concentrations or by deleting *cysA* or *cysC*, which repress or inactivate the sulphate assimilation pathway, respectively [146].

E. coli encodes three types of RNRs (see section 1.2.6.3). RNRI (NrdAB, class Ia), the only functional enzyme during the aerobic growth of *E. coli* [147], is reduced *in vitro* and *in vivo* by TrxA, TrxC and GrxA [148] [149]. Double or triple *E. coli* deletes *trxA trxC grxA*, *trxB gshA*, *trxB gor*, *trxA trxC gshA* are aerobically inviable as consequence of defective RNR reduction, suggesting that TrxA, TrxC and GrxA are alternative electron donors for RNRI.

E. coli OxyR and Hsp33 reduction are other processes where both Trx and GSH/Grx systems overlap. OxyR is a transcription factor, which acts as a redox sensor to control the induction of antioxidant genes upon oxidative stress. It is inactive when it is reduced, but

upon formation of a disulphide or glutathionylation it exerts its function and triggers an antioxidant response. When the oxidative stress is diminished, both TrxA and GrxA reduce the generated disulphide, although only GrxA is able to catalyse deglutathionylation [150] [151]. Hsp33 is a chaperone regulated by thiol-disulphide exchange. When it is a monomer, it has low chaperone activity, but under oxidative stress it forms a homodimer through a disulphide bond, being then able to bind unfolded proteins. Again, this homodimer can be reduced and deactivated by Trx and GSH/Grx systems [152] [153].

1.2.5.2 *S. cerevisiae*

In yeast, GSH is indispensable by itself, independently of the Trx pathway, contrasting with *E. coli* (or at least this still considered in the literature in spite of characterization of *E. coli* Grx4, see above section 1.2.5.1). Thus, *S. cerevisiae* mutants lacking the rate-limiting enzyme in the GSH biosynthetic pathway (*Δgsh1*) are inviable unless some external GSH is provided [154]. The cause of lethality is not related to reduction of substrates, since a *grx1 grx2* double mutant is viable, but to defects related to iron homoeostasis and metabolism [119] [120]. However, lack of glutathione reductase (*Δglr1*) is dispensable (this is not the case in *S. pombe*, see section 1.2.4.4). This mutant has accumulated levels of oxidized GSSG, but it also has enough levels of GSH to support cell growth [155]. Since Glr1 is the only glutathione reductase of *S. cerevisiae*, the presence of reduced GSH in this mutant is suggestive of an alternative GSSG reducing system. In a recent work, this role was attributed to the Trx system. Thus, Glr1 activity was required for the survival of a *trx1 trx2* mutant, moreover over-expression of Trx1 and Trx2 in a *glr1* mutant diminished the amount of GSSG and increased the amount of GSH, and the contrary, deletion of *trx1* and *trx2* increased GSSG and decreased GSH [156]. These results are in concordance with those showed in a report in *Drosophila melanogaster*, in which a genuine GR is absent, being GSSG reduced by TrxR through *Dm*Trx2 [157].

S. cerevisiae lacking either cytoplasmic Trx (Trx1 or Trx2) have no appartent phenotype, but *Δtrx1 Δtrx2* mutants have an extended S-phase, a lower pool of deoxyribonucleotides and an increased fraction of oxidized RNR. Nevertheless, these mutants are still viable, suggesting a role for the GSH pathway in (inefficient) RNR reduction. Hence, a cuadruple mutant lacking both cytoplasmic Trxs and both cytoplasmic Grxs (*trx1 trx2 grx1 grx2*) was inviable [158] [159] [160]. Also, *S. cerevisiae Δtrx1 Δtrx2* is auxotroph for sulphur aminoacids, suggesting an exclusive role for the cytoplasmic Trxs in reducing PAPS reductase [159]. Regarding this aspect, there is a work suggesting that in a low oxygen atmosphere or in the absence of functional mitochondria, PAPS reductase can be also inefficiently reduced by means of the GSH/Grx pathway [158].

1.2.5.3 Higher eukaryotes

Human *GRX2*, coding for both a mitochondrial and a nuclear Grx2, depending on the transcribed exons, is another particular case where Trx and GSH/Grx systems overlap. Grx2, a monthiol Grx with an atypical CSYC motif (see section 1.2.4.2), is the first characterized Fe-S protein member within the Trx fold family (see section 1.2.4.2). Grx2 has three Cys, which upon oxidation can form an intra-molecular disulphide bond as well as a mixed disulphide with GSH. The particularity of Grx2 is that both the intra-molecular disulphide and the mixed disulphide are not only substrates of GSH but also substrates of mammalian TrxR (mitochondrial and cytoplasmic). At sufficiently oxidative stress conditions, where mitochondrial GSH is consumed or effluxed, the presence of TrxR as an alternative reducing system might help in rescuing the redox balance, avoiding blocking of the mitochondrial electron transport chain and apoptosis [126].

1.2.6 Thioredoxin and glutaredoxin substrates

1.2.6.1 Peroxiredoxins

Peroxiredoxins (Prxs) are a ubiquitous family of proteins, highly expressed in cells (up to 1% of total protein [9]), that function not only as major antioxidant enzymes but also as mediators of H_2O_2 signalling in eukaryotes [161]. Differently than in other types of peroxidases (heme peroxidases) that imply substrate-metal binding, Prxs use a mechanism of nucleophilic substitution type 2 (SN_2) where a thiolate reduces, with high order rates ($\sim 10^7$ M^{-1} s^{-1}) and high specificity, peroxide substrates. Thus, under normal cellular conditions, eukaryotic Prxs are responsible of detoxifying 90% of mitochondrial H_2O_2 [162] and almost 100% of cytoplasmic H_2O_2. This can be explained in other words, in mammalian cells, 10000 times more H_2O_2 would react with Prxs before it can react with GSH [9].

All Prxs have in common an universally conserved PXXXTXXC$_P$ motif, at their catalytic site, which closely resembles a Trx fold (in fact, evidence suggest that Prxs have evolved from a Trx-like precursor, being the only difference between the Trx fold the Prx motif a Tyr replacing the catalytic Cys in the former [162]). The mode of catalysis is also common in Prxs, including a conformational step, as well as at least three chemical steps (**figure 1.10**). Thus, in the first step of the catalytic cycle, the peroxide substrate (either an alkyl hydroperoxide or H_2O_2) enters the fully-folded (FF) conformation of the substrate binding pocket, where it directly reacts with the thiolate of the peroxidatic Cys (C$_P$) (step 1 in **figure 1.10**). In this way, the peroxide becomes reduced to its corresponding alcohol and C$_p$ is oxidized to a sulphenic acid form (S$_P$OH). In the second step (step 2 in **figure 1.10**), or the resolution step, a free 'resolving' thiol (S$_R$H), either present in the same or in another subunit of the Prx, attacks the S$_P$OH to form a disulphide and release water.

Because C_P is hidden inside the active site pocket in the FF conformation, to make it more accesible and allow disulphide formation, it is necessary, at least, local unfolding of the active site. Once the disulphide is formed, it remains locked in this local unfolded (LU) conformation until recycling (step three in **figure 1.10**). In this third step, the disulphide is reduced to regenerate free thiols in C_P and C_R and the Prx is freed again to adopt the FF conformation, completing in this way the catalytic cycle. Recycling requires a protein or small molecule thiols, but for most Prxs this step involves a Trx-like protein or domain [163].

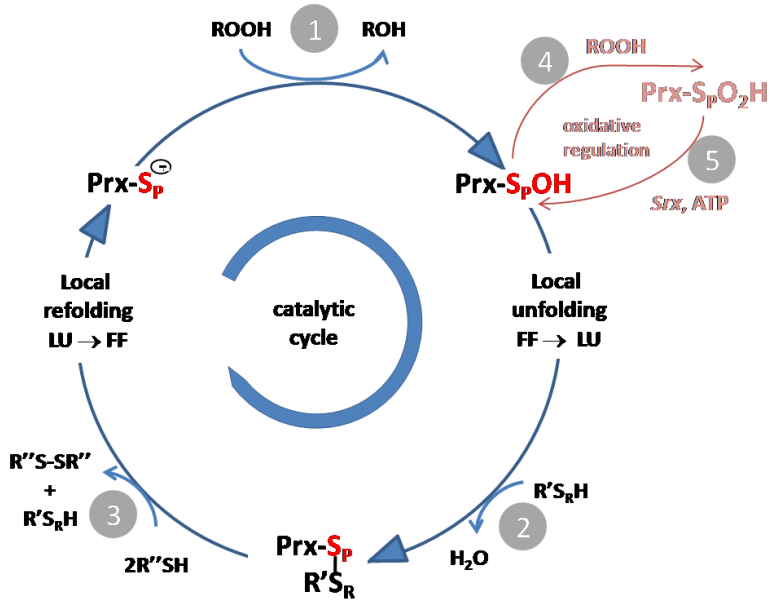

Figure 1.10: The catalytic cycle of peroxiredoxins. Adapted from [162], see text for details

.

In competition with the resolution step, there is an over oxidation reaction (steps 4 and 5 in **figure 1.10**). In this reaction, S_POH, in the FF conformation, can react with more peroxide molecules to form sulphinic (S_PO_2H) or sulphonic (S_PO_3H) acids. These over oxidized forms render an inactive enzyme, although S_PO_2H can be recycled by sulfiredoxins to S_POH, at the expense of ATP consumption. It has been suggested that this inactivation may have an important role in peroxide signal transduction [163].

Why Prxs are such effective catalyts? In order to find an explanation for the high catalytic rates of Prxs towards peroxide substrates, it is necessary to explore the structure and conformation of their catalytic active-site. As mentioned above, the catalytic cycle of Prxs starts with a nucleophilic attack of the thiolate of C_P on the peroxide substrate. For this to happen, C_P needs to be a good nucleophile. At neutral pH, pK_a values below 7 increase thiolate availability and thus increase nucleophilicity (although this is only truth

for a very tight range of pH, once the thiolate is formed, its nucleophilicity decreases as its pK_a is lowered [90]). Hydrogen-bond interactions, at the Prxs active-site, stabilize the thiolate and render pK_a values below 7 [162]. One could expect the thiolate to be one of the major contributors in Prxs reactivity, nevertheless studies based on small molecule thiols, indicate that the lowered pK_a at the active-site can only account for rates around 20 $M^{-1}s^{-1}$, leaving unexplained enhanced rates of 10^5 to 10^7. For catalysis, more important than interactions between enzyme and substrate is the stabilization of the transition state of the reaction. Hall A. *et al* [162] proposed, based on all known structures of Prxs-substrate complexes up to 2011, a model for the conformation of the active-site at the transition-state, which could truly explain the high catalytic rates of Prxs towards their substrates. Thus, they show how the Prx active-site is perfectly organized to stabilize the transition state, which would have a partial bond formed between the S_P and one of the oxygens of ROOH, and a partial bond broken between both oxygens of ROOH. In fact, the important contributions to catalysis of the active-site are both the activation of C_P as a potent nucleophile and the activation of the peroxide itslef to be attacked.

Prx families and classification Although a single Prx contains at their active-site all necessary residues required for catalysis, only one Prx, the BCP from *S. cerevisiae*, is monomeric. The remaining Prxs have quaternary structures that include two distinct types of dimers (A-type and B-type interfaces) as well as octamers, decamers and dodecamers. So far, Prxs are classified as members of PrxI, PrxV, PrxVI, Tpx, BCP and AhpE subfamilies, and in brief, known members of PrxI and PrxVI subfamilies form B-type dimers, with most oligomerizing to decamers through the A-type interface, known members of PrxV, Tpx and AhpE subfamilies only form A-type dimers, and BCP subfamily members exist either as monomers or as A-type dimers [162]. Oligomerization is a dynamic process, and dimers and decamers exist in an equilibrium, *in vivo* mainly affected by the redox state and phosphorylation. The physiological role of this process is still not understood, but there is a link between decamer assembly and the catalytic cicle. Studies with the alkyl hydroperoxide reductase C (AhpC) from *Salmonella typhimurium* showed that the decameric form is stabilized in all redox states of the Prx (S_PH, S_POH, S_PO_2H and S_PO_3H) but in the disulphide form. In the latter, the unfolding of the C_P loop destabilizes the decamer-building interactions yielding more stable dimers. Mutations in the AhpC designed to weaken the decameric formation were 100-fold less active than wild-type enzymes, solely due to a K_m effect [162] [161] [164].

Independently of the subfamily in which Prxs are classified, these can be referred as 1-Cys peroxiredoxins, if the resolving Cys belongs to a small molecule or a second protein, or as 2-Cys peroxiredoxins if the resolving Cys comes from within the Prx (atypical 2-Cys peroxiredoxins) or from another Prx chain in the dimer (typical 2-Cys peroxiredoxins). All members of PrxI and PrxVI families are typical 2-Cys peroxiredoxins, whereas members of the remaining subfamilies are either 1-Cys or 2-Cys peroxiredoxins [161].

Robust and sensitive 2-Cys peroxiredoxins A typical characteristic, mainly of some typical eukaryotic 2-Cys peroxiredoxins, is their high susceptibility to hyperoxidation (see above in section 1.2.6.1 and step 4 of **figure 1.10**). For human PrxI, it has been shown that at 100 μM H_2O_2, the half-life for inactivation during the catalytic cycle is about 2 min, and kinetic analysis at low steady-state levels of H_2O_2 ($<$1 μM) indicated that the enzyme was hyperoxidized at a rate of 0.072% per turnover at 30°C. Curiously, the presence of H_2O_2 alone was not sufficient to induce the *in vitro* hyperoxidation of PrxI, rather all catalytic components (H_2O_2, Trx, and TrxR) were required [165].

In contrast with these "sensitive" Prxs, some other members of the typical 2-Cys Prxs, for instance *S. typhimurium* AhpC, are more "robust", requiring at least 100-fold more concentration of H_2O_2 for being inactivated. Wood Z.A. *et al* [166] compared the sequences and structures of sensitive *vs* robust 2-Cys Prxs and found that sensitive 2-Cys Prxs harbour a conserved GGLG motif and a C-terminal extension associated with a conserved Tyr-Phe sequence, the YF motif. Hyperoxidation appears to occur when the disulphide formation between C_P and C_R ($\sim$ 13 Å apart) is slow enough to allow the reaction of C_PSOH with peroxide. The YF motif, which is not part of the peroxidatic active site itself, forms a helix that packs above the active site in the FF conformation of the protein limiting the active-site dynamics hindering it from unfolding, therefore disfavouring the resolving reaction (step 2 in **figure 1.10**) and making the C_PSOH longer lived and more susceptible to attack by another H_2O_2 molecule [166] [161] [167]. As an example, the sensitive typical 2-Cys peroxiredoxin Tpx1 from *S. pombe*, lacking the C-terminal part of the protein, resulted insensitive to inactivation by H_2O_2, although it is worth mentioning that it also lowers the Km for H_2O_2 [168]. What remains to be explained is why a C169S mutant of the same protein, *S. pombe* Tpx1, is not prone to hyperoxidation. The reason for the GGLG motif is less clear, but it is thought to be required for rescuing the sulphinic form, by forming part of the ATP binding site, in the sulfiredoxin-dependent reduction [161].

Physiological roles of hyperoxidized 2-Cys peroxiredoxins Prxs over-oxidation seems to have been selected during evolution to serve to some purpose. Different roles have been attributed to over-oxidized 2-Cys peroxiredoxins, being probably, one of the most important, their involvement in cellular signalling pathways.

In *S. pombe*, the peroxiredoxin Tpx1 is the major intracellular scavenger of H_2O_2, as it is essential for aerobic growth, it is highly abundant (0.1-1% of total soluble protein) and it has high affinity for its substrate (K_m 2 μM) [52]. Although it can inefficiently work as a 1-Cys peroxiredoxin (a mutant of Cys_R to Ser is able to grow under aerobic conditions), it is classified as a typical 2-Cys Prx, belonging to the subfamily PrxI, which is inactivated at doses of 1 mM H_2O_2 [169]. In *S. pombe*, at least two independent pathways are activated depending on the intracellular concentrations of H_2O_2: the Pap1 and the Sty1 pathways (see **figure 1.11**). At low H_2O_2 concentrations, the AP-1-like transcription factor Pap1

triggers a specific antioxidant gene response; thus, H_2O_2 promotes the formation of an intra-molecular disulphide bond between distant Cys residues, masking the accessibility of the nuclear exporter Crm1 to the Pap1 C-terminal nuclear export signal, resulting in its nuclear accumulation and in Pap1-dependent gene expression. Nevertheless, H_2O_2 does not directly oxidise Pap1 Cys residues, rather Tpx1 is oxidized to form a disulphide between C_P and C_R and then, by a mechanism still not understood, transfers the oxidation state to Pap1 [169]. In this case, Tpx1 is working as an upstream sensor of H_2O_2, being essential for the up-regulation of the Pap1 transcriptional activity. On the contrary, the MAPK Sty1, which can also be activated by other types of stresses, such as heat shock, nutritional starvation or osmotic stress, preferentially responds to higher doses of H_2O_2 ($\sim$ 1 mM H_2O_2) [56], doses at which Tpx1 is over-oxidized. In this case, Sty1 becomes phosphorylated, accumulates in the nucleus and phosphorilates, among others, its main substrate, the transcription factor Atf1 [74], which then binds to a wide number of promoters and up-regulates their gene products in response to stress. Therefore, as the adaptative response of Pap1 is being inactivated (or delayed), the survival response triggered by Sty1 is being activated at 1 mM H_2O_2. The sulfiredoxin Srx1 is one of the gene products which are induced upon Sty1-Atf1 pathway activation, and as a result, Tpx1 sulphinic form is eventually reduced to its peroxidatic active form, which in turn lowers the intracellular H_2O_2 concentration, yielding the Pap1 pathway active again. In this regard, a strain lacking Srx1 is not able to reduce over-oxidized Tpx1 and therefore to reactivate the Pap1 pathway upon 1 mM H_2O_2 stress [169]. Thus, H_2O_2, by influencing in the redox state of Tpx1, is a key messenger in the regulation of the two independent transcription pathways.

Additionally, it was suggested that Tpx1 was required for the peroxide-induced activation of Sty1. In this report, it was shown that Tpx1 activated Sty1, downstream of previously identified redox sensors, by a mechanism involving formation of a peroxide-induced disulphide complex between Tpx1 and Sty1 [170].

Other proposed role for *S. pombe* hyperoxidized Tpx1 is related with maintenance of Trx activity and cell viability under conditions of oxidative stress. Under low oxidative stress conditions, Tpx1, the main *S. pombe* Trx1 substrate competitively inhibits Trx-mediated reduction of other oxidized proteins. However, upon higher oxidative stress, Tpx1 becomes hyperoxidized, no longer being a Trx1 substrate. This allows Trx1 to act on other substrates, therefore ensuring repair of other oxidized proteins [171].

Finally, other suggested role of over oxidized Prxs, not linked with peroxide-driven signal transduction pathways, is their function as molecular chaperones. In fact, as mentioned above, in section 1.2.6.1, sulphinic forms of the enzyme favour higher olimeric states, such as decamers, which can further aggregate under oxidative stress situations, exhibiting enhanced chaperone and super-chaperone activities [167].

Electron donors of Prxs Although other thiol-containing electron donors, such as GSH or GSH transferase π [172] [173] can recycle oxidized Prx, this process is usually driven

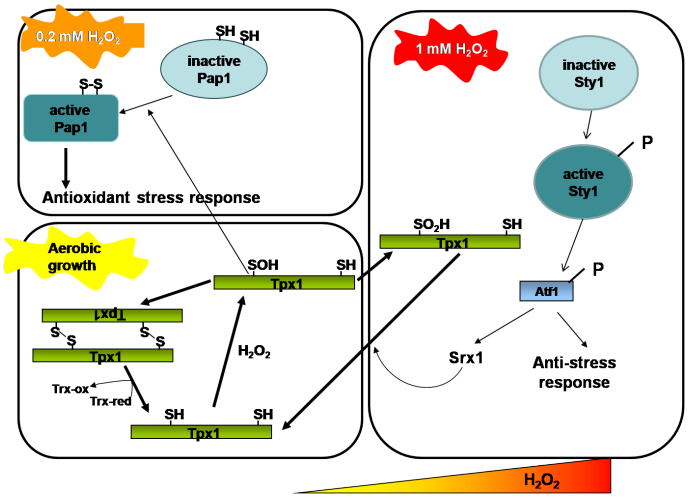

Figure 1.11: *S. pombe* Tpx1 key messenger upon H_2O_2 stress. At low H_2O_2 concentrations (0.2 mM H_2O_2), Tpx1 is oxidized to form an inter-molecular disulphide and then, by a mechanism still not understood, transfers the oxidation state to Pap1. On the contrary, the MAPK Sty1 preferentially responds to higher doses of H_2O_2 ($\sim$ 1 mM H_2O_2), doses at which Tpx1 is over oxidized and the Pap1 pathway is inactive. The sulfiredoxin Srx1 is one of the gene products which are induced upon Sty1-Atf1 pathway activation. As a result, Tpx1 sulphinic is eventually reduced to its peroxidatic active form, which in turn lowers the intracellular H_2O_2 concentration, yielding the Pap1 pathway active again. Adapted from [169]

.

by Trx. There is not too much known about how Trx approaches and engages the Prxs since there is only one crystallised structure with both proteins complexed, the *S. cerevisiae* alkyl hydroperoxide reductase Ahp1 complexed with Trx2 [174]. Ahp1 is a typical 2-Cys peroxiredoxin that belongs to the PrxV subfamily, which has the peroxidatic Cys (Cys-62) extraneously positioned, in the primary sequence, after the resolving Cys (Cys-31). It exists as a dimer in solution and reduces organic hydroperoxides, such as *t*-butyl hydroperoxide (*t*-BOOH) more efficiently than H_2O_2. At the stage of Ahp1 regeneration, the Cys-31 of the inter-molecular disulphide bond (Cys-62-Cys-31) in the dimer is subjected to attack by Cys-31 of Trx2. Probably, two Trx2 molecules attack the dimeric Ahp1 from both sides at the same time. The interface between the Ahp1 dimer and the Trx2 monomer buries a total surface area of 1200 Å, typical from short-lived complexes, with four main-chain hydrogen bonds, conserved among previously reported Trx2-complexed structures [174].

Peroxiredoxins and specificity in redox signalling Oxidation and reduction of thiol proteins is one of the main mechanisms by which ROS integrate into cellular signalling pathways. To meet signalling criteria it is necessary to preferentially oxidise a specific subset of proteins, in a fast and reversible way. Several are the proposed mechanisms for redox regulation (**figure 1.12**). One is based on the thermodynamic principle that all thiol/disulphide couples are in equilibrium, with the ratio of the oxidized to reduced forms determined by the redox potential of the cell. Thus, changes in the GSH/GSSG

ratio would lead to re-equilibration of the rest of the thiol/disulphide couples. However, direct thiol/disulphide exchange is slow and, as previously mentioned (section 1.2.1), equilibrium does not necessarily reflect thiol/disulphide status of the proteins, making this mechanism unreliable for signal transduction. Other proposed mechanism is a more specific cellular response to an oxidant, based on the kinetic properties of few sensitive targets. These proteins would be transiently oxidized to allow signal transmission, and then enzymatically reduced to their basal oxidation state. Thus, the existence of proteins with different oxidant sensitivities would enable the activation of different pathways depending on the oxidant exposure. A handicap for this mechanism would be that these thiols must be sufficiently reactive to undergo oxidation in the presence of cellular antioxidants, or competing antioxidants must be depleted before oxidation of the target occurs. A third proposed mechanism, a variation of the former, relies on the presence of very reactive thiol proteins, called sensor proteins, that once oxidized would facilitate the oxidation of other target proteins through selective protein-protein interactions and thiol exchange. According to this last proposed mechanism of signal transduction, Prxs, due to their low pK_a, their constant rates and their ubiquity and abundance, would be the only cellular thiol proteins with enough reactivity for being direct targets of H_2O_2, and therefore behaving as sensor proteins which act in signalling cascades [29].

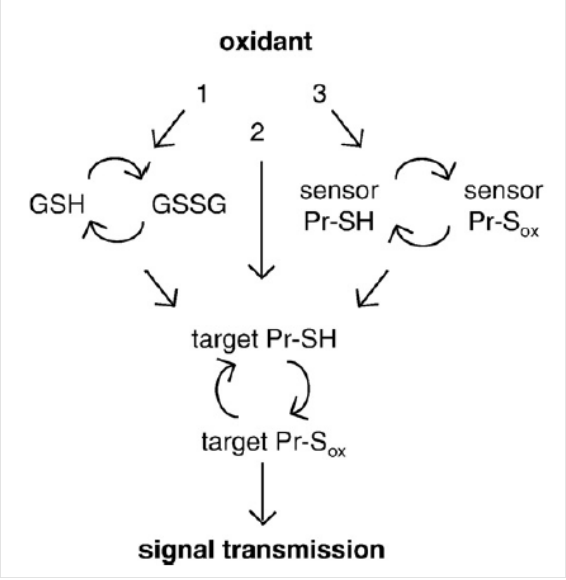

Figure 1.12: General mechanisms of redox signalling. (1) Alterations in cellular redox buffers such as GSH may result in oxidation of thiol proteins depending on the redox potential of target Cys. (2) The local environment of specific target Cys considerably enhances their reactivity to the oxidant. (3) Extremely reactive sensor proteins scavenge the signalling oxidant and then facilitate the oxidation of target proteins through specific protein interactions and thiol transfer reactions. Reprinted from [29].

1.2.6.2 Methionine sulphoxide reductases

Methionine sulphoxide reductases (Msrs) are enzymes ubiquitously distributed in nature [175], which activity consists on reducing methionine sulphoxide Met-O to methionine (Met) inside cells. Met, either free in the cell or bound to proteins, is one of the amino acids more readily oxidized by ROS. When exposed to mild oxidizing conditions, a mixture of two enantiomers of Met-O are formed, *L*-methionine-*S*-sulphoxide (Met-*S*-O) and *L*-methionine-*R*-sulphoxide (Met-*R*-O), which can be further oxidized to Met sulphone if stronger oxidizing conditions are applied [176].

Met-*S*-O and Met-*R*-O can be enzymatically reduced to Met, with the help of an electron donor such as Trx, through the action of Msrs. It is now known that at least two different enzymatic activities are required to reduce each of the Met(O) enantiomers. Thus, Msrs type A (MsrA) reduce Met-*S*-O [177] whereas Msrs type B (MsrB) reduce the *R* enantiomer [178] [179]. In some cases, such as in the *Neisseria gonorrhoeae* PilB protein, both activities are fused in tandem (MsrA/B). Moreover, in this particular case, a Trx-like domain is also located at the N-terminus of the protein [178].

MsrA and MsrB are separately conserved across life kingdoms and are structurally unrelated [175], nevertheless both have signature Cys-containing motifs (GCFWG in MsrA [177] and RXCXN near the C-terminus of MsrB [178]) required for their similar catalytic mechanism (**figure 1.13**). Thus, in the first step of this mechanism, the catalytic Cys of the Msrs nucleophillically attacks on the sulphur atom of the Met(O) leading to the formation of a sulphenic acid intermediate, with the concomitant release of Met. Then, the recycling Cys nucleophillically attacks on the sulphenic acid intermediate and an intra molecular disulphide is formed, with the release of a water molecule. Finally, return of the active site to a fully reduced state happens with the reduction of the Msr disulphide bond by reduced Trx or Grx [180] [181] [182] [183].

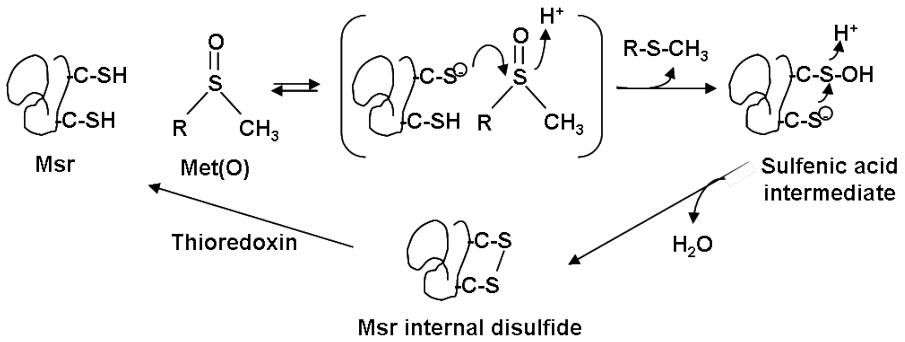

Figure 1.13: Msrs catalytic mechanism. See text for details

Methionine sulphoxide reductases and oxidative stress Reversible oxidation of Met in proteins has been suggested i) to be a mechanism for modulating protein activity, and

therefore for cellular regulation (providing there is a specific Met oxidase, a role that has been also suggested for MsrA [184]), ii) to be an efficient mechanism for ROS scavenging (surface exposed Met residues can be easily oxidized, without significant changes in protein activity, and protect other internal residues of further oxidation [185]), or iii) to alter the properties of the protein such as function, activity, structure or degradation resistance (reviewed in [186]). Consequently, Msrs, by reducing Met(O), may act i) as modulators of cell signalling, ii) as antioxidant enzymes or iii) as repairing enzymes.

The role of MsrA acting as a repairing enzyme was first published in the 80's. In this work it was reported an activity able to restore *in vitro* the biological activity of the *E. coli* ribosomal protein L12 when some internal Met(O) residues were reduced to Met. This enzymatic activity was initially called 'peptide methionine sulphoxide reductase' [187], now called MsrA, to differentiate it from other previously reported activities able to reduce Met(O) [188] [189] which could only use free Met(O) as a substrate.

MsrA acting as an antioxidant enzyme was consistently demonstrated in several works. Thus, an *E. coli* strain deleted in the *msrA* gene survived worse than a wild type strain upon H_2O_2 [190]. Also, a *S. cerevisiae* strain lacking MsrA showed higher sensitivity to 1 mM of H_2O_2 than a wild type strain in liquid cultures and accumulated Met(O), both free and in proteins [191]. Flies, human T cells and yeast over expressing MsrA survived better than their wild types when treated with the same oxidant [192] [193]. Mice lacking the *msrA* genes exhibited a neurological disorder in the form of ataxia ("tip toe walking"), shortened their life span, presented higher sensitivity to oxidative stress and were less able to up regulate TrxR under stress conditions [194], also suggesting a role for this enzyme in ageing and neurodegenerative disorders.

The participation of Msrs (or the reversible Met oxidation-reduction) on cell signalling and regulation is less clear, although it is an idea that has been frequently postulated. The pre-requisite would be the presence of a stereospecific Met oxidase. Regarding this issue, there is only a very recent work reporting MsrA not only working as a Met(O)reductase, but also as a stereospecific Met oxidase, able to catalyse its own auto-oxidation as well as oxidation of Met, both free and in proteins [184].

Msrs type B have been less studied and their role in protecting cells from oxidative stress is less clear. The first work presenting Met-*R*-O as a substrate for MsrB dates from 2002, in a study in bacteria [178]. Nevertheless, this activity resulted important only to reduce Met-*R*-O in proteins and not free Met-*R*-O [179]. To reduce the latter, a structurally unrelated MsrB protein (called free MsrB) was later found, although resulted an enzyme not very widely distributed among species [195] [196]. In fact, MsrB is not as ubiquitous as MsrA, what may suggest, apart from the unexpected biological bias towards one of the epimers of Met(O) [175] (Met ROS oxidation should lead to the same amount of both enantiomers), MsrB being less important for the antioxidant defences in cells.

In *S. pombe*, putative MsrA and MsrB can be found by sequence homology (free

MsrB seems to be absent), but the role of these proteins in the antioxidant defence, as repairing enzymes or as modulators of cell signalling, still remains to be characterized.

1.2.6.3 Ribonucleotide reductases

Ribonucleotide reductases (RNRs) are the enzymes that catalyse the conversion of ribonucleotides to their 2'-deoxyribonucleotide counterparts (dNTPs), providing the precursors needed for DNA synthesis and repair. dNTPs pools need to be very tightly controlled since mutation rates increase hugely if the levels of the four dNTPs are either unbalanced or too high. Since RNRs are main players in this homoeostasis, they are highly regulated by allosteric and transcriptional control, by protein-protein interactions and by subunit compartmentation.

Three main classes of RNR enzymes have been discovered depending on the different metal cofactors required for their catalytic activity. However, all three classes have in common a conserved Cys residue at their active site which is converted into a thiyl radical. The function of the thiyl radical is to abstract an H from the 3'-carbon of the ribose ring, generating in this way a substrate radical [197].

Class I enzymes are oxygen-dependent, ubiquitously distributed, they contain a diiron-oxygen cluster (Fe-O-Fe), and they are further divided into two classes (Ia and Ib), depending on their polypeptide sequence and allosteric regulation [198]. Class Ia enzymes exist in eukaryotes, prokaryotes, viruses, and bacteriophages, whereas class Ib enzymes have been found only in prokaryotes. Both classes are tetrameric enzymes $\alpha_2\beta_2$. The substrate binding active site is located in the large α_2 homodimer which is called R1. The small β_2 homodimer contains a binding site for two iron ions in each polypeptide chain and is called R2. In the active form, these R2 proteins contain a stable tyrosil radical close to the iron centres. Class II enzymes are found in facultative anaerobic bacteria and also in some of their phages. They utilize adenosylcobalamin, a vitamin B12 derivative, which directly interacts with the active site Cys to form the thiyl radical needed for ribonucleotide reduction. Finally, class III enzymes are found in strict or facultative anaerobic bacteria and some bacteriophages. The large α_2 subunit contains the active and allosteric sites and the smaller β_2 subunit, or the activase, carries a 4Fe-4S cluster, which reacts with S-adenosylmethionine (SAM), and generates a glycyl radical in the large subunit. This glycyl radical is then able to generate the thyil radical at the active site when the right set of allosteric activators and substrates are bound (reviewed in [117]).

RNR catalytic mechanism and regeneration Although the generation of the thyil radical differs among the RNRs, once it is formed the reaction mechanisms of class I and II RNRs are quite similar. The more studied is class I RNR of *E. coli* (**figure 1.14**). The thyil radical on the conserved C439 abstracts a hydrogen atom from the 3'-carbon of the ribose ring generating a substrate radical. The ribose radical makes its 2'-OH group more

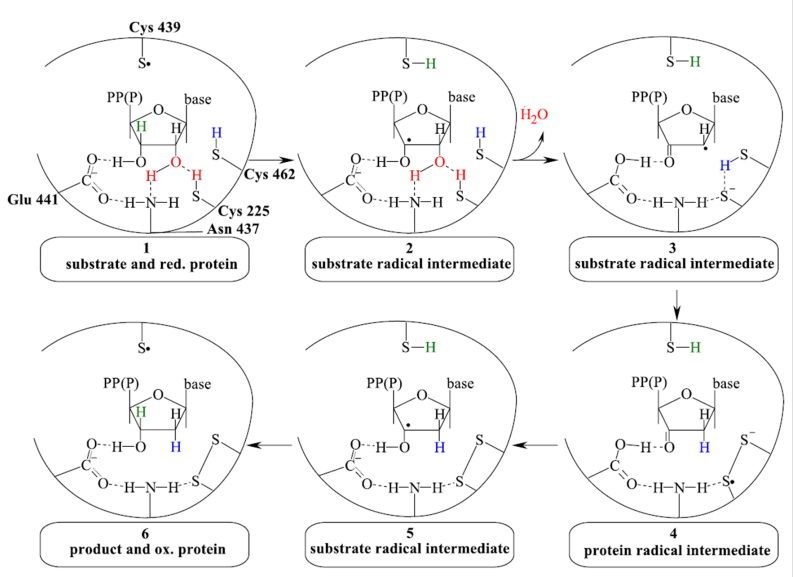

Figure 1.14: *E. coli* RNRs class I and II catalytic mechanism. The thyil radical on the conserved C439 abstracts a hydrogen atom from the 3'-carbon of the ribose ring generating a substrate radical. The ribose radical makes its 2'-OH group more accessible to acid catalysis and results protonated by Cys225, releasing a water molecule and yielding a 2'-ketyl radical. Upon transferring the hydrogen atom to the substrate, Cys225 forms a disulphide anion radical with Cys462. The excess radical electron is next transferred to the 2'-position of the substrate via a chain of hydrogen-bonded active-site residues, regenerating a substrate radical. For completion of the deoxyribonucleotide product, the substrate radical abstracts the hydrogen from Cys439 restoring the RNR thyil radical. Reprinted from [117].

accessible to acid catalysis and results protonated by Cys225, releasing a water molecule and yielding a 2'-ketyl radical. Upon transferring the hydrogen atom to the substrate, Cys225 forms a disulphide anion radical with Cys462. The excess radical electron is next transferred to the 2'-position of the substrate via a chain of hydrogen-bonded active-site residues, regenerating a substrate radical. For completion of the deoxyribonucleotide product, the substrate radical abstracts the hydrogen from Cys439 restoring the RNR thyil radical. Each catalytic cycle generates an intra-molecular disulphide bond (Cys225-Cys462), and this must be reduced for a complete RNR turnover. The active site is too narrow to allow external electron donors to make direct reduction of the active-site Cys, therefore reduction is first performed by the two additional Cys which are located on the flexible C-terminus (Cys754 and Cys759) of the R1 subunit. Then, a second reduction by an external electron donor (Trx, Grx or GSH) returns RNR to its basal reduced status and it is ready again for the next catalytic cycle (**figure 1.15**). Class III RNRs enzymatic mechanism is quite different from the above explained and *in vitro* studies show that they use formate as the final electron donor [199].

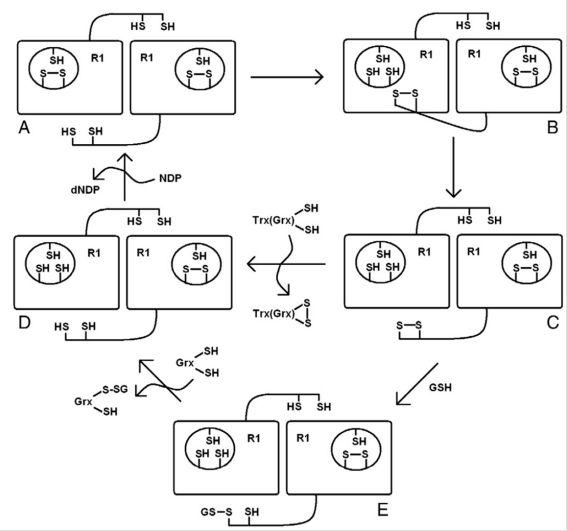

Figure 1.15: Trx and GSH/Grx sytems in RNR regeneration. (A) Upon each cycle of catalysis a disulphide bond is formed between the conserved Cys pair at the RNR active site (showed as a circle). (B) Reduction of the R1 active site is mediated by the C-terminal CXXC motif of the neighbouring subunit. (C to D) The resulting disulphide bond is reduced by the Trx and Grx systems through disulphide exchange resulting in an active R1. (D to A) The reaction allows the RNR reaction cycle to continue. (E to D) The monothiol mechanism involves glutathionylation. Reprinted from [199].

RNRs in *E. coli* *E. coli* encodes three RNRs, two oxygen-dependent from class I, NrdAB (class Ia) and NrdEF (class Ib), and one oxygen-sensitive NrdDG, from class III. NrdAB is essential for *E. coli* aerobic growh [147] and it is induced by DNA damage or by inhibition of DNA replication. Both Trx and Grx were found to reduce NrdAB *in vitro* and *in vivo* [148] [149], and at least one, GrxA, TrxA or TrxC is required for the areobic viability of this organism. GrxA, with 10-fold less K_m than Trx, but with equal V_{max}, is the most efficient donor for *E. coli* NrdAB. NrdEF is induced upon oxidative stress, in minimal media and by lack of Trx and Grx [200]. It is expressed together with two small open reading frames (ORFs), *nrdH* and *nrdI* encoding a Grx-like protein and a protein which stimulates NrdEF activity, respectively [201]. NrdH is structurally a Grx-like protein, although it lacks the specific GSH-binding sequence. Its active site, CM/VQC, differs from the canonical CPYC Grx active site, and it is unexpectedly reduced by TrxR, both *in vitro* and *in vivo* [202] [203]. NrdH is essential to efficiently reduce NrdEF *in vivo*, although it can be partially replaced by GrxA in *E. coli* mutants lacking *trxB*. The physiological role of this RNR is unknown. Normally this is a cryptic enzyme, which, only if expressed, is able to suppress the aerobic lethality of an *E. coli* mutant lacking NrdAB [203]. Finally, NrdDG is expressed in anaerobiosis. According to *in vitro* studies, formate is the electron donor for this class of RNR, although this remains to be demonstrated *in vivo* [204]. However, the thiol groups located at the C-terminus require reduction in order to keep NrdDG active. This reduction probably relies on the Trx or GSH/Grx systems, since an *E. coli* mutant lacking *nrdAB*, *nrdEF*, *trxB* and *gor* was not able to grow anaerobically [203]. Under strict

anaerobic conditions, NrdAB can partially rescue an *E. coli* strain lacking NrdDG [203].

RNRs in *S. cerevisiae* *S. cerevisiae* has a class Ia RNR with unique characteristics. Two separate versions of R1 are coded by two genes, *rnr1* and *rnr3* [205], and two genes encode two R2-like proteins, Rrn2 [206] and Rrn4 [207]. Rnr3 is barely expressed in normal conditions, and cells lacking *rnr3* do not have any apparent phenotype, even after DNA damage when it is strongly induced. However, over expression of Rnr3 can rescue *rnr1* null mutants [208]. The two R2-like proteins, Rnr2 and Rnr4, are both required to provide a functional reductase. Rnr4 does not bind iron, cannot form the tyrosyl radical and only has a structural function, whereas Rnr2 appears to bind the di-iron centre [209]. Rnr4 and Rnr2 form the heterodimer of the small subunit that, together with the large subunit, form the active $\alpha_2\beta\beta$' heterotetramer [207]. This is an unusual subunit compositon, since in other organisms, such in the case of *S. pombe*, the classical heterodimer $\alpha_2\beta_2$ is formed instead (in the case of *S. pombe* the only large regulatory subunit is coded by *cdc22*, whereas the small subunit is coded by *suc22* [210]) [117].

S. cerevisiae cytoplasmic Trxs are the major *in vivo* electron donors for RNR. Thus, *Δtrx1 Δtrx2* cells have an elongated S-phase, a reduced pool of dNTPs in S-phase [160] [211] and accumulate oxidized R1 [160]. Grxs are also able to reduce RNR, although less efficiently and only in substitution of the Trx system, as it is demonstrated by the lack of phenotype of a *grx1 grx2* double mutant and by the lack of viability of the quadruple mutant *trx1 trx2 grx1* and *grx2*. Over-expression of Rnr1 in the *Δtrx1 Δtrx2* double mutant diminished the elongation of the S-phase and increased dNTPs concentrations. The conserved Cys in *S. cerevisiae* are Cys218, Cys443, Cys883 and Cys886, being equivalent to *E. coli* Cys225, Cys462, Cys754 and Cys759, respectively [160].

Mammalian RNRs In mammalian cells, the R2 subunit is made in the late G1 phase before DNA replication, and disappears in late S or early G2. In contrast, the R1 subunit is produced throughout the cell cycle [212]. During mitosis, R2 is degraded by ubiquitination and proteolysis through KEN box binding to the Cdh1-anaphase-promoting complex [213] [214]. Importantly, in resting cells, the R2 gene is neither transcribed nor up-regulated after DNA damage. It is a different protein (p53R2) that, together with R1, provides dNTPs for DNA repair. In contrast to R2, p53R2 is expressed at a low level throughout the whole cell cycle, it is induced upon DNA damage and this induction is dependent on the tumour supressor protein p53 [213] [215] [216] [217]. This is why the R1-R2 complex was suggested to be associated with DNA replication and the R1-p53R2 complex was suggested to be required for basal DNA repair [218].

There is only one study regarding the electron donors for S phase mammalian RNR, which used as a model recombinant mouse RNR. Trx1 and Grx1 resulted equally efficient (K_{cat}/K_m) in reducing this RNR, although the activity with the Grx system resulted highly dependent on the GSH concentration. Thus with 4 mM GSH, Grx1 showed a higher affinity

in comparison with Trx1, which displayed higher apparent K_{cat}, suggesting its major role in S phase DNA replication. Moreover, Grx2 was equally active as Grx1, and a Grx2.C40S mutant was found to be active with RNR, suggesting a deglutathionylation mechanism for Grx catalysis, in contrast to the dithiol mechanism for Trx. The authors of this work hypothesized that this monothiol mechanism could be an advantage for mitochondrial DNA synthesis, where there are very low levels of R1, or in tumour cells where there are high levels of RNR and no or low Trx expression [219].

***S. pombe* RNRs** In the fission yeast, the two subunits of RNR, Cdc22 (R1) and Suc22 (R2) are transcriptionally induced at the transition G1 to S phase by the MBF transcription complex [210], although their levels do not change dramatically neither during the cell cycle nor upon checkpoint activation [220]. A significant proportion of RNR regulation in cycling cells is thus occurring post-translationally [221]. For instance, R2 is localized to the nucleus in non S-phase cells, but it is re-localized to cytosol in response to either S-phase entry or upon DNA damage and checkpoint activation [222]. Since Cdc22 (R1) is constitutively cytoplasmic, the re-localization was proposed to promote RNR holoenzyme formation. It was found that Spd1, an inhibitory protein, prior to DNA replication and in response to DNA damage, is degraded under the control of the COP9/signalosome and Ddb1 leading to R1 activation [223]. Also, other related RNR-regulatory roles were attributed to this protein, some of them related to R2 localization, but the exact mechanisms remain to be explained [221]. No works regarding the electron donors for RNR reduction have been performed yet.

1.2.6.4 PAPS reductase

Prototrophic bacteria or fungi mainly use inorganic sulphate as the only sulphur source for the biosynthesis of amino acids and essential cofactors. Sulphate assimilation takes place in five enzymatic steps. First, sulphate is activated to 5'-adenylylsulphate (APS) and 3'-phospho-5'-adenylylsulphate (PAPS) by ATP sulphurylase and APS kinase, respectively. PAPS is then reduced to sulphite by PAPS reductase, and sulphite is reduced to sulphide by sulphite reductase. From sulphide, different steps lead to synthesis of Met, Cys and their derivatives. PAPS reductase catalyses the first reductive step in this sequence, and to be recycled, it needs electrons provided by either the Trx or the GSH/Grx systems.

The reaction mechanism was first described for *E. coli* PAPS reductase. Structural and functional data established a ping-pong mechanism for the enzyme homodimer in which Trx reduced the enzyme, in a first reaction, forming a stable reduced enzyme isoform, and then, PAPS oxidized PAPS reductase to give sulphite and adenosine 3',5'-bis-phosphate (PAP) [225]. Nevertheless, the sequence of events for PAPS reduction was later challenged [226], and even a Trx-PAPS reductase complex from *E. coli* was crystallized [227], further supporting a new proposed mechanism (**figure 1.17**). *E. coli* PAPS reductase (CysH)

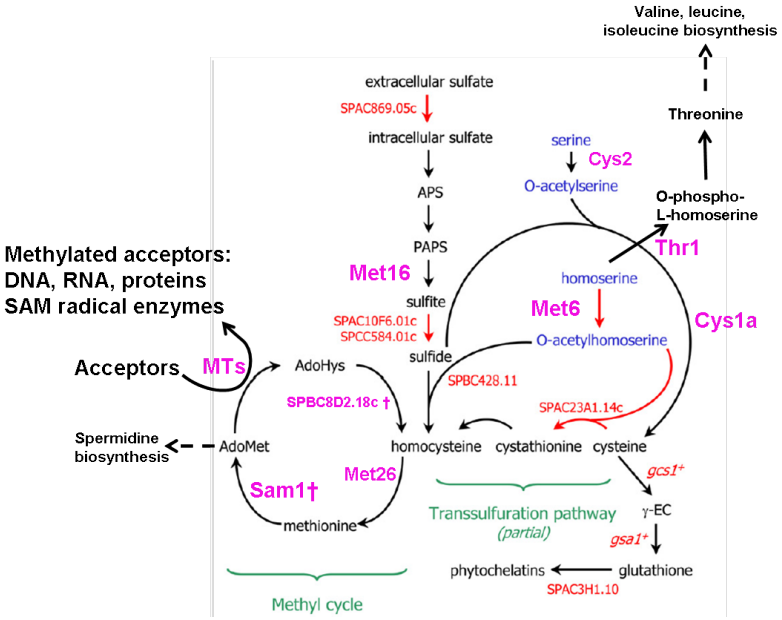

Figure 1.16: Sulphate assimilation pathway in *S. pombe*. SPAC869.05c sulphate transporter, Met16 phosphoadenosine phosphosulphate reductase, SPAC10F6.01c and SPCC584.01c sulphite reductases, Cys2 homoserine O-acetyltransferase, Thr1 homoserine kinase, Met6 homoserine O-acetyltransferase, Cys1a cysteine synthase, SPBC428.11 homocysteine synthase, SPAC23A1.14c trans-sulphuration enzyme, Gcs1 glutamate-cysteine ligase, Gsa1 glutathione synthetase, SPAC3H1.10 phytochelatin synthetase, SPBC8D2.18c adenosylhomocysteinase, Met26 homocysteine methyltransferase, Sam1 S-adenosylmethionine synthetase, MTs methyl transferases. Adapted from [224].

contains a single Cys in a conserved cluster KXECGI/LH [225]. This Cys performs a SN_2 attack on the sulphonucleotide sulphate group of PAPS to yield a S-sulphocysteine intermediate (E-Cys-S_γ-SO_3^-). Then, the N-terminal Cys of Trx active site attacks on the Sγ of the intermediate forming a mixed disulphide, and releasing sulphite. Finally, a thiol/disulphide exchange with the C-terminal Trx Cys would yield oxidized Trx and reduced PAPS reductase [226].

In *E. coli*, PAPS reductase recycling is carried out mainly by TrxA and GrxA, as a double mutant lacking both proteins is not viable in mimimal media plates, due to toxic PAPS accumulation. Thus, increased levels of Cys or mutations in *cysA* or *cysC* genes, which repress or inactivate the sulphate assimilation pathway, respectively, allowed survival of this double mutant [146]. Restricted growth of combined null mutants for *gor* and *grxA grxB grxC* on minimal media suggested that at least one Grx is required for sulphate to sulphite reduction, and improved cell growth on minimal media for *gor* mutants expressing only GrxB or GrxBC12S lead to the discovery that a monothiol mechanism could be regulating the activity of PAPS reductase [228].

In *S. cerevisiae* loss of both cytoplasmic Trxs renders cells auxotrophic for Met. In this case, Trxs are the sole reductants for PAPS reductase, although in low aeration conditions

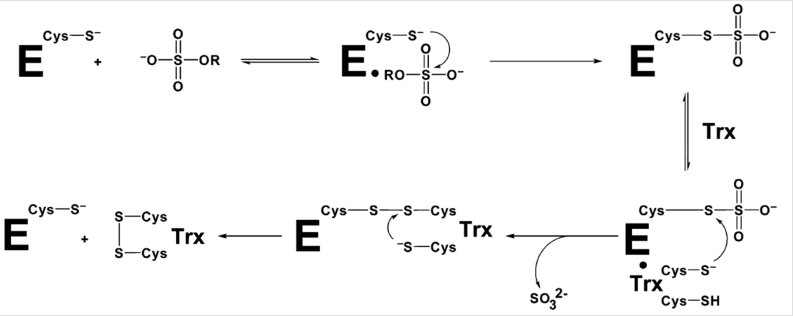

Figure 1.17: Mechanism for sulphonucleotide reduction and PAPS reductase regeneration. The single Cys of the *E. coli* PAPS reductase performs a SN_2 attack on the sulphonucleotide sulphate group to yield a S-sulphocysteine intermediate. Then, the N-terminal Cys of the Trx active site attacks on the Sγ of the intermediate forming a mixed disulphide, and releasing sulphite. Finally, a thiol/disulphide exchange with the C-terminal Trx Cys would yield oxidized Trx and reduced PAPS reductase. Reprinted from [226].

or in the absence of functional mitochondria, *trx1 trx2* mutants were able to assimilate sulphate. This results suggested an alternative electron donor for PAPS reductase, which is normally functioning in the repair of oxidative-mediated damage, but under low ROS production, it can alternatively serve as an inefficient PAPS reductase electron donor [158]. Importantly, *S. cerevisiae trr1* mutants are not auxotrophic for Met, suggesting that they still retain Trx activity [119]. *S. pombe* is quite similar to *S. cerevisiae* in this aspect, as cells lacking Trx (*Δtrx1*) are Cys auxotrophs [99].

1.3 Protein quality control and oxidative stress

Proteins, which virtually determine almost every aspect of life, due to their diverse enzymatic and structural properties, are at the same time vulnerable molecules inside the physiological environment of living cells. Protein folding and stability are continuously challenged in the different processes of a protein life, from biogenesis through translation, intermediate folding or subunit assembly. All of them are processes in which hydrophobic regions are frequently exposed leading to structurally unstable products that tend to aggregate and precipitate. Accumulation of aggregation-prone proteins interferes with normal cellular functions. In addition, failure to clear aggregated proteins is common in many human disorders including Parkinson disease, Huntington disease, Alzheimer disease, cataracts, or diabetes [229]. Under stress conditions, as in the case of oxidative stress, and also in unbalanced protein synthesis, metabolic stress, heat or heavy metals exposure, generation of abnormal proteins is enhanced and thus their accumulation. To cope with protein damage, cells trigger cellular protein quality control (PQC) pathways that either sort proteins for repair, mediated by chaperones, or for degradation, by the ubiquitin proteasome system (UPS) or by macroautophagy [230].

1.3.1 Ubiquitin proteasome system (UPS)

Degradation of a protein by the UPS involves two successive steps: covalent attachment of multiple ubiquitin molecules and degradation of the ubiquitin-tagged substrate by the 26S proteasome complex, with release of free and reusable ubiquitin. This last step is mediated by deubiquitinating enzymes (DUBs).

Attachment of ubiquitin, a highly evolutionary conserved 76 residue polypeptide, to a protein substrate takes place in three different steps (**figure 1.18**). First, the ubiquitin activating enzyme, or E1, activates ubiquitin in an ATP-requiring reaction to yield a high energy thiol ester intermediate, E1-S∼ubiquitin. One of the various ubiquitin conjugating enzymes, E2 or UBCs, transfer the activated ubiquitin moiety from E1, via a different high energy thiol ester intermediate, E2-S∼ubiquitin, to the substrate which is specifically bound to a member of the ubiquitin-protein ligase family or E3. If the E3 contains a HECT domain, the ubiquitin is transferred once again from the E2 enzyme to an active site Cys residue on the E3, to generate a third high energy thiol ester intermediate, E3-S∼ubiquitin, before its transfer to the ligase-bound substrate. On the contrary, RING finger E3s catalyze direct transfer of the activated ubiquitin moiety to the E3-bound substrate. E3s catalyze the last step in the attachment of the ubiquitin to the substrate, therefore playing an important role by specifically recognizing substrates to be degraded. Ubiquitin is normally transferred to an ε-NH_2 group of an internal Lys residue in the substrate to generate a covalent isopeptide bond, although in some cases, ubiquitin is conjugated to the NH_2 terminal amino group of the substrate. By successive addition of ubiquitin moieties to internal Lys residues on the initial conjugated ubiquitin molecule, a polyubiquitin chain is synthesized.

Chains of at least four molecules of isopeptide-linked ubiquitin, in which the C-terminus of one ubiquitin is attached to Lys48 of the next ubiquitin, efficiently promote binding of the modified protein to the 26S proteasome. On the contrary, monoubiquitination or attachment of short Lys63-linked ubiquitin chains to a protein may serve as a cellular targeting or localization signal, but it does not target proteins to proteasome. Importantly, chains of four ubiquitins bind 100 times better to the proteasome than chains of two ubiquitins. The quaternary structure of ubiquitin polymers and also the spatial relationship between each subunit molecule is also critical for targeting substrates for degradation by the proteasome. For instance, modification of proteins by polyubiquitin chains linked by Lys-63 instead of Lys48 plays a role in signalling and DNA repair but not in substrate degradation.

There are a lot of cellular proteins targeted by ubiquitin, such as cell cycle regulators, tumour suppressors, transcriptional activators and their inhibitors, cell surface receptors, endoplasmic reticulum proteins and finally mutated and denatured/misfolded proteins. It is in the latter where this system plays a key role in cellular quality control and defence mechanisms (reviewed in [231]).

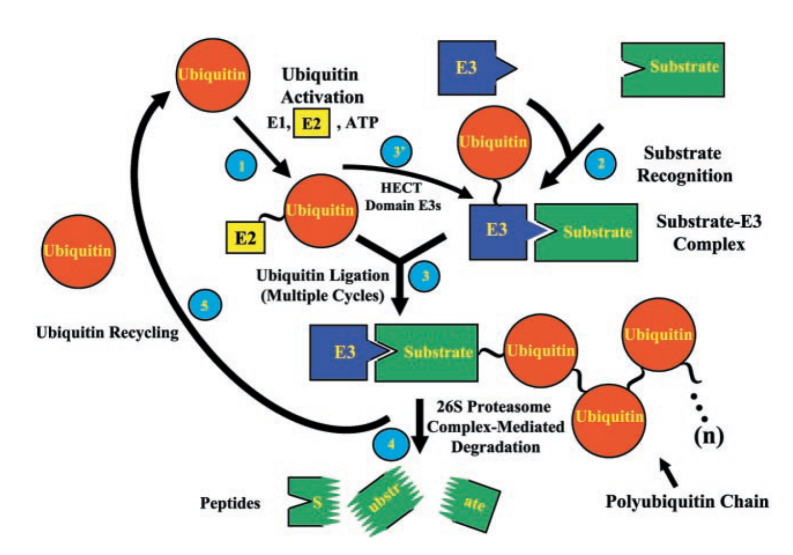

Figure 1.18: The ubiquitin proteolytic pathway. (1) Activation of ubiquitin by E1, E2, and ATP. (2) Binding of the protein substrate to a specific E3. (3) Synthesis of a polyubiquitin chain. E2 transfers the first activated ubiquitin moiety directly to the E3-bound substrate, and in following cycles, to a previously conjugated ubiquitin moiety. Direct transfer of activated ubiquitin from E2 to the E3-bound substrate occurs in substrates targeted by RING finger E3s. (3) As in 3, but the activated ubiquitin moiety is transferred from E2 to a high-energy thiol intermediate on E3, before its conjugation to the E3-bound substrate or to the previously conjugated ubiquitin moiety. This reaction is catalyzed by HECT domain E3s. (4) Degradation of the ubiquitin-tagged substrate by the 26S proteasome complex with release of short peptides. (5) Ubiquitin is recycled via the activity of DUBs. Reprinted from [231]

.

1.3.1.1 The proteasome

The proteasome is a large, 26S, multicatalytic protease, which degrades polyubiquitinated proteins to small peptides. It is formed by two different subcomplexes: a core particle or 20S, which carries the catalytic activity, and a regulatory particle or 19S. The 20S is a 700-kDa complex composed of two copies of 14 different gene products arranged in four axially heptameric rings (α1-7, β1-7, β1-7, α1-7). The α subunits form the gates of the cylindrical structure of the 20S and the β subunits carry the catalytic sites that line the central lumen of the proteolytic chamber. Substrates reach this proteolytic chamber via 13-Å pores formed by the α-subunit rings at either end of the cylinder.

Each extremity of the 20S barrel can be capped by the 19S regulatory particle, the latter behaving as a gatekeeper for substrate entry into the 20S proteasome. The 19S is formed by six different AAA-family ATPases (Rpt1-6) together with three non-ATPases (Rpn1, -2, and -10). The lid of the 19S is a complex made up of eight of the remaining non-ATPase subunits (Rpn3, -5, -7, -8, -9, -11, 12) that can be released from the proteasome under certain conditions. The 19S particle participates in the ATP dependent opening of the pores of the 20S, providing an acces portal for substrates to the catalytic core. Also the

ATPase subunits of 19S contribute to substrate unfolding and delivery into the 20S. Some of the non-ATPase subunits of the 19S have deubiquitinating activity, and others participate in ubiquitin-interaction processes which allow substrate recognition. As a whole, the 26S proteasome-catalyzed process is energy consuming depending on ATP hydrolisis. Once the substrate is degraded, both short peptides from the substrate as well as free reusable ubiquitin are released (reviewed in [231] [232]).

1.3.1.2 The ubiquitin conjugating machinery: E1, E2 and E3

Typically, eukaryotic organisms code for a single ubiquitin-activating enzyme. For instance, the *S. cerevisiae* genome encodes for a single and essential ubiquitin-activating enzyme, Uba1, responsible of activating ubiquitin by a two-step intra-molecular and ATP-dependent reaction yielding the high-energy intermediate E1-S$\sim$ubiquitin [233].

E2s share an active-site ubiquitin-binding Cys residue, and they present a UBC domain required for E3 binding. They catalyze the covalent attachment of ubiquitin to substrate proteins, or, when acting along with HECT domain E3s, transfer the activated ubiquitin to a high energy E3$\sim$ubiquitin intermediate. In the *S. cerevisiae* genome 11 E2s have been identified (Ubc1-8, 10, 11, 13). Two additional enzymes Ubc9 and Ubc12 are UBC family members, although they conjugate the ubiquitin-like proteins Smt3 [234] and Rub1 [235], respectively, and not ubiquitin. In higher organisms there are up to 40 E2s [236]. These small number of conjugating enzymes suffices for targeting numerous substrates, since each E2 is able to interact with several different ligases.

E3 ubiquitin ligases are the enzymes responsible for the specific recognition of the multitude of different substrates of the UPS. E3s are proteins or protein complexes which bind both to E2-conjugating enzymes and to substrates. Interaction with the substrate can be direct or mediated by ancillary proteins. In the case of RING finger domain E3s, these serve as scaffold that bring together E2s and substrates to allow efficient ubiquitin transfer. HECT domain E3s play a catalytical role by transferring the activated ubiquitin from the E2 to an internal Cys residue on E3, before ubiquitin conjugation to a NH_2 group in the target. In addition, there are an extra subset of E3s called E4s (U-box domain) which serve as scaffold to help in the transfer of ubiquitin to a previously conjugated ubiquitin moiety, resulting in elongation of polyubiquitin chains [237]. In yeast, E4 binds to the ubiquitin chains of preformed short conjugates, catalyzing ubiquitin chain elongation both in conjunction with E1, E2 and E3 or independently of E3 [238]. Hence, E4 render preferred substrates for proteasomal degradation [239].

HECT domain E3s have a sequence of 350-aminoacid homologous to the carboxy-terminal domain of the prototypical member of the family E6-AP (E6-associated protein) [240] [241]. This is the domain which harbours the conserved Cys involved in the uptake of the E2 transferred ubiquitin [242]. On the contrary, substrate recognition is probably

located on the amino-terminal region of the protein, since this is a highly variable region amongst E2s.

RING finger domain-containing E3s proteins are ubiquitin ligases which transfer ubiquitin to both heterologous substrates as well as to the RING proteins themselves [243]. They harbour a pattern of conserved Cys and His residues, which form a cross-brace structure probably binding two Zn^{2+} cations [244]. This family is composed of two different subgroups, single and multisubunit proteins. For example, Mdm2 [245], Ubr1 [246] and Parkin [247] are monomers or homodimers which contain both the RING finger domain and the substrate-binding recognition site in the same molecule. In the case of APC, involved in cell cycle regulators degradation [248], the von-Hippel Lindau-Elongins B and C (VBC)-Cul2-RING finger complex [249], involved in HIFI-α degradation or the Skp1-Cullin/Cdc53-F-box protein (SCF)-RING finger involved in signal- and cell cycle-induced phosphorylated proteins degradation [250], E3s are part of multisubunit complexes. Regarding the SCF complex, the RING finger component is involved in E2 recruitment and assembly of other parts of the complex, but not in substrate recognition. It is a different subunit, the F-box protein which carries out the substrate recognition function [250].

1.3.2 Molecular chaperones

Molecular chaperones are defined by their ability to associate with non-native proteins. They participate in the folding of newly synthesized polypeptides, in protein transport across membranes and in the assembly of protein complexes. They are widely considered as cellular folding and assembly factors [251]. However, as it was shown over the last few years, molecular chaperones are key in protein degradation pathways. This new activity still relies in their ability of selectively associate with non-native proteins or unfolded proteins, however, instead of directing these proteins onto a folding pathway, they are driven to the degradation machinery. Therefore, chaperones initially bind to non-native proteins preventing their aggregation and then triage decisions directing protein towards folding or to degradation [252].

There are diverse groups of molecular chaperones, but those more directed involved in chaperone-assisted degradation in eukaryotic cells are the Hsp90 and Hsp70 families. The activity of both chaperone families relies on similar functional principles. In both cases a cycle of ATP binding and hydrolisis gives rise to a dynamic cycle of substrate binding and release [253] [254]. Moreover, both chaperones cooperate with a quite number of co-chaperones, which regulate the ATPase cycle, assist substrate loading onto the chaperones, and recruit Hsp70 and Hsp90 to different protein complexes and subcellular localizations. This means that the cooperation with different subsets of co-chaperones is what directs engagement of Hsp90 or Hsp70 in specific cellular processes, forming the chaperone/co-chaperone complex the functional entity in cells [255].

The importance of Hsp90s in PQC has been unravelled by studying the fate of Hsp90 client protein kinases and transcription factors upon specific Hsp90 inhibition with the benzoquinoid ansamycin geldanamycin [256]. Geldanamycin inhibition results in the rapid degradation via the UPS for many, although not all, Hsp90 clients. Hsp90 functions at the distal end of the pathway of chaperone interactions for newly made transcription factors and protein kinases. Upon geldanamycin inhibition, for protein kinases, concomitantly with a reduction of Hsp90 binding, there is an increase in Hsp70 binding, eviction of the co-chaperone Cdc37 and recruitment of the heat shock protein (Hsp)-organizing protein co-chaperone Sti1 [257]. This correlates with the role of Hsp70 in the degradation process [258].

Hsp70 chaperones function early in the protein folding process by interacting with nascent polypeptide chains, co-translationally or immediatly after translation. The Hsp40 family of co-chaperones are responsible for polypeptide loading onto the Hsp70 chaperones [259]. The former are a diverse and large protein family, but all have in common a conserved 'J' domain, which functions in stimulating Hsp70's ATPase. Therefore, once a polypeptide is bound to Hsp70, the Hsp40 J domain, by stimulating the Hsp70's ATPase, stabilizes the interaction by leading to closure of a helical lid structure over the polypeptide binding site [260]. Initial binding of unfolded peptides to either Hsp70 or Hsp40 is directed by hydrophobic interactions, preventing in this way polypeptide aggregation [260]. It was shown that Hsp70s and Hsp40s promote targeting of polypeptides to degradation. For instance, the *S. cerevisiae* Hsp40s Ydj1 promotes the degradation of cytoplasmic short-lived and abnormal proteins [261] [262], also the neuronal HSJ1, which directly interacts with polyubiquitin chains via a ubiquitin interaction motif, promotes ubiquitination of polypeptides in association with CHIP/Ubc5 conjugation machinery [263]. Curiously, an opposite role was found for *S. cerevisiae* Ydj1 regarding protein kinase degradation. In this case, Ydj1 resulted important for maintaining steady-state levels of protein kinases during or immediately after synthesis, in a similar way as the Hsp90 kinase specific co-chaperone Cdc37 does [264]. In fact, Cdc37 served to protect around 75% of all protein kinases in yeast against rapid degradation, either during or shortly after translation, via the UPS [265]. Cdc37 and Ydj1 acted non-redundantly as one could not substitute for the other in the protection of the newly made protein kinases. This specificity suggested that they interact with a unique region of the newly made kinase client prior to transfer to Hsp70 (via Ydj1) or to Hsp90 (via Cdc37) [266].

Evidence for the active and specific chaperone participation in protein degradation was demonstrated in a study of the degradation of misfolded variants of a heterologously expressed cytoplasmic protein in yeast, the VHL tumour suppressor (**figure 1.19**). Evidence pointed to a hierarchy of chaperone interactions in controlling the different fates of the protein. Thus, both folding and degradation required Hsp70 (*S. cerevisiae* Ssa1), the chaperonin TRiC resulted essential for folding but dispensable for degradation. Conversely, Hsp90 was dispensable for folding and for keeping misfolded VHL solubility, but was required for degradation. Finally, the co-chaperone Sti1/HOP was important for the PQC

by probably bridging the Hsp70-Hsp90 interaction [267].

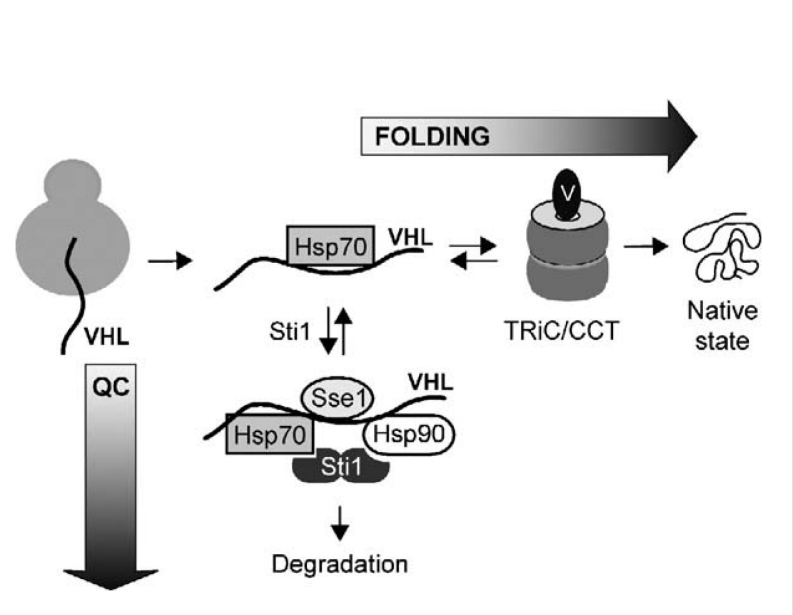

Figure 1.19: VHL folding and VHL quality control. VHL folding and degradation require the Hsp70 Ssa1, the chaperonin TRiC is essential for folding but dispensable for degradation. Conversely, Hsp90 is dispensable for folding and for keeping misfolded VHL solubility, but is required for degradation. Finally, the co-chaperone Sti1 is important for the PQC by probably bridging the Hsp70-Hsp90 interaction. Reprinted from [267].

1.3.3 Chaperones, co-chaperones and the UPS in PQC

The activity of chaperone-associated ubiquitin ligases is key in labelling chaperone substrates for degradation. The E3 C terminus of Hsp70-interacting protein, CHIP (with no yeast homolog) is a main linker between chaperones and the proteasome. This modular protein contains three chaperone-interacting domains at the amino terminus, which confer binding to Hsp70 and Hsp90 [268], and a U-box with E3 ligase activity at the carboxy terminus. The E2s that function with CHIP belong to the mammalian UBCH5 family, closely related to yeast Ubc4 and Ubc5 conjugating enzymes [269]. CHIP and its E2 partner mediate the ubiquitination of chaperone substrates presented by either Hsp90 or Hsp70, initiating sorting to the proteasome and degradation [270]. In this regard, the chaperone/CHIP/E2 complex may be viewed as a multi-subunit ubiquitin ligase complex, in which the chaperone acts as the main substrate recognition factor [271].

Chaperone substrates targeted by CHIP can be both proteins that undergo conformational changes in association with Hsp90 or Hsp70 as a result of their cellular regulation, such as the glucocorticoid hormone receptor or the oncogenic receptor tyrosine kinase

ErbB2 [272], or aggregation-prone proteins recognized by chaperones during protein quality control, such as the immature cystic fibrosis transmembrane conductance regulator (CFTR) [273], whose mutations cause cystic fibrosis, or hyperphosphorylated tau that accumulates in patients with Alzheimer's disease [274]. Regarding PQC, CHIP partially unravels the long-standing question as to how the ubiquitin/proteasome system recognizes non-native proteins for degradation. Thus, this chaperone- associated ubiquitin ligase is key in switching chaperone activity from protein folding to protein degradation [255] [252].

In *S. cerevisiae* the ubiquitin-conjugating enzymes Ubc4 and Ubc5 mediate the selective degradation of short-lived and abnormal proteins. These E2s are closely related in sequence and complementing in function, they are induced upon heat shock, comprising the major part of total ubiquitin conjugating activity in stressed cells, and generate high molecular weight ubiquitin-protein conjugates *in vivo*. Lack of both *ubc4* and *ubc5* impairs cell growth and renders cells inviable at high temperatures [275].

One of the E3 ligases that was found to work together with Ubc4 is the RING finger E3 Ubr1 [276]. Ubr1 is the main enzyme which participates in the N-end rule degradation pathway, where the identity of the N-terminal amino acid determines a protein's half life [277]. Surprisingly, Ubr1 is responsible for targeting misfolded cytoplasmic protein to proteasomal degradation [278] and to promote degradation of protein kinases in geldanamycin-treated yeast (Hsp90 clients), this function enhanced by Hsp70 [279]. Ubr1 appears to directly interact with its misfolded protein substrates, but their ubiquitination is Hsp70 and Sse1 (Hsp110 co-chaperone)-dependent [280]. These latter findings suggest that Hsp70 and Sse1 form a substrate recognition module that works directly with Ubr1, in a manner analogous to CHIP [280] [281].

Ubr1 has a paralog, Ubr2 that does not function via the N-end rule pathway, but promotes ubiquitination of Rpn4, a transcription factor involved in regulating genes encoding proteasome subunits [282]. Nevertheless, its role in protein degradation is mild compared with a *Δubr1* strain [279].

Similarly to Ubr1, the nuclear ubiquitin ligase San1 (*sir* antagonist) also mediates chaperone-dependent ubiquitination of numerous misfolded cytoplasmic proteins, via direct protein-substrate interaction. Nevertheless, in this case, it remains to be determined whether chaperones are required to prevent cytoplasmic aggregation of substrates, to assist in nuclear transport, or to present substrates to San1 in the nucleus [280].

PQC in the nucleus is totally dependent on the UPS, since it lacks the autophagy-lysosomal system [283]. *S. cerevisiae* San1, together with the E2s Cdc34 and Ubc1 specifically targets four different mutant nuclear proteins for ubiquitination and destruction by the proteasome [284]. Similarly, *S. pombe* San1 was found to specifically target Asf1-30, the mutant form of the histone chaperone Asf1, for proteasomal degradation. Unexpectedly, a different E2 enzyme, Ubc4, was identified to work together with San1

[285]. In mammals, both ectopic expression of *S. cerevisae* San1 and the nuclear E3 ligase UHRF-2 promote polyglutamine (pQ) aggregate degradation and rescued pQ-induced cytotoxicity in cultured cells and primary neurons [286]. The expansion of trinucleotide repeats encoding pQ within the mutant gene product causes polyglutamine diseases such as Hungtington disease [287].

1.3.4 Deubiquitination

Despite of being covalently linked to many substrates targeted for degradation, ubiquitin itself is a highly stable protein *in vivo*. This is due to the efficient removal of ubiquitin from its conjugates prior to proteolysis by deubiquitinating enzymes (DUBs). Several roles have been ascribed to DUBs, important in the UPS. First, DUBs carry out activation of the ubiquitin pro-proteins probably cotranslationally. Ubiquitin is always expressed as a linear polyubiquitin pro-protein fused to one of two ribosomal proteins, thus, in order to obtain the mature ubiquitin monomer it must be first processed. Then, DUBs may also recycle accidentally trapped ubiquitin by the reaction of small cellular nucleophiles with the thiol ester intermediates involved in protein ubiquitination. Also, DUBs reverse ubiquitination or ubiquitin-like modification of proteins, antagonizing in this way the ubiquitination of proteins, negatively regulating protein degradation. Conversely, deubiquitination of proteolytic substrates is also necessary for sustaining normal rates of proteolysis by helping to maintain a sufficient pool of free ubiquitin within the cell. Finally, DUBs are responsible for regenerating monoubiquitin from unanchored polyubiquitin (free polyubiquitin *de novo* synthesized or released from target proteins by other DUBs) and for keeping the 26S proteasome free of unanchored ubiquitin chains that can compete with ubiquitinated substrates for ubiquitin-binding sites (reviewed in [288]).

DUBs are highly conserved Cys proteases or zinc-dependent metalloproteases, which can be classified according to their catalytic domain structure: ubiquitin C-terminal hydrolases (UCHs), ubiquitin specific proteases (USPs), ovarian tumour proteases (OTUs), Machado-Joseph disease proteases and JAB1/MPN/Mov34 metalloenzymes (JAMMs) [289].

Specific roles of different DUBs have been elucidated. In particular, Uch2/UCH37 (with no *S. cerevisiae* ortholog), Rpn11/POH1 and Ubp6/USP14, are directly involved in protein degradation, since they process polyubiquitinated proteins at the proteasome [288].

UCH37 is activated upon 19S proteasome-association. It inhibits the degradation of ubiquitinated proteins by removing ubiquitin from the distal end of a polyubiquitin chain. Thus, UCH37 depletion led to an accelerated hydrolysis of model proteasome substrates with a concomitant decrease in the levels of cellular polyubiquitinated proteins [290].

Similarly to UCH37, Ubp6 and its human ortholog USP14 are also activated upon association with the 19S regulatory particle ($\sim$300 fold increase in ubiquitin hydrolase

activity) [291] [292] [293]. Ubp6 is found in nearly stoichiometric amounts in the 19S, and the direct association with the 19S happens via an UBL domain at its N-terminus. Deletion of *S. cerevisiae* Ubp6, or USP14 in human cells, led to accelerated protein degradation and to reduced levels of free ubiquitin [294], which means that Ubp6 delays protein degradation [295] [296]. Intriguingly, this inhibition of protein degradation, which has been proposed to provide a time window for gradual substrate deubiquitination, resulted independent of its deubiquitinating activity but relied on its association with the 19S. It has been found that Ubp6 acts catalytically in cooperation with Hul5, a proteasomal associated E3 ligase, and both regulate the length of polyubiqutin chains on the substrate from the distal end. This dynamic elongation and shortening of polyubiquitin chains, was suggested to represent a balance for keeping in the one hand the substrate associated with the proteasome, and in the other hand polyubiquitin removal from the substrate as it is translocated into the proteasome [297]. According to this, a *Δhul5* suppressed the phenotype of a *Δubp6*.

S. cerevisiae Rpn11 (human POH1), is a deubiquitinating enzyme which is an integral part of the 19S regulatory particle [298]. This DUB belongs to the JAMM domain family and it is the only essential DUB in yeast. Similarly, depletion of POH1 by RNAi inhibited cellular growth, showed an increase in polyubiquitinated proteins, it was defective in cellular protein degradation and had compromised proteasomal activity [290]. A D121A active-site mutation in the *S. cerevisiae* Rpn11 caused a defect in protein degradation but not in cell viability. Rpn11-dependent deubiquitination is linked to association of Rpn11 with the lid of the 19S and with ATP hydrolisis, suggesting that deubiquitination may be linked to protein unfolding by the ATPases of the base subcomplex. Differently from Ubp6/USP14 or Uch2/UCH37, Rpn11 cleaves polyubiquitin chains from the substrate at the proximal end of the chains, or in other words, it releases polyubiquitin chains in bloc [299] [288].

Although no directly interacting with the proteasome, deletion of the DUB Ubp14 in *S. cerevisiae* (IsoT in mammalian), led to defects in the degradation of model substrates of the UPS. These were ascribed to inhibition of the proteasome by excess of unanchored polyubiquitin, which may competitively inhibit polyubiquitinated substrate binding to the proteasome [300].

Additionally, the vacuole/lysosome protein degradation [301] system equally requires ubiquitination prior to degradation [302]. Substrates of this pathway are mostly membrane proteins, such as cell surface proteins, which are endocytosed and directed to the vacuole by monoubiquitination or anchoring of short Lys63-linked ubiquitin oligomers. *S. cerevisiae* Doa4 is involved in recovering ubiquitin from these involuting membrane proteins before complete vesiculation. Consistently, mutants of Doa4 resulted in the internalization of ubiquitinated receptors by the vacuole and depletion of free ubiquitin [303] [304].

Recently, a work characterizing the entire family of DUBs in *S. pombe* has been published. In contrast to mammalian cells, which approximately code for $\sim$ 95 DUBs, *S. pombe* codes for only 20 putative DUBs, belonging to four of the five subfamilies (UCH,

USP, OTU and JAMM) [305]. Similarly, to *S. cerevisiae* only Rpn11 is essential and curiously, the UCH37 ortholog, absent in *S. cerevisiae*, is present in *S. pombe* (Uch2) [306].

1.3.5 ER associated degradation (ERAD) and the unfolded protein response (UPR)

More than thirty percent of the cellular proteins are proteins of the secretory pathway. They fold in the lumen or membrane of the ER from where they are sorted to their site of action. However, if folding is delayed or an illegitimate conformation arises, these proteins are selected for degradation in a process known as ER-associated degradation or ERAD, a highly conserved pathway among eukaryotes. Importantly, the final degradation machinery of misfolded ER proteins is the UPS, localized in the cytosol or in the nucleus. This means that misfolded proteins must be recognized and retrotranslocated across the ER membrane back into the cytosol, where they are polyubiquitinated and degraded. For misfolded ER lumenal proteins the retro-translocon complex (RTC) includes the Hrd-Der ubiquitin ligase complex of the ER membrane, linked to the Derlin Der1 and the Sec61 translocon, and the ubiquitin conjugating enzyme Ubc7. Once in the cytoplasmic side of the ER, a Cdc48-Ufd1-Npl4 segregation machinery, also linked to the RTC, delivers the polyutibiquitinated proteins to the proteasome for their degradation (ERAD-L pathway). In the case of misfolded membrane proteins with lesions in the cytosol, polyubiquitination is performed by the ubiquitin ligase Doa10 together with the E2s Ubc6 and Ubc7, previously to Cdc48-Ufd1-Npl4 proteasome delivery (ERAD-C pathway) (reviewed in [307] [308] [230]).

Accumulation of unfolded proteins in the ER can trigger the unfolded protein response (UPR), through a signal transmission cascade, which in yeast is solely initiated by the inositol-requiring protein 1 (Ire1). This is an ER-localized transmembrane protein with a luminal stress sensor domain and a cytoplasmic, bifunctional Ser/Thr kinase and endoribonuclease effector domain. Under unstressed conditions, the immunoglobulin binding protein (BiP) binds Ire1 in the ER lumen and maintains the enzyme in an inactive state. Conversely, ER stress titrates away BiP to bind to misfolded substrates, leading to oligomerization of Ire1, resulting in *trans*-phosphorylation of the cytoplasmic kinase domains and induction of the endoribonuclease activity. The activated endoribonuclease activity catalyses an unconventional cytoplasmic splicing process that specifically splices an intron in the mRNA that encodes Hac1 (homologous to ATG6/CREB). This allows translation of the Hac1 transcription factor, which translocates to the nucleus, binds to UPR elements (UPREs) in the promoter region of target genes and activates their transcription, reviewed in [309] [308] [230]).

1.3.6 Role of UPS in degradation of oxidatively damaged proteins

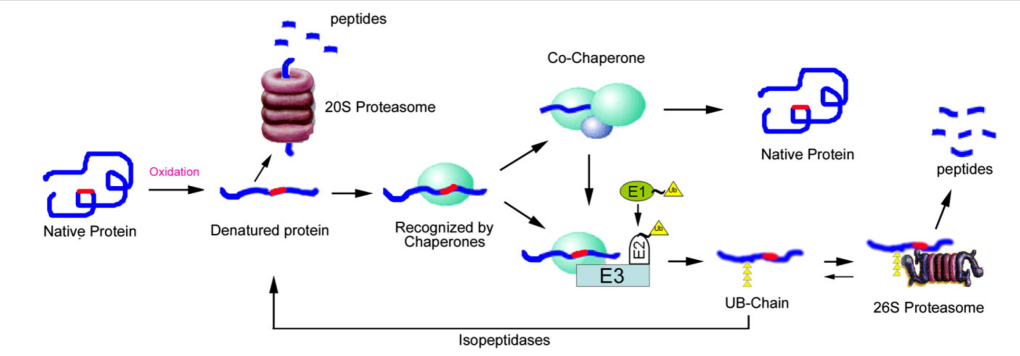

Figure 1.20: Recognition and degradation of unfolded proteins by the UPS. This model predicts that most proteins have intrinsic signals for interaction with molecular chaperones or the ubiquitination system. These signals (red) are hidden in properly folded native proteins and they are not recognized by the PQC. Upon oxidative stress, proteins become unfolded showing the recognition signals. Some of the unfolded proteins can be directly recognized and degraded by the 20S proteasome, whereas others are recognized by molecular chaperones. These, with the help of other chaperones or cofactors, are capable of refolding the denatured proteins. But, if the denatured proteins cannot be refolded rapidly, the chaperone-bound substrates are ubiquitinated (yellow triangles) by chaperone-interacting ubiquitin ligases, such as CHIP. The ubiquitinated substrates are then recognized and degraded by the 26S proteasome. If the ubiquitinated proteins were deubiquitinated by DUBs, the denatured proteins would have a second chance to be refolded by molecular chaperones. The parallel/competitive functional relationship between the UPS and the molecular chaperones ensures the efficiency of PQC systems at getting rid of abnormal proteins. Reprinted from [232].

Whereas antioxidants and antioxidant enzymes quench or metabolize ROS, oxidatively modified proteins (carbonylated proteins) are either repaired by molecular chaperones or targeted to degradation by the proteasome (see **figure 1.20**). Although many publications suggest that oxidized proteins are degraded by the 20S proteasome independently of ubiquitin (reviewed in [310] and [311]), there is also solid evidence supporting the involvement of ubiquitination in degradation of some oxidized proteins [312] [150] [313] [314] [315] [296]. Thus, some works studied the involvement of PQC components in protein degradation in yeast, not only under oxidative stress but also upon heat-shock, cadmium exposure or other stresses able to produce misfolded proteins. Hence, the ubiquitin ligases Ubc4/5, the proteasomal subunit Rpn10, and the Cdc48 AAA family ATPase and its associated partners Ufd1 and Npl4 were found to be involved in the degradation of newly synthesized proteins upon exposure to the ROS generators paraquat and cadmium, to *sod1* (superoxide dismutase) deletion or to 38°C. Failure to clear these proteins, by lack of any of those components, led to accumulation of the nondegraded polypeptides as aggregates [312]. Likewise, HECT Hul5 ubiquitin ligase was found to be involved in degradation of short-lived misfolded proteins upon heat-shock [316]. Deletion of the ubiquitin-conjugating enzymes *ubc4*, *ubc7* and *ubc1* made cells hypersensitive to cadmium, a thiol reactant group that can substitute for zinc in certain proteins [317]. In contrast, overexpression of Ubc4 and Cdc34 (Ubc3) conferred cadmium resistance, in the case of Cdc34

by accelerating the ubiquitination of Met4, and therefore inactivating its transcriptional activity, and in the case of Ubc4 by ubiquitinating proteins other than Met4, and hence accelerating their degradation [318].

It still remains to be elucidated how oxidatively modified proteins are recognized by the UPS. Several studies show that oxidized proteins are partially unfolded due to loss of secondary and tertiary structures, within the domain receiving the oxidative impact [319] [320]. A consequence of the oxidation-induced unfolding is the exposure of hydrophobic patches from the interior of the protein to the surface, and this exposition may be a molecular switch for recognition of oxidized proteins by chaperones or by the proteasome, in a similar manner that other forms of damaged or abnormal proteins. Clues for UPS-substrate recognition were found by studying the way in which the *S. cerevisiae* nuclear ubiquitin ligase San1, involved in PQC, directly recognize its variety of misfolded substrates. Thus, San1 harbours intrinsically disordered amino and carboxy terminus domains, which serve as San1 substrate-recognition sites [321]. Moreover, San1 recognition is triggered by exposure of as few as five contiguous hydrophobic residues. This hydrophobicity recognized by San1 can cause aggregation and cellular toxicity, underscoring the fundamental protective role for San1-mediated PQC degradation of misfolded nuclear proteins [322].

The ability of the UPS to degrade proteins in cells is altered in response to oxidative stress. Upon exposure to mild oxidative stress there is a transient increase in the intracellular degradation of both short-lived and long-lived proteins. This is due to both an increase on substrate availability and to an enhancement of the ubiquitination and degradation capabilities of the cell. Nevertheless, all components of the UPS, including E1, E2s, some E3s, the proteasome and deubiquitinating enzymes may be affected by extensive oxidative insults [323] [324] [325] [326]. Thus, mild to moderate oxidative stress increases protein susceptibility to degradation whereas severe oxidation, by impairing the functions of the UPS, leads to reduced intracellular protein degradation concomitantly with their accumulation and aggregation [232].

Efficiency of the PQC is also affected by ageing, thus accumulation of aberrant protein species in the form of carbonylated proteins, aggregates, amyloids and inclusion bodies increase with age [27] [327] [328]. Additionally to PQC, it has been discovered that cells possess a spatial protein quality control (SQC). This encompasses the formation of aggresomes, which has been suggested to be a cytoprotective response that sequesters toxic misfolded proteins and facilitates their removal by autophagy, which concludes with lysosomal degradation. This formation and processing of aggresomes also involves ubiquitin ligases, deubiquitinating enzymes and histone deacetylase 6 (HDAC6) [329] [330]. HDAC6 is a microtubule associated deacetylase that belongs to the aggresome. HDAC6 has the ability of binding both poliubiquitin misfolded proteins and dynein motors, and acts by recruiting misfolded protein cargo to dynein motors for transport to aggresomes. Hence, *Δhdac6* cells fail to clear misfolded protein aggregates, cannot form aggresomes and are hypersensitive to the accumulation of misfolded proteins [331].

Curiously, aggregated proteins are segregated in the process of cytokinesis, in such a way that the germ-like lineage is kept free of damage whereas progenitor cells retain the oxidized proteins (reviewed in [332]). This process is Sir2 [333] and Hsp104-dependent [334] in yeast and proteasome-dependent in mice [335] and in worms [336].

1.3.7 Role of UPS in cellular redox regulation

The UPS is also involved in cellular redox regulation. In mammals it is involved in the degradation of the nuclear factor-E2-related factor 2 (Nrf2), a bZIP transcription factor which induces a transcriptional response upon oxidative stress [337]. Nrf2 binds to the antioxidant-response element (ARE) and regulates ARE-mediated expression of antioxidant enzymes together with the expression of proteasome subunits [338]. As with many other transcription factors, Nrf2 abundance is regulated by the UPS [339]. The Kelch-like ECH-associating protein or Keap1 is a cytoplasmic inhibitor of Nrf2, whose main function relays on serving as an adapter for the cullin 3-dependent ubiquitin ligase (Cul3). Keap1 binds both to Cul3 via its amino terminus BTB/POZ domain and to Nrf2 via its carboxy terminus Kelch domain, leading to Nrf2 ubiquitination followed by 26S proteasome degradation. Under basal conditions, Nrf2 is constantly ubiquitinated by the Keap1/Cul3/Rbx1 complex and degraded by the proteasome, nevertheless upon oxidative stress, Nrf2 dissociates from the Keap1/Cul3 complex and translocates into the nucleus, leading to activation of the ARE-mediated gene expression (reviewed in [340]).

Similarly, the UPS was also found to participate in the antioxidant response in yeast. In *S. pombe*, deletion of the ubiquitin ligase *ubr1* increased the nuclear levels of the transcription factor Pap1, rendering *S. pombe* cells more resistant to oxidative stress and caffeine treatments [341]. Moreover, over-expression of the proteasomal deubiquitinase Rpn11 or Pad1, confers Pap1-dependent drug resistance [342] [343]. In *S. cerevisiae*, the transcription factor Yap1 translocates from the cytoplasm to the nucleus upon oxidative stress. Nuclear-localized and DNA-bound Yap1 is targeted by the ubiquitin ligase Not4 for proteasomal degradation. Constitutively nuclear Yap1 is degraded even in the absence of an oxidant signal, suggesting a pathway for regulation of the oxidative stress response that serves to temporally limit the duration of Yap1-dependent transcriptional activation [344].

1.4 Methodologies to characterize oxidized proteomes

1.4.1 Proteomic study of reversibly oxidized cysteines

Due to the highly reactive nature of the thiolate anion and to the dynamism of the intracellular redox events, a major difficulty at the time of studying reversible Cys oxidations is to

obtain a snapshot of the *in vivo* Cys redox status at a desired particular time. To overcome this problem, cell lysis is usually performed in the presence of trichloroacetic acid (TCA), which not only rapidly protonates all redox-active thiolate anions by shifting the pH below their pK_a, but also stops thiol-disulphide exchanges by precipitating and denaturing proteins [345] [346]. Alternatively, since thiolates are good nucleotides, membrane-permeable alkylating agents, such as iodoacetamide (IAM) or maleimide derivatives, can also be used for freezing the thiol-redox status.

By following the mentioned above premises, several proteomic approaches have been undertaken to assess the *in vivo* global redox changes of thiol proteomes in different cellular backgrounds or upon oxidative stress. One of these methods, termed diagonal SDS-PAGE, was adapted to identify cytoplasmic proteins which suffer disulphide bond formation after cell exposure to oxidative stress [347]. This methodology consists on separating oxidized proteins in a first dimension by non-reducing electrophoresis. Then, a lane containing the separated proteins is excised from the gel and placed horizontally in a second gel to perform a second electrophoretic dimension under reducing conditions. This results in an atypical 2D gel containing a diagonal line of proteins representing the majority of proteins which do not form disulphide bonds. However, some proteins appear as spots in the right side of the diagonal, these are proteins forming inter-molecular disulphide bonds, which have lower electrophoretic migration rates in the first dimension. On the contrary, proteins forming intra-molecular disulphide bonds migrate faster in the first dimension, therefore appearing in the left side of the diagonal upon the second electrophoretic dimension. Although a very clever strategy, its major limitation is the use of a technique such as 2D electrophoresis, since it lacks sensitivity, as most of the identified proteins in this type of global analysis are normally only those highly expressed in cells. Specificity is also a major issue, especially when using the new generation of mass spectrometers, with enhanced sensitivity. In this case, several proteins are found in a single 2D gel spot, being almost impossible to discern which one of them is specifically labelled at their Cys residue/s.

To circumvent some of these limitations, other type of strategy was designed, initially developed to detect cysteine S-nitrosylation [348], which was called the biotin switch assay. In this strategy Cys oxidation is detected as an increase of probe incorporation in reducible thiols. To do so, initial reduced Cys are first blocked with an alkylating agent (IAM or maleimide), then reversibly oxidized thiols are reduced with a reducing agent and the newly appearing reduced Cys are alkylated with IAM- or maleimide-biotin derivatives. In this case, the use of biotin allows sample enrichment by affinity purification and therefore notable improvements in the sensitivity and the specificity of the technique. Remarkably, the nature of the reducing agent determines the type of Cys oxidation to be detected, thus S-nitrosylations can be detected upon incubation with ascorbate/$CuCl_2$ [349], sulphenated Cys can be specifically detected upon reduction with arsenite [350], Grx specifically reduces S-glutathionylated Cys [351], and dithiothreitol (DTT) or tris (2-carboxyethyl) phosphine hydrochloride (TCEP) non-specifically reduce all Cys reversible oxidations. This approach, in combination with 2D electrophoresis, allowed to successfully

detect many redox-sensitive proteins in different organisms, including bacteria [345], yeast [352] and cells from higher eukaryotes [353], although still coping with the intrinsic limitations of a technique such as 2D electrophoresis. Moreover, these methodologies are semi-quantitative, at best, and unable to identify the specific oxidized Cys residues within the polypeptide.

An important improvement to these limitations was the adaptation of the quantitative isotope coded affinity tag (ICAT) technology [354] to redox proteomics [355] [355] [356]. ICAT moieties are alkylating agents consisting of an IAM linked to a biotin tag through a 9-carbon linker, which exists in an isotopically light (^{12}C-ICAT) and a 9-Da-heavier isotopically heavy form (^{13}C-ICAT). This technique was optimized to be used as an adaptation of the biotin switch methodology, either for the quantification of the absolute oxidation status of proteins in a single sample, which was called OxICAT [357], or for the comparison of two samples at once [358].

In the OxICAT methodology, initially reduced Cys are labelled with light ICAT, whereas upon reduction, newly appearing reduced Cys are labelled with heavy ICAT. After trypsinization, the biotin side of the ICAT moiety allows affinity purification and enrichment of only those Cys-containing peptides, which are then processed by HPLC and quantified and identified by MS and tandem MS/MS analysis, respectively. Importantly, the fact that the light and heavy ICAT reagents are chemically identical allows them to co-elute from the HPLC system and to behave equally in the mass spectrometer. Thus, differences of 9-Da, or multiples of 9-Da, reflect the number of oxidized Cys in a peptide. Moreover, relative peak areas of a peptide containing a Cys labelled with both heavy and light ICAT reagents reflects its absolute oxidation status. Several are the strengths of this technique, it is quantitative, it allows the identification of thousands of peptides at the same time and the identification of the involved redox-sensitive Cys and its *in vivo* oxidation status, and it is immune to changes in protein expression or protein turnover. In fact, it was successfully applied to detect Cys oxidations in *E. coli* [357], in yeast [359] or in *C. elegans* [360] [361]. However, as 90 % of intracellular Cys are in their reduced state [362], there is a big disproportion between the amounts of Cys labelled with one of the ICAT reagents in comparison with the other one, yielding a sample with a high level of complexity. In order to be analyzed, this requires extensive fractionation [up to 192 liquid chromatography (LC) fractions] making data analysis a very difficult issue, even requiring specific software development, and a time consuming event.

One of the goals of this thesis is to optimize a simpler gel-free methodology to identify and quantify oxidized Cys in complex samples.

1.4.2 Proteomic study of carbonylated proteins

The fact that carbonyl compounds are major products of ROS-mediated oxidation reactions led to development of several highly sensitive methods for their quantification. These generally include the specific reaction of the carbonyl group with hydrazine or hydrazide derivatives (e.g. the classical one, dinitrophenylhydrazine (DNPH) which reacts with carbonyl groups to form stable 2,4-dinitrophenyl (DNP) hydrazone products) followed by spectrophotometric measurements or immunodetection with specific antibodies [363]. Althouth recently, it has been reported that DNPH does not react selectively only with carbonyl groups, but it can also form hydrazone derivatives with thioaldehyde derived from sulphenic acid [364].

The majority of proteomic studies of protein carbonylation that have been performed so far have used 2D coupled with MS for their separation, quantification and identification.

The most widely used system for detecting carbonylated proteins on 2D gels is based on DNPH derivatisation and immunodetection with anti-DNPH antibody. Depending on when the DNPH derivatisation step is performed, there are three variants of the protocol. Thus, derivatisation can be carried out before isoelectrofocusing [365]; right after isoelectrofocusing [366] or post electrophoretically [367]. DNPH derivatisation changes protein mobility, therefore by performing pre-electrophoretic DNPH derivatisation is not possible to directly compare the patterns of carbonylated and non-carbonylated proteins. However, post-electrophoretic or isoelectrophoretic staining overcomes those problems and allows direct comparison between labelled and non-labelled proteins, facilitating the quantitation process and MS identification.

Other type of carbonyl-reactive probes, for example fluorescent hydroxylamine [368] or fluorescein-5-thiosemicarbazide [369] were also used to detect protein carbonylation by 2D electrophoresis coupled to MS spectrometry. Nevertheless, all these approaches are susceptible to the intrinsic limitations of the 2D electrophoresis methodology (see section 1.4.1).

Specifity and sensitivity can be improved with the use of biotin-hydrazide, to label protein carbonyls, and then enrichment with immobilized avidin or streptavidin resins. This approach has been used in a number of proteomic studies to enrich for carbonylated peptides and identify carbonylation in complex protein mixtures including yeast [370] [371], rat plasma [372] and human plasma [373].

Attempts to detect protein carbonylations with gel-free approaches have been also undertaken. Thus, relative quantification studies using stable isotope coding allows comparing the degree of oxidation of a particular site between two or more samples. Hydrazide-functionalized isotope-coded affinity tag (HICAT) [374], isobaric tags for relative and absolute quantitation (iTRAQ) [375] [376], and most recently, targeted ^{18}O-labeling [377] have been used in relative quantification studies of carbonylated proteins. A major limita-

tion in using these approaches is that little is known about the fraction of any particular protein or protein site being oxidized in selected condition making difficult comparison between samples.

However, what makes analysis of oxidised proteins exceptionally challenging is the fact that there are many types of modifications of proteins that result in creation of carbonyl residues. Also, MS-based analysis of proteins requires the enzymatic degradation of proteins to peptides. Normally, the enzyme of choice is trypsin, which has high cleavage specificity by cleaving C terminally to Arg or Lys residues. However, oxidised Lys and Arg residues become inaccessible to trypsin proteolysis, leading to a higher number of missed cleavages than normal [378].

In spite of this, $\sim$ 450 carbonylation sites have been identified. They show a tendency to cluster in RKPT-rich regions, and many have been identified in the mitochondrion, a major site of ROS production in the cell (reviewed in [379]).

Chapter 2

OBJECTIVES

Objectives

These are the main objectives to be developed along this thesis:

1. Establishment of a protocol for studying reversible thiol oxidations at the proteomic level.

2. Characterize reversible thiol oxidations upon environmental (H_2O_2) and endogenous (lack of the thioredoxin system) oxidative stress.

3. Characterization of the *S. pombe* methionine sulphoxide reductases.

4. Characterization of the main scavengers of H_2O_2 in *S. pombe*.

5. Establishment of a protocol for studying irreversible protein modifications (protein carbonylations) at the proteomic level.

6. Characterization of the routes that follow the carbonylated proteins for their degradation.

Chapter 3

RESULTS

Results

The results chapter of the thesis is divided in four major sections. Section 3.1 is presented as a paper complemented with additional results (section 3.1.1). Also, section 3.2 is presented with a paper, including some complementary results (section 3.2.1). Sections 3.3 and 3.4 are presented as manuscripts in preparation. Finally, section 3.5 is presented as results.

3.1 Characterization of reversible thiol oxidations in *S. pombe* upon H_2O_2

In this section, we present a protocol for studying reversible thiol oxidations *in vivo* at the proteomic level (ICAT adapted methodology). Moreover, we show data obtained with this protocol when comparing untreated vs H_2O_2 treated wild-type cells. This data was published in one paper, that is presented in the results section. I contributed to the paper as a first co-author, together with Susanna Boronat.

3.2 Cys homoeostasis in *S. pombe* cells lacking a functional Trx system

In this section, we present the results obtained from studying reversible thiol oxidations both, by 1D electrophoresis and by a proteomic gel-free approach (ICAT methodology, described in the previous results section). This data was published in one paper, together with some complementary results, that is presented in the results section. I contributed to the paper as a first co-author, together with Susanna Boronat.

3.3 Characterization of *S. pombe* methionine sulphoxide reductases

In this section, we deeply characterize the *S. pombe* Msrs. They role in reducing oxidized free Met, together with their role as antioxidants. Results are shown as a manuscript; my contribution is as a first author.

3.4 Characterization of *S. pombe* H_2O_2 scavengers

In this results section, we genetically characterize the major H_2O_2 scavengers in *S. pombe*. Results are shown as a manuscript; my contribution is as a first co-author, together with Isabel Calvo.

3.5 Identification and homoeostasis of irreversible protein modifications: protein carbonylation

This results section, for which I closely worked with Susanna Boronat, is divided into two sub-sections:

3.5.1 Troubleshooting of different protocols to study protein modifications by carbonylation

Here we present the troubleshooting performed to set up a good protocol to identify and quantify protein carbonylations in different environmental or genetic conditions.

3.5.2 Protein homoeostasis upon oxidative damage

In this section we present the data obtained from a genetic screening aimed to identify mutants involved in the homoeostasis of carbonylated proteins generated by oxidative damage.

Appendix Moreover, in the Appendix, I present two papers in which I contributed as a middle-author. These papers were the result of a genetic screening from a collection of *S. pombe* deletion mutants. In this screening, two members of the laboratory, Isabel Calvo and Natalia Gabrielli, identified genes participating in wild-type tolerance to oxidative stress.

7.1 Mitochondrial dysfunction increases oxidative stress and decreases chronological life span in fission yeast

Zuin A, Gabrielli N, Calvo IA, García-Santamarina S, Hoe KL, Kim DU, Park HO, Hayles J, Ayté J, Hidalgo E. PLoS One. 2008 Jul 30;3(7):e2842.

Out of a collection of 2,700 haploid yeast deletion mutants, 51 were sensitive to growth on both respiratory-proficient media and H_2O_2-containing fermentable media. From these 51, 19 were related to mitochondrial function, 12 of them lacked components of the electron transport chain. These respiration-deficient mutants displayed elevated steady-state levels of ROS, probably due to enhanced electron leakage from their defective electron transport chains, compromising the viability of chronologically-aged cells.

7.2 Genome-wide screen of genes required for caffeine tolerance in fission yeast

Calvo IA, Gabrielli N, Iglesias-Baena I, García-Santamarina S, Hoe KL, Kim DU, Sansó M, Zuin A, Pérez P, Ayté J, Hidalgo E. PLoS One. 2009 Aug 12;4(8):e6619.

Out of a collection of 2,700 haploid yeast deletion mutants, 98 were sensitive to caffeine, and many of these mutants were related with the H_2O_2-induced Pap1 and Sty1 pathways. In this paper, it is shown that both the Pap1 and the Sty1 pathways are required for normal tolerance to by caffeine, but only the Sty1 pathway is activated by the drug. Cells lacking Pap1 are caffeine sensitive because they have decreased expression of the efflux pump Hba2. Thus, constitutive activation of the Pap1 pathway renders cells resistant to caffeine in a Hba2-dependent manner.

3.1 Characterization of reversible thiol oxidations in *S. pombe* upon H_2O_2

Irreversible and reversible protein modifications are common outcomes of ROS reactivity in situations of oxidative stress. Whereas irreversible protein modifiactions cause loss-of-function in proteins, reversible protein modifications in thiol groups from Cys are profited by the cell to trigger redox signalling pathways in a gain-of-function process.

In the paper presented in this results section, we demonstrate the reversible nature of thiol oxidation to low oxidation states upon H_2O_2, a modification that happens to solvent exposed thiols and to thiols with specially low pK_a values. We also optimized a thiol-labelling approach, which is based on the ICAT reagents, to characterize the H_2O_2-induced reversible thiol oxidations in the proteome of the fission yeast.

García-Santamarina S, Boronat S, Espadas G, Ayté J, Molina H, Hidalgo E. The oxidized thiol proteome in fission yeast—Optimization of an ICAT-based method to identify H2O2-oxidized proteins. J Proteomics. 2011 Oct 19;74(11):2476–86. DOI: 10.1016/j.jprot.2011.05.030

3.1.1 H_2O_2 sensor proteins *vs* general thiol oxidation

This small section is to complement the results presented as a paper entitled The oxidized thiol proteome in fission yeast-Optimization of an ICAT-based method to identify H_2O_2-oxidized proteins.

Intracellular redox regulation through reversible Cys oxidation is possible because not all Cys in proteins react equally with H_2O_2, when this is acting as a second messenger. Rather, for a Cys to react with H_2O_2, it must be in the form of a thiolate anion. This chemical form ot the thiol moiety is present only in few Cys along the proteome, those that have proper local charged environments that allow proton loose at physiological pH.

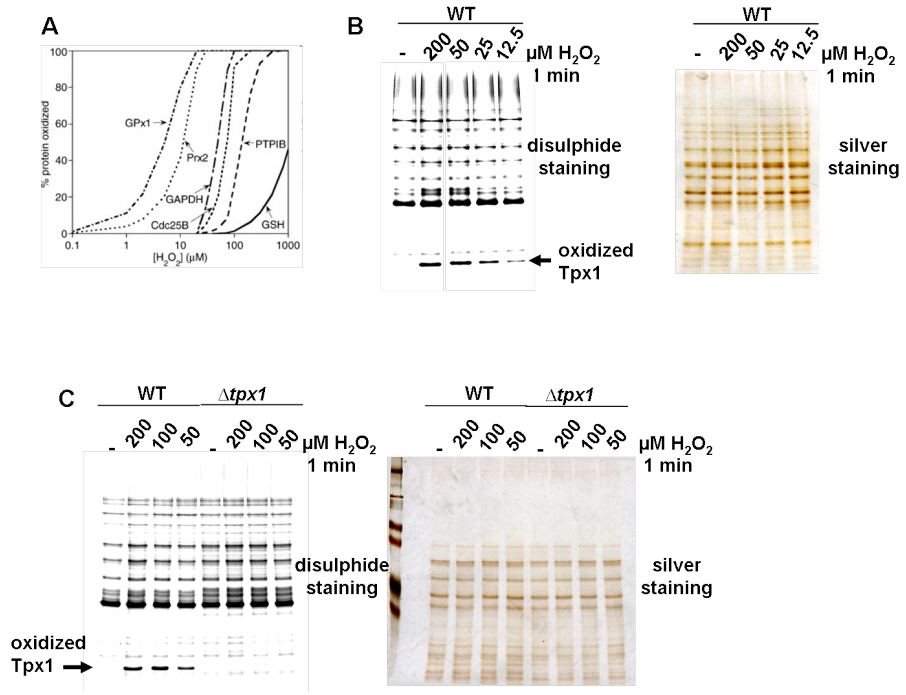

Figure 3.1: Thiol reactivity towards H_2O_2: toxicity *vs* redox sensing. **A** Schematic representation of thiol reactivity toward protein thiols and low molecular weight thiols. Reprinted from [29]. **B** Low levels of H_2O_2 trigger Tpx1 oxidation before general protein oxidations. Free thiols in TCA protein extracts from untreated or treated (with the indicated amounts of H_2O_2) 972 (WT) were alkylated with iodoacetamide. Upon reduction of oxidised thiols, resulting thiols were alkylated with a fluorescently labelled iodoacetamide derivative. Samples were analysed by fluorescent 1D electrophoresis (oxidised thiols) and with silver staining, as a control of protein loading). Oxidized Tpx1 is indicated with an arrow. **B** Lack of Tpx1 does not avoid general thiol oxidation upon low levels of H_2O_2. Free thiols in TCA protein extracts from untreated or treated (with the indicated amounts of H_2O_2) 972 (WT) and MJ11 (Δ*tpx1*) were alkylated with iodoacetamide. Upon reduction of oxidised thiols, resulting thiols were alkylated with a fluorescently labelled iodoacetamide derivative. Samples were analysed by fluorescent 1D electrophoresis (oxidised thiols) and with silver staining, as a control of protein loading). Oxidized Tpx1 is indicated with an arrow.

Among the proteins more reactive with H_2O_2 are found the Prxs. As it is shown in

figure 3.1 A, at least 10,000 times more H_2O_2 would react with a Prx before than reacting with GSH. In fact, these proteins are amongst the most easily oxidized proteins in cells, and mediate antioxidant signalling pathways including the *S. pombe* Pap1 pathway.

We wondered if general disulphides are oxidized concomitantly with Tpx1. As it is shown in **figure 3.1 B**, Tpx1 is oxidized at very low concentrations (12.5 μM), whereas in order to observe general disulphide oxidation, it is required, at least, 4 times this concentration.

Also, it has been suggested that Prxs act as 'sensor' proteins, due to their high reactivity with H_2O_2, which, upon their oxidation, are signal transmitters, that transfer the information to specific target proteins, triggering in this way, specific signalling cascades. This seems to be the case for *S. pombe* Tpx1 and the transcription factor Pap1, as in cells lacking Tpx1, H_2O_2 is not able to activate the Pap1 pathway. We wondered if this would also be the case for the rest of proteins in *S. pombe*. However, as it is shown in **figure 3.1 C**, not only cells lacking Tpx1 have higher levels of thiol oxidation, probably reflecting increased intracellular concentrations of H_2O_2 (Tpx1 is the main scavenger of intracellular H_2O_2), but also disulphide levels increase at all tested H_2O_2 concentrations. The latter result probably indicating direct general thiol oxidation by H_2O_2.

3.2 Cys redox homoeostasis in *S. pombe* cells lacking a functional Trx system

Two are the major roles of the Trx and GSH/Grx systems in cells. On the one hand, they are important to keep general thiols in their reduced state, and on the other hand, they recycle enzymes that use the reversible nature of the modification thiol/disulphide in their catalytic cycles.

We decided to use the ICAT methodology (and also 1D electrophoresis) to study the disulphide proteome of *S. pombe* cells lacking a functional Trx system. We found that in a strain devoid of Trx1, the main cytoplasmic *S. pombe* Trx, there is oxidation only of classical Trx substrates. However, in the absence of the reductase, Trr1, there is a massive generation of reversible oxidized thiols. This general oxidation depending on the presence of Trxs, suggesting that in the absence of their reductase, Trxs become powerful oxidants triggering general thiol oxidation (disulphide stress). Surprisingly, we found that classical Trx substrates could still be weakly recycled in this background, suggesting the presence of an alternative electron donor for Trx.

García-Santamarina S, Boronat S, Calvo IA, Rodríguez-Gabriel M, Ayté J, Molina H, et al. Is oxidized thioredoxin a major trigger for cysteine oxidation? Clues from a redox proteomics approach. Antioxid Redox Signal. 2013 May 1;18(13):1549–56. DOI: 10.1089/ars.2012.5037

3.2.1 Alternative electron donors in *S. pombe* cells missing a functional thioredoxin system

This section is to complement the part of the results presented as a paper entitled Is oxidized thioredoxin a major trigger for cysteine oxidation? Clues from a redox proteomics approach.

In that publication we presented data obtained from a proteomic analysis of Cys oxidations in strains deleted in the major components of the *S. pombe* thioredoxin system, *trx1* and *trr1*. The results obtained in this proteomic analysis led us to conclude that the absence of *trx1* barely increases Cys oxidation, only classical thioredoxin substrates, including PAPS reductase Met16, the methionine sulphoxide reductases Mxr1 and Mxr2, the thioredoxin peroxidase Tpx1 and the glutatione peroxidase Gpx1 appeared with oxidized Cys in this background. However, cells devoided of *trr1*, the only known *S. pombe* thioredoxin reductase, had massive thiol oxidation. We proposed that in the absence of the reductase, oxidized thioredoxins become powerful oxidants and trigger general thiol oxidation. Intriguingly, we also observed that, even though Trxs are very oxidized in a Δ*trr1* background, at least one of their substrates, Met16, remained functional.

In many cases, enzymes that require disulphide reduction in their catalytic cycles, are able to use alternative electron donors. So, if their main electron donor is absent, they can, although probably with less efficiency, switch to a different enzymatic source of electrons, even if this source belongs to a different reducing system (i.e. functional switching between the Trx and the GSH/Grx systems). This seems to be the case for RNRs [121] [117] or Msrs [188] [178] [380], among others. However, in the case of the recycling of *S. pombe* Met16, it seems that the only involved enzyme is Trx1, since cells a single deletion in *trx1* renders cells auxotrophic for Cys. Curiously, this is not the case for cells lacking Trr1, these cells can grow in minimal media without external sources of Cys. This led us to hypothesize, that in the absence of *trr1*, Trx1 is still able to reduce substrates, and that an alternative reducing system may be operating in recycling Trx1.

3.2.1.1 Ratio of GSH/GSSG is lower in cells lacking Trr1, however this ratio increases if Trx are absent in this background

GSH/GSSG ratios are often used as a measurement of the redox potential of the intracellular milieu. Low GSH/GSSG ratios represent oxidising intracellular environments, in which the GSH/Grx system is probably very active in reducing thiol oxidations. Since *S. pombe* cells lacking Trr1 have massive thiol oxidations, we decided to test GSH/GSSG ratios in this strain. We found that the GSH/GSSG ratio is decreased by ∼2-fold in this strain, when compared with a wild-type strain (**figure 3.2 A**), accordingly with a oxidising intracellular environment.

I mentioned above that, in the absence of Trr1, Trx1 was functional at least in reducing Met16. In order to check if the GSH/Grx system is a possible electron donor for Trxs in cells lacking their reductase, we also measured GSH and GSSG levels in cells lacking Trr1 and one or the two *S. pombe* thioredoxins (Trx1 and Trx3). We clearly observed a huge decrease on the ratio of GSH/GSSG in these backgrounds (**figure 3.2 A**), consistently with a role of the GSH/Grx system in reducing Trxs in the absence of TrxR.

These results led us to hypothesize that the GSH pool may act as alternative electron donor for Trx1, when the reductase of the Trx system is missing.

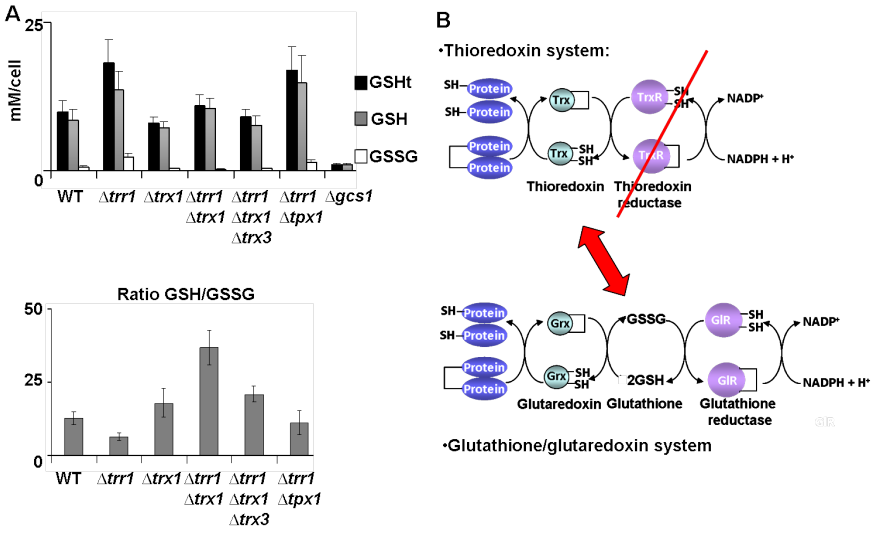

Figure 3.2: GSH/Grx system in the absence of TrxR. **A** Glutathione levels in different mutant backgrounds. Upper panel, GSH_t (total GSH), GSH (reduced GSH) and GSSG (oxidised GSH) concentrations measured for 972 (WT), MJ15 (Δ*trx1*), SG167 (Δ*trr1*), PG22 (Δ*trr1* Δ*trx1*), SG185 (Δ*trr1* Δ*trx1* Δ*trx3*), SG164 (Δ*trr1* Δ*tpx1*), and NG78 (Δ*gcs1*) . Lower panel, ratio of GSH/GSSG was calculated for the previous strains. **B** Schematic representation of the proposed pathway for Trx reduction in the absence of TrxR (see text for details).

3.2.1.2 An extracellular source of GSH partially restores the fitness of a *S. pombe* Δ*trr1* strain

We have shown in the paper that a Δ*trr1* strain has very high levels of reversible Cys oxidations, and that removing both cytoplasmic Trxs (Trx1 and Trx3), or Trx1, together with its major *S. pombe* substrate Tpx1, leads to a significant decrease of Cys oxidations. These remained almost at the same level when all Trxs and Tpx1 were deleted at the same time in a Δ*trr1* background (**figure 3.3 A**). I also described in the previous figure (**figure 3.2**) that GSH consumption is very high in Δ*trr1* cells, and that this consumption decreases when cytoplasmic Trxs (*trx1* and/or *trx3*) or *tpx1* (the main substrate of *S. pombe* Trx1) are deleted together with *trr1*.

We wanted to check the fitness of cells deleted in *trr1* alone or together with the rest of the components of the Trx system, or with *tpx1*, to see if fitness correlates with oxidised/reduced Cys or with GSH/GSSG ratio (**figure 3.3 B**). In general, cells devoid of Trr1 are worse fitted than those cells lacking Trr1 and both cytoplasmic Trxs or Tpx1. Cells lacking Trr1 and a single Trx (Trx1 or Trx3) grow as bad as Δ*trr1* strain. These results highly correlate with increased Cys oxidation levels in the different strains, except in the case where *trr1* is deleted together with *tpx1*. This strain grows better than a strain lacking only *trr1*. However, this correlation does not apply to GSH/GSSG ratios, in this case, by simply deleting *trx1* to a Δ*trr1* background, GSH/GSSG ratio is back (or even superior) to wild-type levels.

Since a Δ*trr1* strain has a low GSH/GSSG ratio, we wondered if adding GSH to the culture media would improve fitness of this strain. As it can be observed in **figure 3.3 B**, by adding GSH is to the media, cells lacking Trr1 only improve fitness a little, to a similar extent that untreated cells incubated under an anaerobic atmosphere. However, neither GSH addition nor anaerobiosis allow Δ*trr1* cells to reach the same growth and colony size as a wild-type strain, probably indicating specific roles for the Trx system that can not be overcome by the GSH/Grx system.

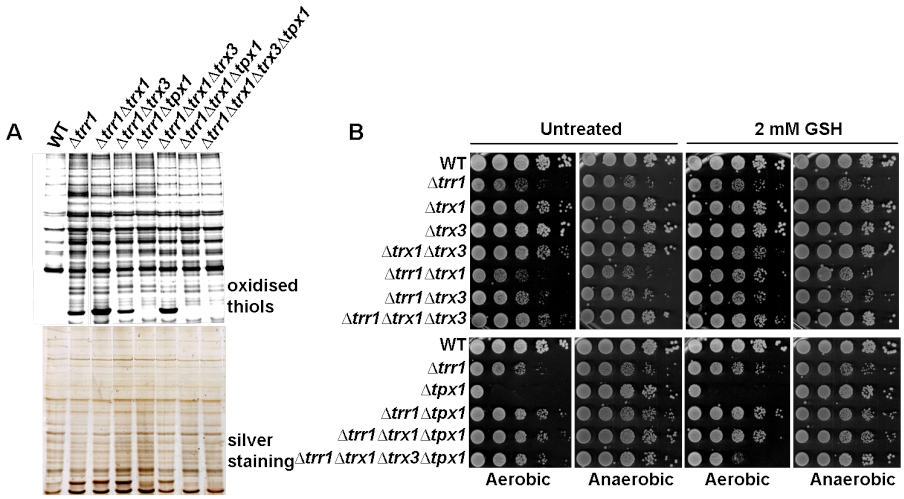

Figure 3.3: GSH partially restores the fitness of a Δ*trr1* strain. **A** Labelling of reversibly oxidised Cys for 1D electrophoresis. Free thiols in TCA protein extracts from strains 972 (WT), SG167 (Δ*trr1*), PG22 (Δ*trr1* Δ*trx1*), SG187 (Δ*trr1* Δ*trx3*), SG164 (Δ*trr1* Δ*tpx1*), SG185 (Δ*trr1* Δ*trx1* Δ*trx3*), SG170 (Δ*trr1* Δ*trx1* Δ*tpx1*), and SG219 (Δ*trr1* Δ*trx1* Δ*trx3* Δ*tpx1*) were alkylated with iodoacetamide. Upon reduction of oxidised thiols, resulting thiols were alkylated with a fluorescently labelled iodoacetamide derivative. Samples were analysed by fluorescent 1D electrophoresis (oxidised thiols) and with silver staining, as a control of protein loading. **B** GSH partially restores growth of *S. pombe* cells lacking Trr1. Exponentially growing cultures of 972 (WT), SG167 (Δ*trr1*),MJ15 (Δ*trx1*), SG189 (Δ*trx3*, SG260 (Δ*trx1* Δ*trx3*), PG22 (Δ*trr1* Δ*trx1*), SG187 (Δ*trr1* Δ*trx3*), SG185 (Δ*trr1* Δ*trx1* Δ*trx3*), MJ11 (Δ*tpx1*), SG164 (Δ*trr1* Δ*tpx1*), SG170 (Δ*trr1* Δ*trx1* Δ*tpx1*), and SG219 (Δ*trr1* Δ*trx1* Δ*trx3* Δ*tpx1*) were serial diluted and spotted on YE5S either untreated or treated with 2 mM GSH. Plates were grown under aerobic or anaerobic conditions as indicated.

3.2.1.3 GSH/Grx system is essential in cells lacking Trr1, unless they also lack the peroxiredoxin Tpx1

When trying to understand the overlapping roles between the GSH/Grx system and the Trx system, we decided to construct several mutant strains in order to check their phenotypes. We tried to construct the double deletions *trr1* and *gcs1* (*gcs1* codes for glutamate-cysteine ligase, the rate-limiting enzyme on the GSH bio synthesis), or *trr1* and *grx1*, however they resulted not viable. We were very surprised to find out that a viable Δ*trr1* Δ*grx1* was so because it contained a mutation which provoked the truncation of the gene coding for *tpx1*. With this information, we tried to construct a triple deletion mutant Δ*trr1* Δ*tpx1* Δ*grx1*, which in fact resulted viable.

All these double or triple deleted strains are anaerobic, however, adding GSH to the media partially restored the growth of Δ*trr1* Δ*trx1* Δ*grx1* and Δ*trr1* Δ*tpx1* Δ*grx1* (**figure 3.4**). Curiously, growth of strains devoid of Trr1 and Tpx1 (either by mutation or by gene deletion) was not equal in the tested conditions.

Importantly, a strain without both cytoplasmic Trx and Grx1 (Δ*trx1* Δ*trx3* Δ*grx1*) is viable only under anaerobic conditions. Since the main Trx substrate required for the aerobic growth of *S. pombe* is the peroxiredoxin Tpx1, it can be argued that lack of both cytoplasmic Trx and also Grx1 may affect the Tpx1 cycle, and this may be the reason for the anaerobiosis of the triple deleted strain. Thus, adding 2 mM GSH completely restores aerobic growth of a Δ*trx1* Δ*trx3* Δ*grx1* strain (**figure 3.4**).

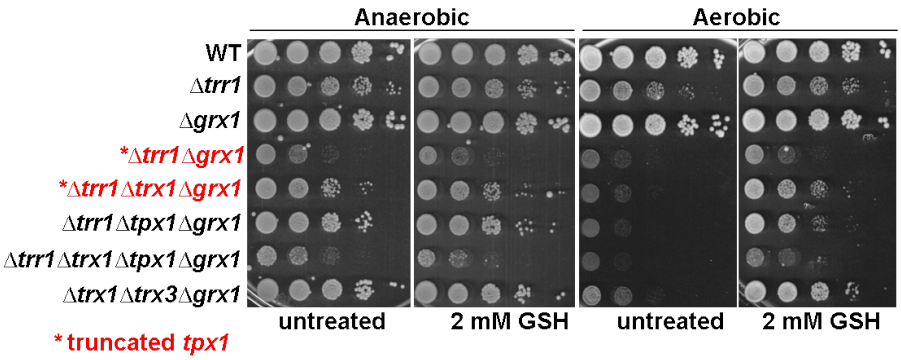

Figure 3.4: Fitness of *S. pombe* cells lacking *trr1* and *grx1*. Exponentially growing cultures of 972 (WT), SG167 (Δ*trr1*),SG180 (Δ*grx1*), SG195 (Δ*trr1* Δ*grx1*), SG211 (Δ*trr1* Δ*trx1* Δ*grx1*), SG270 (Δ*trr1* Δ*tpx1* Δ*grx1*), SG278 (Δ*trr1* Δ*trx1* Δ*tpx1* Δ*grx1*) and SB160 (Δ*trx1* Δ*trx3* Δ*grx1*) were serial diluted and spotted on YE5S either untreated or treated with 2 mM GSH. Plates were grown under aerobic or anaerobic conditions as indicated.

3.3 Characterization of *S. pombe* methionine sulphoxide reductases

Met is one of the aminoacids more prone to oxidation, either free in the cell or bound to proteins. Under mild oxidizing conditions, two enantiomeric forms of Met sulphoxide (Met-O) are generated, Met-*S*-O and Met-*R*-O. These can be reduced to Met again in a stereo-specific manner by Msrs, thus MsrA reduce the S form, whereas MsrB and free MsrB reduce the R form (in proteins and free in the cell, respectively). Stronger oxidizing conditions oxidise Met to the irreversible form of Met sulphone.

S. pombe contains two uncharacterised families of Msrs, Mxr1/MsrA and Mxr2/MsrB. In the manuscript presented in this results section, we show that Mxr1 is required to reduce free oxidized Met, whereas Mxr2 is not required for this function. We also show that, although their transcription levels are enhanced by H_2O_2, they are not required for survival upon oxidative stress. There is only one special case, when cells are limiting for Met, that Mxr1 is required for survival upon H_2O_2. Importantly enough, cells auxotrophic for Met are as sensitive as cells lacking to Pap1 to oxidative stress, what suggests that free Met acts as a first barrier in the defence to oxidative stress.

García-Santamarina S, Boronat S, Ayté J, Hidalgo E. Methionine sulphoxide reductases revisited: free methionine as a primary target of H_2O_2stress in auxotrophic fission yeast. Mol Microbiol. 2013 Dec;90(5):1113–24. DOI: 10.1111/mmi.12420

3.4 Characterization of *S. pombe* H_2O_2 scavengers

Previously in the laboratory, the Prx Tpx1 was characterized as the main H_2O_2 scavenger in aerobic conditions, thus cells lacking Tpx1 are only able to grow in plates under semi-anaerobic conditions. We found that the gene coding for TrxR, *trr1*, is a suppressor of the sensitivity to aerobic growth of Δ*tpx1* cells. We show in this results section, presented as a manuscript, that cells lacking Trr1 suppress the anaerobic phenotype, because they have constitutive active Pap1, which triggers the expression of up to 80 genes, among them, the *ctt1* gene (17-fold increase). Thus, we show that Ctt1 over-expression suffices to grow Δ*tpx1* cells under an aerobic atmosphere.

We also studied the potential role of other Trx-dependent Prxs (Gpx1, Pmp20, and BCP) in the detoxification of peroxides. We only found a secondary role for Gpx1 when extracellular peroxides are added.

An integrative genetic approach to study H_2O_2 scavenging in fission yeast

Sarela García-Santamarina[1], Isabel A. Calvo[1], Esther Paulo, Alba Domenech, José Ayté and Elena Hidalgo*

Oxidative Stress and Cell Cycle Group, Departament de Ciències Experimentals i de la Salut, Universitat Pompeu Fabra, C/ Dr. Aiguader 88, E-08003 Barcelona, Spain

*Corresponding author: Elena Hidalgo, Universitat Pompeu Fabra, C/ Dr. Aiguader 88, E-08003 Barcelona, Spain (elena.hidalgo@upf.edu; Tel: 34-93-316-0848; Fax: 34-93-316-0901)
[1]The first two authors contributed equally to this work

The main peroxiredoxin in *Schizosaccharomyces pombe*, Tpx1, is essential to sustain aerobic growth, and cells lacking this protein are only able to grow on solid plates under semi-anaerobic conditions. We have found that the gene coding for thioredoxin reductase is a suppressor of the sensitivity to aerobic growth of Δ*tpx1* cells, so that cells lacking both proteins are able to grow on solid plates in the presence of oxygen. We have investigated this suppression effect, and determined that it depends on the expression of catalase, which is constitutively expressed in Δ*trr1* cells in a transcription factor Pap1-dependent manner. A complete characterization of the repertoire of hydrogen peroxide scavenging activities in fission yeast suggests that Tpx1 is the only enzyme with sufficient sensitivity for peroxides as to control the low levels produced during aerobic growth, catalase being the next barrier of detoxification when the steady state levels of peroxides are increased in Δ*tpx1* cells. Gpx1, the only glutathione peroxidase encoded by the *S. pombe* genome, only has a secondary role when extracellular peroxides are added. Our study proposes non-overlapping roles for the different hydrogen peroxide scavenging activities of this eukaryotic organism.

Reactive oxygen species (ROS) such as superoxide and hydrogen peroxide (H_2O_2) are produced during aerobic growth mainly as by-products during the transfer of electrons in mitochondrial respiration. A battery of cellular activities scavenge superoxide and H_2O_2, so that an equilibrium between production and detoxification is achieved, reaching physiological, non-toxic steady-state levels of these ROS.

Regarding H_2O_2 detoxification, at least three families of enzymes cooperate to reach nanomolar intracellular levels: catalases, glutathione peroxidases (Gpxs) and thioredoxin peroxidases, also known as peroxiredoxins (Prxs). Catalases dismutase two molecules of H_2O_2, to generate water and oxygen at the expense of the reversible oxidation-reduction of iron at their heme group. Gpxs ant Prxs decompose H_2O_2 to water with the concomitant oxidation of two cysteine residues to a disulfide bond; reduction of the disulfide to the thiol form will require the participation of glutathione or thioredoxin, respectively, at the expense of reduced cofactor.

The *Schizosaccharomyces pombe* genome contains three genes coding for Prx isoforms (Tpx1, Pmp20 and BCP/SPBC1773.02c), one gene coding for a Gpx (Gpx1), and another one coding for catalase, Ctt1. While cells lacking *ctt1* (Mutoh *et al.*, 1999), *gpx1* or *pmp20* (Vivancos *et al.*, 2005) do not seem to display growth defects on aerobic plates, strain Δ*tpx1* cannot grow on solid agar unless semi-anaerobic conditions are used (Vivancos *et al.*, 2005; Jara *et al.*, 2007), which prompted us to hypothesize that Tpx1 is the main H_2O_2 scavenger during aerobic growth in fission yeast. It is worth pointing out that growth on aerobic plates is always more extreme to microbial cells than growth on liquid cultures: cells lacking Tpx1 are able to duplicate in liquid, while single cells cannot initiate colony formation on solid plates.

Gpxs and, especially, Prxs have been proposed to have an additional role in transmitting the H_2O_2-dependent oxidizing signal to transduction pathways, so that antioxidant responses can be triggered. In these signalling events, reversible oxidation of thiols in pathway components as an activation step cannot be achieved directly by H_2O_2, since reactivity of peroxide towards most cysteine residues is rather limited. Only proteins such as Prx1 and Gpxs have very high rate constants per H_2O_2, and may be able not only to sense and react with peroxides but also to transmit the signal and oxidize other secondary targets in signal transduction pathways (for a review, see (Winterbourn and Hampton, 2008). In particular,

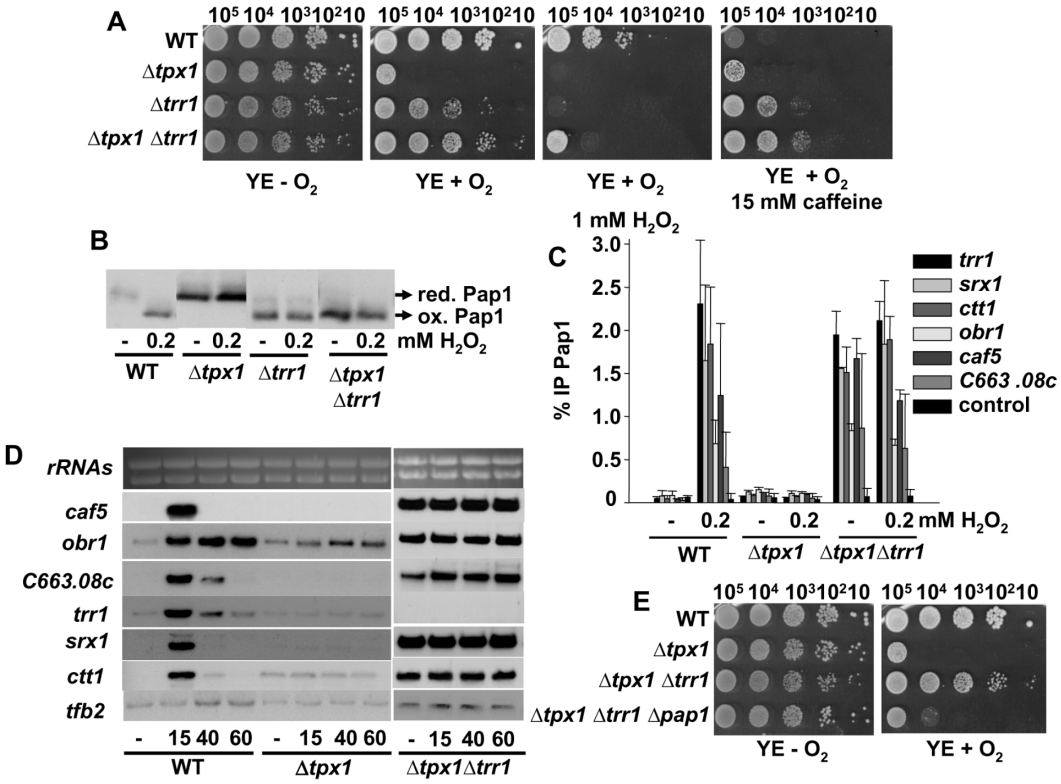

FIGURE 1. **Tpx1 is essential for aerobic conditions and the combination of the deletion of Trr1 and Tpx1 rescues the phenotype in a Pap1-dependent manner.** *A* Deletion of *trr1* supresses the aerobic growth defects of cells lacking Tpx1. Sensitivity to H_2O_2 and caffeine exposure. Strains 972 (WT), MJ11 (Δ*tpx1*), SG167 (Δ*trr1*) and SG164 (Δ*tpx1* Δ*trr1*) were grown in liquid YE media, and the indicated number of cells were spotted onto plates with or without 1 mM H_2O_2 and 15 mM caffeine. (B, C and D) Pap1 is active in *Δtrr1* cells in a Tpx1-independent manner. *B* *In vivo* oxidation of Pap1. Cultures of strains used in Fig. 1A were treated or not with 0.2 mM H_2O_2 for 5 min. Reduced/inactive (red.) and oxidized/active (ox.) Pap1 forms are indicated with arrows. *C* Oxidized/nuclear Pap1 is recruited to all Pap1-dependent promoters in Δ*tpx1* Δ*trr1* background prior to stress. Cultures of strains 972 (WT), MJ11 (Δ*tpx1*) and SG164 (Δ*tpx1* Δ*trr1*) were treated with 0.2 mM H_2O_2 for 5 min. ChIP experiments using anti-Pap1 antibody, were performed using primers covering only promoter regions of *trr1, srx1, ctt1, caf5, obr1* and *SPCC663.08c* genes. Primers of an intergenic region were used as a negative control (control). Error bars (SD) for all ChIP experiments were calculated from biological triplicates. *D* Constitutive activation of Pap1 dependent genes in Δ*tpx1* Δ*trr1* background. Cultures of strains used in Figure 1C were treated or not with 0.2 mM H_2O_2 for the indicated times. Total RNA was obtained and analysed by northern blot with probes for *trr1, srx1, ctt1, caf5, obr1* and SPCC663.08 c. Ribosomal RNA (rRNAs) and tfb2 are shown as loading controls. *E* Survival to anaerobic and aerobic conditions in YE media plates. Strains 972 (WT), MJ11 (Δ*tpx1*), SG164 (Δ*tpx1* Δ*trr1*) and SG224 (Δ*tpx1* Δ*trr1* Δ*pap1*) were grown in liquid YE media, and the indicated number of cells were spotted onto plates.

upon mild extracellular oxidative stress Tpx1 is an upstream activator of the transcription factor Pap1 (Bozonet *et al.*, 2005; Vivancos *et al.*, 2005), which then accumulates in the nucleus to induce up to 80 genes and develop an adaptation response (Chen *et al.*, 2008). Among the many genes triggered by oxidized Pap1 is *ctt1,* whose transcription is activated 17-fold in response to mild extracellular oxidative stress (Chen *et al.*, 2008). The activation of Pap1 can also be achieved by genetic ablation of the thioredoxin system in a H_2O_2-independent manner: cells lacking thioredoxin reductase, Trr1, display massive disulfide stress in an oxidized thioredoxin-dependent manner, and Pap1 is fully active under these conditions (Vivancos *et al.*, 2004; Garcia-Santamarina *et al.*, 2012).

Due to the prevalent role of Tpx1 not only in aerobic H_2O_2 scavenging but also in signalling towards the Pap1 pathway, we decided to confirm the first one by searching for suppressors of the aerobic growth defects of cells lacking Tpx1. We show here that over-expression of catalase, Ctt1, either after constitutive activation of the Pap1 pathway by deletion of the Trr1-coding gene or from a heterologous promoter, is able to rescue the limitation to grow on solid plates of cells lacking Tpx1. We also show that the ability of Δ*tpx1* to grow on semi-anaerobic plates depends on the presence of Ctt1, which is probably able to sense

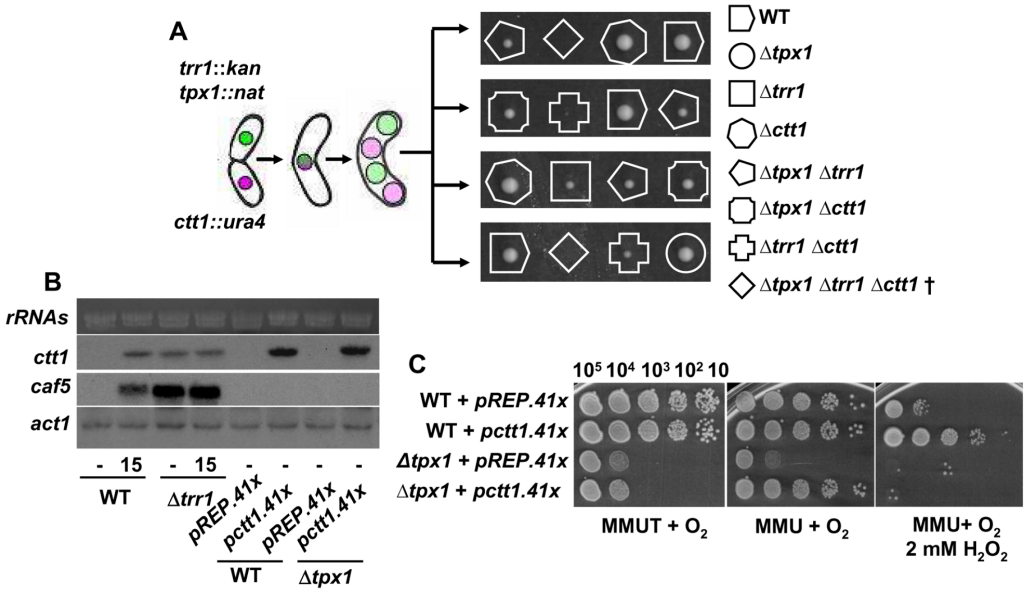

FIGURE 2. **Over-expression of catalase improve the phenotype of WT and Δ*tpx1* strains.** *A* Schematic representation of tetrad dissection. *B* Northern blot analysis of several Pap1-dependent genes of 972 (WT), SG167 (Δ*trr1*), PN513 (WT) and SG5 (Δ*tpx1*) over-expressing *pREP.41x* (053) and *pctt1.41x* (p418.41x). These strains were treated or not with 0.2 mM H_2O_2 for 15 min and were analysed as described in Figure 1D. *C* Sensitivity to H_2O_2 exposure of strains PN513 (WT) and SG5 (Δ*tpx1*) over-expressing *pREP.41x* and *pctt1.41x*. The survival of these strains was analyzed by sequential spotting as described in Figure 1A.

the enhanced steady state levels of peroxides in this strain background. Furthermore, Ctt1 is the main H_2O_2 scavenger when supplied extracellularly, while the other three putative peroxide detoxification activities, Gpx1, Pmp20 and BCP, do barely display a phenotype when multiple deletions accumulate. Our experiments demonstrate that in fission yeast Tpx1 is the first and only line of defence to control H_2O_2 generated during aerobic growth, while catalase has a major role controlling high levels of peroxides.

EXPERIMENTAL PROCEDURES

Yeast strains and growth conditions—The origins and genotypes of strains used in this study are outlined in Table 1. Cells were grown in rich medium (YE) or in synthetic minimal medium (MM) as described previously (Alfa *et al.*, 1993).

Plasmids—The *ctt1* and *atf1* coding sequences were PCR amplified from an *S. pombe* cDNA library by using primers specific for the *ctt1* and *atf1*-coding genes. *ctt1* was cloned into the *nmt* (no message in thiamine)-driven expression vector pREP.41x (053) (Maundrell, 1993) to yield plasmid p418.41x. *nmt* promoter was *PstI/XhoI* digested from plasmid p418.41x and this fragment was replaced by a *PstI/XhoI* digested PCR amplification of 797 bp upstream from the ATG of *sty1* gene, to yield plasmid p419 (p*sty1'::ctt1*). *atf1* was cloned into the *S. pombe* vectors pRep.41x. A DNA fragment coding for the HA epitope was inserted between the *nmt* promoter and the atf1 ORFs of the plasmid to yield p151.41x (pHA-atf1.41x).

H_2O_2 sensitivity assay—For survival on solid plates, *S. pombe* strains were grown, diluted and spotted in YE5S agar plates or minimal media plates, containing 0.3, 0.5 and 1 mM H_2O_2 or 15 mM caffeine, as described previously (Calvo *et al.*, 2009).

Preparation of S. pombe TCA extracts and immunoblot analysis—To analyze the *in vivo* redox state of Pap1, trichloroacetic acid (TCA) extracts were prepared as described elsewhere (Vivancos *et al.*, 2005). Pap1 was immuno-detected using polyclonal anti-Pap1 antibodies (Vivancos *et al.*, 2004).

Chromatin immuno-precipitation—The *in vivo* binding of Pap1 to stress promoters was analyzed as described previously (Calvo *et al.*, 2012), using polyclonal antibodies against Pap1 (Vivancos *et*

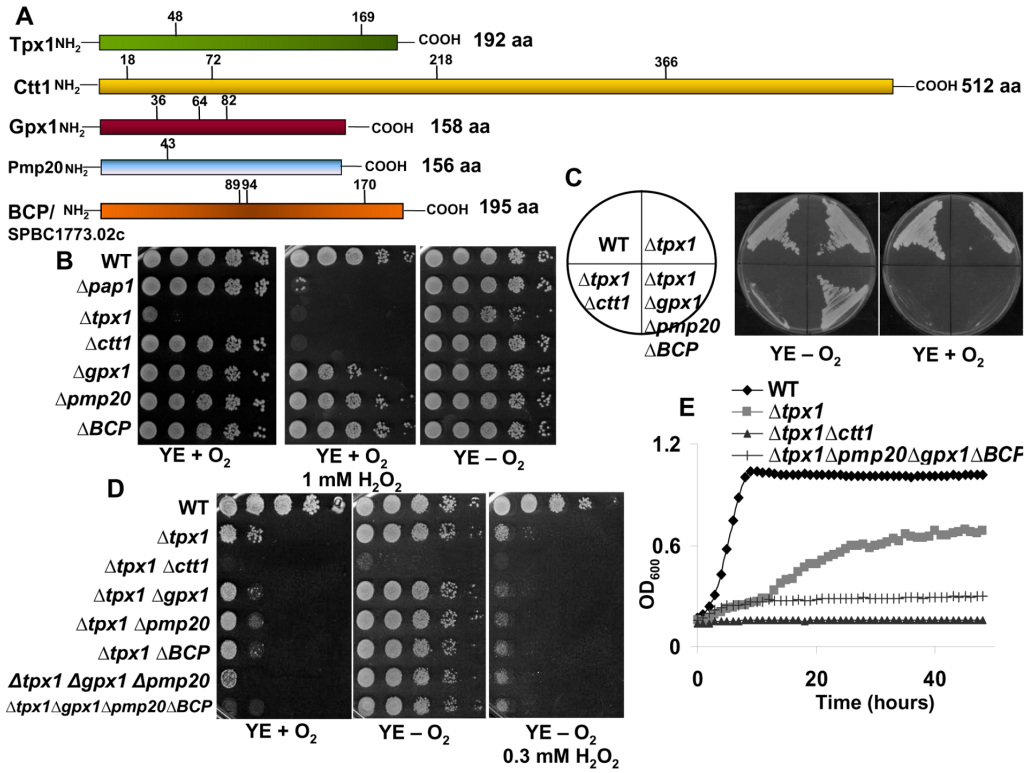

FIGURE 3. **The peroxiredoxin Tpx1 and Catalase perform important roles in H_2O_2 detoxification.** *A* Schematic representation of some H_2O_2 scavengers, Ctt1, Gpx1 and Prx of *S. pombe*. *B* Serial dilutions from cultures of strains 972 (WT), AV25 (*Δpap1*), MJ11 (*Δtpx1*), CN513 (*Δctt1),* EA37 *(Δgpx1),* EA49 *(Δpmp20)* and SG253 *(ΔBCP)* were spotted in YE media plates with or without 1 mM H_2O_2. Sensitivity to anaerobic, aerobic conditions and H_2O_2 exposure were analysed as described in Figure 1A. *C* Cuadruple mutant, SG259 strain (*Δtpx1 Δgpx1 Δpmp20 ΔBCP)* grows better than double mutant, SG267 (*Δtpx1 Δctt1)* in anaerobic conditions. *D* Sensitivity to 0.3 mM H_2O_2 exposure of strains 972 (WT), MJ11 (*Δtpx1*), SG267 (*Δtpx1 Δctt1),* SG232 (*Δtpx1 Δgpx1),* SG256 (*Δtpx1 Δpmp20),* SG258 (*Δtpx1 ΔBCP)*, SG255 (*Δtpx1 Δgpx1 Δpmp20) and* SG259 (*Δtpx1 Δgpx1 Δpmp20 ΔBCP).* The survival of these strains was analyzed by sequential spotting as described in Figure 1A. *E* Growth curves of cultures of strains used in Fig 3C. Log-phase cultures at an OD_{600} of 0.1 were grown into microculture wells. Growth was monitored by measuring OD_{600} every 10 min at 30º for 48 h. (*Δmet6*), SG136 (*Δmxr1 Δmet6*), SG143 (*Δmxr2 Δmet6*), and SG137 (*Δmxr1 Δmxr2 Δmet6*) were serial diluted and spotted on MM plates containing 0.08 mM Met either without or with the indicated concentrations of H_2O_2.

al., 2004).

RNA analysis—Total RNA from *S. pombe* minimal media cultures was obtained, processed and transferred to membranes as described previously (Castillo *et al.*, 2002). Membranes were hybridized with [α-32P] dCTP-labelled *caf5*, *obr1*, *SPCC663.08c*, *trr1*, *srx1* or *ctt1* probes, containing the complete open reading frames. We used ribosomal RNA or *tfb2* as loading controls.

Tetrads dissection—A tiny bit of asci was ressuspended in 1 ml of sterile water, and then 15 µl were streaked on a YE5S plate. Asci were identified and with the use of a micromanipulator they were moved away from the streak onto a line parallel to the streak. Asci were allowed to break their walls by incubating them at 37ºC for 4 hours. Spores from each ascus were micromanipulated so that all four spores from each ascus was again in a streak line. Plates were incubated at 30ºC under anaerobiosis to allow germination of the spores.

Growth curves in liquid—To measure cellular growth, we used an assay based on automatic measurements of optical densities for small (100 µl) cell cultures. Cells were grown to an OD_{600} of 0.5 under continuous shaking in Erlenmeyer flasks and then diluted to an OD_{600} of 0.1. 100 µl of the diluted cultures (treated or not with the indicated amounts of stressors) were placed into a 96-well non-coated polystyrene microplate covered with an adhesive plate seal. A Power Wave microplate scanning spectrophotometer (Bio-Tek) was used to

obtain the growth curves. The OD_{600} was automatically recorded using Gen5 software. The software was set as follows: OD was measured at 600 nm, incubation temperature was kept at 30ºC, the microplates were subjected to continuous shaking and the readings were done every 10 min during 48 hours.

Measurement of intracellular H_2O_2 levels—Cells were grown at OD600 ~0.3 in YE5S and relative intracellular peroxide levels were determined using the redox-sensitive fluorescent probe DHR123 (Invitrogen), using a second dye, iodurum propide (IP) (Sigma-Aldrich), to differentiate between living and dead cells as described (Zuin *et al.*, 2010).

H_2O_2 scavenging by total protein extracts—Cell cultures were grown aerobically to OD600~0.5. Cells were pelleted, and pellets were washed twice with PBS 1X. Pellets were then resuspended in 300 µl of 50 mM potassium phosphate buffer, pH 7.8, and disrupted with glass beads during 5 min in a vortex in a cold chamber. 0.25 µg/µl of protein extracts for each condition were then treated with 10 µM H_2O_2. At the indicated times, 50 µl of the protein extract were mixed with 25 µl of 0.02 mg/ml horseradish peroxidise (HRP) (Sigma) and 25 µl of 200 µM amplex red (AR, Molecular Probes) (Seaver and Imlay, 2001), and fluorescence was measured at 530 nm λ_{ex} 530 nm and λ_{em} 590 nm. A blank was obtained with untreated samples, and this value was subtracted from the rest of measured fluorescence values. Relative fluorescent values were calculated using the maximum fluorescence value for each condition.

RESULTS

Deletion of trr1 suppresses the aerobic growth defects of cells lacking Tpx1—We had previously demonstrated that cells lacking Tpx1 are able to grow aerobically in liquid media, but they are unable to grow on solid plates under normal aerobic conditions, since probably the oxygen tension is higher for individual cells exposed to the atmosphere than to the oxygen dissolved in aqueous solutions (Jara *et al.*, 2007). Cells deficient in *trr1,* the only *S. pombe* gene coding for a thioredoxin reductase, are able to grow on aerobic plates (Fig. 1A), but they display pronounced sensitivity to the presence of extracellular peroxides (Fig. 1A). Surprisingly, cells deleted in both the Tpx1- and the Trr1-coding genes do not longer display defects to grow on solid plates, what indicates that deletion of *trr1* suppresses the phenotypic defect of Δ*tpx1* cells (Fig. 1A).

Tpx1 and Trr1 had been reported to antagonistically regulate the activity of the antioxidant transcription factor Pap1: Δ*trr1* cells display constitutive oxidation/activation of Pap1 (Vivancos *et al.*, 2004), while in cells lacking Tpx1 the transcription factor Pap1 cannot sense H_2O_2 stress (Bozonet *et al.*, 2005; Vivancos *et al.*, 2005). Constitutive oxidation/activation of Pap1 can be easily tested through the resistance to caffeine (Benko *et al.*, 1998; Calvo *et al.*, 2009). The double mutant Δ*tpx1* Δ*trr1* displays all the hallmarks of constitutive Pap1 activation: it is resistant to caffeine (Fig. 1A), Pap1 is constitutively oxidized according to non-reducing electrophoresis (Fig. 1B), the transcription factor is bound to promoters even prior to stress as determined by chromatin immuno-precipitation (Fig. 1C) and the Pap1-dependent gene expression program is engaged in the absence of peroxides (Fig. 1D).

We then tested whether constitutive Pap1 activation is required for the suppression effect of *trr1* deletion on Δ*tpx1* strain. As shown in Fig. 1E, a triple mutant Δ*tpx1* Δ*trr1* Δ*pap1* is no longer able to grow on solid plates. This suggests that one or several of the Pap1-dependent gene products is able to rescue the aerobic growth defects of cells lacking Tpx1.

Over-expression of catalase is sufficient to support aerobic growth in cells lacking Tpx1—We then speculated than one or several of the four putative H_2O_2-scavenging activities left in cells lacking Tpx1, namely catalase/Ctt1, Gpx1 or the Prxs Pmp20 and BCP/SPBC1773.02c, could be over-expressed in Δ*tpx1* Δ*trr1* in a Pap1-dependent manner, and that would suppress the aerobic growth defect of cells lacking Tpx1. According to transcriptomic studies of cells exposed to H_2O_2, only the *ctt1* gene responds to sub-toxic doses of peroxides, those known to activate Pap1 (Chen *et al.*, 2008), which pointed to catalase as the activity overcoming the lack of Tpx1. We first tried to obtain a triple Δ*tpx1* Δ*trr1* Δ*ctt1* strain, but tetrad analysis demonstrated that cells lacking all three genes were not viable (Fig. 2A). We then transformed wild-type cells and cells lacking Tpx1 with a plasmid containing the *ctt1* gene under the control of the thiamine-repressible *nmt* promoter. As shown in Fig. 2B, upon thiamine depletion both plasmid-containing cells types (wild-type and Δ*tpx1*) express the *ctt1* mRNA. These levels of expression were sufficient to enhance the tolerance of wild-type cells to grow in the presence of H_2O_2 (Fig. 2C). As we were expecting, those high catalase levels accomplished after thiamine withdrawal were also sufficient to suppress the growth defects of Δ*tpx1* cells on solid plates (Fig. 2C, central panel).

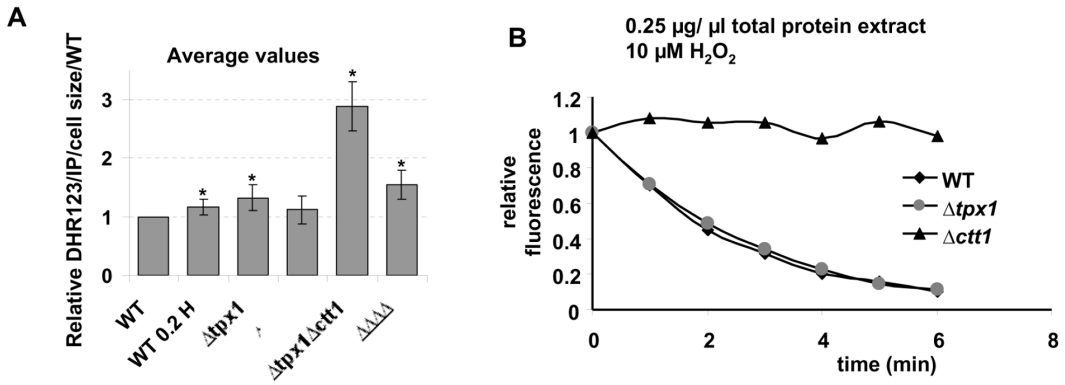

FIGURE 4. **Some mutants display an increase of intracellular ROS levels.** *A* Relative intracellular H_2O_2 levels of wild-type (972) with or without of H_2O_2 and mutant strains, MJ11 (Δ*tpx1*), CN513 (Δ*ctt1),* SG267 (Δ*tpx1* Δ*ctt1), and* SG259 (Δ*tpx1* Δ*gpx1* Δ*pmp20* Δ*BCP)* were analysed as indicated in Materials and Methods. Significant differences between wild-type and mutant cells were determined by the Student's t-test. *p,0.05 compared with untreated wild-type cells. Data in both panels were obtained from three independent experiments and are expressed as mean±SEM. *B* Protein extracts obtained from strains wild-type (972), MJ11 (Δ*tpx1*), and CN513 (*Δctt1*) were treated with 10 µM H_2O_2. At various time points after addition of H_2O_2, fluorescence (equivalent to H_2O_2 concentration) was measured as described in Materials and Methods.

Only Tpx1 and Ctt1 have significant roles in H_2O_2 scavenging—Given the previous experiments, Tpx1 and catalase having specific roles in H_2O_2 detoxification, we decided to determine whether the other three putative peroxide scavengers, namely Gpx1, Pmp20 and BCP, also had a role in H_2O_2 scavenging (Fig. 3A). We compared the growth of each one of the five deletion strains on aerobic plates containing or not H_2O_2. As shown in Fig. 3B, only Tpx1 is required for aerobic growth, whereas deletion of *ctt1* renders cells extremely sensitive to the presence of exogenously added H_2O_2. Regarding Gpx1, Pmp20 and BCP, only Δ*gpx1* cells display a mild sensitivity to H_2O_2.

Tpx1 seems to be the only enzyme able to detoxify peroxides arising from aerobic metabolism. However, the enhanced levels of H_2O_2 of Δ*tpx1* cells can be partially scavenged by either Ctt1 or combination of Gpx1, Pmp20 and BCP, as observed by the enhanced anaerobic growth phenotypes of Δ*tpx1* Δ*ctt1* and Δ*tpx1* Δ*gpx1* Δ*pmp20* Δ*BCP* strains (Fig. 3C, 3D and 3E).

We used a fluorescent dye, DHR123, to measure relative levels of peroxides in different mutant strains. As shown in Fig. 4A, a small but significant increase in the levels of intracellular peroxides could be measured in cells lacking Tpx1, but not Ctt1. The increment, however, was almost 3-fold in cells lacking both Tpx1 and Ctt1, what confirms the idea that in the absence of the peroxiredoxin Tpx1 the enhanced levels of peroxides are partially scavenged by catalase. We also measured the activity of Tpx1 and Ctt1 in total extracts from wild-type and mutant strains, and showed that the sensitivity of the method (10 µM H_2O_2 in the assay) only allowed us to follow the H_2O_2 scavenging activity of catalase.

Over-expression of catalase is the main cellular strategy for the adaptation to H_2O_2 stress—Our data confirms the role of Tpx1 in general H_2O_2 homeostasis during aerobic growth and in activation of signalling cascades. Catalase, on the contrary, only participates in peroxide scavenging when the levels of H_2O_2 arise in a Δ*tpx1* background, or upon addition of peroxides to the growth media. Up-regulation of the *ctt1* gene seems to be a common theme in the cellular adaptation to peroxides. In fission yeast, mild concentrations of H_2O_2 activate the Tpx1-Pap1 pathway, which trigger transcription of around 50 genes meant to mount an adaptive response to peroxides, one of them being *ctt1* (Chen *et al.*, 2008) (Fig. 5A). Higher doses of peroxides, however, temporarily halt Pap1 activation while maximally trigger a cascade of phosphorylations which end up activating the MAP kinase Sty1 and its transcription factor Atf1/Pcr1; the transcription of up to 300 genes is then activated, and again *ctt1* is at the top of the list (Chen *et al.*, 2008) (Fig. 5A).

To test the prevalent role of catalase up-regulation in the response of fission yeast to peroxides, we tested whether over-expression of Ctt1 from an episomal plasmid and using a strong and constitutive promoter could be sufficient to complements some of the H_2O_2 defects of cells mutated in components of either the Sty1-Atf1 or the Pap1 pathways. As shown in Figure 5B, over-

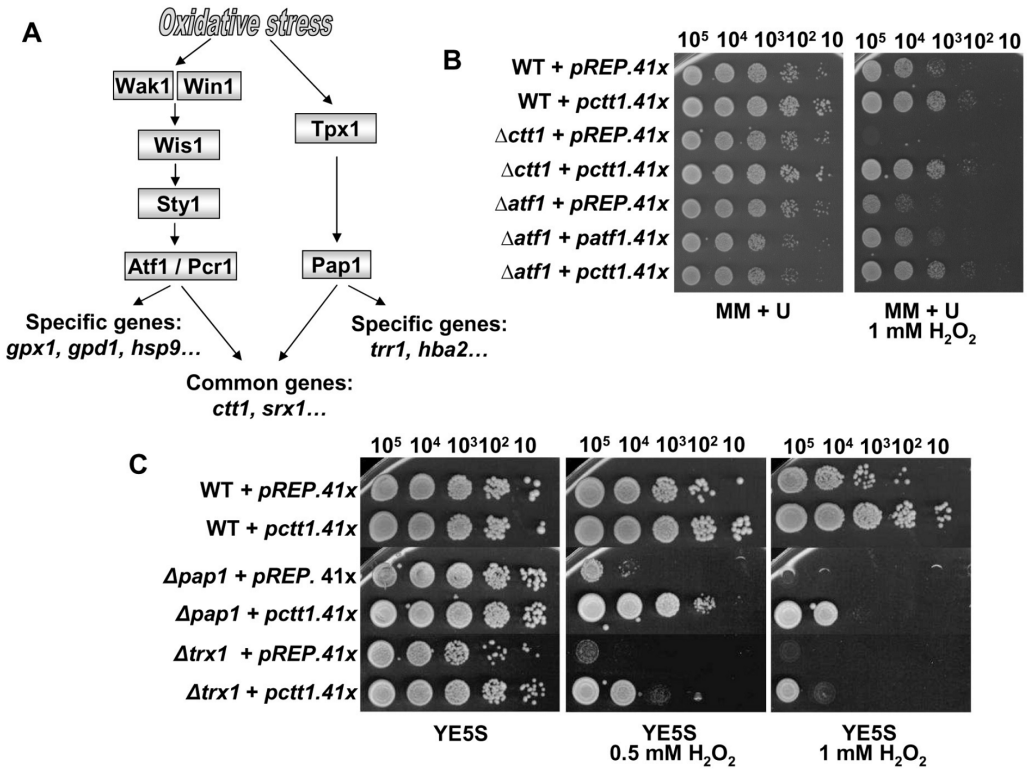

FIGURE 5. **Over-expression of catalase decreases the sensitivity to H_2O_2 in Δ*ctt1*, Δ*atf1*, Δ*pap1 and* Δ*trx1* strains.** *A* Scheme of the activation of the MAP kinase Sty1 and specific sensor Pap1 pathways by oxidative stress. Other upstream and downstream components of the pathways are indicated. *B* Sensitivity to H_2O_2 exposure of strains PN513 (WT), EP197 (Δ*ctt1*), and EP193 (Δ*atf1*) over-expressing *pREP.41x* (053) and *pctt1.41x* (p419.41x). These strains were grown in liquid MMU media, and the indicated number of cells were spotted with or without 1 mM H_2O_2 and was analysed as described in Figure 1A. *C* Serial dilutions from cultures of strains PN513 (WT), IC1 (*Δpap1*) and MJ2 (Δ*trx1*) over-expressing *pREP.41x* (053) and *pctt1.41x* (p419.41x) were spotted onto YE5S plates with or without 0.5 and 1 mM H_2O_2. The survival of these strains was analyzed by sequential spotting as described in Figure 1A.

expression of catalase was sufficient to fully complement the sensitivity to peroxides of cells lacking the transcription factor Atf1. A similar, although more limited, complementation could be observed in cells lacking Pap1 (Fig. 5C). Interestingly enough, over-expression of Ctt1 was sufficient to partially restore the growth on H_2O_2-containing plates of cells lacking Trx1, the main cytosolic thioredoxin, required to recycle the peroxiredoxin Tpx1 (Fig. 5C).

DISCUSSION

Aerobic organisms express a battery of antioxidant activities to counteract the toxic effects of reactive oxygen species. Often, several enzymes seem to be redundant in terms of their antioxidant activity. In an attempt to provide an integrative view of H_2O_2 scavenging in fission yeast, we have performed an *in vivo* analysis of cells lacking each one of the five proteins encoded by the fission yeast genome meant to scavenge peroxides: catalase (Ctt1), the glutathione peroxidase Gpx1, and the peroxiredoxins Tpx1, Pmp20 and BCP. We have confirmed here the essential role of Tpx1 not only in signalling towards the Pap1 pathway, but specially in aerobic H_2O_2 scavenging. Searching for suppressors of the aerobic growth defects of cells lacking Tpx1, we have found that deletion of *trr1* gene is able to restore growth on aerobic plates due to the constitutive activation of Pap1 and concomitant overexpression of catalase, Ctt1. Furthermore, Ctt1 is the main H_2O_2 scavenger when peroxides are supplied extracellularly, while cells lacking any of the other three putative peroxide detoxification activities, Gpx1, Pmp20 and BCP, do not display sensitivity to peroxides. Our experiments demonstrate that in *S. pombe* the peroxiredoxin Tpx1, with high sensitivity for peroxides, is the first line of defence

to control H_2O_2 generated during aerobic metabolism, while catalase has a major role controlling high levels of peroxides. Probably, the activity of Tpx1 can be saturated upon high doses of H_2O_2 (either by temporary shut down of NADH reducing power, required for its recycling, or by over-oxidation and inactivation to sulfinic acid) (Bozonet *et al.*, 2005; Vivancos *et al.*, 2005). Under these circumstances of severe H_2O_2 stress, catalase may be better suited to become the predominant peroxide scavenger. Indeed, over-expression of Ctt1 seems to be a critical strategy to survive a severe threat of H_2O_2: a plasmid constitutively expressing catalase is sufficient to totally or partially complement the oxidative stress sensitivity of several mutants of the H_2O_2-responding Sty1 and Pap1 pathways.

In bacteria, similar studies have provided genetic and biochemical evidences to demonstrate that putative H_2O_2 scavengers really perform such a role, and whether they have overlapping functions (for a review, see (Mishra and Imlay, 2012). In particular, the main peroxiredoxin of *Escherichia coli,* AhpC, was demonstrated to act as the primary scavenger of peroxides generated endogenously during aerobic growth, while catalase may specifically act when the peroxiredoxin becomes saturated (Seaver and Imlay, 2001). Then, why are *E. coli* cells lacking AhpC able to grow under aerobic conditions on solid plates? Interestingly enough, both in *S. pombe* (Fig. 3 and Fig. 4A) and in *E. coli,* catalase seems to have a back up role in cells lacking the peroxiredoxin Tpx1 and AhpC, respectively. In fact, expression of catalase in *E. coli* is dependent of the main sensor of peroxides and transcription factor OxyR. Thus, cells lacking AhpC display higher levels of intracellular peroxides, and OxyR-dependent over-expression of catalase, which allows aerobic growth (Seaver and Imlay, 2001). In *S. pombe*, since *ctt1* activation at low doses of peroxides is Pap1-dependent and Pap1 activation is Tpx1-dependent, cells lacking Tpx1 cannot activate *ctt1* transcription and therefore cannot grow under aerobic conditions. The fact that fission yeast uses Tpx1 as both a H_2O_2 scavenger and as a sensor and transducer of the oxidative signal impedes the over-expression of catalase in a Δ*tpx1* background.

It is surprising to observe that the only over-expression of catalase is sufficient to rescue the sensitivity to peroxides of Δ*atf1* or Δ*pap1* cells, even though these two pathways are able to trigger many different genes in response to peroxides. Regarding the Sty1-Atf1 pathway (Fig. 5A), it is worth mentioning that several other types of life-threatening environmental stresses, such as osmotic stress, heat shock or nutrient deprivation, are also able to activate this MAP kinase signalling pathway, what could explain why hundreds of genes are up-regulated while over-expression of only catalase is sufficient to counteract the H_2O_2–mediated toxicity.

It may sound like a good strategy to increase the levels of catalase to become more tolerant to oxidative threats, even prior to H_2O_2 imposition. However, excessive amounts of catalase may be deleterious for growth, either by decreasing the steady-state levels of H_2O_2 and minimizing signalling events, or by activating other signalling cascades. Indeed, we have determined that constitutive over-expression of catalase induces the iron starvation response, probably through sequestering available iron during reconstitution of the heme group (data not shown). Constitutive activation of the iron starvation response can halt cell growth, by repressing the transcription of many genes coding for essential iron-containing proteins (for a review, see (Labbe *et al.*, 2007).

Acknowledgements—This work was supported by the Spanish Ministry of Economy and Competitiveness, Grant BFU2012-32045 and FEDER, by the Spanish program Consolider-Ingenio 2010 Grant CSD 2007-0020, and by SGR2009-196 from Generalitat de Catalunya (Spain) to E.H. E. H. and J.A. are recipients of ICREA Academia Awards (Generalitat de Catalunya).

REFERENCES

Benko, Z., Sipiczki, M., and Carr, A.M. (1998). Cloning of caf1+, caf2+ and caf4+ from Schizosaccharomyces pombe: their involvement in multidrug resistance, UV and pH sensitivity. Mol.Gen.Genet. 260, 434-443.

Bozonet, S.M., Findlay, V.J., Day, A.M., Cameron, J., Veal, E.A., and Morgan, B.A. (2005). Oxidation of a eukaryotic 2-Cys peroxiredoxin is a molecular switch controlling the transcriptional response to increasing levels of hydrogen peroxide. J Biol Chem 280, 23319-23327.

Calvo, I.A., Gabrielli, N., Iglesias-Baena, I., Garcia-Santamarina, S., Hoe, K.L., Kim, D.U., Sanso, M., Zuin, A., Perez, P., Ayte, J., and Hidalgo, E. (2009). Genome-wide screen of genes required for caffeine tolerance in fission yeast. PLoS One 4, e6619.

Chen, D., Wilkinson, C.R., Watt, S., Penkett, C.J., Toone, W.M., Jones, N., and Bahler, J. (2008). Multiple pathways differentially regulate global oxidative stress responses in fission yeast. Mol Biol Cell 19, 308-317.

Garcia-Santamarina, S., Boronat, S., Calvo, I.A., Rodríguez-Gabriel, M., Ayte, J., Molina, H., and Hidalgo, E. (2012). Is oxidized thioredoxin a major trigger for cysteine oxidation? Clues from a redox proteomics approach. Antioxid Redox Signal (in press).

Jara, M., Vivancos, A.P., Calvo, I.A., Moldon, A., Sanso, M., and Hidalgo, E. (2007). The peroxiredoxin Tpx1 is essential as a H2O2 scavenger during aerobic growth in fission yeast. Mol Biol Cell 18, 2288-2295.

Labbe, S., Pelletier, B., and Mercier, A. (2007). Iron homeostasis in the fission yeast Schizosaccharomyces pombe. Biometals 20, 523-537.

Maundrell, K. (1993). Thiamine-repressible expression vectors pREP and pRIP for fission yeast. Gene 123, 127 -130.

Mishra, S., and Imlay, J. (2012). Why do bacteria use so many enzymes to scavenge hydrogen peroxide? Arch Biochem Biophys 525, 145-160.

Mutoh, N., Nakagawa, C.W., and Yamada, K. (1999). The role of catalase in hydrogen peroxide resistance in fission yeast Schizosaccharomyces pombe. Can J Microbiol 45, 125-129.

Seaver, L.C., and Imlay, J.A. (2001). Alkyl hydroperoxide reductase is the primary scavenger of endogenous hydrogen peroxide in Escherichia coli. J Bacteriol 183, 7173-7181.

Vivancos, A.P., Castillo, E.A., Biteau, B., Nicot, C., Ayte, J., Toledano, M.B., and Hidalgo, E. (2005). A cysteine-sulfinic acid in peroxiredoxin regulates H2O2-sensing by the antioxidant Pap1 pathway. Proc Natl Acad Sci U S A 102, 8875-8880.

Vivancos, A.P., Castillo, E.A., Jones, N., Ayte, J., and Hidalgo, E. (2004). Activation of the redox sensor Pap1 by hydrogen peroxide requires modulation of the intracellular oxidant concentration. Mol Microbiol 52, 1427-1435.

Winterbourn, C.C., and Hampton, M.B. (2008). Thiol chemistry and specificity in redox signaling. Free Radic Biol Med 45, 549-561.

Zuin, A., Carmona, M., Morales-Ivorra, I., Gabrielli, N., Vivancos, A.P., Ayte, J., and Hidalgo, E. (2010). Lifespan extension by calorie restriction relies on the Sty1 MAP kinase stress pathway. Embo J 29, 981-991.

García-Santamarina et al. Supplementary data

Includes: Supplementary Table S1

Add caption

Strain	Phenotype	Origin
972	*h*$^-$	[1]
MJ11	*h*$^-$ *tpx1::kanMX6*	This work
SG167	*h*$^+$ *trr1::natMX6*	[2]
SG164	*h*$^-$ *tpx1::natMX6 trr1::kanMX6*	This work
SG224	*h*$^+$ *pap1::ura4+ tpx1::natMX6 trr1::kanMX6 ura4-D18 ade6-M210 leu1-32*	This work
HM123	*h*$^-$ *leu1-32*	[3]
SG5	*h*$^+$ *tpx1::natMX6 leu1-32*	This work
AV25	*h*$^-$ *pap1::kanMX6*	This work
CN513	*h*$^-$ *ctt1::ura4+ ura4-D18 ade6-M216 leu1-32*	[4]
EA37	*h*$^-$ *gpx1::kanMX6 leu1-32*	[3]
EA49	*h*$^-$ *pmp20::KanMX6 leu1-32*	[3]
SG253	*h*$^-$ *SPBC1773.02c/BCP::hph*	This work
SG267	*h*$^+$ *ctt1::ura4+ tpx1::kanMX6 ura4-D18*	This work
SG232	*h*$^+$ *tpx1::natMX6 gpx1::kanMX6*	This work
SG256	*h*$^+$ *pmp20::kanMX6 tpx1::natMX6*	This work
SG258	*h*$^-$ *SPBC1773.02c/BCP::hph tpx1::natMX6*	This work
SG255	*h*$^-$ *pmp20::kanMX6 tpx1::natMX6 gpx1::kanMX6*	This work
SG259	*h*$^+$ *SPBC1773.02c/BCP::hph tpx1::natMX6 pmp20::kanMX6 gpx1::kanMX6*	This work
PN513	*h- ura4-D18 leu1-32*	This work
EP197	*h- ctt1::natMX6 ura4-D18 leu1-32*	This work
EP193	*h- atf1::natMX6 leu1-32*	This work
IC1	*h- pap1::ura4+ ura4-D18 leu1-32*	[5]
MJ2	*h- trx1::kanMX6 ura4-D18 leu1-32*	[2]

[1] Leupold U. Genetical methods for *Schizosaccharomyces pombe*. Methods in Cell Biology 1970 4:169-177.

[2] García-Santamarina S, Boronat S, Calvo IA, Rodríguez-Gabriel, M, Ayté J, Molina H, Hidalgo E. Is oxidized thioredoxin a major trigger for cysteine oxidation? Clues from a redox proteomics approach. Antioxidants & redox signaling 2012 [Epub ahead of print].

[3] Vivancos AP, Castillo EA, Biteau B, Nicot C, Ayté J, Toledano, MB, Hidalgo E. A cysteine-sulfinic acid in peroxiredoxin regulates H_2O_2-sensing by the antioxidant Pap1 pathway. PNAS 2005 102(25):8875.

[4] Nakagawa CW, Yamada K, Mutoh N. Two distinct upstream regions are involved in expression of the catalase gene in *Schizosaccharomyces pombe* in response to oxidative stress. J Biochem. 1998 Jun;123(6):1048-54.

[5] Calvo IA, GarcÃa P, AytÃ© J, Hidalgo E. The transcription factors Pap1 and Prr1 collaborate to activate antioxidant, but not drug tolerance, genes in response to H_2O_2. Nucleic Acids Res. 2012 Jun;40(11):4816-24.

3.5 Identification and homoeostasis of irreversible protein modifications: protein carbonylation

3.5.1 Troubleshooting of different protocols to study protein modifications by carbonylation

3.5.1.1 Fluorescent derivatives to label protein carbonyls

As described in section 1.4.2 of the Introduction, the most frequent way of detecting protein carbonyls generally include the specific reaction of the carbonyl group with a hydrazine or a hydrazide derivative, being the classical one dinitrophenylhydrazine (DNPH), which reacts with carbonyl groups to form stable 2,4-dinitrophenyl (DNP) hydrazone products. These can be then immunodetected with specific antibodies [363].

While the use of this reagent perfectly works for 1D electrophoresis, difficulties arise at the time of performing more complicated techniques such as 2D electrophoresis. In the case of using DNPH, carbonylated proteins will appear as spots upon immunodetection in a membrane. In order to be identified, they have to be matched with their protein of origin in a stained gel (silver stained, coomassie blue stained or fluorescent stained) loaded in parallel. To avoid the use of two different gels for 2D electrophoresis (one for total protein staining and the other one for immunoblotting), we decided to set up a protocol which included the use of fluorescent hydrazine or hydrazide derivatives to specifically label protein carbonyls. Theoretically, this would allow us to use a single 2D electrophoresis gel both for detecting protein carbonyls and for quantifying protein levels. In this way, carbonyl-labelled proteins will appear as fluorescent spots, and upon scanning for fluorescence, the same gel can be later stained for protein concentrations by any of the different available technologies (silver staining, coomassie-staining or fluorescent staining).

To set up the protocol, we initially tested fluorescein-5-thiosemicarbazide (FTC), a fluorescent semicarbazide, to label and detect protein carbonyls upon 1D electrophoresis (**figure 3.5, upper panel**) [369]. This reagent was also tested for 2D electrophoresis, however, since this is a charged molecule (it contains a -COOH), it was impossible to match the FTC-labelled spots with the spots reflecting their protein concentration, even using a specific software for image-analysis (PDQuest, BioRad). The explanation for this is that probably carbonylation is not affecting the same to all molecules of a protein (i.e. it will be always a small percentage of carbonylated protein mixed with another percentage of unmodified protein). Upon labelling with FTC, with a molecular weight of 421 g/mol, that small percentage of carbonylated molecules of a protein, will migrate differently that the bigger percentage of molecules of the same protein in the 2D gel. Therefore, spots from proteins labelled with FTC will appear displaced from visible spots belonging to the

same protein when checking for protein concentration, even when using highly sensitive fluorescent staining.

To overcome this difficulty, a different fluorescent derivative was checked, BODIPY Fl Hydrazide (Bodipy) (**figure 3.5, lower panel**). Even though its molecular weight is 306 g/mol, this is not a charged molecule. Therefore, in this case, protein carbonyls were labelled and appeared as spots upon 2D electrophoresis, which were easily matched with the spots reflecting protein concentration.

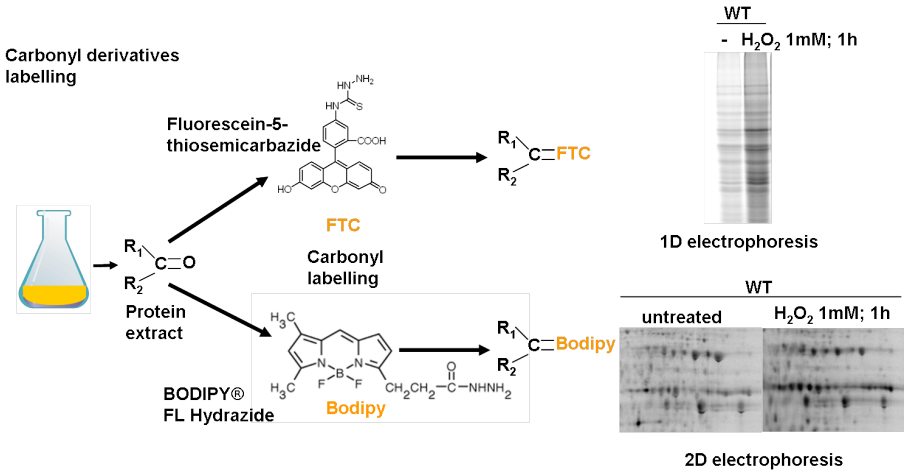

Figure 3.5: Use of fluorescents to label protein carbonyls. Upon obtaining a protein extract, two different types of reagents are used depending on the purpose of the detection. Fluorescein-5-thiosemicarbazide (FTC) is used for carbonyl detection in 1D electrophoresis (upper panel). As an example, an experiment of FTC-labelled protein extracts from wild-type cells untreated (-) or treated with 1 mM H_2O_2 for 1 hour is shown. BODIPY Fl Hydrazide (Bodipy) is used for labelling protein carbonyls if 2D electrophoresis is to be performed (lower panel). As an example, an experiment of Bodipy-labelled protein extracts from wild-type cells untreated or treated with 1 mM H_2O_2 for 1 hour is shown.

3.5.1.2 2D gel electrophoresis is not an appropriate technique to detect and quantify protein carbonylation

Theoretically, performing 2D electrophoresis for studying protein carbonylations would allow us to identify and quantify which particular proteins would be carbonylated upon an environmental or a genetic condition at the proteome level of the fission yeast. However, a major intrinsic limitation of the technique provoked us to change the strategy. As it is shown in **figure 3.6**, up to 22 proteins were identified upon MS analysis of a single-excised spot. This made impossible to discern which protein/s from the list were those modified with the fluorescent label. Even being this possible, due to the lack of specificity of this technique, an added difficulty would be the normalization of protein carbonylation to protein expression levels.

Different strategies were tested to improve protein separation, both in the first and in the second dimension.

In the first dimension of a 2D electrophoresis, proteins are separated on the bases of differences on their pI, the pH at which they do not have net charge. To improve protein-separations in the this dimension, we used large (17 cm) immobilized pH gradient (IPG) strips with narrow pH intervals. In the second dimension, proteins are separated based on their size. Improvements in the this dimension also included the use of large gels (up to 17 cm).

Since the *S. pombe* proteome is amongst the smaller eukaryotic proteomes, we thought that these improvements would suffice to obtain good protein separations. However, this was not the case, and it was still impossible to obtain one protein (or at least a list with two or three proteins) from excised spots. This led us to conclude that the use of 2D electrophoresis is not appropriate for studying protein carbonylation at the proteome level.

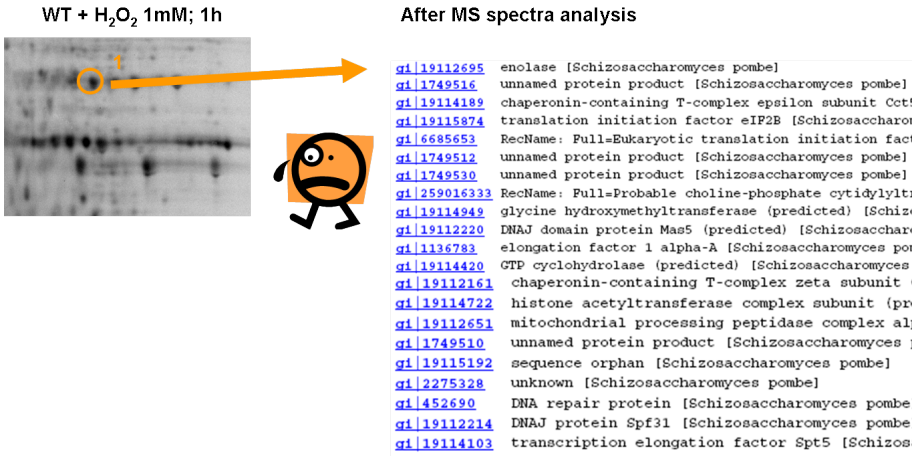

Figure 3.6: Tenths of proteins can be identified in a single spot of a 2D electrophoresis gel. BODIPY Fl Hydrazide (Bodipy) was used for labelling protein carbonyls in a protein extract from H_2O_2 treated wild-type cells. Upon analysis with a specific software, one spot, theoretically corresponding to a single protein, was excised for protein identification (left panel). After MS analysis, 22 proteins were identified from the excised spot (right panel).

3.5.1.3 Testing a gel-free approach for the proteomic study of protein carbonylation

Once established that 2D electrophoresis is not an appropriate technique for the identification of protein carbonyls, we decided to try a gel-free approach with the same purpose. We considered bovine serum albumin (BSA) a good protein to set up the protocol. BSA is a very well known protein, and easily available in the laboratory. Also, a recent publication described a pattern of protein carbonylation for BSA upon *in vitro* metal-catalysed oxidation (MCO) [381].

As described in **figure 3.7 A**, two different situations were compared. Either BSA was kept reduced the whole protocol, and used as a control, or it was *in vitro* oxidised by a metal-catalysed system, $FeCl_3$ and ascorbic acid (MCO treatment) [382]. Both samples were treated the same along the protocol. To perform the oxidation, the initial buffer containing the BSA was changed by dialysis. Upon oxidation (or 'non-oxidation' in the case of the control sample), EDTA was added to halt the reaction. The MCO system ($FeCl_3$ and ascorbic acid) was removed by dialysing again the sample. At this time, carbonyl derivatization was performed with DNPH, and TCA precipitation was used to remove excess DNPH. Pellets were re-suspended, reduced, alkylated, and trypsinized with two different enzymes, chemotrypsin and trypsin, for MS analysis. The reason for using two different enzymes for protein digestion, is that lysines are among the amino acids more prone to carbonylation upon oxidative stress. Therefore, carbonyls at lysines will not be recognized by trypsin, generating long-sized peptides, which will not easily 'fly' in the mass spectrometer.

Labelling of protein carbonyls was followed by 1D electrophoresis and immunodetection with α-DNP antibodies (**figure 3.7 B**).

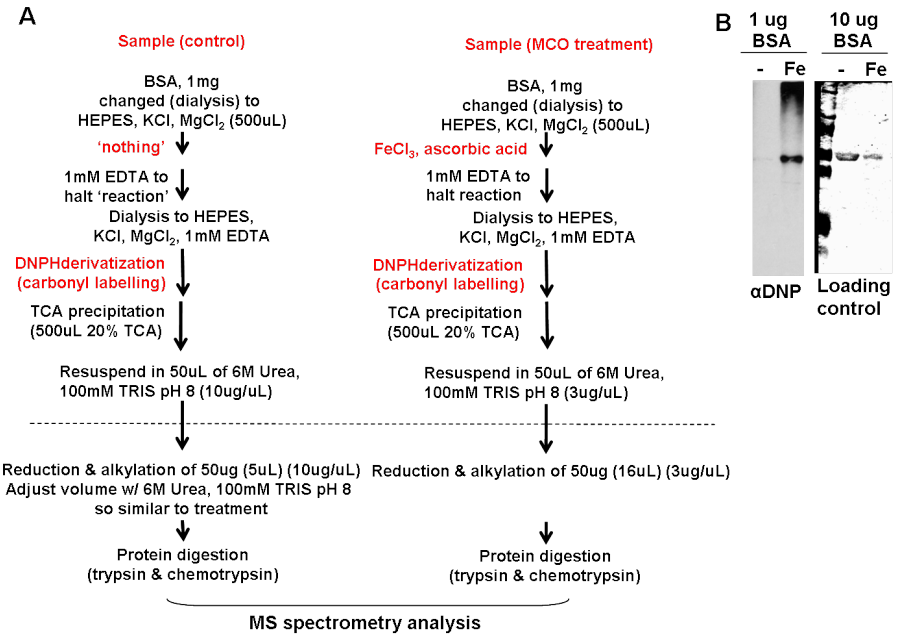

Figure 3.7: **A.** Bovine serum albumin (BSA) was tested for a gel-free carbonylation assay. 1 mg of either reduced sample (control) or oxidised sample (MCO treatment) were digested and analysed by MS upon following the steps marked with arrows (see text for details). **B.** Carbonyl-labelling test. 1 ug of reduced (-) or metal-catalysed oxidized BSA (Fe) was checked for protein oxidation by labelling protein carbonyls with DNPH and immunodetection with DNP antibodies (αDNP). 10 ug of reduced (-) or metal-catalysed oxidized (Fe) BSA were used for Ponceau staining as a loading control.

We started the optimization of a gel-free approach in order to facilitate the identification and quantification of protein carbonyls upon oxidative stress. However, changes

of amino acid residues by protein carbonylation are not 'easy' modifications. Many are the residues that may be carbonylated upon an oxidative stress burst (see section 1.1.2.3 in the Introduction). Moreover, the complexity of the sample increases if one considers that probably protein digestion will be only partial. Also, at the time of performing search algorithms, many are the modifications that must be introduced in the software in order to match peptides with protein identifiers in the data bases (**figure 3.8**).

Having into account this high level of complexity, we were unable to obtain any valuable data from the MS analysis of MCO BSA. Therefore, establishing a good protocol to identify protein carbonyls at the proteome level is still an unresolved matter.

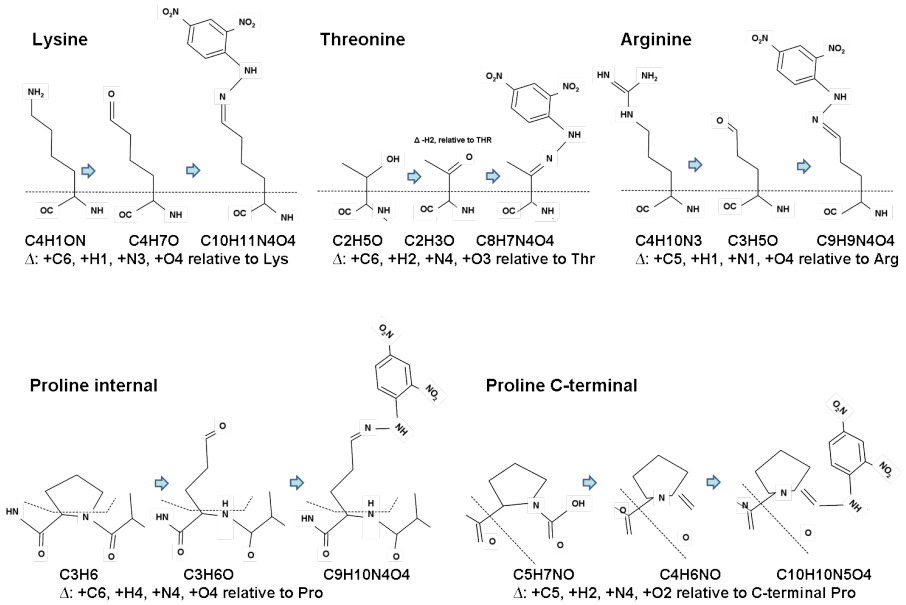

Figure 3.8: Modifications of different amino acids upon protein carbonylation and derivation with DNPH. Δ represents mass increase of the oxidized peptide derivatized with DNPH when compared with the non-oxidized aminoacid

3.5.2 Protein homoeostasis upon oxidative damage

3.5.2.1 Screening of *S. pombe* deletion mutants related with degradation pathways

Irreversible protein modifications are a frequent outcome of ROS reactivity with biomolecules. These irreversible modifications provoke protein unfolding and either their targeting for degradation, or in the worst of the situations, their accumulation as toxic aggregates.

A controversy exists regarding how oxidative unfolded proteins are targeted and degraded by cellular proteases. Some reports suggest that ubiquitination, a common tag

which labels unfolded proteins for degradation, is not involved in this process, being in this case only the 20S proteasome the protease required for their degradation (reviewed in [310] and [311]). However, almost the same amount of reports suggest the requirement of the ubiquitin tag to label proteins prior to their degradation by the 26S proteasome [312] [150] [313] [314] [315] [296].

Having into account these premises, we decided to study which pathways in *S. pombe* regulate the levels of carbonylation in proteins after H_2O_2 stress. To do so, we performed a screening of 67 *S. pombe* deletion mutants related with different routes of protein catabolism, including components of the UPR, the ERAD, ubiquitination-related proteins (E2 conjugating enzymes, RING finger, HECT domain, and F-box E3 ligases, ubiquitin fused with ribosome, ubiquitin-related proteins), proteasome components, deubiquitinases, chaperones, translation, and transcription factors (**table 3.1**).

Most of these deletion strains were derived from a *S. pombe* deletion collection (Bioneer, [383]). Many were PCR-verified and crossed with a wild-type strain to eliminate auxotrophies. All mutants were selected due to their relationship with protein catabolism, and this info was obtained either from published data or inferred from protein databases. Other considered variables were gene induction upon oxidative stress, heat shock or both [56] [85].

Table 3.1. Mutants used in the screening for degradation of carbonylated proteins

Protein	Function	Origin
UPR/ERAD		
SPAC167.01/Ppk4	Member of the ribonuclease 2-5A family, contains a protein kinase domain. Low similarity to *S. cerevisiae* Ire1p, which is a protein kinase and a site-specific endoribonuclease involved in the UPR	Bioneer
SPBC17D11.02c/Hrd1	HMG-coA reductase degradation, RING E3 involved in ERAD	Bioneer
SPBC14F5.07/Doa10	RING E3, has weak similarity to *S. cerevisiae* Ssm4p, which is an E3 involved in Alpha2p degradation, associated with the UPR	Bioneer
SPAC1565.08/Cdc48	Protein with high similarity to *S. cerevisiae* Cdc48p, which is an ATPase required for homotypic membrane fusion, member of the ATPase family associated with various cellular activities, contains a cell division protein 48 (CDC48) N-terminal domain	cdc48-353 Yanagida M. [384]
SPAC2C4.15c/ Ubx2	Protein that interacts with Cdc48p and binds multiubiquitin	Bioneer
SPBC21C3.11/Ubx4	Protein that interacts with Cdc48p and binds multiubiquitin	Bioneer
UBIQUITINATION		
E2 conjugating		
Ubc13	Protein involved in post-replication DNA repair and resistance to DNA damaging agents	Bioneer
SPAC1250.03/Ubc14	Protein with high similarity to *S. cerevisiae* Ubc4p, which is an E2 involved in degradation of short-lived and abnormal proteins	Bioneer
SPBC1198.09 / Ubc16	Protein with moderate similarity to ubiquitin-conjugating enzyme E2D2 (human UBE2D2), which marks cellular proteins for degradation	Bioneer
SPAC18B11.07c/Ubc2/Rhp6	E2 that ubiquitinates histone H2B, which has a positive role in transcription elongation by RNA polymerase II, also involved negative regulation of heterochromatin silencing by affecting histone H3 methylation	Bioneer

Protein	Function	Origin
SPBC119.02/Ubc4	E2 required for ubiquitin chain elongation, mitotic transition, and cytokinesis. Mediates the selective degradation of short-lived and abnormal proteins	Ubc4P61S Seino H. [385]
E3 ligases		
RING finger		
SPBC19C7.02/Ubr1	Required for ubiquitin-proteasome dependent degradation of Mei2p	Bioneer
SPAC15A10.11/Ubr11	Member of the ATP-dependent Clp protease adaptor protein ClpS family, and the putative zinc finger in N-recognin family	Bioneer
SPAC6B12.07c	Member of the SPX (SYG1, Pho81 and XPR1) domain containing family	Bioneer
SPBC2A9.04c/San1	Homologous to *S. cerevisiae* San1, which is involved in the proteasome-dependent degradation of aberrant nuclear proteins	Bioneer
SPBC947.10Â /Dsc1	Homologous to *S. cerevisiae* Tul1, which is involved in ubiquitinating and sorting membrane proteins that contain polar transmembrane domains to multivesicular bodies for delivery to the vacuole for quality control purposes	Bioneer
SPAC2F3.16	Protein with a region of moderate similarity to human RCHY1, which is a ubiquitin ligase that interacts with the androgen receptor (human AR) and with TIP160 (human HTATIP)	Bioneer
SPBP8B7.23	Zinc finger protein of unknown function	Bioneer
SPBC29A3.03c	Protein of unknown function	Bioneer
SPAC11E3.05	Protein containing five WD domains (WD-40 repeat), which may mediate protein-protein interactions	Bioneer
HECT domain		
SPAC167.07c	Protein homologous to *S. cerevisiae* Hul5, which is an E4 with opposing roles to Ubp6p, a branched polyubiquitin protease; required for retrograde transport of misfolded proteins during ERAD	Bioneer
SPAC12B10.01c/Ufd4	Protein homologous to *S. cerevisiae* Ufd4, which interacts with Rpt4p and Rpt6p, two subunits of the 19S particle of the 26S proteasome	Bioneer
SPAC11G7.02 / Pub1	Ubiquitin ligase, involved in regulating Cdc25p and leucine uptake	Bioneer
SPBC16E9.11c/Pub3	Putative ubiquitin ligase that may be functionally redundant with Pub1p, contains a HECT domain, a C2 domain, and three central WW domains	Bioneer
F-BOX domain		
SPAC4D7.03 / Pop2	Protein involved in Cig2 degradation.	Bioneer
SPAC6F6.02c / Pof5	Protein of unknown function	Bioneer
SPBC3H7.06c / Pof9	Similar to *S. cerevisiae* YBR280C, involved in chromosome condensation	Bioneer
SPAC29E6.01 / Pof11	Protein with low similarity to beta-transducin repeat containing, which is a subunit of the Ikappa B-ubiquitin ligase complex that binds HIV-1 Vpu and inhibits NF-kB activation	Bioneer
SPAC13D6.01 / Pof14	Protein that binds to and decreases Erg9 activity in vitro, involved in ergosterol biosynthesis	Bioneer
Fusion with ribosome		
SPAC11G7.04 / Ubi1	Ubiquitin fusion protein	Bioneer
SPAC589.10c/Ubi5	Ubiquitin fusion protein	Bioneer
Ubi-related proteins		
SPCC548.04/Urm1	Protein with moderate similarity to S. cerevisiae Urm1p, which is a ubiquitin-related protein that is conjugated to other proteins by Uba4p	Bioneer
SPAC1486.02c / Ucp14	Protein containing a UBA (ubiquitin associated) or TS-N domain	Bioneer
PROTEASOME		
SPBC4.07c/ mts2	Essential ATPase subunit of the 19S regulatory complex of the 26S proteasome	Colin Gordon [386]

Protein	Function	Origin
SPBC16G5.01/mts3	Regulatory subunit of the 26S proteasome, involved in the ATP-dependent degradation of ubiquitinated proteins. Involved in chromosome segregation and required for the degradation of ubiquitin-conjugated proteins	Colin Gordon [387]
SPAC1782.01 / Ecm29	Protein with weak similarity to *S. cerevisiae* Ecm29p, which associates proteasome 19S regulatory particles with 20S core particle forming the 26S proteasome	Bioneer
SPCC1682.16 / Rpt4	Protein with high similarity to *S. cerevisiae* Rpt4p, which is a component of the 19S regulatory cap complex of the 26S proteasome complex	Bioneer
SPAC26A3.16 / Dph1	Protein involved in the spindle checkpoint pathway, binds polyubiquitinated protein conjugates	Bioneer
DEUBIQUITINASES		
SPAC328.06/ Ubp2	Protein with low similarity to *S. cerevisiae* Ubp2p, which cleaves at the C terminus of ubiquitin	Bioneer
SPBP8B7.21/Ubp3	Protein with weak similarity to ubiquitin specific protease 12 (ubiquitin hydrolyzing enzyme 1, human USP12)	Bioneer
SPBC18H10.08c/Ubp4	Protein that acts late in the proteolytic pathway in conjunction with the 26S proteasome. Plays a role in avoiding DNA overreplication	Bioneer
SPCC188.08c/Ubp5	Protein with moderate similarity to *S. pombe* Ubp21p, which is a ubiquitin-specific protease that may regulate Prp4p function	Bioneer
SPAC6G9.08/Ubp6	Protease that recognizes and hydrolyzes a peptide bond at the C-terminal glycine of ubiquitin.Component of the 26S proteosome. Interacts with Rpn1.	Bioneer
SPAC23G3.08c/Ubp7	Protein with weak similarity to ubiquitin specific protease 16 (human USP16), which deubiquitinates histone H2A and H2B	Bioneer
SPAC13A11.04c/Ubp8	Protein with low similarity to *S. cerevisiae* Ubp8p, involved in protein deubiquitination	Bioneer
SPBC1703.12/Ubp9	Protein with low similarity to ubiquitin-specific protease 3 (human USP3), which removes ubiquitin from ubiquitin-conjugated proteins	Bioneer
SPBC19C2.04c/ Ubp11	Protein with low similarity to *S. cerevisiae* Ubp8p, which is a ubiquitin C-terminal hydrolase	Bioneer
SPBC6B1.06c/Ubp14	Protein with low similarity to human USP5, which acts in deubiquitination	Bioneer
SPCC1682.12c/Ubp16	Protein with low similarity to deubiquitinating enzyme 1 (mouse Dub1)	Bioneer
SPAC27F1.03c/Uch1	Protein with low similarity to mouse Uchl3, which is involved in swallowing control by the central nervous system via neuron maintenance	Bioneer
SPBC409.06 / Uch2	Primary deubiquitinating enzyme associated with the 26S proteasome	Bioneer
SPAC24C9.14/Otu1	Member of the ovarian tumor (OTU)-like cysteine protease family	Bioneer
SPAC1952.03/Otu2	Member of the ovarian tumor (OTU)-like cysteine protease family	Bioneer
SPAC19B12.10/Sst2	Suppressor of ste12, required for vacuolar sorting of carboxypeptidase through the multivesicular body	Bioneer
SPAC31G5.13/Pad1/Rpn11	Subunit of the 26S proteasome, required for the degradation of ubiquitin-conjugated proteins and for proper centromere function	Colin Gordon [388]
CHAPERONES/ HSPs		
SPBC1734.11/Mas5	Protein highly similar to *S. cerevisiae* Ydj1p, which acts in numerous cellular events including protein import into mitochondria and ER, member of the DnaJ central domain (4 repeats) and C-terminal region families	Bioneer
SPBC530.03c/ Bag102	Member of the Bcl-2-associated athanogene 1	Bioneer
SPBC947.09	Protein with similarity to *E. coli* Hsp31; member of the DJ-1/ThiJ/PfpI superfamily, which includes human DJ-1 involved in Parkinson's disease	Bioneer

Protein	Function	Origin
SPAC5H10.02c	Protein with similarity to *E. coli* Hsp31; member of the DJ-1/ThiJ/PfpI superfamily, which includes human DJ-1 involved in Parkinson's disease	Bioneer
SPAC4G9.19	Protein containing a DnaJ domain, which are part of chaperone (protein folding) system that mediates interaction with heat shock proteins	Bioneer
SPAP8A3.04c/Hsp9	Heat shock-induced protein	Bioneer
SPBC3E7.02c/Hsp16	Heat shock protein that may be regulated by Ras1p	Bioneer
SPCC63.13	Protein containing a DnaJ domain, which are part of chaperone (protein folding) system that mediates interaction with heat shock proteins	Bioneer
SPAC13G7.02c/Ssa1	Member of the Hsp70 family, which are stress-induced protein chaperones	Bioneer
TRANSLATION/TF		
SPAC637.07/Moe1	Protein required for generation of a mitotic spindle and microtubule dynamics, component of the Moe1p-Mal3p-Int6p complex which functions in microtubule organization and chromosome stability	Bioneer
SPBC1105.14/Rsv2	Protein containing two C2H2 type zinc finger domains, which bind nucleic acids, has weak similarity to *S. cerevisiae* Rpn4p, which is a proteasome regulatory particle subunit that binds DNA and is a positive regulator of proteasome gene expression	Bioneer

To perform the screening, we treated cells (wild-type and deletion mutants) with high concentrations of H_2O_2 (2.5 mM H_2O_2) for long times (4 or 5 hours), to allow extensive protein carbonylation. Upon this stress, we analysed different variables:

(i) Protein carbonylation: in this case, we correlated increased carbonylation levels with decreased protein turnover. We decided to use this assay because by looking at protein carbonylation levels we are looking only to those proteins modified by oxidation.

(ii) Sensitivity to H_2O_2 in plates: we expect that deletion mutants with decreased protein turnover display higher sensitivity to H_2O_2, when compared with a wild-type strain.

(iv) Survival to H_2O_2 in liquid: strains are grown in liquid, either in untreated or treated conditions. Then, survival is checked by plating the cells. In this case, we expect that deletion mutants leading to decreased protein degradation rates will survive worse than a wild-type strain upon the stress.

(v) Lag times in liquid cultures before and after stress: we expect to find higher lag times for those mutants leading to decreased protein degradation rates upon stress, when compared with a wild-type strain.

(iii) Sensitivity to heat (37°C) in plates: we expect a cross-talk between mutants involved in protein turnover in the two types of stresses (heat shock and H_2O_2).

Due to space limitations, I am not showing the entire sets of data obtained from this screening, however in **table 3.2** there is a summary of the main results obtained from the screening, and in the subsections below a description of some of the most interesting results is presented.

Table 3.2. Results of the screening of strains checked for degradation of carbonylated proteins

Protein	Carbonylation	Survival plates	Sensitivity plates	Sensitivity 37°C	Lag-time (liquid)
UPR/ERAD					
Ppk4	**Decreased**	**As WT**	**As WT**	**No**	**As WT**
Hrd1	**As WT**				
Doa10	**As WT**	**As WT**	**As WT**		**Increased**
Cdc48 (ts)	**As WT**				
Ubx2	**As WT**				
Ubx4	**Decreased**	**Increased**	**As WT**	**No**	**As WT**
UBIQUITINATION					
E2 conjugating					
Ubc13	**As WT**				
Ubc14	**Increased**	**Diminished**	**Increased**	**Yes**	**Increased**
Ubc16	**As WT**				
Ubc2	**Decreased**	**Increased**	**Diminished**	**No**	**As WT**
Ubc4 (ts)	**Increased**				
E3 ligases					
RING finger					
Ubr1	**Decreased**	**Increased**	**Diminished**	**Yes**	**As WT**
Ubr11	**Decreased**	**As WT**	**As WT**	**No**	**As WT**
SPACB12.07c	**As WT**				
San1	**Decreased**	**Increased**	**Diminished**	**No**	**Decreased**
Dsc1	**As WT**				
SPAC2F3.16	**As WT**				
SPBP8B7.23	**As WT**				
SPAC29A3.03c	**As WT**				
SPAC11E3.05	**As WT**				
HECT domain					
SPAC167.07C	**Decreased**	**Increased**	**Decreased**	**No**	**Decreased**
Ufd4	**As WT**				
Pub1	**Decreased**	**Increased**	**Diminished**	**Yes**	**Decreased**
Pub3	**As WT**				
F-BOX domain					
Pop2	**As WT**	**Increased**	**Diminished**		**As WT**
Pof5	**As WT**				**Increased**
Pof9	**As WT**				**As WT**
Pof11	**As WT**	**As WT**	**As WT**		**Increased**
Pof14	**As WT**				**Increased**
Fusion ribosome					
Ubi1	**Decreased**	**As WT**	**As WT**		**Decreased**
Ubi5	**WT**	**Increased**	**Diminished**		
Ubi-related proteins					
Urm1	**As WT**				
Ucp14	**Decreased**	**Increased**	**Diminished**		**Decreased**
PROTEASOME					
mts2	**As WT**				
mts3	**As WT**				
Ecm29	**As WT**			**No**	
Rpt4	**Decreased**	**Increased**	**Diminished**		**Decreased**
Dph1	**As WT**	**As WT**	**As WT**		
DEUBIQUITINASES					
Ubp2	**Decreased**	**As WT**	**As WT**	**No**	**Increased**
Ubp3	**As WT**	**As WT**	**As WT**	**No**	**Decreased**
Ubp4	**Decreased**	**As WT**	**As WT**	**No**	**Increased**
Ubp5	**As WT**	**As WT**	**As WT**	**No**	**As WT**
Ubp6	**Decreased**	**As WT**	**As WT**	**No**	**As WT**
Ubp7	**As WT**	**As WT**	**As WT**	**No**	**Decreased**
Ubp8	**As WT**	**As WT**	**As WT**	**No**	**As WT**
Ubp9	**As WT**	**As WT**	**As WT**	**No**	**As WT**
Ubp11	**As WT**	**As WT**	**As WT**	**No**	**As WT**
Ubp14	**As WT**	**As WT**	**As WT**	**No**	**As WT**
Ubp16	**Decreased**	**Increased**	**Diminished**	**No**	**Decreased**

Protein	Carbonylation	Survival plates	Sensitivity plates	Sensitivity 37°C	Lag-time (liquid)
Uch1	**As WT**	**As WT**	**As WT**	**No**	**Decreased**
Uch2	**As WT**	**As WT**	**As WT**	**No**	**As WT**
Otu1	**Decreased**	**As WT**	**As WT**	**No**	**As WT**
Otu2	**Increased**	**As WT**	**As WT**	**No**	**Increased**
Sst2	**As WT**	**Diminished**	**Increased**	**Yes**	**Increased**
Rpn11	**As WT**				
CHAPERONES					
Mas5	**Decreased**	**Increased**	**Diminished**	**Yes**	**Increased**
Bag102	**As WT**				
SPBP947.09	**As WT**				
SPAC5H10.02c	**As WT**				
SPACG9.19	**As WT**				
Hsp9	**As WT**				
Hsp16	**As WT**				
SPCC63.13	**As WT**				
Ssa1	**As WT**	**As WT**	**As WT**	**No**	**As WT**
TRANSLATION/TF					
Moe1	**Increased**	**Decreased**	**Increased**		**Decreased**
Rsv2	**As WT**	**Decreased**	**As WT**		**Decreased**

3.5.2.2 Lack of Ubc14, an E2 conjugating enzyme, leads to decreased protein degradation upon oxidative stress in *S. pombe*

E2 conjugating enzymes are required in the ubiquitination process, since they contain an UBC domain for E3 ligases binding. These proteins catalyse the covalent attachment of ubiquitin to target proteins, or, when acting with HECT domain E3s, they transfer the activated ubiquitin to a high energy E3∼ ubiquitin intermediate, which is then conjugated to the substrate.

Since these proteins are involved in the conjugation of ubiquitin to substrates, we expected to find accumulation of carbonylated proteins upon stress in some of the E2 deleted mutants. This would reflect lack of ubiquitination of E2 substrates, and therefore decreased protein degradation. In our screening, we checked *S. pombe* deletion mutants for Ubc1, -2, -4, -13, -14, -15, and -16 (**tables 3.1** and **3.2**).

From these, clear phenotypes were found for *ubc2*, *ubc4*, and *ubc14* deleted *S. pombe* cells. Ubc2 and Ubc4 were previously shown to participate in intracellular protein quality control processes in *S. cerevisiae* [275] [313] [280] [316], and Ubc4 in *S. pombe* [285]. Accordingly, we found increased carbonylation leves upon H_2O_2 when the Ubc4 is impaired (*ubc4* in *S. pombe* is essential, for checking this strain in the screening we used a termo-sensitive (ts) mutant, which grows as a wild-type at 25°C, but that behaves as a deletion mutant at 37°C). However, in the case of Δ*ubc2*, we unexpectedly found decreased carbonylation levels upon oxidative stress, which may correlate with increased protein turnover, since this strain was also less sensitive to H_2O_2 in plates, and survived better than a wild-type upon oxidative stress. We speculate that in the absence of Ubc2 a compensatory effect (i.e. increased levels of Ubc4) may be the reason for the enhanced degradation of oxidized proteins.

Increased carbonylation levels, together with higher sensitivity to H_2O_2, less survival in liquid upon stress, and higher lag-time upon treatment were found for a strain lacking Ubc14 (**figure 3.9**), a result expected for a mutant of the ubiquitin-conjugating machinery, provided that ubiquitination is involved in the degradation of oxidative modified misfolded proteins.

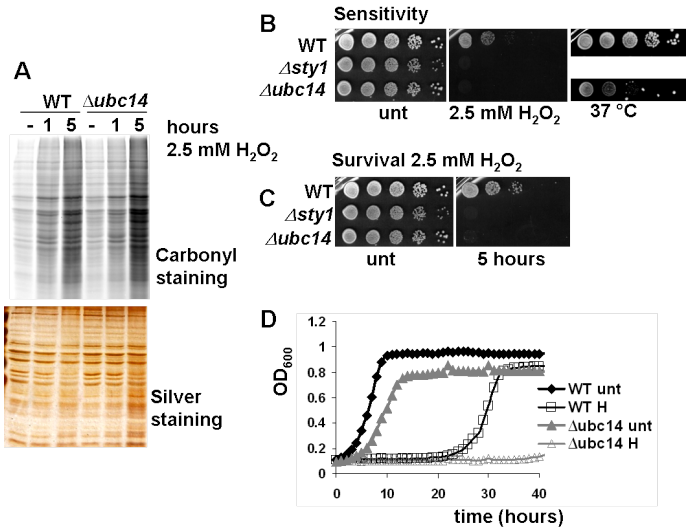

Figure 3.9: Ubc14 is involved in protein degradation upon oxidative stress. **A** Protein carbonylation assay. Protein carbonyls from untreated (-) or treated (2.5 mM H_2O_2 for 1 or 5 hours) extracts of 972 (WT), and SG102 (Δ*ubc14*) were labeled with FTC. Samples were analysed by fluorescent 1D gel electrophoresis (carbonyl staining) and silver staining (as a control of protein loading). **B** *S. pombe* cells lacking Ubc14 are more sensitive to H_2O_2 and heat shock than a wild-type strain. Exponentially growing 972 (WT), AV18 (Δ*sty1*), and SG102 (Δ*ubc14*), cell cultures were serial diluted and spotted on YE5S plates, on YE5S plates containing 2.5 mM H_2O_2 and on YE5S plates incubated at 37°C. **C** *S. pombe* cells lacking Ubc14 survive worse than a wild-type strain upon oxidative stress. Exponentially growing cell cultures of untreated (-) or treated (2.5 mM H_2O_2 for 5 hours) 972 (WT), AV18 (Δ*sty1*), and SG102 (Δ*ubc14*), were serial diluted and spotted on YE5S plates. **D** Δ*ubc14 S. pombe* cells have higher lag-time than a wild-type strain upon oxidative stress in liquid culture. Growth curves of untreated (unt) or treated (2.5 mM H_2O_2 (H)) cell cultures at OD_{600} 0.1 of 972 (WT), and SG102 (Δ*ubc14*) in YE5S liquid medium. OD_{600} was recorded at the indicated times.

As above mentioned, E2 conjugating enzymes are involved in tagging ubiquitin to misfolded substrates, and this ubiquitin is recognized as a signal which directs these proteins for degradation. If these enzymes are absent, their specific protein substrates will not be ubiquitinated and therefore will accumulate inside cells (**figure 3.10 A**). In the case of oxidative misfolded proteins, this protein accumulation is probably correlated with increased levels of protein carbonylation.

As shown above, we propose that Ubc14 is involved in the targeting and degradation of oxidatively unfolded proteins. This protein has not known *S. cerevisiae* orthologs, however it is very close in sequence to both *S. pombe* (**figure 3.10 B**) and *S. cerevisiae* Ubc4, a protein extensively described in different organisms to be involved in degradation

of misfolded proteins, both cytoplasmic and nuclear [275] [313] [280] [316] [285].

To confirm whether this protein is involved or not in targeting ubiquitin to oxidative misfolded substrates, we decided to over-express ubiquitin in a wild-type strain and in a Δ*ubc14* strain and to check for protein carbonylation levels upon oxidative treatment. As it is shown in **figure 3.10 C**, over-expression of ubiquitin highly decreased carbonylation levels of a wild-type strain upon H_2O_2 treatment, reinforcing the idea that ubiquitination is involved in the degradation of carbonylated proteins. However, this was not the outcome for Δ*ubc14* cells. In this case, protein carbonyls remained almost to the same level upon H_2O_2, independently of ubiquitin expression. This led us to conclude that ubiquitination pathways are involved in the degradation of carbonylated proteins, and that *S. pombe* Ubc14 is directly involved in the ubiquitination of oxidative misfolded proteins.

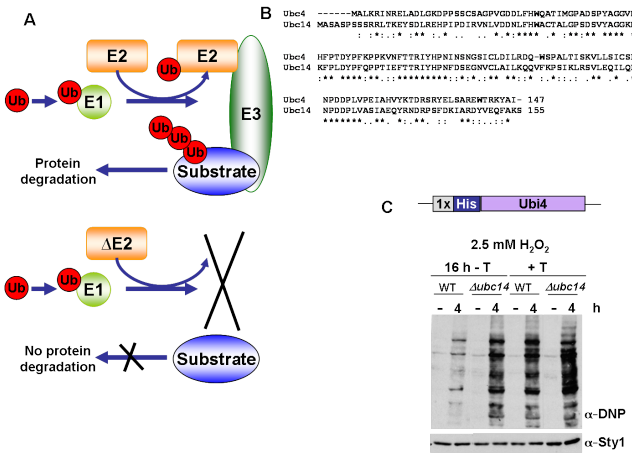

Figure 3.10: Ubc14 conjugates ubiquitin to oxidatively misfolded proteins in *S. pombe*. **A** Schematic representation of substrates ubiquitination. Upper panel, in the presence of E2 conjugating enzymes, substrates are ubiquitinated and later degraded by the proteasome. Lower panel, in the absence of E2 conjugating enzymes, substrates are not ubiquitinated and therefore accumulate in the cell, since they are not targeted for degradation. **B** *S. pombe* Ubc14 and Ubc4 proteins are very close in sequence. Sequence alignment between Ubc14 and Ubc4 according to ClustalW. **B** Protein carbonyls from extracts of 666 (WT), and Δ*ubc14*, collection, expressing [without thiamine (16 h -T)] or not [with thiamine (+T)] ubiquitin from an episomal plasmid with a 1X driven nmt promoter, either untreated or treated with 2.5 mM H_2O_2 for 4 hours, were labelled with DNPH. Samples were analysed by immunoblotting with αDNP antibodies. Immunoblotting with αSty1 antibodies was used as a control of protein loading.

3.5.2.3 Screening of the involvement of E3 ligases in the degradation of oxidatively modified proteins in *S. pombe*

E3 ligases also participate in the ubiquitination pathway. These enzymes are responsible for the specific recognition of the different substrates of the ubiquitin-proteasome system. RING finger domain E3 ligases act as scaffolds that bring together E2s and substrates, whereas HECT domain E3 ligases have a catalytical role, since they are responsible of

transferring the activated ubiquitin from the E2 to an internal Cys residue in the E3, before ubiquitin conjugation to the susbstrate. F-box proteins are substrate-recognition subunits of the SCF complex, generally involved in the degradation of signal- and cell cycle-induced phosphorylated proteins.

We checked this three classes of E3 ligases in our screening. Unexpectedly, we did not find any E3 ligase-coding gene which deletion led to increased carbonylation levels upon oxidative stress. However, for many mutants, including those deleted in *ubr1*, *ubr11*, *SPAC167.07c* (*S. cerevisiae hul5* homologue), *san1* and *pub1*, we found decreased levels of protein carbonylation, together with decreased sensitivity to H_2O_2, and in most of the cases increased survival and lower lag-time in liquid upon stress, phenotypes probably indicating increased degradation rates of oxidative modified proteins. Among them, the most impressing phenotypes were found for cells lacking *pub1* (**figure 3.11**). In this case, carbonylation levels barely changed upon stress (**figure 3.11 A**), and the lag time of liquid cultures of Δ*pub1* cells upon H_2O_2 exposure was much shorter than in wild-type cells (**figure 3.11 D**). Sensitivity to heat-shock was found for mutants lacking Ubr1 and Pub1 (**table 3.2**).

Curiously, Ubr1, San1, and Hul5 are proteins that have been previously described to be involved in protein quality control of misfolded proteins [280] [279] [389][285] [316] [297]. However, little is known about Pub1 regarding its involvement in protein degradation pathways. Pub1 is a HECT domain ubiquitin ligase, that belongs to the Nedd4/Rsp5 subfamily [390]. Described roles for this protein are regulation of the G2/M transition via ubiquitination of Cdc25 [391], involvement in cell viability in low pH medium and in leucine uptake [392] [393].

3.5.2.4 Lack of Ubp16, a *S. pombe* deubiquitinase, show high protein turnover upon oxidative stress

Deubiquitinases are involved in many processes related with ubiquitin maintenance. These enzymes participate in the activation of ubiquitin, which is always expressed as a polyubiquitin pro-protein fused to ribosomal proteins. Also, they participate in recycling ubiquitin unspecifically bound to small cellular nucleophiles. They may negatively regulate protein degradation, since they can reverse the ubiquitination of proteins, and conversely, appropriate deubiquitination of substrates is also necessary for maintaining normal rates of substrate proteolysis, by helping to maintain ubiquitin levels in the cell. With these plethora of functions, it results difficult to predict which are the expected levels of protein carbonylation upon oxidative stress in DUB deleted strains.

As it is shown in **table 3.2**, a decrease in protein carbonylation levels was observed for most of the deleted strains showing a phenotype. Only in one case, in the strain deleted in *otu2*, slightly increased carbonylation levels were found, but with no changes in oxidative stress sensitivity when compared with a wild-type.

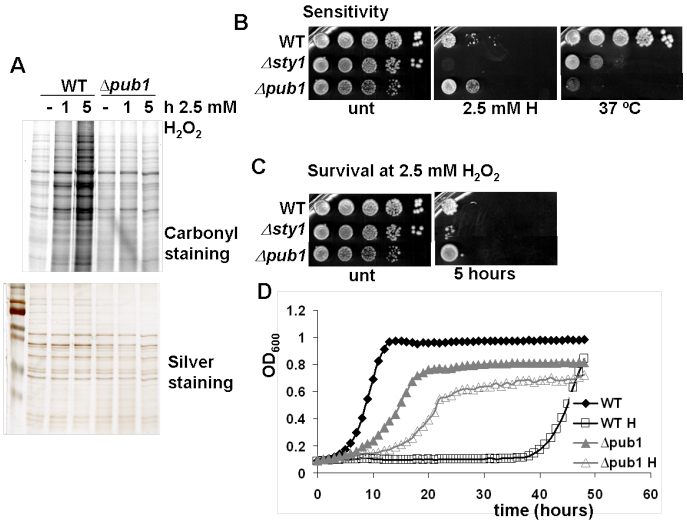

Figure 3.11: Lack of Pub1 increases degradation rates of carbonylated proteins upon oxidative stress. **A** Protein carbonylation assay. Protein carbonyls from untreated (-) or treated (2.5 mM H_2O_2 for 1 or 5 hours) extracts of 972 (WT), and SB16 (Δ*pub1*) were labeled with FTC. Samples were analysed by fluorescent 1D gel electrophoresis (carbonyl staining) and silver staining (as a control of protein loading). **B** *S. pombe* cells lacking Pub1 are more resistant to H_2O_2 than a wild-type strain. Exponentially growing 972 (WT), AV18 (Δ*sty1*), and SB16 (Δ*pub1*), cell cultures were serial diluted and spotted on YE5S plates, on YE5S plates containing 2.5 mM H_2O_2 and on YE5S plates incubated at 37°C. **C** *S. pombe* cells lacking Pub1 survive better than a wild-type strain upon oxidative stress. Exponentially growing cell cultures of untreated (-) or treated (2.5 mM H_2O_2 for 5 hours) 972 (WT), AV18 (Δ*sty1*), and SB16 (Δ*pub1*), were serial diluted and spotted on YE5S plates. **D** Δ*pub1 S. pombe* cells have lower lag-time than a wild-type strain upon oxidative stress in liquid culture. Growth curves of untreated (unt) or treated (2.5 mM H_2O_2 (H)) cell cultures at OD_{600} 0.1 of 972 (WT), and SB16 (Δ*pub1*) in YE5S liquid medium. OD_{600} was recorded at the indicated times.

From all checked strains, the most clear phenotype was found for a strain deleted in *ubp16* (**figure 3.12**). In this case, almost no carbonylation was found upon oxidative stress (**figure 3.12 A**), cells were more resistant to oxidative stress in plates (**figure 3.12 B**), survived better (**figure 3.12 C**), and had lower lag-time in liquid upon H_2O_2 (**figure 3.12 D**).

3.5.2.5 Mas5, a *S. pombe* DNAJ domain Hsp40 co-chaperone involved in protein turnover upon oxidative stress

Chaperones are important in the protein degradation process, since not only they bind to misfolded proteins preventing their aggregation, but also they participate in triage decisions which direct proteins either to folding or to degradation pathways (see **figure 1.19** and **figure 1.20** in the Introduction). The chaperones more directly involved in chaperone-assisted protein degradation are those belonging to the Hsp90 and Hsp70 families.

Among all chaperones we tested, we only found a clear phenotype for a strain lacking

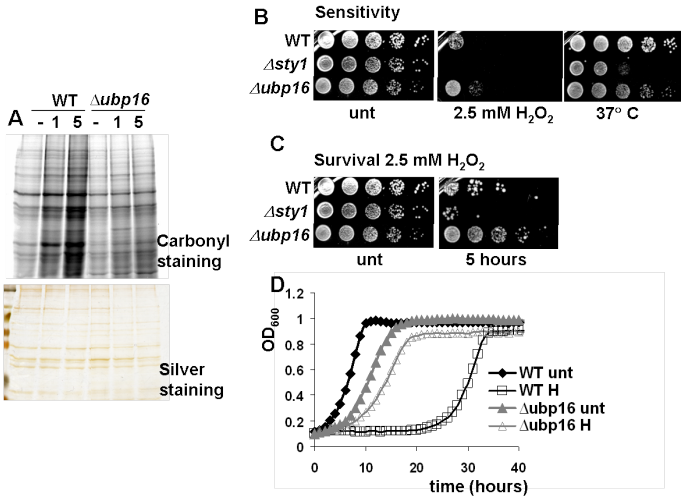

Figure 3.12: Lack of Ubp16 increases degradation rates of carbonylated proteins upon oxidative stress. **A** Protein carbonylation assay. Protein carbonyls from untreated (-) or treated (2.5 mM H_2O_2 for 1 or 5 hours) extracts of 972 (WT), and SG104 (Δ*ubp16*) were labeled with FTC. Samples were analysed by fluorescent 1D gel electrophoresis (carbonyl staining) and silver staining (as a control of protein loading). **B** *S. pombe* cells lacking Ubp16 are more resistant to H_2O_2 than a wild-type strain. Exponentially growing 972 (WT), AV18 (Δ*sty1*), and SG104 (Δ*ubp16*), cell cultures were serial diluted and spotted on YE5S plates, on YE5S plates containing 2.5 mM H_2O_2 and on YE5S plates incubated at 37°C. **C** *S. pombe* cells lacking Ubp16 survive better than a wild-type strain upon oxidative stress. Exponentially growing cell cultures of untreated (-) or treated (2.5 mM H_2O_2 for 5 hours) 972 (WT), AV18 (Δ*sty1*), and SG104 (Δ*ubp16*), were serial diluted and spotted on YE5S plates. **D** Δ*ubp16 S. pombe* cells have lower lag-time than a wild-type strain upon oxidative stress in liquid culture. Growth curves of untreated (unt) or treated (2.5 mM H_2O_2 (H)) cell cultures at OD_{600} 0.1 of 972 (WT), and SG104 (Δ*ubp16*) in YE5S liquid medium. OD_{600} was recorded at the indicated times.

Mas5. This is a *S. pombe* Hsp40 co-chaperone with a DNAJ domain. Hsp40 family of co-chaperones are responsible for polypeptide loading onto the Hsp70 chaperones. Different roles have been attributed to the Hsp40 co-chaperones regarding protein degradation. For instance, *S. cerevisiae* Ydj1 promotes the degradation of cytoplasmic short-lived and abnormal proteins [261] [262], however it also resulted important for maintaining steady-state levels of protein kinases during or immediately after synthesis [264].

Δ*mas5 S. pombe* cells showed no protein carbonylation upon oxidative stress (**figure 3.13 A**), decreased sensitivity to H_2O_2 (**figure 3.13 B**), increased survival and equal lag-time, before and after stress, in liquid culture (**figure 3.13 C and D**). However, this strain was very sensitive to heat-shock (**figure 3.13 B**). These results suggest an important role for this protein in protein turnover upon protein damage by oxidative stress, with a specific role in directing heat-shock-mediated misfolded proteins to refolding, and its depletion triggering massive degradation of both irreversible oxidized proteins and reversibly misfolded proteins.

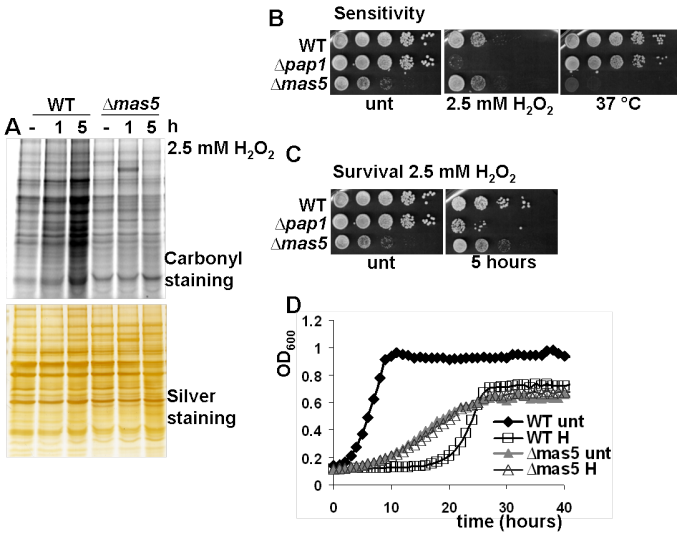

Figure 3.13: Lack of Mas5 increases degradation rates of carbonylated proteins upon oxidative stress. **A** Protein carbonylation assay. Protein carbonyls from untreated (-) or treated (2.5 mM H_2O_2 for 1 or 5 hours) extracts of 972 (WT), and SB26 (Δ*mas5*) were labeled with FTC. Samples were analysed by fluorescent 1D gel electrophoresis (carbonyl staining) and silver staining (as a control of protein loading). **B** *S. pombe* cells lacking Mas5 are more resistant to H_2O_2 than a wild-type strain. Exponentially growing 972 (WT), AV25 (Δ*pap1*), and SB26 (Δ*mas5*), cell cultures were serial diluted and spotted on YE5S plates, on YE5S plates containing 2.5 mM H_2O_2 and on YE5S plates incubated at 37°C. **C** *S. pombe* cells lacking Mas5 survive better than a wild-type strain upon oxidative stress. Exponentially growing cell cultures of untreated (-) or treated (2.5 mM H_2O_2 for 5 hours) 972 (WT), AV25 (Δ*pap1*), and SB26 (Δ*mas5*), were serial diluted and spotted on YE5S plates. **D** Δ*mas5 S. pombe* cells have lower lag-time than a wild-type strain upon oxidative stress in liquid culture. Growth curves of untreated (unt) or treated (2.5 mM H_2O_2 (H)) cell cultures at OD_{600} 0.1 of 972 (WT), and SB26 (Δ*mas5*) in YE5S liquid medium. OD_{600} was recorded at the indicated times.

3.5.2.6 Cross-protection of oxidative protein damage by heat shock

When we were performing carbonylation experiments upon oxidative stress in ts mutants, that require to grow at higher temperature (normally 37°C) in order to show a phenotype, we observed that carbonylation levels remained almost unchanged upon H_2O_2 at that temperature in a wild-type background. This suggests that probably genes that are induced upon heat-shock are somehow protecting cells from oxidative damage. This phenomenon is commonly described as cross-protection, and suggests that either different stress conditions trigger similar defence mechanisms or that there is a general stress response that can confer a basic level of protection to environmental changes [54] [55] [56].

To check if this cross-protection mechanism is operating in *S. pombe*, we decided to compare carbonylation levels upon oxidative stress in wild-type cells, which were pre-incubated at 37°C, either for 15 minutes or for 2 hours, prior to H_2O_2 treatment, and in cells deleted in *sty1* and *atf1*, which were pre-incubated at 37ºC for 2 hours, before applying oxidative stress. As it is shown in **figure 3.14**, carbonylation levels increased in

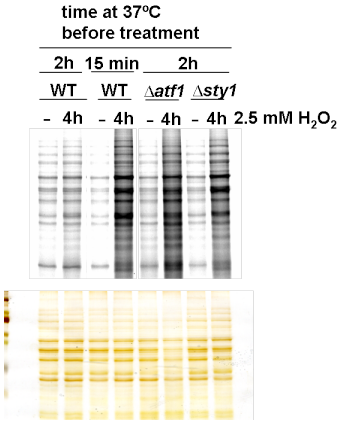

Figure 3.14: Heat shock cross protect cells from oxidative damage. Protein carbonyls from extracts of 972 (WT), MS98 (Δ*atf1*) and AV18 (Δ*sty1*), pre-incubated at 37ºC for the indicated times, untreated or treated with 2.5 mM H_2O_2 for 4 hours were labelled with FTC. Samples were analysed by fluorescent 1D gel electrophoresis (carbonyl staining) and silver staining (as a control of protein loading).

the wild-type strain pre-incubated only for 15 minutes at 37°C. However, pre-incubation of the wild-type for 2 hours rendered cells less sensitive to oxidative protein modifications. Carbonylation levels were restored in Δ*sty1* and Δ*atf1* cells pre-incubated at 37ºC for 2 hours, suggesting the involvement of the heat-shock response, Sty1-dependent, in cross-protecting cells from oxidative damage.

Chapter 4

DISCUSSION

Discussion

4.1 Oxidative stress and protein oxidations

Oxidative stress is defined as an imbalance between ROS production and ROS detoxification. When this situation happens inside cells, either because there is a decrease in ROS scavenging, as it happens in situations where antioxidant enzymes are deficient (for instance lack of catalase, SOD or Prxs), or because there is an increase in ROS production (for instance in mitochondrial dysfunctions or environmental stresses), many cell components are affected, including lipids, proteins and DNA.

In the case of proteins, ROS produce two clear and differentiated outcomes. There are modifications, such as some Cys and Met oxidations, which are reversible as they can be repaired by specific activities in the cell (the Trx and GSH/Grx systems and the Msrs, respectively), and there are modifications, such as protein carbonylations, which are irreversible, and cause protein loss-of-function, protein misfolding, and protein degradation or protein accumulation in the form of toxic aggregates.

Oxidation of specific Cys in proteins by H_2O_2 has been largely described as a cellular mechanism to trigger signalling pathways, such as those triggered by growth factors or cytokines, or the antioxidant responses in microbial systems. In these cases, H_2O_2 accomplishes the requisites of a second messenger, including formation of a specific oxidation in sensor proteins, reversibility and specificity. However, H_2O_2 can be easily transformed to the more reactive $OH^{\cdot}$ species, through the Fenton reaction. This species is the main responsible of formation of protein carbonyls, that can not be repaired and constitute classical marks of oxidative damage.

Along this thesis we were interested in studying and understand two types of ROS reactivity in proteins.

Regarding reversible thiol oxidations, we developed protocols for studying Cys oxidations at the proteome level, in order to characterize which Cys are more sensitive to H_2O_2, and therefore more prone to participate in redox events. We studied the homoeostasis of Cys oxidations in the presence or in the absence of reducing systems such as the Trx system. Regarding the study of irreversible protein modifications we tried protocols for the identification of protein carbonyls, however we were unsuccessful probably due to the complexity of carbonylated samples. Also, we studied the role of PQC systems in clearance of carbonylated proteins. This is a very important issue related with protein toxicity, since lack of clearance, and therefore protein aggregation results toxic for cells.

Close related issues were also the identification and characterization of the main H_2O_2 scavengers in *S. pombe*, the minor role of the *S. pombe* Msrs in the defence against

oxidative stress, and the discovery of free Met as a primary barrier in the defence against H_2O_2 stress.

These results are discussed in the sections below.

4.2 Identification of reversible thiol oxidations

Thiol groups of Cys in proteins are common targets of intracellular oxidations. They can initially be oxidized by H_2O_2 to sulphenic acid, which readily reacts with any close proximal thiol group to generate an intra- or an inter-molecular disulphide. Yet, in the presence of more oxidant it can be further oxidized to sulphinic or sulphonic acids [29] [119]. Non-toxic reversible oxidations (SOH, S-S or mixed S-S) are used as regulatory switches in enzymatic reactions such as the one catalyzed by RNR, and the oxidized proteins can either directly or indirectly be reduced by potent intracellular redox buffers, the Trx and the GSH/Grx systems [143] [87]. Also, redox sensitive proteins undergo reversible thiol oxidations to participate in electron flow pathways and/or trigger signalling cascades [119] [394]. Understanding the effects of genetic and environmental effects on global reversible Cys oxidations is crucial to obtain an understanding of redox signalling events, which eventually modulate many essential intracellular processes.

First, we set up the experimental conditions for studying reversible thiol oxidations by 1D electrophoresis, following the same principle as described in [352], but using a fluorescent IAM-derivative to label reversible thiol oxidations. After 'freezing' the *in vivo* thiol stage of Cys residues by media acidification, we first block reduced thiols in extracts with IAM, and then we sequentially reduce and label reversible oxidized thiols with a fluorescent IAM-derivative. In this way, by simply 1D-gel electrophoreses, we can compare differences in thiol oxidations between strains or environmental conditions.

To further identify and quantify Cys oxidations in two samples to be compared at the proteomic level, we have optimized pre-existing proteomic technologies. The protocol follows the same principle as above, but reversible oxidized thiols are labelled in this case with the biotin-based heavy or light iodoacetamide-derivatives, isotope-coded affinity tag (ICAT) reagents, so that the two samples can be compared at once after combination of the labelled extracts, trypsin digestion, streptavidin-affinity purification of peptides containing oxidized cysteines, liquid chromatography and mass spectrometry analysis (LC-MS/MS). For the same protein extracts, prior to Cys-containing peptide enrichment, individual relative protein concentrations are obtained by stable-isotope dimethyl labelling.

Previous proteomic approaches to study reversible Cys oxidations included the use of 2D gels. Even though it was successfully used for studying thiol oxidations, one of its major limitations is lack of specificity, especially when using the new generation of mass spectrometers, with enhanced sensitivity. In this case, several proteins are found in a single

2D gel spot, being almost impossible to discern which one of them contains the oxidized Cys residue/s.

With our gel-free approach, we believe we improved previous described protocols in several aspects. It is quantitative, it allows the identification of thousands of peptides at the same time, and the identification of the involved redox-sensitive Cys. Also, the use of isotope coded IAM-based biotin tags has several advantages, they allow enrichment of those reversible oxidized peptides and importantly, the fact that the light and heavy ICAT reagents are chemically identical allows them to co-elute from the HPLC system and to behave equally in the mass spectrometer. Thus, differences of 9-Da, or multiples of 9-Da, reflect the number of oxidized Cys in a peptide. Moreover, relative peak areas of a peptide containing a Cys labelled with both heavy and light ICAT reagents reflects the oxidation status of the same peptide in compared samples. Additionally, to make this protocol fully quantitative, we performed an additional step of protein quantification. Thus, individual relative protein concentrations are obtained by stable-isotope dimethyl labelling of the N-terminal group of non-enriched peptides from the same protein extracts [395].

A similar gel-free protocol, called OxICAT, was previously described in the literature [357]. In the OxICAT methodology, initially reduced Cys are labelled with light ICAT, whereas upon reduction, newly appearing reduced Cys are labelled with heavy ICAT. However, as $\sim$90% of intracellular Cys are in their reduced state, as we determined in [396], there is a big disproportion between the amounts of Cys labelled with one of the ICAT reagents in comparison with the other one, yielding a sample with a high level of complexity. A comprehensive analysis requires extensive fractionation [up to 192 liquid chromatography (LC) fractions] [357] and much instrumentation availability. To our knowledge only one laboratory has successfully applied this technique.

Thus, by combining ICAT labelling with dimethyl labelling we are able to obtain a more complete picture at a proteomic level of relative reversible Cys oxidations in two samples to be compared, taking into account changes in the steady-state amounts of individual proteins. This approach has been successfully applied to detect reversible Cys oxidations in *S. pombe* upon different genetic and environmental conditions, as presented in the results section and that has been published in [396] [397].

4.3 Biological relevance of reversible thiol oxidations upon H_2O_2

We used the protocols described above to follow, by 1D electrophoresis or at the proteomic level, reversible thiol oxidations in *S. pombe* upon treating cells with H_2O_2 (exogenous oxidative stress) and upon different genetic conditions (endogenous oxidative stress).

It is generally believed that H_2O_2 has very low reactivity towards general Cys in

proteins. This is due to that pK_a of most cytoplasmic thiols is close to 8.5. This means that, at physiological pH, most thiols are protonated, and therefore they have very low reactivity as nucleophiles. However, there are certain proteins that contain thiols with very low pK_a, due to local environments which withdraw electrons, being these in the form of more reactive thiolates. These are forming part of proteins such as Prxs, which are primary detoxifiers of intracellular levels of H_2O_2. However, Prxs have also other important role, they use their highly sensitive Cys to act as signal transducers (they oxidize their sensors) in redox-signalling pathways, as it is the case of the activation of the antioxidant Pap1 pathway in *S. pombe* upon low doses of ($\sim$ 0.2 mM H_2O_2).

Our results show that we are able to produce general reversible thiol oxidations upon different extracellular concentrations of H_2O_2. This is against the general principle that suggests that H_2O_2 has low reactivity towards general Cys in proteins. However, it is possible that the doses we are testing are high enough to react with a broad range of Cys, including those less reactive (i.e. solvent exposed Cys). This is in accordance with what we show in **figure 3.1 A and B** of the results section 3.1.1. It can be appreciated that Tpx1, the *S. pombe* sensor protein, appears oxidized prior to general disulphides at very low doses of the oxidant.

In *S. pombe*, Tpx1 acts as a H_2O_2 sensor protein to trigger antioxidant pathways. Thus, upon mild concentrations of peroxides, Tpx1 transduces the redox signal to the Pap1 transcription factor, so that it becomes oxidized and activated through the formation of at least one disulphide bond (**figure 1.5** in Introduction) [169] [398]. We wondered if this was also the case for the rest of reversible thiol oxidations that are formed upon H_2O_2 treatment in the cells. So we checked disulphide formation upon the oxidant in wild-type cells and compared it with a strain lacking Tpx1. General disulphides were formed in both strains upon oxidative treatment. Moreover, cells lacking Tpx1 have increased basal levels of disulphides when compared with a wild-type. These results suggest that H_2O_2 is able to directly react with Cys, even in the absence of redox transducers. Or, that in the absence of Tpx1, H_2O_2 reacts more easily with low pK_a and solvent exposed Cys.

The reversible nature of some Cys modifications, makes this residue very important in many enzymatic reactions and metal ion coordination events. This is the case of catalyitic centres of enzymes such as sulphite reductase and aconitase, that use important Cys to coordinate iron, or PAPS reductase, RNR, and Msrs which use oxidation/reduction of Cys in their catalytic cycles. It is possible that H_2O_2 treatment affects some of these Cys (which are probably belonging to the pool of reactive Cys) causing cellular toxicity. However, we have observed, that, at least doses up to 0.2 mM H_2O_2 produce a general increase of reversible thiol oxidations, which is fully reverted to wild-type untreated levels upon some time, as it is shown in **figure 2B** in the paper in section 3.1([396]). This is probably due that cells developed potent systems, the Trx and the GSH/Grx systems, to maintain general Cys in proteins in their reduced state, and to recycle enzymatically oxidized Cys.

As we are using a general reducing agent to identify oxidized Cys, we can not

establish the nature of the oxidations that we see upon H_2O_2. It is possible that many of these are mixed disulphides with low-molecular-weight thiols. In fact, it has been largely suggested that the formation of mixed disulphides with GSH (protein S-glutathionylation) is both a protective mechanism that prevent Cys from being oxidized to higher irreversible oxidation states and a modification that serves to regulate a variety of cellular processes by modulating protein function [364]. The nature of the reducing agent determines the type of Cys oxidation to be detected, thus S-nitrosylations can be detected upon incubation with ascorbate/$CuCl_2$ [349], sulphenated Cys can be specifically detected upon reduction with arsenite [350], Grx specifically reduces S-glutathionylated Cys [351].

By using the ICAT approach, we wanted to identify and characterize which are the Cys oxidations that are produced upon low H_2O_2 concentrations to fish only those more redox sensitive. We treated cells only for few seconds to avoid changes in protein expression, even though, we quantified individual protein levels by dimethyl labelling.

Following this protocol, we were able to characterize Cys oxidations from proteins belonging to different functional categories, including antioxidant enzymes/pathways (Tpx1, Pap1, the thioredoxin peroxidases Pmp20 and Gpx1, Trx1, and Grx1), thioredoxin substrates [RNR (Cdc22), PAPS reductase (Met16), S-adenosylmethionine syntase (Sam1)], proteins from metabolic pathways, mostly belonging to the glycolitic pathway and the linked pyruvate metabolism [glyceraldehyde-3-phosphate dehydrogenase (Tdh1), succinate dehydrogenase (Sdh1), alcohol dehydrogenase (Adh1), pyruvate kinase (Pyk1), and fructose-biphosphate aldolase (Fba1)], ribosomal proteins, proteins from the protein catabolic pathways [E2 ligases (Ubc14), ubiquitin-fusion proteins (Ubi2), and chaperones (Mas5)].

Proteins belonging to the antioxidant enzymes/pathways category served us as internal controls of the procedure, since Tpx1, Pap1, and Trx1 were largely studied in our lab, prior to this work. We also observed that the rest of all peroxiredoxins from *S. pombe* were present in this study (including BCP, which is not in the main table of the paper, since it only appeared in one biological replica), indicating the sensitive nature of their Cys. Classical Trs substrates, Cdc22, Met16, and Sam1, were also identified. These proteins have the particularity that they use redox Cys in their catalytic cycles. Therefore, at this time, we can not discard any out of two possibilities, their Cys appeared more oxidized in our study because their Cys are direct targets of H_2O_2, or because, upon stress, Trx1, their major electron donor is busy in reducing unspecific Cys oxidations, and therefore is less able to reduce their own substrates. Finally, many proteins with oxidized Cys belong to the glycolytic pathway. Glucose has three major fates in the cell: it may be stored, oxidized to pentoses via the pentose phosphate pathway, or oxidized as a three-carbon compound (pyruvate) via glycolisis. Whereas the role of the glycolitic pathway is to produce energy, the role of the pentose phosphate pathway is to generate NADPH, the major intracellular electron donor. Many reports show the inactivation of key enzymes of the the glycolitic pathway to favour the pentose phosphate pathway in conditions of

oxidative stress (reviewed in [399]).

It is worth mentioning that with this protocol we are probably detecting higher oxidation states of Cys in those peptides that appeared with very low ICAT ratios when we compared treated vs untreated condition. However, these types of post-translational modifications would be better studied by 2D gels electrophoresis, where sulphinc or sulphonic acid modifications would make spots to migrate towards the more acidic side of the gel.

4.4 Thiol redox buffers: the Trx and the GSH/Grx systems

After studying the outcome of Cys oxidations upon exogenous oxidative stress, we wondered which would be the outcome upon endogenous oxidative stress. We studied many genetic conditions, for example Cys oxidations in cells lacking Tpx1, as it is shown in **figure 3.1**. However, for a more comprehensive analysis we decided to study the oxidized proteome of cells devoid of the Trx system, the main system involved in keeping reduced Cys in the cytoplasm. So we used strains lacking Trx1 (the main cytoplasmic Trx in *S.pombe*), and the only TrxR in *S. pombe*, Trr1.

We first studied reversible Cys oxidation in these strains by 1D electrophoresis. We were very surprised to find a very different outcome between the two strains (**figure 1** in the paper presented in section 3.2 ([397])). Cys from protein extracts from cells devoid of Trx1 were barely oxidized when compared with a wild-type strain. However, we observed massive thiol oxidation in cells missing Trr1. We were very interested to find out to which proteins belonged those oxidized Cys in both backgrounds, therefore we further studied these strains with the ICAT methodology.

First, we observed that many proteins were over-expressed in these backgrounds. This is due to the constitutive activation of the transcription factor Pap1, specially in the case of Trr1 mutants, as it has been previously shown [58], and also in cells lacking Trx1, although to a lesser extent.

When we looked at the data, we found that oxidized Cys in Δ*trx1* cells were from proteins considered to be classical Trx substrates. However, Cys oxidations were found in proteins belonging to many different functional categories in the Δ*trr1*, a situation most likely representing a disulphide stress. It is worth mentioning that we found very low overlap between oxidized peptides in cells lacking Trr1 and cells treated with H_2O_2.

We found in the literature a similar situation, in which cells lacking Trr1 triggered oxidation, but in this case, of a cytoplasmic-targeted alkaline phosphatase from *E.coli*, whose activity requires the formation of a disulphide bond. Thus, cells devoid of TrxR

triggered oxidation and therefore rendered active the cytoplasmic alkaline phosphatase. This basal disulphide accumulation was largely eliminated in cells lacking both TrxR and Trxs [112], suggesting both that oxidized Trxs are responsible for Cys oxidation in this background and that general disulphides are not easily made in the cytoplasm, unless they are enzyme-catalyzed. We therefore decided to study, by 1D electrophoresis, general disulphide formation in strains lacking Trr1 and one or the two cytoplasmic Trxs (Trx1 and/or Trx3), or their major substrate Tpx1. We observed that it was necessary to eliminate both Trxs or Trx1 and Tpx1 to significantly decrease disulphide stress to cells lacking Trr1. These results suggested that, the absence of the Trx system does not trigger general thiol oxidations, but elimination of Trr1, the only *S. pombe* TrxR, does so through accumulation of oxidized Trxs (Trx1 and Trx3) or their main substrate Tpx1. It is important to mention that Tpx1 is highly oxidized in Δ*trr1* cells.

I explained in the Introduction (section 1.2) that the Trx system has two main roles, one of them is to keep reduced general thiols in proteins, working in this way as an antioxidant system. However, other role is to recycle disulphides from enzymes that have catalytic cycles in which some of steps include Cys oxidation. Therefore, we were also interested in studying how lack of Trx1 or Trr1 affects the function of enzymes that are Trx1-dependent, which we defined as classical Trx substrates. In many cases, recycling of these types of enzymes does not only rely in one electron donor. Many are the examples in the literature were enzymes that are mainly Trx-dependent can use a different enzyme (a different Trx or Grx) or even GSH to be recycled. However, we found that *S. pombe* PAPS reductase recycling is dependent only in Trx1 [99]. Accordingly, *S. pombe* cells lacking Met16, an enzyme that catalyses the reduction of sulphate to sulphite in the Cys and Met biosynthesis pathway (**figure 1.16** in the Introduction), are not able to grow in minimal media unless an external source of Cys or Met is added to the medium. However, it is surprising that this is not the case for Δ*trr1* cells, they are able to grow in minimal media without added Cys or Met. This result led us to hypothesize that there is an alternative electron donor for Trx1 in the absence of its reductase.

In this regard, we explored the role of the GSH/Grx system in reducing Trx1. We found that cells lacking Trr1 have a GSH/GSSG ratio ∼2-fold lower than in a wild-type (**figure 3.2 A**) and that this ratio was back to normal by simply deleting *trx1* in this background. This result suggests that Trx1 recycling may be the reason for that high GSH consumption in Δ*trr1*.

For the rest of substrates, it is possible that the GSH/Grx system plays an important role, since it is impossible to make strains lacking Trr1 and Grx1 or Trr1 and Gcs1 (required for GSH biosynthesis), suggesting again, as it is described in **section 1.2.5** of the Introduction, overlapping roles for the Trx and GSH/Grx systems.

4.5 Msrs and oxidative stress in *S. pombe*

Mxr1/MsrA and Mxr2/MsrB (the *S. pombe* methionine sulphoxide reductases (Msrs)) are two classical Trx substrates that have oxidized Cys in cells lacking Trx1, according to our ICAT data.

Upon oxidative treatment, Met can be reversibly oxidized to a mixture of two enantiomers of methionine sulphoxide (Met-O), methionine-*S*-sulphoxide (Met-*S*-O) and methionine-*R*-sulphoxide (Met-*R*-O), which can be further oxidized to methionine sulphone if stronger oxidizing conditions are applied [176]. Msrs have been described to reduce, with high substrate specificity, these enantiomeric forms of Met-O, being the MsrA family of Msrs responsible for reducing Met-*S*-O (free and in proteins), the MsrB family of Msrs responsible for reducing protein bound Met-*R*-O, and the free Msrs family responsible for reducing free Met-*R*-O.

In *S. pombe* there are only two of these families, MsrA/Mxr1 and MsrB/Mxr2, and since they appeared in our ICAT experiments, and they were described in many organisms to have a role in oxidative stress protection, we decided to further characterize them.

First, we characterized their role as free Msrs, by creating strains auxotrophic for Met, thus we constructed strains deleted for *mxr1* and/or *mxr2* together with a deletion in *met6*. Met6 is a protein required for Met synthesis (see **figure 1.16** in the Introduction), thus cells devoid of Met6 are fully auxotrophic for Met (neither Cys nor GSH can supplement the auxotrophy of this strain). We only found Mxr1 necessary to grow cells in an external source of oxidized Met, containing both enantiomeric forms of the substrate. This suggests a minor role for Mxr2 in reducing free oxidized Met, which is in accordance with published data, for instance in *S. cerevisiae* k_{cat}/K_m of MsrA towards free met-*S*-O is 13.8 x 10^3 $M^{-1}s^{-1}$ whereas k_{cat}/K_m of MsrB towards free met-*R*-O is 0.09 x 10^3 $M^{-1}s^{-1}$, data obtained from a NADPH-coupled Trx system [400].

Many are the works presenting these enzymes as important in the antioxidant defence of different organisms, including *E. coli*, yeast or higher eukaryotes ([191] [401] [186]). However, we were unsuccessful to find any role for these enzymes in the antioxidant defence of *S. pombe*, even though H_2O_2 treatment increased transcription of both genes. We only found a slight increase in the lag time when growing cells in liquid culture and high doses of H_2O_2. These results suggest that Met oxidation in *S. pombe* is not a big issue, probably due to free oxidized Met being rapidly replaced by newly synthesized Met, and because there is not a essential protein function being altered by oxidized Met. Consistenly, we found that cells deficient in Met synthesis and lacking Mxr1 (Δ*mxr1* Δ*met6*) are much more sensitive to oxidative stress than a Δ*met6* strain. Importantly, deletion of *met6* alone renders cells very sensitive to H_2O_2, to a similar extent as cells lacking Pap1. The fact that cells lacking Met6 have such sensitivity to H_2O_2 makes us to think that free Met is a primary line of defence to oxidative stress, a role previously shown in the literature to operate in proteins [185] [402].

4.6 H_2O_2 scavenging in *S. pombe*

Previously in our laboratory, Tpx1 was characterized as a peroxiredoxin with a dual role in *S. pombe*. Thus, on one hand, it was described as the main scavenger of H_2O_2 during the aerobic growth of the fission yeast, as cells lacking Tpx1 do not grow in solid plates, unless they are incubated in an anaerobic atmosphere [169] [52], and on the other hand, Tpx1 was characterized as the H_2O_2 sensor in the Pap1 antioxidant pathway [169] [398].

Intriguingly, it was later observed that deleting *trr1* in a Δ*tpx1* background was enough to recover this anaerobic phenotype, in such a way that cells were able to grow again in solid plates in aerobic conditions. I already mentioned in several places, that Δ*trr1* cells have constitutive active the transcription factor Pap1 [58] (see results section 3.2), which accumulates in the nucleus and induce up to 80 genes, many of them related with antioxidant activities, as it is the case of the *ctt* gene, whose transcription is activated $\sim$17 fold [85].

Taken these results together, we decided to investigate if the activated Pap1 pathway was related with this suppression phenotype provided by cells lacking Trr1. In fact, Δ*tpx1* Δ*trr1* Δ*pap1* cells were again unable to grow under aerobic conditions, pointing to any of the genes triggered by Pap1 responsible for the aerobic phenotype of cells lacking Trr1 and Tpx1. As one of the main genes up-regulated in the Pap1 antioxidant response is *ctt1*, we checked its over-expression in Δ*tpx1* cells. As we expected, high catalase levels were sufficient to suppress the growth defects of Δ*tpx1* cells in solid plates.

These results point to Tpx1 and Ctt1 as the main H_2O_2 scavenging activities in fission yeast.

4.7 Identification of protein carbonylations

Irreversible modifications of proteins, normally protein carbonylation, are associated with protein loss-of-function and degradation or accumulation. These carbonylations are associated to many human disorders, including degenerative diseases such as cardiovascular diseases, diabetes, cancer and neurodegenerative disorders [403] [404]. Also, although oxidative damage to a protein may result in loss-of-function, it is possible that it does not cause a deleterious effect for the whole cell. This is the case for many components of the glycolytic pathway, which have been described to be inactivated under oxidative stress to divert glucose to the pentose phosphate pathway, thus providing NADPH for the antioxidant response (reviewed in [399]). Thus, it is important to have an inventory of those proteins that are irreversible modified upon oxidative stress.

We initially tried to identify carbonylated proteins by derivatizing them with a fluorescent probe, and performing 2D electrophoresis. However, we were unsuccessful, since

upon have set up a whole protocol set up, we found that many proteins were identified in the MS analysis of a single spot in the gel (**figure 3.6** in the results section 3.5.1.2).

Therefore, we tried with a gel-free approach. We successfully used this technology to identify Cys oxidations from proteins in two samples to be compared. This was possible due to many reasons. First, there is a very good available technology to label and enrich those Cys-oxidized peptides, the ICAT reagents. Then, Cys oxidation is only one type of modification. In the case of carbonylations, there are many types of modifications of proteins that result in creation of carbonyl residues.

In the case of carbonylated proteins the available technology is far away from the previous one. Even though similar reagents to the ICAT reagents are described in the literature, the hydrazide-functionalized isotope-coded affinity tag (HICAT) [374], they are not commercial, and seem difficult to handle. Also, peptides will be very different between two samples to be compared (i.e. wild-type untreated *vs* wild-type H_2O_2-treated). Moreover, oxidised Lys and Arg residues become inaccessible to trypsin proteolysis, leading to long-sized peptides with higher number of missed cleavages than normal [378], which do not properly 'fly' in the MS.

The above reasons may suffice to explain why we were unsuccessful even when trying to identify carbonylated peptides from BSA, a very well known protein, upon treatment with a metal-catalysed oxidation system.

Therefore, the identification and quantification of carbonylated proteins is still an unresolved matter.

4.8 PQC of carbonylated modified proteins

Carbonylation of proteins mostly causes loss-of-function and targeting for degradation. If the oxidative damage is high, they aggregate and result inaccessible to the cellular proteases, therefore accumulate inside cells provoking cellular toxicity.

Although many studies have been performed to identify the essential components that target misfolded proteins to degradation, the involvement of different protein quality control (PQC) pathways is still a matter of debate (see results section 3.5.2.1).

Thus, we were interested to study the fate of carbonylated proteins in *S. pombe*, by studying up to 67 gene-deleted strains in components related with protein catabolism, including components of the UPR, ERAD, ubiquitination (E2 conjugating enzymes, E3 ligases, DUBs), proteasome components, and chaperones.

Accumulation of oxidative-misfolded proteins was correlated with increased levels of protein carbonylation, and fitness was studied by cell survival in plates, upon oxidative treatment, either in liquid or in plates, and with differential lag-times in liquid.

By studying the involvement of E2 conjugating enzymes in degradation of carbonylated proteins, we could clearly show the involvement of ubiquitination in their degradation, as it is shown in **figures 3.9** and **3.10** in section 3.5.2.2 from the Results. This is an important result, since many are the reports suggesting that ubiquitination is not required to degrade oxidative-misfolded proteins (reviewed in [310] and [311]). Of course, the involvement of ubiquitination does not discard degradation of misfolded proteins independently of this tag.

More disturbing were the results obtained when we tested E3 ligases, enzymes also required for the proper ubiquitination of substrates targeted for degradation. We found in many cases decreased carbonylation levels, that we attribute to increased degradation of oxidative modified proteins, since in all these cases, the decreased carbonylated levels were accompanied with increased fitness to the oxidative treatment. Curiously, except in one case (the *pub1* deletion), all strains deleted in E3 ligases with decreased carbonylation levels upon oxidative stress were previously shown to be involved in PQC [280] [279] [389][285] [316] [297]. We hypothesize for these deleted strains, compensatory mechanisms may be operating, however these still remain to be elucidated.

Decreased levels of protein carbonylation were also found for a strain lacking Mas5. This is a protein that belongs to the Hsp40 family of co-chaperones, a family with important roles in loading substrates to the Hsp70 family of chaperones, which directly participate in the triage of proteins either for degradation or for refolding pathways. Contrary with their increased fitness upon oxidative stress, cells lacking Mas5 are highly sensitive to heat-shock. This suggests that may be this protein is important in refolding some important misfolded proteins upon heat-shock, that are however dispensable for the oxidative stress response (**figure 3.13** in section 3.5.2.5 from Results).

Finally, we found that inducing some heat shock elements may be protective for survival upon oxidative damage. This cross-protection mechanism [54] [55] [56] was operating in wild-type cells but not in cells lacking Sty1 or Atf1, master regulators of the survival response in both oxidative stress and heat shock. However, we can not still be sure that these protecting activities fully depend on Sty1 or Atf1, since there are many Sty1- and Atf1-dependent genes which are commonly induced in oxidative stress and in heat shock (for instance *ctt1*, which is induced 17-fold upon 15 min of heat shock and 5-fold upon 60 min of heat shock). It is important to notice that we used 2 hours pre-treatment of heat shock prior to H_2O_2 treatment (**figure 3.14** in section 3.5.2.6 of Results).

Chapter 5

CONCLUSIONS

Conclusions

1. The ICAT methodology is appropriate to identify and quantify reversible thiol oxidations at the proteome level.

2. H_2O_2 reversible oxidize solvent-exposed and redox-sensitive cysteines.

3. Reversible oxidation of cysteines in proteins is a transient modification.

4. Lack of Trx1 causes oxidation of cysteines in classical thioredoxin substrates.

5. Lack of Trr1 causes thioredoxin-dependent oxidation of cysteines.

6. Oxidized thioredoxins are the cause of massive thiol oxidations in a Δ*trr1* background.

7. Absence of Trx1 renders inactive its substrates.

8. Trx1 is able to weakly reduce its substrates by an alternative electron donor in the absence of Trr1.

9. Methionine sulphoxide reductases are not required for the antioxidant defence in *S. pombe*.

10. Mxr1 improves survival of a strain auxotrophic for methionine upon oxidative stress.

11. Free methionine is a primary barrier in the defence to oxidative stress.

12. Tpx1 and Ctt1 are the primary H_2O_2 scavengers in *S. pombe*.

13. Gpx1, Pmp20, and BCP do not have a role as H_2O_2 scavengers in *S. pombe*.

14. We could not set up a proper protocol to identify carbonyls in proteins.

15. Ubiquitination is involved in the degradation of carbonylated proteins in *S. pombe*.

16. Chaperones may act in triage decisions in the degradation of carbonylated proteins.

17. Heat shock may act as a cross-protection mechanism in the oxidative modification of proteins.

Chapter 6

MATERIALS AND METHODS

Materials and methods

6.1 Materials

Trichloroacetic acid (TCA) (Merck-Millipore, cat. no. 1008070250), glass beads, 0.4-0.6 mm (Sartorius Stedim Biotech, cat. no. BBI-8541701), acetone (Merck-Millipore, cat. no. 1000142511), iodoacetamide (IAM) (Sigma-Aldrich, cat. no. I1149), tris(hydroxymethyl) aminomethane (Tris base) (Sigma-Aldrich, cat. no. T1378), hydrochloric acid (HCl) (Merck-Millipore, cat. no. 1003172500), urea (Merck-Millipore, cat. no. 1084881000), ethylenediamine tetraacetic acid disodium salt (EDTA) (Sigma-Aldrich, cat. no. E5134), sodium dodecyl sulphate (SDS) (Sigma-Aldrich, cat. no. L4390), tris (2-carboxyethyl) phosphine hydrochloride (TCEP) (Sigma-Aldrich, cat. no. C4706), bradford protein assay (BioRad, cat. no. 500-0006), cleavable ICAT Reagent-10 assay kit (AB Sciex, cat. no. 4339036): contains all of the necessary reagents, buffers, cartridges and instructions with appropriate MSDS data. It contains 10 units of Heavy Cleavable ICAT®Reagent and 11 units of Light Cleavable ICAT®Reagent. Each unit of reagent will label approximately all reduced Cys contained in 100 μg of protein extract, dithiothreitol (DTT) (Sigma-Aldrich, cat. no. D0632), calcium chloride ($CaCl_2$), TPCK-treated trypsin (AB Sciex), formic acid, sequencing grading trypsin (Promega), triethyl-ammonium bicarbonate 1 M, pH 8.5 $\pm$ 0.1 (TEAB) (Sigma-Aldrich), formaldehyde light (CH4O) (37% (vol/vol)) (Sigma-Aldrich), formaldehyde (CD4O) (20%, 98% D) (Sigma-Aldrich), BODIPY®FL C1-IA (FIAM) (Invitrogen, cat. no. D6003), dimethylformamide (DMF) (Merck-Millipore, cat. no. 1030531000), ethanol (Merck, cat. no. K43657683 230), acetic acid (Merck, cat. no. K43573217 224), sodium thiosulphate (Sigma-Aldrich, cat. no. S6672), silver nitrate (Merck, cat. no. K43387312 217), sodium carbonate (Merck, cat. no. A0197592 036, formaldehye (Merck, cat. no. K42566703), EZ-link biotin-HPDP (Thermo-Fisher, cat. no. 21341), sodium chloride (Merck, cat. no. K43132604 207), streptavidin-sepharose beads (Thermo-Fisher, cat. no.), alkaline-phosphatase (Roche, cat. no. 11097075001), sodium acetate (Sigma-Aldrich, cat. no. S8750), hydrogen peroxide (Sigma-Aldrich, cat. no. H1009),L-cysteine (Merck, cat. no. K32952138 527), L-methionine (Sigma-Aldrich, cat. no. M9625), L-methionine-R,S-sulphoxide (Sigma-Aldrich, cat. no. M1126), glutathione (Sigma-Aldrich, cat. no. G4251), dipotassium phosphate (Merck, cat. no. A0187204 125), monopotassium phosphate (Merck, cat. no. A479373 420), Triton X-100 (, cat. no.), sulphosalicilic acid (Sigma-Aldrich, cat. no. S2130), 2-vinylpyridine (Sigma-Aldrich, cat. no. 13229-2), triethanolamine (Sigma-Aldrich, cat. no. 90279), glutathione disulphide (Sigma-Aldrich, cat. no. G4376), 5,5'-dithiobis(2-nitrobenzoic acid) (DTNB) (Sigma-Aldrich, cat. no. D8130), glutathione reductase (Sigma-Aldrich, cat. no. G3664-500U), β-nicotinamide adenine dinucleotide phosphate, reduced (β-NADPH) (Sigma-Aldrich, cat. no. N5130), aprotinine (Sigma-Aldrich, cat. no. A6279), protease cocktail inhibitor

(Sigma-Aldrich, cat. no. P8215), ethyl acetate (Sigma-Aldrich, cat. no. 31990-2), fluorescein-5-thiosemicarbazide (FTC) (Sigma-Aldrich, cat. no. 46985), streptomycin sulphate (Sigma-Aldrich, cat. no. S6501), dinitrophenyl-hydrazine (DNPH) (Fluka, 42210), α-DNP antibody (Sigma-Aldrich, D9656), Bodipy Fl Hydrazide (Invitrogen, cat. no. D-2371), dimethylformamide (DMF) (Merck, cat. no. K33245353 423), Sypro-Rubi (Invitrogen, cat. no. S-12000), thiourea (Sigma-Aldrich, T7875), CHAPS (Sigma-Aldrich, cat. no. C9426), destreak (Amersham, cat. no. 17-6003-18), ReadyStrip IPG strips (BioRad), mineral oil (BioRad, cat. no. 163-2129), agarose for 2D gels (BioRad, cat. no. 163-2111), Brilliant blue G colloidal concentrate B (colloidal Coomassie) (Sigma-Aldrich, cat. no. B2025), methanol (Scharlab, cat. no. ME0301005P).

6.2 Methods

6.2.1 Growth conditions

Strains were grown in standard media (minimal media (MM) or rich media containing 0.25 g/l of lysine, adenine, uracil, leucine, and histidene (YE5S)) as described [405].

6.2.2 Strains

Strains origins from published results or from results presented as manuscripts are described in the same papers/manuscripts. The rest of strains are described in **table 6.1**.

Table 6.1 Strains list

Strains	Genotype	Strains	Genotype
MJ11	*h$^+$ tpx1::kanMX6*	SG25	*h$^-$ pub3::kanMX6*
MJ15	*h$^+$ trx1::kanMX6*	SB18	*h$^-$ pop2::kanMX6*
SG167	*h$^+$ trr1::natMX6*	SB8	*h$^-$ pof5::kanMX6*
PG22	*h$^?$ trr1::natMX6 trx1::kanMX6*	SB25	*h$^-$ pof9::kanMX6*
SG185	*h$^-$ trr1::phleo trx1::natMX6 trx3::kanMX6*	SB7	*h$^+$ pof11::kanMX6*
SG164	*h$^-$ tpx1::natMX6 trr1::kanMX6*	SB9	*h$^-$ pof14::kanMX6*
NG77	*h$^-$ gcs1::kanMX6*	SB82	*h$^-$ ubi1::kanMX6*
SG187	*h$^-$ trr1::natMX6 trx3::kanMX6*	SB17	*h$^-$ ubi5::kanMX6*
SG170	*h$^+$ tpx1::natMX6 trr1::kanMX6 trx1::ura4+ ura4-D18 ade6-M210 leu1-32*	SB19	*h$^-$ urm1::kanMX6*
SG219	*h$^-$ tpx1::natMX6 trr1::kanMX6 trx1::ura4+ trx3::hph ura4-D18*	SB11	*h$^-$ ucp14::kanMX6*
SG189	*h$^-$ trx3::hph*	Δ*ecm29*	*h$^+$ ecm29::kanMX6 ura4-D18 ade6-M210 leu1-32*

Strains	Genotype	Strains	Genotype
SG260	*h⁻ trx1::kanMX6 trx3::natMX6*	SB15	*h⁻ rpt4::kanMX6*
SG180	*h⁻ grx1::hph*	SB10	*h⁻ dph1::kanMX6*
SG195	*h⁻ grx1::kanMX6 trr1::natMX6*	SG92	*h⁻ ubp2::kanMX6*
SG211	*h? trr1::natMX6 trx1::hph grx1::kanMX6*	SG107	*h⁻ ubp3::kanMX6*
SG270	*h? trr1::kanMX6 tpx1::natMX6 grx1::hph*	SG94	*h⁻ ubp4::kanMX6*
SG278	*h? trr1::kanMX6 tpx1::natMX6 grx1::hph trx1::ura4+ ura4-D18*	SG96	*h⁻ ubp5::kanMX6*
SB160	*h⁻ trx3::kanMX6 trx1::natMX6 grx1::hph*	SG108	*h⁻ ubp6::kanMX6*
AV18	*h⁻ sty1::kanMX6*	SG95	*h⁻ ubp7::kanMX6*
AV25	*h⁻ pap1::kanMX6*	SG97	*h⁻ ubp8::kanMX6*
MS98	*h⁻ atf1::natMX6*	SG93	*h⁺ ubp9::kanMX6*
SB6	*h⁻ ppk4::kanMX6*	SB28	*h⁺ ubp11::kanMX6*
SB4	*h⁻ hrd1::kanMX6*	SG103	*h- ubp14::kanMX6*
SB21	*h⁻ doa10::kanMX6*	SG104	*h- ubp16::kanMX6*
SB29	*h⁻ ubx2::kanMX6*	SG91	*h- uch1::kanMX6*
Δ*ubx4*	*h⁺ ubx4::kanMX6 ura4-D18 ade6-M210 leu1-32*	SB23	*h⁻ uch2::kanMX6*
SB12	*h⁻ ubc13::kanMX6*	SG35	*h⁻ otu1::kanMX6*
SB20	*h⁻ ubc14::kanMX6*	SG99	*h⁻ otu2::kanMX6*
SB3	*h- ubc16::kanMX6*	SG101	*h- sst2::kanMX6*
Δ*ubc2*	*h⁺ ubc2::kanMX6 ura4-D18 ade6-M210 leu1-32*	SB26	*h⁻ mas5::kanMX6*
Δ*ubr1*	*h⁺ ubr1::kanMX6 ura4-D18 ade6-M210 leu1-32*	SB13	*h⁻ bag102::kanMX6*
Δ*ubr11*	*h⁺ ubr11::kanMX6 ura4-D18 ade6-M210 leu1-32*	SG23	*h⁻ SPBC947.09::kanMX6*
SG33	*h⁻ SPAC6B12.07c::kanMX6*	SG29	*h⁻ SPAC5H10.02c::kanMX6*
SG31	*h⁻ san1::kanMX6*	SG36	*h⁻ SPAC4G9.19::kanMX6*
SG20	*h⁺ dsc1::kanMX6*	SG26	*h⁻ hsp9::kanMX6*
SG21	*h⁻ SPAC2F3.16::kanMX6*	SG28	*h⁻ hsp16::kanMX6*
SG22	*h⁻ SPBP8B7.23::kanMX6*	Δ*SPCC63.13*	*h⁺ SPCC63.13::kanMX6 ura4-D18 ade6-M210 leu1-32*
SG30	*h⁺ SPBC29A3.03c::kanMX6*	Δ*ssa1*	*h⁺ ssa1::kanMX6 ura4-D18 ade6-M210 leu1-32*
Δ*SPAC11E3.05*	*h⁺ SPAC11E3.05::kanMX6 ura4-D18 ade6-M210 leu1-32*	DC24	*h⁻ moe1::kanMX6*
SB22	*h⁻ SPAC167.07c::kanMX6*	SG32	*h⁻ rsv2::kanMX6*
SB24	*h⁻ ufd4::kanMX6*	666	*h⁺ ura4-D18 ade6-M210 leu1-32*
SB16	*h⁻ pub1::kanMX6*	SG102	*h⁺ ubc14::kanMX6 leu1-32*

6.2.3 Plasmids

Plasmids from results published in papers or presented as manuscripts are described in the same papers/manuscripts. pREP1.His_6-ubiquitin is a gift of Dr Sergio Moreno [406].

6.2.4 Labelling of total disulphides for 1D gel electrophoresis analysis

10 ml of exponentially growing *S. pombe* cells (OD_{600}∼0.5) were pelleted just after addition of 100% TCA to a final concentration of 10%, washed with 20% TCA and lysed by vortexing with glass beads in 12.5% TCA. Cell lysates were then pelleted, washed twice in cold acetone and dried. Free thiols were blocked by re-suspending the pellet in 200 μl of a solution containing 100 mM IAM in ICAT buffer (200 mM Tris-HCl pH 8.5, 6 M urea, 5 mM EDTA and 0.05% SDS), and incubation at 25ºC for 15 min. Aggregates were spun down by centrifugation and proteins were precipitated by addition of 200 μl of 20% TCA and incubation at -20ºC for 10 min. A TCA protein pellet was obtained, washed twice in cold acetone and dried. Reversibly oxidized Cys were then reduced by resuspending the pellet in 200 μl of a solution containing 10 mM TCEP in ICAT buffer and at 30ºC for 30 min. Excess of TCEP was removed by TCA protein precipitation and acetone washing. To label the newly reduced thiols, the resulting pellet was dissolved in 200 μl of a solution containing 40 μM of FIAM in ICAT buffer and incubated at 25ºC in the dark for 1 h. Unbound FIAM was removed by TCA protein precipitation and acetone washing. The resulting pellet was dissolved in ICAT buffer. Protein concentration was determined by Bradford protein assay and 2.5 μg of protein was electrophoretically separated by reducing SDS-PAGE. After electrophoresis, the image of the fluorescent protein on the gel was captured with a Typhoon 8600 (GE Healthcare) using an excitation wavelength of 532 nm and an emission filter of 526 nm with a short-pass filter.

6.2.5 Silver staining

Proteins in gels are fixed in 40 ml EtOH, 10 ml of acetic acid and 50 ml Milli-Q water for 30 min. Then proteins are sensitized in 30% EtOH, and 0.2% sodium thiosulphate in Milli-Q water. After sensitizing, the gel is washed 3 x 5 min with Milli-Q water. The silver reaction is performed with 0.25% of silver nitrate in Milli-Q water. After silver staining, the gel is washed 2 x 1 min in Milli-Q water, and proteins are developed in 2.5% sodium carbonate and freshly added 0.007% formaldehyde in Milli-Q water. Developing is stopped by incubating the gel during 10 min in 1.46% EDTA. Finally, the gel is washed 3 x 5 min with Milli-Q water.

6.2.6 Colloidal Coomassie staining

Use only Milli-Q water along the protocol. Prepare a working solution 1X: Add 800 ml of Milli-Q water to a new bottle (Brilliant blue G-Colloidal Concentrate B) and mix by inversion and with a magnet. Fix proteins in the gel with 40% methanol, 7% acetic acid, and 53% Milli-Q water, minimum for 1 hour. Combine 4 parts of 1X working solution and 1 part of methanol (volume 50 ml). Perform staining by rocking at room temperature during 1 hour. Wash with Milli-Q water until gel is destained.

6.2.7 Analysis of redox state and protein levels by TCA extracts

For in vivo redox state analysis of Pap1, Tpx1, Trx1, or HA-tagged proteins, S. pombe cultures (5 ml) at an OD_{600} of 0.5 were pelleted just after the addition of 100% trichloroacetic acid (TCA) to a final concentration of 10% and washed in 20% TCA. The pellets were lysed by vortexing after the addition of glass beads and 12.5% TCA. Cell lysates were pelleted, washed in acetone, and dried. Alkylation of free thiols was accomplished by resuspension of the pellets in 50 μl of a solution containing 75 mM iodoacetamide, 1% SDS, 100 mM Tris-HCl (pH 8), 1 mM EDTA, and incubation at 25°C for 15 min. In the case of analysing the redox state of Pap1, samples were then dephosphorylated to avoid broad bands after electrophoresis by diluting them 5-fold with alkaline phosphatase buffer to a final concentration of 80 mM Tris-HCl (pH 9.5), 0.08 mM EDTA, and adding 0.04 units/μl of alkaline phosphatase for 30 min at 37°C. The alkylated (and dephosphorylated samples, in the case of Pap1) were electrophoretically separated by non-reducing SDS-PAGE, and proteins were immunodetected with a polyclonal anti-Pap1 [169], polyclonal anti-Tpx1 [52], polyclonal anti-Trx1 [396] or with house-made monoclonal anti-HA antiserum (12CA5). TCA protein extracts and reducing SDS-PAGE (sample buffer containing DTT) were used to detect differences in protein expression.

6.2.8 Labelling of reversibly oxidized Cys with ICAT reagents

With this strategy it is possible to compare two samples at a time.

Freezing thiol-redox status Freeze the thiol-redox status by adding chilled 100% TCA up to a final concentration of 10% directly to the yeast cultures. Allow acidification for a minute before harvesting. TCA has to be added without altering the growing conditions of the culture (i.e. if the culture is growing in a flask with shaking, do not stop shaking).

Preparation of cell lysates During lysis, cells and lysates should be kept at 4ºC at all times. Harvest cells by centrifugation at 2,000 g for 3 min at 4ºC. Collect cells into a 1.5 ml microcentrifuge tube with 1 ml of chilled 20% TCA. Centrifuge at 20,000 g for 30 seconds and take out supernatants. To allow good performance in all following steps, the maximum amount of cells to be collected into a 1.5 ml centrifuge tube is the corresponding to a 50 ml of culture at OD_{600} 0.5 (5 x 10^8 cells). In this step, pellets can be stored at -80ºC at least for 2 weeks. Resuspend pellets in 250 μl of 12.5% TCA. Fill with glass beads up to 85-90% of the volume to allow proper disruption. To disrupt cells, vortex at maximum speed for 5 min in a vortex for microcentrifuge tubes (to avoid overheating of the lysates, keep the vortex in a cold chamber at 4ºC). Pierce two holes, one in the bottom and the other in the top of each 1.5-ml microcentrifuge tube, with a flame-heated needle (0.6 x 25 mm), and place each tube on the top of another 1.5-ml tube. Centrifuge to separate the lysate from the beads at 850 g for 30 sec at 4ºC. Centrifuge the cell lysates at 20,000 g for 20 min at 4ºC. Take out supernatants, and wash pellets with 1 ml of chilled acetone (-20ºC), with the help of the blunt side of a calibrated plastic inoculation loop. Centrifuge at 20,000 g for 5 min at 4ºC. Take out supernatants, and repeat the previous step. Take out supernatants and dry pellets with the help of a vacuum concentrator, by centrifuging 2 min at 37ºC. Alternatively, pellets can be dried by placing them for $\sim$8 min in an oven pre-heated at 55ºC.

Alkylation of reduced Cys Alkylate Cys by resuspending each dried pellet in 500 μl of alkylating buffer A, with the help of the blunt side of a calibrated plastic inoculation loop. Incubate at 25ºC for 15 min in the dark and with shaking. Centrifuge at 20,000 g for 5 min at room temperature to remove aggregates. Collect each supernatant and transfer it to a new 1.5-ml microcentrifuge tube. To precipitate proteins and remove IAM excess, add 500 μl of chilled 20% TCA to each supernatant, mix and place at -20ºC for 10 min. Centrifuge at 20,000 g for 10 min, and remove the supernatants. Wash each pellet with 1 ml of cold acetone. Centrifuge at 20,000 g for 5 min at 4ºC. Remove supernatants and repeat the previous step. Remove supernatants and dry pellets with a vacuum concentrator.

Reduction of reversibly oxidized Cys Reduce the reversibly oxidized Cys by resuspending each pellet in 300 μl of reduction buffer with the help of the blunt side of a calibrated plastic inoculation loop. 30 seconds of sonication at the maximum power in a water bath sonicator may help to resuspend pellets. Incubate for 30 min at 30ºC. At this time, pool all aliquots belonging to the same condition. Determine protein concentration by Bradford assay. In this step, withdrawn 50 μg of each condition for dimethyl labelling. For each condition, precipitate $\sim$2 mg of protein by adding an equivalent volume of chilled 20% TCA, mix and place at -20ºC for 10 min. Centrifuge at 20,000 g for 10 min, and take out the supernatants. Precipitate exactly the same amount of protein for each condition.

Wash each pellet with 1 ml of cold acetone. Centrifuge at 20,000 g for 5 min at 4ºC. Take out supernatants and repeat the previous step. Take out supernatants and dry pellets with the help of a vacuum concentrator.

ICAT labelling of reversibly oxidized Cys Resuspend the pellet belonging to one condition with 1 ml of heavy alkylating buffer, and the pellet belonging to the other condition with 1 ml of light alkylating buffer with the help of the blunt side of a calibrated plastic inoculation loop. 30 seconds of sonication at the maximum power in a water bath sonicator may help to resuspend pellets. Incubate for 2 hours at 37ºC in the dark and with shaking. Stop the ICAT labelling reaction by adding 1.75 μl of 1 M DTT (10-fold molar excess over ICAT reagent). Allow the reaction to take place by incubation at room temperature for 5 min.

Trypsin digestion Pool light and heavy reactions in a 15 ml tube. Dilute them by adding 10 ml of 10 mM $CaCl_2$ to reduce the urea concentration to 1 M. Add 100 μg of TPCK-treated trypsin (1:40 ratio) and let the digestion to take place for 16 hours at 37ºC with mild agitation and light protected.

Peptide desalting Peptides must be desalted to remove salts and urea from the digestion buffer. We use Oasis®HLB Plus LP Extraction cartridges which are appropriate for peptide amounts > 10 μg. Wash and condition the cartridge with 5 ml of 100% ACN. Equilibrate with 5 ml of 5% formic acid. Acidify the sample to pH 2-3 with formic acid and load it into the cartridge. Wash with 5 ml of 5% formic acid. Elute with 5 ml of 70% ACN/5% formic acid. Evaporate the sample to dryness with a vacuum concentrator for 1.5 ml microcentrifuge tubes (4-5 hours). Perform cation exchange chromatography, affinity purification and biotin cleavage exactly according to ICAT kit manufacturer instructions. Resuspend dried pellets in 4 ml of cation exchange load buffer of the ICAT kit and further process following manufacturer instructions up to finishing the section of cleaving the ICAT Reagent-Labelled peptides. At this point, the sample is a dry pellet ready to be separated and analyzed by LC-MS/MS.

6.2.9 Liquid chromatography and MS of ICAT-labelled peptides

Peptides were analyzed by LC-MS/MS using an EasyLC (Thermo Fisher Scientific) coupled to an Orbitrap Velos (Thermo Fisher Scientific) via a nano electrospray source

(Thermo Fisher Scientific). Peptides were separated by reversed phase chromatography using a 15 cm column with an inner diameter of 100 μm, packed with 5 μm C_{18} particles (Nikkyo Technos Co.,). Peptides were loaded directly onto the analytical column at 1.5-2 μl/min using a wash volume of 4 to 5 times injection volume and eluted using a gradient delivered at 500 nl/min. The gradient increased from 97% buffer A/3% buffer B (buffer A: 0.1% formic acid, buffer B: 80% acetonitrile, 0.1% formic acid) to 85% buffer A/15% buffer B in 4 min, followed by a less steep increase to 55% buffer A/45% buffer B in 118 min. Following the gradient, the column was washed for 11 min with 10% buffer A/90% buffer B. The Orbitrap Velos was operated in CID mode with a data acquisition cycle composed of a full scan (2 micro scan at 30,000 resolution) in the Orbitrap (AGC target 1 x 10^6) followed by fragmentation of up to 20 of the most intense multiply charged ions in the linear trap (MSn AGC target 3 x 10^4). Dynamic exclusion for the selected ions was set to 30 s. A single ion was used as lock mass (m/z 445.1200) [407].

6.2.10 ICAT data analysis: database searches

MS/MS spectra were extracted using MaxQuant 1.0.13.13 [408]. MS/MS spectra were queried against the *S. pombe* fraction of NCBInr (July 27, 2010) using Mascot v2.2 (Matrix-Science). For protein accession peptides were searched against *S. pombe* GeneDB (Wellcome Trust Sanger Institute, http://old. genedb.org/genedb/pombe/). All search strategies included decoy searches. For all queries, tryptic specificity and allowing up to 3 missed cleavages, was used. The mass tolerance was set to 7 ppm or 15 ppm for precursor ions and 0.5 Da for product ions. When searching the ICAT data the following dynamic modifications were used: oxidation [M], Glu→pyroGlu [N-term. E], Acetyl [Protein N-term] together with the light and heavy ICAT moieties (ICAT-C-^{12}C9 [C] and ICAT-^{13}C9 [C]). Peptides with scores better than 17 (measured false discovery rate of 4.4%, Mascot probability of 0.10 or better) were extracted. Score values of 20 and 27 represent measured false discovery rates of 2.2% and 0.5% with Mascot probabilities better than 0.05 and 0.01, respectively.

6.2.11 ICAT data analysis: quantification analysis

MSQuant 2.0b7 (http://www.msquant.sourceforge.net) was chosen for the quantification of ICAT peptides because this software allows to quantify peptides with multiple Cys differing in modifications (ICAT and carbamidomethylation). In this study, 18% of all matched Cys-containing peptides contained more than one Cys residue. Of those multiple Cys-residue-peptides, more than half (65%) carried both carbamidomethyl and ICAT labels. Since MSQuant 2.0b7, in our hands, is not compatible with Mascot v2.3, ICAT MS/MS data were queried using Mascot v2.2. All peptides were quantified and hereafter sorted based on the following rules: (i) though searched together, peptides from different

biological experiments, and replicates were treated as independent events; (ii) in an ICAT-labelled peptide pair, only the highest scoring peptide was extracted; and (iii) if possible, an average ICAT ratio was calculated for a given peptide sequence using ICAT ratios of this peptide sequence in its different charge states, measured in different LC-MS/MS analysis of the exact same sample and from the peptide sequence carrying modifications assigned as sample handling artefacts (oxidized methionines and pyro-Glutamates at the N-terminal).

6.2.12 Quantification of proteins by dimethyl labelling

A fraction of the two samples subjected to the ICAT experiments was digested using Sequencing Grade trypsin (Promega, Madison, WI, USA), in 25 mM TEAB. Tryptic peptides were labelled with either normal or deuterium labelled formaldehyde, respectively [409] [395]. A modification was added to the dimethyl labelling protocol [395]: the reaction mixture was not acidified prior to mixing, but instead 8 Î¼l of 1% ammonia solution was added. This modification allowed direct sample loading on strong anion exchange columns. The mixed, now differentially labelled peptides, were split into two portions, 1/5 for testing of the labelling and 4/5 as to be used for a more comprehensive analysis. The small portion was acidified, and SDS was removed by a cation exchange (AB Sciex, Foster City, CA, USA) step according to the manufacturer's instructions. The SDS depleted dimethyl labelled peptide mixture was hereafter desalted on a home-made Empore C_{18} column (3M, St. Paul) [410] prior to analysis by LC-MS/MS. The larger portion (4/5) was fractionated by strong anion exchange (Empore anion-SR, 3M, St. Paul) as described by Wisniewski *et al*. [411]. In accordance with this protocol, the peptides were eluted into six pH fractions (11, 8, 6, 5, 4 and 3). Each fraction was purified on home-made Empore C_{18} columns prior to analysis by LC-MS/MS.

6.2.13 Quantification of proteins by dimethyl labelling: data analysis

Proteome Discoverer v1.2.0.208 (Thermo Fisher Scientific) was used to extract MS/MS spectra which were queried using Mascot v2.3. All Cys were treated as being carbamidomethylated while variable modifications were: oxidation [M], Glu→pyro-Glu [N-term. E] together with modification of lysines and N-terminals by normal ($^{12}C_2{}^1H_4$) and heavy ($^{12}C_2{}^2H_4$) labelled dimethyl. Identified peptides (5% false discovery rate) were quantified using Proteome Discoverer v1.2.0.208. We observed that not all dimethyl labelled peptide pairs co-eluted and to compensate for this we increased the default quantification window from $\pm$0.2 min to $\pm$0.5 min. A mass precision window of 3 ppm was used for the quantification. Protein ratios are reported as the median of the measured peptide ratios for a given protein.

6.2.14 Validation of ICAT results by Western blot

To confirm the ICAT results for individual oxidized proteins, 50 ml of exponentially growing cells were processed as described above (section 6.2.42) except that the labelling step of disulphides was performed with a biotin-linked reversible alkylating agent, biotin-HPDP. After labelling, excess unbound biotin-HPDP was removed by TCA protein precipitation and acetone washing. The dried pellet was resuspended in ICAT buffer plus 50 mM NaCl, and quantified. A total of 1 mg of biotin-HPDP-reacted proteins, in a final volume of 300 μl, was added to 15 μl of streptavidin-sepharose beads, previously washed with PBS/1% NP-40/0.1% SDS, and incubation proceeded overnight at 4°C with continuous tumbling. Beads were washed twice with PBS/1% NP-40/0.1% SDS, twice with PBS/1% NP-40/0.1% SDS/0.4 M NaCl and once with 50 mM Tris-HCl pH 7.5. For Pap1 quantification, washed beads were further resuspended in dilution buffer (0.1 M Tris-HCl pH 9.5, 0.1 mM EDTA) containing 2 U of alkaline phosphatase and incubated for 30 min at 37°C. Dephosphorylation of Pap1 was also performed in total labelled extracts, prior to streptavidin purification, and in the unbound fraction, after streptavidin purification, by diluting ten times an aliquot in dilution buffer containing 2 U of alkaline phosphatase and incubating for 30 min at 37°C. Biotinylated proteins were eluted from beads with PAGE sample buffer containing DTT. Proteins were detected by Western blot using Pap1, Tpx1 and Trx1 polyclonal antibodies (described in section 6.2.7).

6.2.15 RNA analysis

Cells, grown in minimal media to a final OD_{600} of 0.5, were left either untreated or treated for the indicated times and concentrations with H_2O_2. Yeast cultures (40 ml) were then centrifuged at 500 g. for 3 min and washed with H_2O. Each sample was then resuspended in 0.4 ml of AE buffer (50 mM sodium acetate pH 5.3, 10 mM EDTA pH 8.0). SDS was then added to a final concentration of 1%, and proteins and DNA extracted by adding 0.3 ml of a mixture of acidic phenol-chloroform, and incubation at 65ºC for 5 min. Samples were cooled down in ice, 0.3 ml of chloroform was added, and the aqueous phase was separated by centrifugation at 10,000 g for 2 min at 4ºC. After chloroform extraction, RNA was precipitated with 100% ethanol plus 0.1 M of sodium acetate pH 5.3 and incubation at -80ºC for 1 hour. Pellets were resuspended in DEPC water after washing them with 70% ethanol. RNA concentration was determined at OD_{260} with a nanodrop system and equal amounts (10 μg) were loaded in formaldehyde agarose gels and transferred to GeneScreen Plus membranes. Hybridization and washes were performed as recommended by the facturer. Membranes were hybridized with [α-^{32}P] dCTP labelled probes containing the open reading frames of the genes indicated in the figure legends. Ribosomal RNA is used as loading control.

6.2.16 Survival and auxotrophy assays by sequential spots

Strains were grown at 30ºC in YE5S media until they reached an OD_{600} 0.5. Cells were then serial diluted from 5 x 10^7 to 5 x 10^2 in serial 1/10 dilutions in a 96-well microplate. 2 μl of each concentration (containing therefore from 10^5 to 10 cells in 1/10 dilutions) were then spotted with a replicator on solid agar plates of YE5S or MM containing the indicated concentrations of stressors or cystheine, methionine, methionine-R,S-sulphoxide, and glutathione. For auxotrophy assays, cells were washed in MM prior to dilution. For stationary phase studies, cell's OD_{600} was considered only for the log-phase day of the experiment.

6.2.17 Growth curves in liquid

To measure cellular growth, we used an assay based on automatic measurements of optical densities for small (100 μl) cell cultures. Cells were grown to an OD_{600} of 0.5 under continuous shaking in Erlenmeyer flasks and then diluted to an OD_{600} of 0.1. 100 μl of the diluted cultures (treated or not with the indicated amounts of stressors) were placed into a 96-well non-coated polystyrene microplate covered with an adhesive plate seal. A Power Wave microplate scanning spectrophotometer (Bio-Tek) was used to obtain the growth curves. The OD_{600} was automatically recorded using Gen5 software. The software was set as follows: OD was measured at 600 nm, incubation temperature was kept at 30ºC, the microplates were subjected to continuous shaking and the readings were done every 10 min during 48 hours.

6.2.18 Quantitative determination of glutathione (GSH) and glutathione disulphide (GSSG) levels

GSH and GSSG levels were quantitatively measured as previously reported [412], with some minor modifications. 50 ml of exponentially growing *S. pombe* cells were pelleted, washed twice with cold 1 x PBS and lysed by vortexing with glass beads in 300 μl of extraction buffer (0.1 M potasium phosphate buffer, pH 7.5, 5 mM EDTA, 0.1% Triton X-100 and 1.3% sulphosalicylic acid). Cell lysates were then pelleted and supernatants were used for measuring total glutathione (GSH + GSSG) and for measuring GSSG. Total glutathione can be directly measured from the supernatants, but to measure GSSG, GSH has to be first quickly blocked by incubating 100 μl of the supernatant with 2 μl of 2-vinylpyridine for 1 hour at room temperature in a fume hood. Reaction was neutralized by incubating 10 min with 6 μl of 1:6 triethanolamine. GSH and GSSG standards were prepared in 0.1 M potassium phosphate buffer pH 7.5 and 5 mM EDTA with concentrations ranging from 26.4 nM/ml to 0.4125 nM/ml. GSSG standards were subjected to the same treatment as supernatants from cell lysates. 20 μl of both, standards and properly dilute

supernatants (in order to fit in the range from the standard curve), were diluted in a 96-well plate. 120 μl of a 1:1 solution of 0.67 mg/ml 5,5'-dithiobis-(2-nitrobenzoic acid) (DTNB) and 13.3 μl/ml of glutathione reductase (250 U/ml) were added to each well and, after incubating 30 sec, 60 μl of 0.67 mg/ml of β-NADPH were also added. Abosrbance was immediately read at 412 nm in a Powerwave HT340 microplate reader (BioTek) with readings every 30 seconds during 5 min. The change in absorbance per min was calculated for each sample and the actual total GSH and GSSG concentrations in the samples were extrapolated from the standard curve. GSH concentration was obtained using the formula GSH_{total}=GSH + 2 x GSSG. Concentration is expressed as mM/cell, considering that, in general, the volume of a *S. pombe* cell is $\sim$ 3.14 x 10^{-8} μl.

6.2.19 Dinitrophenyl hydrazide (DNPH) for labelling protein carbonyls

Obtain cellular pellet by centrifuging 50 ml of cells at 4ºC, 4,000 rpm for 1 min. Pellets can not be frozen. Transfer cells to a 1.5 ml screw cap tube. Add 300 μl of DNPH-carbonylation buffer (50 mM Tris-HCl pH 7.5, 2 mM EDTA, 0.05% NP-40 and freshyl added protease inhibitors (2 mM phenyl-methanesulfonyl-fluoride (PMSF), 5 mM benzamidine, 10 μl/ml aprotinine, and 1 μl/ml of protease inhibitor cocktail (Sigma-Aldrich)) and glass beads. Disrupt cells by bead beating them 3 times for 25 sec, intensity of 4.5. Transfer cell extract to a new eppendorf by pinching a hole with a needle. Centrifuge at 4ºC, 13,200 rpm for 10 min. Supernatant is the native extract. Quantify by Bradford. Because of possible reactivity problems with DNPH, protein extract should be at a concentration between 4-10 μg/μl. If higher, dilute with DNPH-carbonylation buffer and quantify again. Take 50 μg of total protein and take to 12.5 μl final volume (note that 50 μg of protein of a 4 μg/μl extract are contained in a volume of 12.5 μl). Add 12.5 μl of 12% SDS. Boil at 100ºC for 3 min. Let cool back to r.t. Quick spin the samples. Perform the reaction with DNPH 10 min sharp. Add 25 μl of 10 mM DNPH in TFA 10%. Let react for 10 min at 25ºC. Stop the reaction by addition of 25 μl of stopping buffer (30 μl of β-mercaptoethanol to 70 μl of 2M Tris base 30% glycerol). The colour of the samples will change from yellow to orange, as the pH is basic instead of acid. If the colour doesnât change, add more stopping buffer, some 10 μl or so. This buffer contains glycerol, so the samples are dense enough to load in a gel. The orange non-reacted DNPH will provide an electrophoretic front. Load samples in a 10% SDS-acrylamide gel. Perform electrophoresis at 110 V all the time. Transfer, block in 5% milk and inmunodetect with a 1:500 dilution of polyclonal α-DNP (Sigma, D9656) antibody in milk.

6.2.20 Fluorescein-5-thiosemicarbazide (FTC) for labelling protein carbonyls

This protocol is a modification of the protocol published at [369]. Obtain a cellular pellet by centrifuging 50 ml of cells at $OD_{600} \sim 0.5$, at 4ºC, 4,000 rpm for 1 min. Transfer cells to a 1.5 ml eppendorf. Add 300 μl of carbonylation buffer (20 mM sodium phosphate buffer pH 6.0 containing 1 mM EDTA and protease inhibitors (2 mM phenyl-methanesulfonyl-fluoride (PMSF), 5 mM benzamidine, 10 μl/ml aprotinine, and 1 μl/ml of protease inhibitor cocktail (Sigma-Aldrich)) and glass beads. Disrupt cells by beating them 5 min in the eppendorf vortex. Transfer cell extract to a new eppendorf by pinching a hole with a needle. Centrifuge at 4ºC, 13,200 rpm for 10 min. Treat the resulting supernatant with 1% streptomycin sulphate and incubate at 4ºC for 5 min (for precipitating nucleic acids which also contain reactive carbonyl groups). Centrifuge at 4ºC, 13,200 rpm for 5 min. Measure protein concentration in the supernatant by Bradford assay. Dilute protein extract to 2 μg/μl in a final volume of 200 μl in carbonylation buffer. Mix the extract with 8 μl of 50 mM (dissolved in DMF) fluorescein-5-thiosemicarbazide (FTC). Incubate at 37ºC for 150 min in the dark. Precipitate proteins with 200 μl of 20% chilled TCA for 15 min at -20ºC. Centrifuge at room temperature for 10 min at 13,200 rpm. Re-suspend pellet in 1 ml of cold ethanol/ethyl acetate (1:1). Centrifuge at 4ºC at 13,200 rpm for 5 min. Wash at least 3 times, to remove unbound FTC. Dissolve pellets in 50 μl of dissolving buffer (phosphate buffer pH 8.0 containing 1mM EDTA and 8 M urea). Measure protein concentration with Bradford (use 6 μl of sample). For electrophoresis: load 5 μg of protein in 8 μL of dissolving buffer. Add 2 μl of 5 X sample buffer without bromophenol blue. Any empty well in the gel must be filled with 8 μl of dissolving buffer + 2 μl of 5 X sample buffer. Run the gel until the front of the gel is about to migrate to the running buffer. If you leave the front to escape from the gel, FTC leftovers will stain the gel. Capture the fluorescent image with a Typhoon 8600 (GE Healthcare) using an excitation wavelength of 532 nm and an emission filter of 526 nm with a short-pass filter. For loading control, the same gel can be stained with silver staining, as above described 6.2.5.

6.2.21 Bodipy Fl Hydrazide (Bodipy) for labelling protein carbonyls

Obtain a cellular pellet by centrifuging 50 ml of cells at $OD_{600} \sim 0.5$, at 4ºC, 4,000 rpm for 1 min. Transfer cells to a 1.5 ml eppendorf. Add 300 μl of carbonylation buffer (20 mM sodium phosphate buffer pH 6.0 containing 1 mM EDTA and protease inhibitors (2 mM phenyl-methanesulfonyl-fluoride (PMSF), 5 mM benzamidine, 10 μl/ml aprotinine, and 1 μl/ml of protease inhibitor cocktail (Sigma-Aldrich)) and glass beads. Disrupt cells by beating them 5 min in the eppendorf vortex. Transfer cell extract to a new eppendorf by pinching a hole with a needle. Centrifuge at 4ºC, 13,200 rpm for 10 min. Treat the resulting supernatant with 1% streptomycin sulphate and incubate at 4ºC for 5 min (for precipitating nucleic acids which also contain reactive carbonyl groups). Centrifuge at 4ºC,

13,200 rpm for 5 min. Measure protein concentration in the supernatant by Bradford assay. Use 2 ml eppendorf to perform the reaction. Dilute protein extract to 1 μg/μl in a final volume of 1 ml in carbonylation buffer. Mix the extract with 40 μl of 50 mM (dissolved in DMF) Bodipy Fl Hydrazide (Bodipy). Incubate at 37ºC for 15 min in the dark. Precipitate proteins with 1 ml of 20% chilled TCA for 15 min at -20ºC. Centrifuge at r.t. for 10 min, 13,200 rpm. Re-suspend pellet in 1 ml of chilled acetone. Centrifuge at 4ºC, 13,200 rpm for 5 min. Repeat washes 3 times, to remove unbound Bodipy. Dissolve pellets in 150 μl of IEF buffer (7 M urea, 2 M thiourea, 4% CHAPS in 20 mM Tris-HCl, pH 8). Measure protein concentration with Bradford (use 2 μl of sample).

6.2.22 2D gel electrophoresis from Bodipy labelled protein carbonyls

Protein amount and conditions depend on the type of IEF and 2-D you use. Run the gel until the front of the gel is about to migrate to the running buffer. If you leave the front running out from the gel, Bodipy leftovers will stain the gel.

First dimension Once obtained the protein extract (the buffer cannot contain detergents, for example SDS, and the maximum concentration of Tris-HCl that you can use is 20 mM) dissolve it in 0.5 ml of IEF buffer (7 M urea; 2 M thiourea, 4% CHAPS, 20 mM Tris-HCl containing 5% ampholites (with the same pH interval than the strips to be used (BioRad Ready Strip o Amersham IPG buffer), 4.1 μl of 1% bromophenol blue, and 6 μL Destreak.

For 7 cm gels you can load as a standard concentration 75 μg of protein in a final volume of 125 μl of IEF buffer. For 17 cm gels you can load as a standard concentration 350 μg of protein in a final volume of 300 μl of IEF buffer. Once the protein has been dissolved in IEF buffer, centrifuge 5 min at 14,000 rpm at 4ºC and keep the supernatant.

Strips rehydration and sample absorption Make a note with the number of the strip which will correspond with each sample (7 cm strips can be purchased to BioRad or Amersham, but 17 cm strips only in BioRad). Slowly distribute the sample along the tray, leaving approximately 1 cm free in each side of the strip. Remove the piece of plastic from the strips with the forceps. The side of the gel has to contact the sample, avoid bubbles. Leave the sample to be completely absorbed in the strip, 1 hour approximately, and then cover with mineral oil (1.5 ml) and wait for 12 to 16 hours.

Isoelectric focusing (IEF) Set the desired program on the Protean Cell (Bio-Rad) (the manufacturer disposes of pre-set methods with linear slope that are used for both 7 cm and 17 cm strips) according with the size of the strip you are going to use. Conditions can be changed when desired. Cover the electrodes with wet wick papers in mQ water. Change

the strips from the rehydration tray to the tray with the electrodes. First clean the mineral oil from the strips, drying a little the surface with the plastic on absorbent paper. Place the rehydrated strip gel side down in the focusing channel with the end labelled positive at the positive end of the tray. Ensure good contact with electrodes by depressing the strip lightly. Cover the strips with mineral oil, to avoid sample evaporation and run the IEF. At the end of the IEF, the strips can either be prepared straight away for SDS-PAGE second dimension, or they can be placed in a rehydration tray gel side up, wrapped in thin foil and stored at -80ºC.

Equilibration of IPG strips for second dimension SDS-PAGE If strips have been frozen, let them thaw for a few minutes before equilibration. Place the strips in a rehydration tray channel gel side up. Then pipete the equilibration buffer containing DTT (6 M urea, 50 mM Tris-HCl, pH=8.8, 2% SDS, 30% glycerol, and 10 mg/ml of DTT) on top of the IPG strips (2-3 ml/strip). Incubate on a shaker for 10 min, then transfer the strips to clean channels and repeat with equilibration buffer containing iodoacetamide (6 M urea, 50 mM Tris-HCl, pH=8.8, 2% SDS, 30% glycerol, and 25 mg/ml of DTT).

Gel electrophoresis: second dimension After placing the strips on the gel (making sure there are no bubbles between the strip and the gel), place a wet wick paper with protein marker on a side of the strip, and sail the strip on the top with heated agarose.

7 cm strips can be run in small electrophoresis cuvettes, 60 V, 30 min and then at 120 V until the front is leaving the gel. 17 cm strips are run in big electrophoresis cuvettes and under refrigeration (18ºC). The bottom buffer is 1X running buffer (1.5 l) and the upper buffer is 2X running buffer (500 ml). Running conditions are: 16 mA per gel (no per cuvette) for 30 min and then at 24 mA per gel (around 5 hours).

Capture the fluorescent image with a Typhoon 8600 (GE Healthcare) using an excitation wavelength of 532 nm and an emission filter of 526 nm with a short-pass filter. For loading control, the same gel can is stained with Sypro-Rubi (according to manufacturer instructions). Read fluorescence from Sypro-Rubi in the Typhoon at 488 nm λ_{ex}=488 and λ_{em}=610. This image is important to match and quantify spots using the software PDQuest (Bio-Rad). Upon fluorescence staining of total protein concentrations, stain the same gel with colloidal Coomassie, to visualize spots and cut them for analysis in the MS facility.

6.2.23 Metal-catalysed oxidation of BSA

BSA 10 mg/ml from New England Biolabs was used to perform the experiment. 1 mg was keep untreated or used for metal-catalyzed oxidation. In both cases, the original buffer was changed by over-night dialysis to 0.5 ml of oxidation buffer (50 mM HEPES buffer, pH 7.4, containing 100 mM KCl and 10 mM $MgCl_2$). Oxidation was accomplished by

adding ascorbic acid/$FeCl_3$ with final concentrations of 25 mM/100 μM and incubating overnight at 37ºC in a shaking bath. Oxidation was stopped by addition of 1 mM EDTA. Samples were dialysed again at 4ºC against the oxidation buffer supplemented with 1 mM EDTA. Protein carbonyls in the samples were then labelled with DNPH according to section 6.2.19. Upon labelling, samples were precipitated with a final concentration of 10% TCA and washed twice with chilled acetone. Dried pellets were resuspended in 50 μl of 6 M urea, 100 mM Tris-HCl, pH=8. 50 μg of each sample (untreated and oxidized) were reduced and alkylated. Protein digestion was performed with chemotrypsin (ratio 1:40) overnight at 25ºC, and then trypsin (ratio 1:40) during 5 hours at 37ºC.

Chapter 7

APPENDIX

7.1 Mitochondrial dysfunction increases oxidative stress and decreases chronological life span in fission yeast

Zuin A, Gabrielli N, Calvo IA, García-Santamarina S, Hoe KL, Kim DU, Park HO, Hayles J, Ayté J, Hidalgo E. PLoS One. 2008 Jul 30;3(7):e2842.

Zuin A, Gabrielli N, Calvo IA, García-Santamarina S, Hoe K-L, Kim DU, et al. Mitochondrial Dysfunction Increases Oxidative Stress and Decreases Chronological Life Span in Fission Yeast. PLoS One. 2008 Jul 30;3(7):e2842. DOI: 10.1371/journal.pone.0002842

7.2 Genome-wide screen of genes required for caffeine tolerance in fission yeast

Calvo IA, Gabrielli N, Iglesias-Baena I, García-Santamarina S, Hoe KL, Kim DU, Sansó M, Zuin A, Pérez P, Ayté J, Hidalgo E. PLoS One. 2009 Aug 12;4(8):e6619.

Calvo IA, Gabrielli N, Iglesias-Baena I, García-Santamarina S, Hoe K-L, Kim DU, et al. Genome-wide screen of genes required for caffeine tolerance in fission yeast. PLoS One. 2009 Aug 12;4(8):e6619. DOI: 10.1371/journal.pone.0006619

Bibliography

[1] B. Halliwell. Reactive species and antioxidants. redox biology is a fundamental theme of aerobic life. *Plant physiology*, 141(2):312–322, 2006.

[2] J.A. Imlay. Pathways of oxidative damage. *Annual Reviews in Microbiology*, 57(1):395–418, 2003.

[3] J.F. Turrens. Mitochondrial formation of reactive oxygen species. *The Journal of physiology*, 552(2):335–344, 2003.

[4] B. D'Autréaux and M.B. Toledano. ROS as signalling molecules: mechanisms that generate specificity in ROS homeostasis. *Nature Reviews Molecular Cell Biology*, 8(10):813–824, 2007.

[5] E.R. Stadtman and R.L. Levine. Protein oxidation. *Annals of the New York Academy of Sciences*, 899(1):191–208, 2000.

[6] S.S. Fam and J.D. Morrow. The isoprostanes: unique products of arachidonic acid oxidation-a review. *Current medicinal chemistry*, 10(17):1723–1740, 2003.

[7] M.D. Evans, M. Dizdaroglu, and M.S. Cooke. Oxidative DNA damage and disease: induction, repair and significance. *Mutation Research/Reviews in Mutation Research*, 567(1):1–61, 2004.

[8] JA Imlay and I Fridovich. Assay of metabolic superoxide production in *Escherichia coli*. *Journal of Biological Chemistry*, 266(11):6957–6965, 1991.

[9] C.C. Winterbourn. Reconciling the chemistry and biology of reactive oxygen species. *Nature chemical biology*, 4(5):278–286, 2008.

[10] J.D. Lambeth. NOX enzymes and the biology of reactive oxygen. *Nature Reviews Immunology*, 4(3):181–189, 2004.

[11] P.J. Trotter. The genetics of fatty acid metabolism in *Saccharomyces cerevisiae*. *Annual review of nutrition*, 21(1):97–119, 2001.

[12] B.P. Tu and J.S. Weissman. Oxidative protein folding in eukaryotes mechanisms and consequences. *The Journal of cell biology*, 164(3):341–346, 2004.

[13] A.J. Lambert, M.D. Brand, et al. Reactive oxygen species production by mitochondria. *Methods Mol Biol*, 554:165–181, 2009.

[14] R.S. Balaban, S. Nemoto, and T. Finkel. Mitochondria, oxidants, and aging. *Cell*, 120(4):483–495, 2005.

[15] B.M. Bakker, K.M. Overkamp, A.J.A. Maris, P. Kötter, M.A.H. Luttik, J.P. Dijken, and J.T. Pronk. Stoichiometry and compartmentation of NADH metabolism in *Saccharomyces cerevisiae*. *FEMS microbiology reviews*, 25(1):15–37, 2006.

[16] S. Chiron, M. Gaisne, E. Guillou, P. Belenguer, G.D. Clark-Walker, and N. Bonnefoy. Studying mitochondria in an attractive model: *Schizosaccharomyces pombe*. *Methods in molecular biology*, 372:91, 2007.

[17] T. Onishi et al. Mechanism of electron transport and energy conservation in the site I region of the respiratory chain. *Biochimica et biophysica acta*, 301(2):105, 1973.

[18] E. Herrero, J. Ros, G. Bellí, and E. Cabiscol. Redox control and oxidative stress in yeast cells. *Biochimica et Biophysica Acta (BBA)-General Subjects*, 1780(11):1217–1235, 2008.

[19] K.S. Echtay, D. Roussel, J. St-Pierre, M.B. Jekabsons, S. Cadenas, J.A. Stuart, J.A. Harper, S.J. Roebuck, A. Morrison, S. Pickering, et al. Superoxide activates mitochondrial uncoupling proteins. *Nature*, 415(6867):96–99, 2002.

[20] K.J.A. Davies. Oxidative stress, antioxidant defenses, and damage removal, repair, and replacement systems. *IUBMB life*, 50(4-5):279–289, 2000.

[21] S. Avery. Molecular targets of oxidative stress. *Biochem. J*, 434:201–210, 2011.

[22] AJ Hulbert, R. Pamplona, R. Buffenstein, and WA Buttemer. Life and death: metabolic rate, membrane composition, and life span of animals. *Physiological Reviews*, 87(4):1175–1213, 2007.

[23] H. Imai and Y. Nakagawa. Biological significance of phospholipid hydroperoxide glutathione peroxidase (PHGPx, GPx4) in mammalian cells. *Free Radical Biology and Medicine*, 34(2):145–169, 2003.

[24] F.J.G.M. van Kuijk, A. Sevanian, G.J. Handelman, and E.A. Dratz. A new role for phospholipase A2: protection of membranes from lipid peroxidation damage. *Trends in Biochemical Sciences*, 12:31–34, 1987.

[25] J.A. Imlay, S. Linn, et al. DNA damage and oxygen radical toxicity. *Science (New York, NY)*, 240(4857):1302, 1988.

[26] P. Fortini, E. Parlanti, O.M. Sidorkina, J. Laval, and E. Dogliotti. The type of DNA glycosylase determines the base excision repair pathway in mammalian cells. *Journal of Biological Chemistry*, 274(21):15230–15236, 1999.

[27] B.S. Berlett and E.R. Stadtman. Protein oxidation in aging, disease, and oxidative stress. *Journal of Biological Chemistry*, 272(33):20313–20316, 1997.

[28] E. Stadtman and B. Berlett. Reactive oxygen-mediated protein oxidation in aging and disease. *Reactive oxygen species in biological systems*, pages 657–675, 2002.

[29] C.C. Winterbourn and M.B. Hampton. Thiol chemistry and specificity in redox signaling. *Free Radical Biology and Medicine*, 45(5):549–561, 2008.

[30] E.R. Stadtman and B.S. Berlett. Forum on free radical mechanisms of neurotoxicity. *Chem. Res. Toxicol*, 10:485–494, 1997.

[31] Tilman Grune, Tobias Jung, Katrin Merker, and Kelvin JA Davies. Decreased proteolysis caused by protein aggregates, inclusion bodies, plaques, lipofuscin, ceroid, and âaggresomesâ during oxidative stress, aging, and disease. *The international journal of biochemistry & cell biology*, 36(12):2519–2530, 2004.

[32] K.A. Morano, C.M. Grant, and W.S. Moye-Rowley. The response to heat shock and oxidative stress in *Saccharomyces cerevisiae*. *Genetics*, 2011.

[33] M. Zamocky, P.G. Furtmüller, and C. Obinger. Evolution of catalases from bacteria to humans. *Antioxidants & redox signaling*, 10(9):1527–1548, 2008.

[34] P. Chelikani, I. Fita, and PC Loewen. Diversity of structures and properties among catalases. *Cellular and molecular life sciences*, 61(2):192–208, 2004.

[35] L. Domínguez, A. Sosa-Peinado, and W. Hansberg. Catalase evolved to concentrate H2O2 at its active site. *Archives of biochemistry and biophysics*, 500(1):82–91, 2010.

[36] J.M. McCord and I. Fridovich. Superoxide dismutase. *Journal of Biological Chemistry*, 244(22):6049–6055, 1969.

[37] R. Wintjens, C. Noël, A.C.W. May, D. Gerbod, F. Dufernez, M. Capron, E. Viscogliosi, and M. Rooman. Specificity and phenetic relationships of iron- and manganese-containing superoxide dismutases on the basis of structure and sequence comparisons. *Journal of Biological Chemistry*, 279(10):9248–9254, 2004.

[38] CL Dupont, K. Neupane, J. Shearer, and B. Palenik. Diversity, function and evolution of genes coding for putative ni-containing superoxide dismutases. *Environmental microbiology*, 10(7):1831–1843, 2008.

[39] I. Fridovich. Superoxide radical and superoxide dismutases. *Annual review of biochemistry*, 64(1):97–112, 1995.

[40] J.A. Imlay. Cellular defenses against superoxide and hydrogen peroxide. *Annual review of biochemistry*, 77:755, 2008.

[41] C. Michiels, M. Raes, O. Toussaint, and J. Remacle. Importance of Se-glutathione peroxidase, catalase, and Cu/Zn-SOD for cell survival against oxidative stress. *Free Radical Biology and Medicine*, 17(3):235–248, 1994.

[42] T. Tanaka, S. Izawa, and Y. Inoue. GPX2, encoding a phospholipid hydroperoxide glutathione peroxidase homologue, codes for an atypical 2-Cys peroxiredoxin in *Saccharomyces cerevisiae*. *Journal of Biological Chemistry*, 280(51):42078–42087, 2005.

[43] T. Ohdate, K. Kita, and Y. Inoue. Kinetics and redox regulation of Gpx1, an atypical 2-Cys peroxiredoxin, in *Saccharomyces cerevisiae*. *FEMS yeast research*, 10(6):787–790, 2010.

[44] A. Delaunay, D. Pflieger, M.B. Barrault, J. Vinh, and M.B. Toledano. A thiol peroxidase is an H2O2 receptor and redox-transducer in gene activation. *Cell*, 111(4):471–481, 2002.

[45] B.S. Winkler, S.M. Orselli, and T.S. Rex. The redox couple between glutathione and ascorbic acid: a chemical and physiological perspective. *Free Radical Biology and Medicine*, 17(4):333–349, 1994.

[46] D.J. Jamieson. Oxidative stress responses of the yeast *Saccharomyces cerevisiae*. *Yeast*, 14(16):1511–1527, 1998.

[47] C.M. Spickett, N. Smirnoff, and A.R. Pitt. The biosynthesis of erythroascorbate in *Saccharomyces cerevisiae* and its role as an antioxidant. *Free Radical Biology and Medicine*, 28(2):183–192, 2000.

[48] W.K. Huh, B.H. Lee, S.T. Kim, Y.R. Kim, G.E. Rhie, Y.W. Baek, C.S. Hwang, J.S. Lee, and S.O. Kang. D-erythroascorbic acid is an important antioxidant molecule in *Saccharomyces cerevisiae*. *Molecular microbiology*, 30(4):895–903, 1998.

[49] P. Raspor, S. Plesničar, Z. Gazdag, M. Pesti, M. Miklavčič, B. Lah, R. Logar-Marinsek, and B. Poljšak. Prevention of intracellular oxidation in yeast: the role of vitamin E analogue, Trolox (6-hydroxy-2, 5, 7, 8-tetramethylkroman-2-carboxyl acid). *Cell biology international*, 29(1):57–63, 2005.

[50] V. Wood, R. Gwilliam, M.A. Rajandream, M. Lyne, R. Lyne, A. Stewart, J. Sgouros, N. Peat, J. Hayles, S. Baker, et al. The genome sequence of *Schizosaccharomyces pombe*. *Nature*, 415(6874):871–880, 2002.

[51] M. Yanagida et al. The model unicellular eukaryote, *Schizosaccharomyces pombe*. *Genome Biol*, 3(3), 2002.

[52] M. Jara, A.P. Vivancos, I.A. Calvo, A. Moldón, M. Sansó, and E. Hidalgo. The peroxiredoxin Tpx1 is essential as a H2O2 scavenger during aerobic growth in fission yeast. *Molecular biology of the cell*, 18(6):2288–2295, 2007.

[53] Alice Zuin, Natalia Gabrielli, Isabel A Calvo, Sarela García-Santamarina, Kwang-Lae Hoe, Dong Uk Kim, Han-Oh Park, Jacqueline Hayles, José Ayté, and Elena Hidalgo. Mitochondrial dysfunction increases oxidative stress and decreases chronological life span in fission yeast. *PLoS One*, 3(7):e2842, 2008.

[54] Helen C Causton, Bing Ren, Sang Seok Koh, Christopher T Harbison, Elenita Kanin, Ezra G Jennings, Tong Ihn Lee, Heather L True, Eric S Lander, and Richard A Young. Remodeling of yeast genome expression in response to environmental changes. *Molecular biology of the cell*, 12(2):323–337, 2001.

[55] Audrey P Gasch, Paul T Spellman, Camilla M Kao, Orna Carmel-Harel, Michael B Eisen, Gisela Storz, David Botstein, and Patrick O Brown. Genomic expression programs in the response of yeast cells to environmental changes. *Science Signalling*, 11(12):4241, 2000.

[56] D. Chen, W.M. Toone, J. Mata, R. Lyne, G. Burns, K. Kivinen, A. Brazma, N. Jones, and J. Bähler. Global transcriptional responses of fission yeast to environmental stress. *Molecular biology of the cell*, 14(1):214–229, 2003.

[57] J. Quinn, V.J. Findlay, K. Dawson, J.B.A. Millar, N. Jones, B.A. Morgan, and W.M. Toone. Distinct regulatory proteins control the graded transcriptional response to increasing H2O2 levels in fission yeast *Schizosaccharomyces pombe*. *Molecular biology of the cell*, 13(3):805–816, 2002.

[58] A.P. Vivancos, E.A. Castillo, N. Jones, J. Ayté, and E. Hidalgo. Activation of the redox sensor Pap1 by hydrogen peroxide requires modulation of the intracellular oxidant concentration. *Molecular microbiology*, 52(5):1427–1435, 2004.

[59] Andrew Jan Waskiewicz and Jonathan A Cooper. Mitogen and stress response pathways: MAP kinase cascades and phosphatase regulation in mammals and yeast. *Current opinion in cell biology*, 7(6):798–805, 1995.

[60] Genevieve Degols and Paul Russell. Discrete roles of the Spc1 kinase and the Atf1 transcription factor in the UV response of *Schizosaccharomyces pombe*. *Molecular and cellular biology*, 17(6):3356–3363, 1997.

[61] Genevieve Degols, Kazuhiro Shiozaki, and Paul Russell. Activation and regulation of the Spc1 stress-activated protein kinase in *Schizosaccharomyces pombe*. *Molecular and cellular biology*, 16(6):2870–2877, 1996.

[62] Jia-Ching Shieh, Marc G Wilkinson, Vicky Buck, Brian A Morgan, Kozo Makino, and JB Millar. The Mcs4 response regulator coordinately controls the stress-activated Mak1-Wis1-Sty1 MAP kinase pathway and fission yeast cell cycle. *Genes & development*, 11(8):1008–1022, 1997.

[63] Keisuke Aoyama, Hirofumi AIBA, and Takeshi MIZUNO. Genetic analysis of the His-to-Asp phosphorelay implicated in mitotic cell cycle control: involvement of

histidine-kinase genes of *Schizosaccharomyces pombe*. *Bioscience, biotechnology, and biochemistry*, 65(10):2347–2352, 2001.

[64] Vicky Buck, Janet Quinn, Teresa Soto Pino, Humberto Martin, Jose Saldanha, Kozo Makino, Brian A Morgan, and Jonathan Millar. Peroxide sensors for the fission yeast stress-activated mitogen-activated protein kinase pathway. *Science Signalling*, 12(2):407, 2001.

[65] Norihito NAKAMICHI, Hisami YAMADA, Keisuke AOYAMA, Ryusuke OHMIYA, Hirofumi AIBA, and Takeshi MIZUNO. His-to-Asp phosphorelay circuitry for regulation of sexual development in *Schizosaccharomyces pombe*. *Bioscience, biotechnology, and biochemistry*, 66(12):2663–2672, 2002.

[66] Keisuke Aoyama, Yasunori Mitsubayashi, Hirofumi Aiba, and Takeshi Mizuno. Spy1, a histidine-containing phosphotransfer signaling protein, regulates the fission yeast cell cycle through the Mcs4 response regulator. *Journal of bacteriology*, 182(17):4868–4874, 2000.

[67] Aaron Ngocky Nguyen, Albert Lee, Warren Place, and Kazuhiro Shiozaki. Multistep phosphorelay proteins transmit oxidative stress signals to the fission yeast stress-activated protein kinase. *Science Signalling*, 11(4):1169, 2000.

[68] Kazuhiro Shiozaki, Mitsue Shiozaki, and Paul Russell. Mcs4 mitotic catastrophe suppressor regulates the fission yeast cell cycle through the Wik1-Wis1-Spc1 kinase cascade. *Molecular biology of the cell*, 8(3):409, 1997.

[69] Itaru Samejima, Shaun Mackie, Emma Warbrick, Ronit Weisman, and Peter A Fantes. The fission yeast mitotic regulator win1+ encodes an MAP kinase kinase kinase that phosphorylates and activates Wis1 MAP kinase kinase in response to high osmolarity. *Molecular biology of the cell*, 9(8):2325–2335, 1998.

[70] Jia-Ching Shieh, Marc G Wilkinson, and Jonathan BA Millar. The Win1 mitotic regulator is a component of the fission yeast stress-activated Sty1 MAPK pathway. *Molecular biology of the cell*, 9(2):311–322, 1998.

[71] Itaru Samejima, Shaun Mackie, and Peter A Fantes. Multiple modes of activation of the stress-responsive MAP kinase pathway in fission yeast. *The EMBO journal*, 16(20):6162–6170, 1997.

[72] Kazuhiro Shiozaki and Paul Russell. Stress-activated protein kinase pathway in cell cycle control of fission yeast. *Methods in enzymology*, 283:506–520, 1997.

[73] Kazuhiro Shiozaki and Paul Russell. Conjugation, meiosis, and the osmotic stress response are regulated by Spc1 kinase through Atf1 transcription factor in fission yeast. *Genes & development*, 10(18):2276–2288, 1996.

[74] M.G. Wilkinson, M. Samuels, T. Takeda, W.M. Toone, J.C. Shieh, T. Toda, JB Millar, and N. Jones. The Atf1 transcription factor is a target for the Sty1 stress-activated MAP kinase pathway in fission yeast. *Genes & development*, 10(18):2289–2301, 1996.

[75] Frédérique Gaits, Kazuhiro Shiozaki, and Paul Russell. Protein phosphatase 2C acts independently of stress-activated kinase cascade to regulate the stress response in fission yeast. *Journal of Biological Chemistry*, 272(28):17873–17879, 1997.

[76] JB Millar, Vicky Buck, and Marc G Wilkinson. Pyp1 and Pyp2 PTPases dephosphorylate an osmosensing map kinase controlling cell size at division in fission yeast. *Genes & development*, 9(17):2117–2130, 1995.

[77] Aaron Ngocky Nguyen and Kazuhiro Shiozaki. Heat shock-induced activation of stress MAP kinase is regulated by threonine-and tyrosine-specific phosphatases. *Genes & development*, 13(13):1653–1663, 1999.

[78] W Mark Toone and Nic Jones. Stress-activated signalling pathways in yeast. *Genes to Cells*, 3(8):485–498, 1998.

[79] Frédérique Gaits, Geneviève Degols, Kazuhiro Shiozaki, and Paul Russell. Phosphorylation and association with the transcription factor Atf1 regulate localization of Spc1/Sty1 stress-activated kinase in fission yeast. *Genes & development*, 12(10):1464–1473, 1998.

[80] Frédérique Gaits and Paul Russell. Active nucleocytoplasmic shuttling required for function and regulation of stress-activated kinase Spc1/Sty1 in fission yeast. *Molecular biology of the cell*, 10(5):1395–1407, 1999.

[81] Tadayuki Takeda, Takashi Toda, Kin-ichiro Kominami, Asako Kohnosu, M Yanagida, and N Jones. Schizosaccharomyces pombe atf1+ encodes a transcription factor required for sexual development and entry into stationary phase. *The EMBO journal*, 14(24):6193, 1995.

[82] W.M. Toone, S. Kuge, M. Samuels, B.A. Morgan, T. Toda, and N. Jones. Regulation of the fission yeast transcription factor Pap1 by oxidative stress: requirement for the nuclear export factor Crm1 (exportin) and the stress-activated MAP kinase Sty1/Spc1. *Genes & development*, 12(10):1453–1463, 1998.

[83] Nobuaki Kudo, Hiroshi Taoka, Takashi Toda, Minoru Yoshida, and Sueharu Horinouchi. A novel nuclear export signal sensitive to oxidative stress in the fission yeast transcription factor Pap1. *Journal of Biological Chemistry*, 274(21):15151–15158, 1999.

[84] Esther A Castillo, Jose Ayte, Cristina Chiva, Alberto Moldón, Montse Carrascal, Joaquín Abián, Nic Jones, and Elena Hidalgo. Diethylmaleate activates the transcrip-

tion factor Pap1 by covalent modification of critical cysteine residues. *Molecular microbiology*, 45(1):243–254, 2002.

[85] D. Chen, C.R.M. Wilkinson, S. Watt, C.J. Penkett, W.M. Toone, N. Jones, and J. Bähler. Multiple pathways differentially regulate global oxidative stress responses in fission yeast. *Molecular biology of the cell*, 19(1):308–317, 2008.

[86] I.A. Calvo, P. García, J. Ayté, and E. Hidalgo. The transcription factors Pap1 and Prr1 collaborate to activate antioxidant, but not drug tolerance, genes in response to H2O2. *Nucleic Acids Research*, 2012.

[87] A. Vlamis-Gardikas. The multiple functions of the thiol-based electron flow pathways of *Escherichia coli*: Eternal concepts revisited. *Biochimica et Biophysica Acta (BBA)-General Subjects*, 1780(11):1170–1200, 2008.

[88] H.F. Gilbert. Molecular and cellular aspects of thiol-disulfide exchange. *Advances in enzymology and related areas of molecular biology*, pages 69–172, 1993.

[89] K.S. Jensen, R.E. Hansen, and J.R. Winther. Kinetic and thermodynamic aspects of cellular thiol-disulfide redox regulation. *Antioxidants & Redox Signaling*, 11(5):1047–1058, 2009.

[90] G. Ferrer-Sueta, B. Manta, H. Botti, R. Radi, M. Trujillo, and A. Denicola. Factors affecting protein thiol reactivity and specificity in peroxide reduction. *Chemical Research in Toxicology*, 2011.

[91] C. Berndt, C.H. Lillig, and A. Holmgren. Thioredoxins and glutaredoxins as facilitators of protein folding. *Biochimica et Biophysica Acta (BBA)-Molecular Cell Research*, 1783(4):641–650, 2008.

[92] Zhiyong Cheng, Jinfeng Zhang, David P. Ballou, and Charles H. Williams. Reactivity of thioredoxin as a protein thiol-disulfide oxidoreductase. *Chemical Reviews*, 111(9):5768–5783, 2011.

[93] E.C. Moore, P. Reichard, L. Thelander, et al. Enzymatic synthesis of deoxyribonucleotides. V. purification and properties of thioredoxin reductase from *Escherichia Coli* B. *The Journal of biological chemistry*, 239:3445, 1964.

[94] J.F. Collet and J. Messens. Structure, function, and mechanism of thioredoxin proteins. *Antioxidants & redox signaling*, 13(8):1205–1216, 2010.

[95] Shingo Izawa, Keiko Maeda, Kei-ichi Sugiyama, Junâichi Mano, Yoshiharu Inoue, and Akira Kimura. Thioredoxin deficiency causes the constitutive activation of Yap1, an AP-1-like transcription factor in *Saccharomyces cerevisiae*. *Journal of Biological Chemistry*, 274(40):28459–28465, 1999.

[96] CH Williams Jr. Mechanism and structure of thioredoxin reductase from *Escherichia coli*. *The FASEB journal*, 9(13):1267–1276, 1995.

[97] B.W. Lennon, C.H. Williams, and M.L. Ludwig. Twists in catalysis: alternating conformations of *Escherichia coli* thioredoxin reductase. *Science*, 289(5482):1190, 2000.

[98] D. Mustacich and G. Powis. Thioredoxin reductase. *Biochemical Journal*, 346(Pt 1):1, 2000.

[99] J.Y. Song and J.H. Roe. The role and regulation of Trxl, a cytosolic thioredoxin in *Schizosaccharomyces pombe*. *The Journal of Microbiology*, 46(4):408–414, 2008.

[100] J.Y. Song, J. Cha, J. Lee, and J.H. Roe. Glutathione reductase and a mitochondrial thioredoxin play overlapping roles in maintaining iron-sulfur enzymes in fission yeast. *Eukaryotic cell*, 5(11):1857–1865, 2006.

[101] J.Y. Song, K.D. Kim, and J.H. Roe. Thiol-independent action of mitochondrial thioredoxin to support the urea cycle of arginine biosynthesis in *Schizosaccharomyces pombe*. *Eukaryotic cell*, 7(12):2160–2167, 2008.

[102] K.M. Andersen, C. Jensen, F. Kriegenburg, A.M.B. Lauridsen, C. Gordon, and R. Hartmann-Petersen. Txl1 and Txc1 are co-factors of the 26S proteasome in fission yeast. *Antioxidants & Redox Signaling*, 14(9):1601–1608, 2011.

[103] A. Jiménez, L. Mateos, J.R. Pedrajas, A. Miranda-Vizuete, and J.L. Revuelta. The *txl1+* gene from *Schizosaccharomyces pombe* encodes a new thioredoxin-like 1 protein that participates in the antioxidant defence against *tert*-butyl hydroperoxide. *Yeast*, 24(6):481–490, 2007.

[104] D. Casso, D. Beach, D. Casso, and D. Beach. A mutation in a thioredoxin reductase homolog suppresses p53-induced growth inhibition in the fission yeast *Schizosaccharomyces pombe*. *Molecular and General Genetics MGG*, 252(5):518–529, 1996.

[105] G.D. Pearson and G.F. Merrill. Deletion of the *Saccharomyces cerevisiae trr1* gene encoding thioredoxin reductase inhibits p53-dependent reporter gene expression. *Journal of Biological Chemistry*, 273(10):5431–5434, 1998.

[106] Z. Benko, I. Miklos, A.M. Carr, and M. Sipiczki. Caffeine-resistance in *S. pombe*: mutations in three novel caf genes increase caffeine tolerance and affect radiation sensitivity, fertility, and cell cycle. *Current genetics*, 31(6):481–487, 1997.

[107] Z. Benko, M. Sipiczki, and AM Carr. Cloning of *caf1+*, *caf2+* and *caf4+* from *Schizosaccharomyces pombe*: their involvement in multidrug resistance, UV and pH sensitivity. *Molecular and General Genetics MGG*, 260(5):434–443, 1998.

[108] Z. Benko, C. Fenyvesvolgyi, M. Pesti, and M. Sipiczki. The transcription factor Pap1/Caf3 plays a central role in the determination of caffeine resistance in *Schizosaccharomyces pombe*. *Molecular Genetics and Genomics*, 271(2):161–170, 2004.

[109] I.A. Calvo, N. Gabrielli, I. Iglesias-Baena, S. García-Santamarina, K.L. Hoe, D.U. Kim, M. Sansó, A. Zuin, P. Pérez, J. Ayté, and Hidalgo E. Genome-wide screen of genes required for caffeine tolerance in fission yeast. *PloS one*, 4(8):e6619, 2009.

[110] S.M. Hong, H.W. Lim, I.H. Kim, K. Kim, E.H. Park, and C.J. Lim. Stress-dependent regulation of the gene encoding thioredoxin reductase from the fission yeast. *FEMS microbiology letters*, 234(2):379–385, 2004.

[111] A.I. Derman, W.A. Prinz, D. Belin, and J. Beckwith. Mutations that allow disulfide bond formation in the cytoplasm of *Escherichia coli*. *Science*, 262(5140):1744, 1993.

[112] E.J. Stewart, F. Åslund, and J. Beckwith. Disulfide bond formation in the *Escherichia coli* cytoplasm: an in vivo role reversal for the thioredoxins. *The EMBO journal*, 17(19):5543–5550, 1998.

[113] L. Debarbieux and J. Beckwith. The reductive enzyme thioredoxin 1 acts as an oxidant when it is exported to the *Escherichia coli* periplasm. *Proceedings of the National Academy of Sciences*, 95(18):10751, 1998.

[114] D. Spector, J. Labarre, and M.B. Toledano. A genetic investigation of the essential role of glutathione. *Journal of Biological Chemistry*, 276(10):7011–7016, 2001.

[115] C.H. Lillig, C. Berndt, and A. Holmgren. Glutaredoxin systems. *Biochimica et Biophysica Acta (BBA)-General Subjects*, 1780(11):1304–1317, 2008.

[116] S.J. Kim, H.G. Kim, B.C. Kim, K. Kim, E.H. Park, and C.J. Lim. Transcriptional regulation of the gene encoding gamma-glutamylcysteine synthetase from the fission yeast *Schizosaccharomyces pombe*. *Journal of microbiology*, 42(3):233–238, 2004.

[117] M. Kolberg, K.R. Strand, P. Graff, and K. Kristoffer Andersson. Structure, function, and mechanism of ribonucleotide reductases. *Biochimica et Biophysica Acta (BBA)-Proteins & Proteomics*, 1699(1):1–34, 2004.

[118] Katalin Sipos, Heike Lange, Zsuzsanna Fekete, Pascaline Ullmann, Roland Lill, and Gyula Kispal. Maturation of cytosolic iron-sulfur proteins requires glutathione. *Journal of Biological Chemistry*, 277(30):26944–26949, 2002.

[119] M.B. Toledano, C. Kumar, N. Le Moan, D. Spector, and F. Tacnet. The system biology of thiol redox system in *Escherichia coli* and yeast: differential functions in oxidative stress, iron metabolism and DNA synthesis. *FEBS letters*, 581(19):3598–3607, 2007.

[120] C. Kumar, A. Igbaria, B. D'Autreaux, A.G. Planson, C. Junot, E. Godat, A.K. Bachhawat, A. Delaunay-Moisan, and M.B. Toledano. Glutathione revisited: a vital function in iron metabolism and ancillary role in thiol-redox control. *The EMBO journal*, 30(10):2044–2056, 2011.

[121] A. Holmgren. Hydrogen donor system for *Escherichia coli* ribonucleoside-diphosphate reductase dependent upon glutathione. *Proceedings of the National Academy of Sciences*, 73(7):2275, 1976.

[122] E. Herrero, J. Ros, J. Tamarit, and G. Belli. Glutaredoxins in fungi. *Photosynthesis research*, 89(2):127–140, 2006.

[123] Z.R. Gan and W.W. Wells. The primary structure of pig liver thioltransferase. *Journal of Biological Chemistry*, 262(14):6699–6703, 1987.

[124] G.P. Johnson, S.J. Goebel, M.E. Perkus, S.W. Davis, J.P. Winslow, and E. Paoletti. Vaccinia virus encodes a protein with similarity to glutaredoxins. *Virology*, 181(1):378–381, 1991.

[125] M. Lundberg, C. Johansson, J. Chandra, M. Enoksson, G. Jacobsson, J. Ljung, M. Johansson, and A. Holmgren. Cloning and expression of a novel human glutaredoxin (Grx2) with mitochondrial and nuclear isoforms. *Journal of Biological Chemistry*, 276(28):26269–26275, 2001.

[126] C. Johansson, C.H. Lillig, and A. Holmgren. Human mitochondrial glutaredoxin reduces S-glutathionylated proteins with high affinity accepting electrons from either glutathione or thioredoxin reductase. *Journal of Biological Chemistry*, 279(9):7537–7543, 2004.

[127] D. Shenton, G. Perrone, K.A. Quinn, I.W. Dawes, and C.M. Grant. Regulation of protein S-thiolation by glutaredoxin 5 in the yeast *Saccharomyces cerevisiae*. *Journal of Biological Chemistry*, 277(19):16853–16859, 2002.

[128] D. Shenton and C.M. Grant. Protein S-thiolation targets glycolysis and protein synthesis in response to oxidative stress in the yeast *Saccharomyces cerevisiae*. *Biochemical Journal*, 374(Pt 2):513, 2003.

[129] C.H. Lillig, C. Berndt, O. Vergnolle, M.E. Lönn, C. Hudemann, E. Bill, and A. Holmgren. Characterization of human glutaredoxin 2 as iron-sulfur protein: a possible role as redox sensor. *Proceedings of the National Academy of Sciences of the United States of America*, 102(23):8168, 2005.

[130] W.H. Chung, K.D. Kim, Y.J. Cho, and J.H. Roe. Differential expression and role of two dithiol glutaredoxins Grx1 and Grx2 in *Schizosaccharomyces pombe*. *Biochemical and biophysical research communications*, 321(4):922–929, 2004.

[131] H.G. Kim, J.H. Kim, B.C. Kim, E.H. Park, and C.J. Lim. Carbon source-dependent regulation of a second gene encoding glutaredoxin from the fission yeast *Schizosaccharomyces pombe*. *Molecular biology reports*, 32(1):15–24, 2005.

[132] W.H. Chung, K.D. Kim, and J.H. Roe. Localization and function of three monothiol glutaredoxins in *Schizosaccharomyces pombe*. *Biochemical and biophysical research communications*, 330(2):604–610, 2005.

[133] K.D. Kim, W.H. Chung, H.J. Kim, K.C. Lee, and J.H. Roe. Monothiol glutaredoxin Grx5 interacts with Fe-S scaffold proteins Isa1 and Isa2 and supports Fe-S assembly and DNA integrity in mitochondria of fission yeast. *Biochemical and biophysical research communications*, 392(3):467–472, 2010.

[134] G. Bellí, M.M. Molina, J. García-Martínez, J.E. Pérez-Ortín, and E. Herrero. *Saccharomyces cerevisiae* glutaredoxin 5-deficient cells subjected to continuous oxidizing conditions are affected in the expression of specific sets of genes. *Journal of Biological Chemistry*, 279(13):12386–12395, 2004.

[135] U. Mühlenhoff, J. Gerber, N. Richhardt, and R. Lill. Components involved in assembly and dislocation of iron-sulfur clusters on the scaffold protein Isu1p. *The EMBO journal*, 22(18):4815–4825, 2003.

[136] R. Alves, E. Herrero, and A. Sorribas. Predictive reconstruction of the mitochondrial iron-sulfur cluster assembly metabolism. II. Role of glutaredoxin Grx5. *Proteins: Structure, Function, and Bioinformatics*, 57(3):481–492, 2004.

[137] M. Jbel, A. Mercier, and S. Labbé. Grx4 monothiol glutaredoxin is required for iron limitation-dependent inhibition of Fep1. *Eukaryotic Cell*, 10(5):629–645, 2011.

[138] A. Mercier and S. Labbé. Both Php4 function and subcellular localization are regulated by iron via a multistep mechanism involving the glutaredoxin Grx4 and the exportin Crm1. *Journal of Biological Chemistry*, 284(30):20249, 2009.

[139] K.D. Kim, H.J. Kim, K.C. Lee, and J.H. Roe. Multi-domain CGFS-type glutaredoxin Grx4 regulates iron homeostasis via direct interaction with a repressor Fep1 in fission yeast. *Biochemical and biophysical research communications*, 2011.

[140] P. Vachon, A. Mercier, M. Jbel, and S. Labbé. The monothiol glutaredoxin Grx4 exerts an iron-dependent inhibitory effect on Php4 function. *Eukaryotic Cell*, 11(6):806–819, 2012.

[141] L. Ojeda, G. Keller, U. Muhlenhoff, J.C. Rutherford, R. Lill, and D.R. Winge. Role of glutaredoxin-3 and glutaredoxin-4 in the iron regulation of the Aft1 transcriptional activator in *Saccharomyces cerevisiae*. *Journal of Biological Chemistry*, 281(26):17661–17669, 2006.

[142] J. Lee, I.W. Dawes, and J.H. Roe. Isolation, expression, and regulation of the *pgr1+* gene encoding glutathione reductase absolutely required for the growth of *Schizosaccharomyces pombe*. *Journal of Biological Chemistry*, 272(37):23042–23049, 1997.

[143] Y. Meyer, B.B. Buchanan, F. Vignols, and J.P. Reichheld. Thioredoxins and glutaredoxins: unifying elements in redox biology. *Annual review of genetics*, 43:335–367, 2009.

[144] A.P. Fernandes, M. Fladvad, C. Berndt, C. Andrésen, C.H. Lillig, P. Neubauer, M. Sunnerhagen, A. Holmgren, and A. Vlamis-Gardikas. A novel monothiol glutaredoxin (Grx4) from *Escherichia coli* can serve as a substrate for thioredoxin reductase. *Journal of Biological Chemistry*, 280(26):24544–24552, 2005.

[145] M. Fladvad, M. Bellanda, A.P. Fernandes, S. Mammi, A. Vlamis-Gardikas, A. Holmgren, and M. Sunnerhagen. Molecular mapping of functionalities in the solution structure of reduced Grx4, a monothiol glutaredoxin from *Escherichia coli*. *Journal of Biological Chemistry*, 280(26):24553–24561, 2005.

[146] M. Russel, P. Model, and A. Holmgren. Thioredoxin or glutaredoxin in *Escherichia coli* is essential for sulfate reduction but not for deoxyribonucleotide synthesis. *Journal of bacteriology*, 172(4):1923–1929, 1990.

[147] R. Ortenberg, S. Gon, A. Porat, and J. Beckwith. Interactions of glutaredoxins, ribonucleotide reductase, and components of the DNA replication system of *Escherichia coli*. *Proceedings of the National Academy of Sciences of the United States of America*, 101(19):7439, 2004.

[148] F. Aslund, B. Ehn, A. Miranda-Vizuete, C. Pueyo, and A. Holmgren. Two additional glutaredoxins exist in *Escherichia coli*: glutaredoxin 3 is a hydrogen donor for ribonucleotide reductase in a thioredoxin/glutaredoxin 1 double mutant. *Proceedings of the National Academy of Sciences*, 91(21):9813, 1994.

[149] W.A. Prinz, F. Åslund, A. Holmgren, and J. Beckwith. The role of the thioredoxin and glutaredoxin pathways in reducing protein disulfide bonds in the *Escherichia coli* cytoplasm. *Journal of Biological Chemistry*, 272(25):15661–15667, 1997.

[150] F. Åslund, M. Zheng, J. Beckwith, and G. Storz. Regulation of the oxyR transcription factor by hydrogen peroxide and the cellular thiol-disulfide status. *Proceedings of the National Academy of Sciences*, 96(11):6161, 1999.

[151] S.O. Kim, K. Merchant, R. Nudelman, W.F. Beyer, T. Keng, J. DeAngelo, A. Hausladen, and J.S. Stamler. OxyR: a molecular code for redox-related signaling. *Cell*, 109(3):383–396, 2002.

[152] PCF Graf and U. Jakob. Redox-regulated molecular chaperones. *Cellular and molecular life sciences*, 59(10):1624–1631, 2002.

[153] J.H. Hoffmann, K. Linke, P.C.F. Graf, H. Lilie, and U. Jakob. Identification of a redox-regulated chaperone network. *The EMBO journal*, 23(1):160–168, 2003.

[154] C.M. Grant, F.H. MacIver, and I.W. Dawes. Glutathione is an essential metabolite required for resistance to oxidative stress in the yeast *Saccharomyces cerevisiae*. *Current genetics*, 29(6):511–515, 1996.

[155] EG Muller. A glutathione reductase mutant of yeast accumulates high levels of oxidized glutathione and requires thioredoxin for growth. *Molecular biology of the cell*, 7(11):1805, 1996.

[156] S.X. Tan, D. Greetham, S. Raeth, C.M. Grant, I.W. Dawes, and G.G. Perrone. The thioredoxin-thioredoxin reductase system can function *in vivo* as an alternative system to reduce oxidized glutathione in *Saccharomyces cerevisiae*. *Journal of Biological Chemistry*, 285(9):6118, 2010.

[157] Z. Cheng, L.D. Arscott, D.P. Ballou, and C.H. Williams Jr. The relationship of the redox potentials of thioredoxin and thioredoxin reductase from *Drosophila melanogaster* to the enzymatic mechanism: reduced thioredoxin is the reductant of glutathione in *Drosophila*. *Biochemistry*, 46(26):7875–7885, 2007.

[158] T. Draculic, I.W. Dawes, and C.M. Grant. A single glutaredoxin or thioredoxin gene is essential for viability in the yeast *Saccharomyces cerevisiae*. *Molecular microbiology*, 36(5):1167–1174, 2000.

[159] EG Muller. Thioredoxin deficiency in yeast prolongs S phase and shortens the G1 interval of the cell cycle. *Journal of Biological Chemistry*, 266(14):9194–9202, 1991.

[160] S. Camier, E. Ma, C. Leroy, A. Pruvost, M. Toledano, and M.C. Marsolier-Kergoat. Visualization of ribonucleotide reductase catalytic oxidation establishes thioredoxins as its major reductants in yeast. *Free Radical Biology and Medicine*, 42(7):1008–1016, 2007.

[161] A. Hall, P.A. Karplus, and L.B. Poole. Typical 2-Cys peroxiredoxins-structures, mechanisms and functions. *Febs Journal*, 276(9):2469–2477, 2009.

[162] A. Hall, K. Nelson, L.B. Poole, and P.A. Karplus. Structure-based insights into the catalytic power and conformational dexterity of peroxiredoxins. *Antioxidants & redox signaling*, 15(3):795–815, 2011.

[163] P.A. Karplus and A. Hall. Structural survey of the peroxiredoxins. *Peroxiredoxin systems*, pages 41–60, 2007.

[164] Z.A. Wood, L.B. Poole, R.R. Hantgan, and P.A. Karplus. Dimers to doughnuts: redox-sensitive oligomerization of 2-cysteine peroxiredoxins. *Biochemistry*, 41(17):5493–5504, 2002.

[165] K.S. Yang, S.W. Kang, H. Woo, S.C. Hwang, H.Z. Chae, K. Kim, and S.G. Rhee. Inactivation of human peroxiredoxin I during catalysis as the result of the oxida-

tion of the catalytic site cysteine to cysteine-sulfinic acid. *Journal of Biological Chemistry*, 277(41):38029, 2002.

[166] Z.A. Wood, L.B. Poole, and P.A. Karplus. Peroxiredoxin evolution and the regulation of hydrogen peroxide signaling. *Science's STKE*, 300(5619):650, 2003.

[167] S.G. Rhee and H.A. Woo. Multiple functions of peroxiredoxins: peroxidases, sensors and regulators of the intracellular messenger H2O2, and protein chaperones. *Antioxidants & redox signaling*, 15(3):781–794, 2011.

[168] M. Jara, A.P. Vivancos, and E. Hidalgo. C-terminal truncation of the peroxiredoxin Tpx1 decreases its sensitivity for hydrogen peroxide without compromising its role in signal transduction. *Genes to Cells*, 13(2):171–179, 2008.

[169] A.P. Vivancos, E.A. Castillo, B. Biteau, C. Nicot, J. Ayté, M.B. Toledano, and E. Hidalgo. A cysteine-sulfinic acid in peroxiredoxin regulates H2O2-sensing by the antioxidant Pap1 pathway. *Proceedings of the National Academy of Sciences of the United States of America*, 102(25):8875, 2005.

[170] E.A. Veal, V.J. Findlay, A.M. Day, S.M. Bozonet, J.M. Evans, J. Quinn, and B.A. Morgan. A 2-Cys peroxiredoxin regulates peroxide-induced oxidation and activation of a stress-activated MAP kinase. *Molecular cell*, 15(1):129–139, 2004.

[171] A.M. Day, J.D. Brown, S.R. Taylor, J.D. Rand, B.A. Morgan, and E.A. Veal. Inactivation of a peroxiredoxin by hydrogen peroxide is critical for thioredoxin-mediated repair of oxidized proteins and cell survival. *Molecular cell*, 2012.

[172] Z.A. Wood, E. Schröder, J. Robin Harris, and L.B. Poole. Structure, mechanism and regulation of peroxiredoxins. *Trends in biochemical sciences*, 28(1):32–40, 2003.

[173] L.A. Ralat, Y. Manevich, A.B. Fisher, and R.F. Colman. Direct evidence for the formation of a complex between 1-cysteine peroxiredoxin and glutathione S-transferase π with activity changes in both enzymes. *Biochemistry*, 45(2):360–372, 2006.

[174] F.M. Lian, J. Yu, X.X. Ma, X.J. Yu, Y. Chen, and C.Z. Zhou. Structural snapshots of yeast alkyl hydroperoxide reductase Ahp1 peroxiredoxin reveal a novel two-cysteine mechanism of electron transfer to eliminate reactive oxygen species. *Journal of Biological Chemistry*, 287(21):17077–17087, 2012.

[175] X.H. Zhang and H. Weissbach. Origin and evolution of the protein-repairing enzymes methionine sulphoxide reductases. *Biological Reviews*, 83(3):249–257, 2008.

[176] H. Weissbach, L. Resnick, and N. Brot. Methionine sulfoxide reductases: history and cellular role in protecting against oxidative damage. *Biochimica et Biophysica Acta (BBA)-Proteins & Proteomics*, 1703(2):203–212, 2005.

[177] J. Moskovitz, J.M. Poston, B.S. Berlett, N.J. Nosworthy, R. Szczepanowski, and E.R. Stadtman. Identification and characterization of a putative active site for peptide methionine sulfoxide reductase (MsrA) and its substrate stereospecificity. *Journal of Biological Chemistry*, 275(19):14167–14172, 2000.

[178] W.T. Lowther, H. Weissbach, F. Etienne, N. Brot, and B.W. Matthews. The mirrored methionine sulfoxide reductases of *Neisseria gonorrhoeae* pilB. *Nature Structural & Molecular Biology*, 9(5):348–352, 2002.

[179] F. Etienne, D. Spector, N. Brot, and H. Weissbach. A methionine sulfoxide reductase in *Escherichia coli* that reduces the R enantiomer of methionine sulfoxide. *Biochemical and biophysical research communications*, 300(2):378–382, 2003.

[180] S. Boschi-Muller, S. Azza, S. Sanglier-Cianferani, F. Talfournier, A. Van Dorsselear, and G. Branlant. A sulfenic acid enzyme intermediate is involved in the catalytic mechanism of peptide methionine sulfoxide reductase from *Escherichia coli*. *Journal of Biological Chemistry*, 275(46):35908, 2000.

[181] A. Olry, S. Boschi-Muller, M. Marraud, S. Sanglier-Cianferani, A. Van Dorsselear, and G. Branlant. Characterization of the methionine sulfoxide reductase activities of PilB, a probable virulence factor from *Neisseria meningitidis*. *Journal of Biological Chemistry*, 277(14):12016, 2002.

[182] S. Boschi-Muller, A. Gand, and G. Branlant. The methionine sulfoxide reductases: Catalysis and substrate specificities. *Archives of biochemistry and biophysics*, 474(2):266–273, 2008.

[183] H.Y. Kim. Glutaredoxin serves as a reductant for methionine sulfoxide reductases with or without resolving cysteine. *Acta biochimica et biophysica Sinica*, 44(7):623–627, 2012.

[184] Jung Chae Lim, Zheng You, Geumsoo Kim, and Rodney L. Levine. Methionine sulfoxide reductase A is a stereospecific methionine oxidase. *Proceedings of the National Academy of Sciences*, 108(26):10472–10477, 2011.

[185] R.L. Levine, L. Mosoni, B.S. Berlett, and E.R. Stadtman. Methionine residues as endogenous antioxidants in proteins. *Proceedings of the National Academy of Sciences*, 93(26):15036, 1996.

[186] D.B. Oien and J. Moskovitz. Substrates of the methionine sulfoxide reductase system and their physiological relevance. *Current topics in developmental biology*, 80:93–133, 2007.

[187] N. Brot, L. Weissbach, J. Werth, and H. Weissbach. Enzymatic reduction of protein-bound methionine sulfoxide. *Proceedings of the National Academy of Sciences*, 78(4):2155, 1981.

[188] Simon Black, Eileen M. Harte, Blondel Hudson, and Leonard Wartofsky. A specific enzymatic reduction of L-methionine sulfoxide and a related nonspecific reduction of disulfides. *Journal of Biological Chemistry*, 235(10):2910–2916, 1960.

[189] SI Ejiri, H. Weissbach, and N. Brot. Reduction of methionine sulfoxide to methionine by *Escherichia coli*. *Journal of bacteriology*, 139(1):161, 1979.

[190] J. Moskovitz, M.A. Rahman, J. Strassman, S.O. Yancey, S.R. Kushner, N. Brot, and H. Weissbach. *Escherichia coli* peptide methionine sulfoxide reductase gene: regulation of expression and role in protecting against oxidative damage. *Journal of bacteriology*, 177(3):502, 1995.

[191] J. Moskovitz, B.S. Berlett, J.M. Poston, and E.R. Stadtman. The yeast peptide-methionine sulfoxide reductase functions as an antioxidant *in vivo*. *Proceedings of the National Academy of Sciences*, 94(18):9585, 1997.

[192] J. Moskovitz, E. Flescher, B.S. Berlett, J. Azare, J.M. Poston, and E.R. Stadtman. Overexpression of peptide-methionine sulfoxide reductase in *Saccharomyces cerevisiae* and human T cells provides them with high resistance to oxidative stress. *Proceedings of the National Academy of Sciences*, 95(24):14071, 1998.

[193] H. Ruan, X.D. Tang, M.L. Chen, MA Joiner, G. Sun, N. Brot, H. Weissbach, S.H. Heinemann, L. Iverson, C.F. Wu, et al. High-quality life extension by the enzyme peptide methionine sulfoxide reductase. *Proceedings of the National Academy of Sciences*, 99(5):2748, 2002.

[194] J. Moskovitz, S. Bar-Noy, W.M. Williams, J. Requena, B.S. Berlett, and E.R. Stadtman. Methionine sulfoxide reductase (MsrA) is a regulator of antioxidant defense and lifespan in mammals. *Proceedings of the National Academy of Sciences*, 98(23):12920, 2001.

[195] Z. Lin, L.C. Johnson, H. Weissbach, N. Brot, M.O. Lively, and W.T. Lowther. Free methionine-(R)-sulfoxide reductase from *Escherichia coli* reveals a new GAF domain function. *Proceedings of the National Academy of Sciences*, 104(23):9597, 2007.

[196] D.T. Le, B.C. Lee, S.M. Marino, Y. Zhang, D.E. Fomenko, A. Kaya, E. Hacioglu, G.H. Kwak, A. Koc, H.Y. Kim, et al. Functional analysis of free methionine-R-sulfoxide reductase from *Saccharomyces cerevisiae*. *Journal of Biological Chemistry*, 284(7):4354, 2009.

[197] H. Eklund, U. Uhlin, M. Färnegårdh, D.T. Logan, and P. Nordlund. Structure and function of the radical enzyme ribonucleotide reductase. *Progress in biophysics and molecular biology*, 77(3):177–268, 2001.

[198] A. Jordan, E. Pontis, M. Atta, M. Krook, I. Gibert, J. Barbe, and P. Reichard. A second class I ribonucleotide reductase in *Enterobacteriaceae*: characterization

of the *Salmonella typhimurium* enzyme. *Proceedings of the National Academy of Sciences*, 91(26):12892, 1994.

[199] A. Holmgren and R. Sengupta. The use of thiols by ribonucleotide reductase. *Free Radical Biology and Medicine*, 49(11):1617–1628, 2010.

[200] F. Monje-Casas, J. Jurado, M.J. Prieto-Álamo, A. Holmgren, and C. Pueyo. Expression analysis of the nrdHIEF operon from *Escherichia coli*. *Journal of Biological Chemistry*, 276(21):18031–18037, 2001.

[201] A. Jordan, E. Aragall, I. Gibert, and J. Barbé. Promoter identification and expression analysis of salmonella typhimurium and *Escherichia coli* nrdEF operons encoding one of two class I ribonucleotide reductases present in both bacteria. *Molecular microbiology*, 19(4):777–790, 1996.

[202] A. Jordan, F. Åslund, E. Pontis, P. Reichard, and A. Holmgren. Characterization of *Escherichia coli* Nrdh. *Journal of Biological Chemistry*, 272(29):18044, 1997.

[203] S. Gon, M.J. Faulkner, and J. Beckwith. *In vivo* requirement for glutaredoxins and thioredoxins in the reduction of the ribonucleotide reductases of *Escherichia coli*. *Antioxidants & redox signaling*, 8(5-6):735–742, 2006.

[204] E. Mulliez, S. Ollagnier, M. Fontecave, R. Eliasson, and P. Reichard. Formate is the hydrogen donor for the anaerobic ribonucleotide reductase from *Escherichia coli*. *Proceedings of the National Academy of Sciences*, 92(19):8759, 1995.

[205] SJ Elledge and RW Davis. Two genes differentially regulated in the cell cycle and by DNA-damaging agents encode alternative regulatory subunits of ribonucleotide reductase. *Genes & development*, 4(5):740–751, 1990.

[206] S.J. Elledge and R.W. Davis. Identification and isolation of the gene encoding the small subunit of ribonucleotide reductase from *Saccharomyces cerevisiae*: DNA damage-inducible gene required for mitotic viability. *Molecular and cellular biology*, 7(8):2783–2793, 1987.

[207] M. Huang and S.J. Elledge. Identification of RNR4, encoding a second essential small subunit of ribonucleotide reductase in *Saccharomyces cerevisiae*. *Molecular and cellular biology*, 17(10):6105–6113, 1997.

[208] V. Domkin, L. Thelander, and A. Chabes. Yeast DNA damage-inducible Rnr3 has a very low catalytic activity strongly stimulated after the formation of a cross-talking Rnr1/Rnr3 complex. *Journal of Biological Chemistry*, 277(21):18574–18578, 2002.

[209] P.J. Wang, A. Chabes, R. Casagrande, X.C. Tian, L. Thelander, and T.C. Huffaker. Rnr4p, a novel ribonucleotide reductase small-subunit protein. *Molecular and cellular biology*, 17(10):6114–6121, 1997.

[210] M.J.F. Sarabia, C. McInerny, P. Harris, C. Gordon, and P. Fantes. The cell cycle genes *cdc22+* and *suc22+* of the fission yeast *Schizosaccharomyces pombe* encode the large and small subunits of ribonucleotide reductase. *Molecular and General Genetics MGG*, 238(1):241–251, 1993.

[211] A. Koc, C.K. Mathews, L.J. Wheeler, M.K. Gross, and G.F. Merrill. Thioredoxin is required for deoxyribonucleotide pool maintenance during S phase. *Journal of Biological Chemistry*, 281(22):15058–15063, 2006.

[212] G. Lozano and S.J. Elledge. Cancer: p53 sends nucleotides to repair DNA. *Nature a-z index*, 404(6773):24–25, 2000.

[213] A. Chabes and L. Thelander. Controlled protein degradation regulates ribonucleotide reductase activity in proliferating mammalian cells during the normal cell cycle and in response to DNA damage and replication blocks. *Journal of Biological Chemistry*, 275(23):17747–17753, 2000.

[214] A.L. Chabes, C.M. Pfleger, M.W. Kirschner, and L. Thelander. Mouse ribonucleotide reductase R2 protein: a new target for anaphase-promoting complex-Cdh1-mediated proteolysis. *Proceedings of the National Academy of Sciences*, 100(7):3925, 2003.

[215] Z.P. Lin, M.F. Belcourt, J.G. Cory, and A.C. Sartorelli. Stable suppression of the R2 subunit of ribonucleotide reductase by r2-targeted short interference rna sensitizes p53(-/-) HCT-116 colon cancer cells to DNA-damaging agents and ribonucleotide reductase inhibitors. *Journal of Biological Chemistry*, 279(26):27030–27038, 2004.

[216] K. Nakano, E. Balint, M. Ashcroft, K.H. Vousden, et al. A ribonucleotide reductase gene is a transcriptional target of p53 and p73. *Oncogene*, 19(37):4283, 2000.

[217] H. Tanaka, H. Arakawa, T. Yamaguchi, K. Shiraishi, S. Fukuda, K. Matsui, Y. Takei, and Y. Nakamura. A ribonucleotide reductase gene involved in a p53-dependent cell-cycle checkpoint for DNA damage. *Nature*, 404(6773):42–49, 2000.

[218] P. Nordlund and P. Reichard. Ribonucleotide reductases. *Annu. Rev. Biochem.*, 75:681–706, 2006.

[219] F.Z. Avval and A. Holmgren. Molecular mechanisms of thioredoxin and glutaredoxin as hydrogen donors for mammalian S phase ribonucleotide reductase. *Journal of Biological Chemistry*, 284(13):8233–8240, 2009.

[220] A. Watson, J. Mata, J. Bähler, A. Carr, and T. Humphrey. Global gene expression responses of fission yeast to ionizing radiation. *Molecular biology of the cell*, 15(2):851–860, 2004.

[221] K. Nestoras, A.H. Mohammed, A.S. Schreurs, O. Fleck, A.T. Watson, M. Poitelea, C. O'Shea, C. Chahwan, C. Holmberg, B.B. Kragelund, et al. Regulation of ribonu-

cleotide reductase by Spd1 involves multiple mechanisms. *Genes & development*, 24(11):1145–1159, 2010.

[222] C. Liu, K.A. Powell, K. Mundt, L.J. Wu, A.M. Carr, and T. Caspari. Cop9/signalosome subunits and Pcu4 regulate ribonucleotide reductase by both checkpoint-dependent and-independent mechanisms. *Genes & development*, 17(9):1130–1140, 2003.

[223] P. Håkansson, L. Dahl, O. Chilkova, V. Domkin, and L. Thelander. The *Schizosaccharomyces pombe* replication inhibitor Spd1 regulates ribonucleotide reductase activity and dNTPs by binding to the large Cdc22 subunit. *Journal of Biological Chemistry*, 281(3):1778–1783, 2006.

[224] P Baudouin-Cornu and J Labarre. Regulation of the cadmium stress response through SCF-like ubiquitin ligases: comparison between *Saccharomyces cerevisiae*, *Schizosaccharomyces pombe* and mammalian cells. *Biochimie*, 88(11):1673–1685, 2006.

[225] U. Berendt, T. Haverkamp, A. Prior, and J.D. Schwenn. Reaction mechanism of thioredoxin: 3'-phospho-adenylylsulfate reductase investigated by site-directed mutagenesis. *European Journal of Biochemistry*, 233(1):347–356, 1995.

[226] K.S. Carroll, H. Gao, H. Chen, C.D. Stout, J.A. Leary, and C.R. Bertozzi. A conserved mechanism for sulfonucleotide reduction. *PLoS biology*, 3(8):e250, 2005.

[227] J. Chartron, C. Shiau, C.D. Stout, and K.S. Carroll. 3'-phosphoadenosine-5'-phosphosulfate reductase in complex with thioredoxin: a structural snapshot in the catalytic cycle. *Biochemistry*, 46(13):3942–3951, 2007.

[228] A. Vlamis-Gardikas, A. Potamitou, R. Zarivach, A. Hochman, and A. Holmgren. Characterization of *Escherichia coli* null mutants for glutaredoxin 2. *Journal of Biological Chemistry*, 277(13):10861–10868, 2002.

[229] H. Kubota. Quality control against misfolded proteins in the cytosol: a network for cell survival. *Journal of biochemistry*, 146(5):609–616, 2009.

[230] A. Buchberger, B. Bukau, and T. Sommer. Protein quality control in the cytosol and the endoplasmic reticulum: brothers in arms. *Molecular cell*, 40(2):238–252, 2010.

[231] M.H. Glickman and A. Ciechanover. The ubiquitin-proteasome proteolytic pathway: destruction for the sake of construction. *Physiological reviews*, 82(2):373–428, 2002.

[232] F. Shang and A. Taylor. Ubiquitin-proteasome pathway and cellular responses to oxidative stress. *Free Radical Biology and Medicine*, 2011.

[233] J.P. McGrath, S. Jentsch, and A. Varshavsky. Uba1: an essential yeast gene encoding ubiquitin-activating enzyme. *The EMBO journal*, 10(1):227, 1991.

[234] E.S. Johnson and G. Blobel. Ubc9p is the conjugating enzyme for the ubiquitin-like protein Smt3p. *Journal of Biological Chemistry*, 272(43):26799–26802, 1997.

[235] L. Gong and E.T.H. Yeh. Identification of the activating and conjugating enzymes of the NEDD8 conjugation pathway. *Journal of Biological Chemistry*, 274(17):12036–12042, 1999.

[236] A.L. Goldberg et al. Protein degradation and protection against misfolded or damaged proteins. *Nature*, 426(6968):895–899, 2003.

[237] M. Koegl, T. Hoppe, S. Schlenker, H.D. Ulrich, T.U. Mayer, and S. Jentsch. A novel ubiquitination factor, E4, is involved in multiubiquitin chain assembly. *Cell*, 96(5):635–644, 1999.

[238] S. Hatakeyama, M. Yada, M. Matsumoto, N. Ishida, and K.I. Nakayama. U box proteins as a new family of ubiquitin-protein ligases. *Journal of Biological Chemistry*, 276(35):33111–33120, 2001.

[239] E.S. Johnson, P.C.M. Ma, I.M. Ota, and A. Varshavsky. A proteolytic pathway that recognizes ubiquitin as a degradation signal. *Journal of Biological Chemistry*, 270(29):17442–17456, 1995.

[240] JM Huibregtse, M. Scheffner, and P.M. Howley. Cloning and expression of the cDNA for E6-AP, a protein that mediates the interaction of the human papillomavirus E6 oncoprotein with p53. *Molecular and cellular biology*, 13(2):775–784, 1993.

[241] J.M. Huibregtse, M. Scheffner, S. Beaudenon, and P.M. Howley. A family of proteins structurally and functionally related to the E6-AP ubiquitin-protein ligase. *Proceedings of the National Academy of Sciences*, 92(7):2563–2567, 1995.

[242] M. Scheffner, U. Nuber, and J.M. Huibregtse. Protein ubiquitination involving an E1-E2-E3 enzyme ubiquitin thioester cascade. *Nature*, 373(6509):81–83, 1995.

[243] CA Joazeiro, A.M. Weissman, et al. Ring finger proteins: mediators of ubiquitin ligase activity. *Cell*, 102(5):549, 2000.

[244] K.L.B. Borden. Ring domains: master builders of molecular scaffolds? *Journal of molecular biology*, 295(5):1103–1112, 2000.

[245] R.K. Geyer, Z.K. Yu, C.G. Maki, et al. The MDM2 RING-finger domain is required to promote p53 nuclear export. *Nature cell biology*, 2(9):569–573, 2000.

[246] Y.T. Kwon, Y. Reiss, V.A. Fried, A. Hershko, J.K. Yoon, D.K. Gonda, P. Sangan, N.G. Copeland, N.A. Jenkins, and A. Varshavsky. The mouse and human genes

encoding the recognition component of the N-end rule pathway. *Proceedings of the National Academy of Sciences*, 95(14):7898–7903, 1998.

[247] H. Shimura, N. Hattori, S. Kubo, Y. Mizuno, S. Asakawa, S. Minoshima, N. Shimizu, K. Iwai, T. Chiba, K. Tanaka, et al. Familial Parkinson disease gene product, parkin, is a ubiquitin-protein ligase. *Nature genetics*, 25(3):302–305, 2000.

[248] AM Page and P. Hieter. The anaphase-promoting complex: new subunits and regulators. *Annual review of biochemistry*, 68(1):583–609, 1999.

[249] K. Iwai, K. Yamanaka, T. Kamura, N. Minato, R.C. Conaway, J.W. Conaway, R.D. Klausner, and A. Pause. Identification of the von Hippel-Lindau tumor-suppressor protein as part of an active E3 ubiquitin ligase complex. *Proceedings of the National Academy of Sciences*, 96(22):12436–12441, 1999.

[250] RJ Deshaies. Scf and Cullin/Ring H2-based ubiquitin ligases. *Annual review of cell and developmental biology*, 15(1):435–467, 1999.

[251] R.J. Ellis. Molecular chaperones: assisting assembly in addition to folding. *Trends in biochemical sciences*, 31(7):395–401, 2006.

[252] V. Arndt, C. Rogon, and J. Höhfeld. To be, or not to be-molecular chaperones in protein degradation. *Cellular and molecular life sciences*, 64(19):2525–2541, 2007.

[253] MP Mayer and B. Bukau. Hsp70 chaperones: cellular functions and molecular mechanism. *Cellular and Molecular Life Sciences*, 62(6):670–684, 2005.

[254] L.H. Pearl and C. Prodromou. Structure and mechanism of the Hsp90 molecular chaperone machinery. *Annu. Rev. Biochem.*, 75:271–294, 2006.

[255] A.J. McClellan, S. Tam, D. Kaganovich, and J. Frydman. Protein quality control: chaperones culling corrupt conformations. *Nature cell biology*, 7(8):736–741, 2005.

[256] L. Whitesell, E.G. Mimnaugh, B. De Costa, C.E. Myers, and L.M. Neckers. Inhibition of heat shock protein Hsp90-Pp60v-Src heteroprotein complex formation by benzoquinone ansamycins: essential role for stress proteins in oncogenic transformation. *Proceedings of the National Academy of Sciences*, 91(18):8324–8328, 1994.

[257] W.G. An, T.W. Schulte, L.M. Neckers, et al. The heat shock protein 90 antagonist geldanamycin alters chaperone association with p210 Bcr-Abl and v-Src proteins before their degradation by the proteasome. *Cell growth & differentiation: the molecular biology journal of the American Association for Cancer Research*, 11(7):355, 2000.

[258] N. Kettern, M. Dreiseidler, R. Tawo, and J. Höhfeld. Chaperone-assisted degradation: multiple paths to destruction. *Biological chemistry*, 391(5):481–489, 2010.

[259] EA Craig, P. Huang, R. Aron, and A. Andrew. The diverse roles of J-proteins, the obligate Hsp70 co-chaperone. *Reviews of physiology, biochemistry and pharmacology*, pages 1–21, 2006.

[260] C.Y. Fan, S. Lee, and D.M. Cyr. Mechanisms for regulation of Hsp70 function by Hsp40. *Cell stress & chaperones*, 8(4):309, 2003.

[261] D.H. Lee, M.Y. Sherman, and A.L. Goldberg. Involvement of the molecular chaperone Ydj1 in the ubiquitin-dependent degradation of short-lived and abnormal proteins in *Saccharomyces cerevisiae*. *Molecular and cellular biology*, 16(9):4773–4781, 1996.

[262] S.H. Park, N. Bolender, F. Eisele, Z. Kostova, J. Takeuchi, P. Coffino, and D.H. Wolf. The cytoplasmic Hsp70 chaperone machinery subjects misfolded and endoplasmic reticulum import-incompetent proteins to degradation via the ubiquitin-proteasome system. *Molecular biology of the cell*, 18(1):153–165, 2007.

[263] B. Westhoff, J.P. Chapple, J. van der Spuy, J. Höhfeld, and M.E. Cheetham. Hsj1 is a neuronal shuttling factor for the sorting of chaperone clients to the proteasome. *Current biology*, 15(11):1058–1064, 2005.

[264] A.K. Mandal, N.B. Nillegoda, J.A. Chen, and A.J. Caplan. Ydj1 protects nascent protein kinases from degradation and controls the rate of their maturation. *Molecular and cellular biology*, 28(13):4434–4444, 2008.

[265] A.K. Mandal, P. Lee, J.A. Chen, N. Nillegoda, A. Heller, S. DiStasio, H. Oen, J. Victor, D.M. Nair, J.L. Brodsky, et al. Cdc37 has distinct roles in protein kinase quality control that protect nascent chains from degradation and promote posttranslational maturation. *The Journal of cell biology*, 176(3):319–328, 2007.

[266] M.A. Theodoraki and A.J. Caplan. Quality control and fate determination of Hsp90 client proteins. *Biochimica et Biophysica Acta (BBA)-Molecular Cell Research*, 1823(3):683–688, 2012.

[267] A.J. McClellan, M.D. Scott, and J. Frydman. Folding and quality control of the VHL tumor suppressor proceed through distinct chaperone pathways. *Cell*, 121(5):739–748, 2005.

[268] C.A. Ballinger, P. Connell, Y. Wu, Z. Hu, L.J. Thompson, L.Y. Yin, and C. Patterson. Identification of CHIP, a novel tetratricopeptide repeat-containing protein that interacts with heat shock proteins and negatively regulates chaperone functions. *Molecular and cellular biology*, 19(6):4535–4545, 1999.

[269] Z. Xu, K.I. Devlin, M.G. Ford, J.C. Nix, J. Qin, and S. Misra. Structure and interactions of the helical and U-box domains of CHIP, the C terminus of Hsp70 interacting protein. *Biochemistry*, 45(15):4749–4759, 2006.

[270] P. Connell, C.A. Ballinger, J. Jiang, Y. Wu, L.J. Thompson, J. Höhfeld, and C. Patterson. The co-chaperone CHIP regulates protein triage decisions mediated by heat-shock proteins. *Nature cell biology*, 3(1):93–96, 2000.

[271] C. Esser, S. Alberti, and J. Höhfeld. Cooperation of molecular chaperones with the ubiquitin/proteasome system. *Biochimica et Biophysica Acta (BBA)-Molecular Cell Research*, 1695(1):171–188, 2004.

[272] W. Xu, M. Marcu, X. Yuan, E. Mimnaugh, C. Patterson, and L. Neckers. Chaperone-dependent E3 ubiquitin ligase CHIP mediates a degradative pathway for c-Erbb2/Neu. *Proceedings of the National Academy of Sciences*, 99(20):12847–12852, 2002.

[273] G.C. Meacham, C. Patterson, W. Zhang, J.M. Younger, and D.M. Cyr. The Hsc70 co-chaperone CHIP targets immature CFTR for proteasomal degradation. *Nature Cell Biology*, 3(1):100–105, 2000.

[274] L. Petrucelli, D. Dickson, K. Kehoe, J. Taylor, H. Snyder, A. Grover, M. De Lucia, E. McGowan, J. Lewis, G. Prihar, et al. Chip and Hsp70 regulate tau ubiquitination, degradation and aggregation. *Human molecular genetics*, 13(7):703–714, 2004.

[275] W. Seufert and S. Jentsch. Ubiquitin-conjugating enzymes UBC4 and UBC5 mediate selective degradation of short-lived and abnormal proteins. *The EMBO journal*, 9(2):543, 1990.

[276] C. Byrd, G.C. Turner, and A. Varshavsky. The N-end rule pathway controls the import of peptides through degradation of a transcriptional repressor. *The EMBO journal*, 17(1):269–277, 1998.

[277] A. Mogk, R. Schmidt, B. Bukau, et al. The N-end rule pathway for regulated proteolysis: prokaryotic and eukaryotic strategies. *Trends in cell biology*, 17(4):165–172, 2007.

[278] F. Eisele and D.H. Wolf. Degradation of misfolded protein in the cytoplasm is mediated by the ubiquitin ligase Ubr1. *FEBS letters*, 582(30):4143–4146, 2008.

[279] N.B. Nillegoda, M.A. Theodoraki, A.K. Mandal, K.J. Mayo, H.Y. Ren, R. Sultana, K. Wu, J. Johnson, D.M. Cyr, and A.J. Caplan. Ubr1 and Ubr2 function in a quality control pathway for degradation of unfolded cytosolic proteins. *Molecular biology of the cell*, 21(13):2102–2116, 2010.

[280] J.W. Heck, S.K. Cheung, and R.Y. Hampton. Cytoplasmic protein quality control degradation mediated by parallel actions of the E3 ubiquitin ligases Ubr1 and San1. *Proceedings of the National Academy of Sciences*, 107(3):1106–1111, 2010.

[281] S.B. Qian, H. McDonough, F. Boellmann, D.M. Cyr, and C. Patterson. CHIP-mediated stress recovery by sequential ubiquitination of substrates and Hsp70. *Nature*, 440(7083):551–555, 2006.

[282] L. Wang, X. Mao, D. Ju, and Y. Xie. Rpn4 is a physiological substrate of the Ubr2 ubiquitin ligase. *Journal of Biological Chemistry*, 279(53):55218–55223, 2004.

[283] A. Iwata, J.C. Christianson, M. Bucci, L.M. Ellerby, N. Nukina, L.S. Forno, and R.R. Kopito. Increased susceptibility of cytoplasmic over nuclear polyglutamine aggregates to autophagic degradation. *Proceedings of the National Academy of Sciences of the United States of America*, 102(37):13135–13140, 2005.

[284] R.G. Gardner, Z.W. Nelson, and D.E. Gottschling. Degradation-mediated protein quality control in the nucleus. *Cell*, 120(6):803–815, 2005.

[285] Y. Matsuo, H. Kishimoto, K. Tanae, K. Kitamura, S. Katayama, and M. Kawamukai. Nuclear protein quality is regulated by the ubiquitin-proteasome system through the activity of Ubc4 and San1 in fission yeast. *Journal of Biological Chemistry*, 286(15):13775–13790, 2011.

[286] A. Iwata, Y. Nagashima, L. Matsumoto, T. Suzuki, T. Yamanaka, H. Date, K. Deoka, N. Nukina, and S. Tsuji. Intranuclear degradation of polyglutamine aggregates by the ubiquitin-proteasome system. *Journal of Biological Chemistry*, 284(15):9796–9803, 2009.

[287] H.Y. Zoghbi and H.T. Orr. Glutamine repeats and neurodegeneration. *Annual review of neuroscience*, 23(1):217–247, 2000.

[288] F.E.R. Turcu, K.H. Ventii, and K.D. Wilkinson. Regulation and cellular roles of ubiquitin-specific deubiquitinating enzymes. *Annual review of biochemistry*, 78:363, 2009.

[289] A.Y. Amerik and M. Hochstrasser. Mechanism and function of deubiquitinating enzymes. *Biochimica et Biophysica Acta (BBA)-Molecular Cell Research*, 1695(1):189–207, 2004.

[290] E. Koulich, X. Li, and G.N. DeMartino. Relative structural and functional roles of multiple deubiquitylating proteins associated with mammalian 26S proteasome. *Molecular biology of the cell*, 19(3):1072–1082, 2008.

[291] D.S. Leggett, J. Hanna, A. Borodovsky, B. Crosas, M. Schmidt, R.T. Baker, T. Walz, H. Ploegh, and D. Finley. Multiple associated proteins regulate proteasome structure and function. *Molecular cell*, 10(3):495–507, 2002.

[292] A. Borodovsky, B.M. Kessler, R. Casagrande, H.S. Overkleeft, K.D. Wilkinson, and H.L. Ploegh. A novel active site-directed probe specific for deubiquitylating en-

zymes reveals proteasome association of USP14. *The EMBO journal*, 20(18):5187–5196, 2001.

[293] M. Hu, P. Li, L. Song, P.D. Jeffrey, T.A. Chernova, K.D. Wilkinson, R.E. Cohen, and Y. Shi. Structure and mechanisms of the proteasome-associated deubiquitinating enzyme USP14. *The EMBO journal*, 24(21):3747–3756, 2005.

[294] A.Y. Amerik, S.J. Li, and M. Hochstrasser. Analysis of the deubiquitinating enzymes of the yeast *Saccharomyces cerevisiae*. *Biological chemistry*, 381(9-10):981–992, 2000.

[295] J. Hanna, N.A. Hathaway, Y. Tone, B. Crosas, S. Elsasser, D.S. Kirkpatrick, D.S. Leggett, S.P. Gygi, R.W. King, and D. Finley. Deubiquitinating enzyme Ubp6 functions noncatalytically to delay proteasomal degradation. *Cell*, 127(1):99–111, 2006.

[296] B.H. Lee, M.J. Lee, S. Park, D.C. Oh, S. Elsasser, P.C. Chen, C. Gartner, N. Dimova, J. Hanna, S.P. Gygi, et al. Enhancement of proteasome activity by a small-molecule inhibitor of USP14. *Nature*, 467(7312):179–184, 2010.

[297] B. Crosas, J. Hanna, D.S. Kirkpatrick, D.P. Zhang, Y. Tone, N.A. Hathaway, C. Buecker, D.S. Leggett, M. Schmidt, R.W. King, et al. Ubiquitin chains are remodeled at the proteasome by opposing ubiquitin ligase and deubiquitinating activities. *Cell*, 127(7):1401–1413, 2006.

[298] R. Verma, L. Aravind, R. Oania, W.H. McDonald, J.R. Yates III, E.V. Koonin, and R.J. Deshaies. Role of Rpn11 metalloprotease in deubiquitination and degradation by the 26S proteasome. *Science Signalling*, 298(5593):611, 2002.

[299] T. Yao, L. Song, W. Xu, G.N. DeMartino, L. Florens, S.K. Swanson, M.P. Washburn, R.C. Conaway, J.W. Conaway, and R.E. Cohen. Proteasome recruitment and activation of the Uch37 deubiquitinating enzyme by Adrm1. *Nature cell biology*, 8(9):994–1002, 2006.

[300] A.Y. Amerik, S. Swaminathan, B.A. Krantz, K.D. Wilkinson, and M. Hochstrasser. *In vivo* disassembly of free polyubiquitin chains by yeast Ubp14 modulates rates of protein degradation by the proteasome. *The EMBO journal*, 16(16):4826–4838, 1997.

[301] J.D. Shaw, K.B. Cummings, G. Huyer, S. Michaelis, and B. Wendland. Yeast as a model system for studying endocytosis. *Experimental cell research*, 271(1):1–9, 2001.

[302] S. Dupré, C. Volland, R. Haguenauer-Tsapis, et al. Membrane transport: ubiquitylation in endosomal sorting. *Current Biology*, 11(22):932, 2001.

[303] S. Swaminathan, A.Y. Amerik, and M. Hochstrasser. The Doa4 deubiquitinating enzyme is required for ubiquitin homeostasis in yeast. *Molecular biology of the cell*, 10(8):2583–2594, 1999.

[304] A.Y. Amerik, J. Nowak, S. Swaminathan, and M. Hochstrasser. The Doa4 deubiquitinating enzyme is functionally linked to the vacuolar protein-sorting and endocytic pathways. *Molecular biology of the cell*, 11(10):3365–3380, 2000.

[305] I. Kouranti, J.R. McLean, A. Feoktistova, P. Liang, A.E. Johnson, R.H. Roberts-Galbraith, and K.L. Gould. A global census of fission yeast deubiquitinating enzyme localization and interaction networks reveals distinct compartmentalization profiles and overlapping functions in endocytosis and polarity. *PLoS biology*, 8(9):e1000471, 2010.

[306] M. Stone, R. Hartmann-Petersen, M. Seeger, D. Bech-Otschir, M. Wallace, C. Gordon, et al. Uch2/Uch37 is the major deubiquitinating enzyme associated with the 26S proteasome in fission yeast. *Journal of molecular biology*, 344(3):697, 2004.

[307] N. Ismail and D.T.W. Ng. Have you HRD? understanding ERAD is DOAble! *Cell*, 126(2):237–238, 2006.

[308] S.S. Vembar and J.L. Brodsky. One step at a time: endoplasmic reticulum-associated degradation. *Nature Reviews Molecular Cell Biology*, 9(12):944–957, 2008.

[309] D. Ron and P. Walter. Signal integration in the endoplasmic reticulum unfolded protein response. *Nature Reviews Molecular Cell Biology*, 8(7):519–529, 2007.

[310] R. Shringarpure, T. Grune, and KJA Davies. Protein oxidation and 20S proteasome-dependent proteolysis in mammalian cells. *Cellular and Molecular Life Sciences*, 58(10):1442–1450, 2001.

[311] T. Grune, K. Merker, G. Sandig, and K.J.A. Davies. Selective degradation of oxidatively modified protein substrates by the proteasome. *Biochemical and biophysical research communications*, 305(3):709–718, 2003.

[312] B. Medicherla and A.L. Goldberg. Heat shock and oxygen radicals stimulate ubiquitin-dependent degradation mainly of newly synthesized proteins. *The Journal of Cell Biology*, 182(4):663–673, 2008.

[313] H. HIRAISHI, M. MOCHIZUKI, and H. TAKAGI. Enhancement of stress tolerance in *Saccharomyces cerevisiae* by overexpression of ubiquitin ligase Rsp5 and ubiquitin-conjugating enzymes. *Bioscience, biotechnology, and biochemistry*, 70(11):2762–2765, 2006.

[314] F. Shang, T.R. Nowell, and A. Taylor. Removal of oxidatively damaged proteins from lens cells by the ubiquitin-proteasome pathway. *Experimental eye research*, 73(2):229–238, 2001.

[315] EJ Dudek, F. Shang, P. Valverde, Q. Liu, M. Hobbs, and A. Taylor. Selectivity of the ubiquitin pathway for oxidatively modified proteins: relevance to protein precipitation diseases. *The FASEB journal*, 19(12):1707–1709, 2005.

[316] N.N. Fang, A.H.M. Ng, V. Measday, and T. Mayor. Hul5 HECT ubiquitin ligase plays a major role in the ubiquitylation and turnover of cytosolic misfolded proteins. *Nature Cell Biology*, 13(11):1344–1352, 2011.

[317] J. Jungmann, H.A. Reins, C. Schobert, and S. Jentsch. Resistance to cadmium mediated by ubiquitin-dependent proteolysis. 1993.

[318] G.W. Hwang, T. Furuchi, and A. Naganuma. The ubiquitin-conjugating enzymes, Ubc4 and Cdc34, mediate cadmium resistance in budding yeast through different mechanisms. *Life sciences*, 82(23):1182–1185, 2008.

[319] RE Pacifici, Y. Kono, and KJ Davies. Hydrophobicity as the signal for selective degradation of hydroxyl radical-modified hemoglobin by the multicatalytic proteinase complex, proteasome. *Journal of Biological Chemistry*, 268(21):15405–15411, 1993.

[320] P. Lasch, T. Petras, O. Ullrich, J. Backmann, D. Naumann, and T. Grune. Hydrogen peroxide-induced structural alterations of RNAse A. *Journal of Biological Chemistry*, 276(12):9492–9502, 2001.

[321] J.C. Rosenbaum, E.K. Fredrickson, M.L. Oeser, C.M. Garrett-Engele, M.N. Locke, L.A. Richardson, Z.W. Nelson, E.D. Hetrick, T.I. Milac, D.E. Gottschling, et al. Disorder targets misorder in nuclear quality control degradation: a disordered ubiquitin ligase directly recognizes its misfolded substrates. *Molecular cell*, 41(1):93–106, 2011.

[322] E.K. Fredrickson, J.C. Rosenbaum, M.N. Locke, T.I. Milac, and R.G. Gardner. Exposed hydrophobicity is a key determinant of nuclear quality control degradation. *Molecular biology of the cell*, 22(13):2384–2395, 2011.

[323] J. Jahngen-Hodge, M.S. Obin, X. Gong, F. Shang, T.R. Nowell Jr, J. Gong, H. Abasi, J. Blumberg, and A. Taylor. Regulation of ubiquitin-conjugating enzymes by glutathione following oxidative stress. *Journal of Biological Chemistry*, 272(45):28218–28226, 1997.

[324] M. Obin, F. Shang, X. Gong, G. Handelman, J. Blumberg, and A. Taylor. Redox regulation of ubiquitin-conjugating enzymes: mechanistic insights using the thiol-specific oxidant diamide. *The FASEB journal*, 12(7):561–569, 1998.

[325] X. Zhang, J. Zhou, A.F. Fernandes, J.R. Sparrow, P. Pereira, A. Taylor, and F. Shang. The proteasome: a target of oxidative damage in cultured human retina pigment epithelial cells. *Investigative ophthalmology & visual science*, 49(8):3622–3630, 2008.

[326] K.S. Doris, E.L. Rumsby, and B.A. Morgan. Oxidative stress responses involves oxidation of a conserved ubiquitin pathway enzyme. *Molecular and Cellular Biology*, 2012.

[327] E.R. Stadtman. Protein oxidation and aging. *Free radical research*, 40(12):1250–1258, 2006.

[328] T. Nyström. Role of oxidative carbonylation in protein quality control and senescence. *The EMBO journal*, 24(7):1311–1317, 2005.

[329] C. Boyault, Y. Zhang, S. Fritah, C. Caron, B. Gilquin, S.H. Kwon, C. Garrido, T.P. Yao, C. Vourcâh, P. Matthias, et al. HDAC6 controls major cell response pathways to cytotoxic accumulation of protein aggregates. *Genes & development*, 21(17):2172–2181, 2007.

[330] LS Chin, JA Olzmann, and L. Li. Aggresome formation and neurodegenerative diseases: therapeutic implications. *Current medicinal chemistry*, 15(1):47–60, 2008.

[331] Y. Kawaguchi, J.J. Kovacs, A. McLaurin, J.M. Vance, A. Ito, and T.P. Yao. The deacetylase HDAC6 regulates aggresome formation and cell viability in response to misfolded protein stress. *Cell*, 115(6):727–738, 2003.

[332] T. Nyström and T. Nyström. Spatial protein quality control and the evolution of lineage-specific ageing. *Philosophical Transactions of the Royal Society B: Biological Sciences*, 366(1561):71–75, 2011.

[333] H. Aguilaniu, L. Gustafsson, M. Rigoulet, and T. Nyström. Asymmetric inheritance of oxidatively damaged proteins during cytokinesis. *Science*, 299(5613):1751–1753, 2003.

[334] N. Erjavec, L. Larsson, J. Grantham, and T. Nyström. Accelerated aging and failure to segregate damaged proteins in *sir2* mutants can be suppressed by overproducing the protein aggregation-remodeling factor Hsp104p. *Genes & development*, 21(19):2410–2421, 2007.

[335] M. Hernebring, G. Brolén, H. Aguilaniu, H. Semb, and T. Nyström. Elimination of damaged proteins during differentiation of embryonic stem cells. *Proceedings of the National Academy of Sciences*, 103(20):7700–7705, 2006.

[336] J. Goudeau and H. Aguilaniu. Carbonylated proteins are eliminated during reproduction in *C. elegans*. *Aging cell*, 9(6):991–1003, 2010.

[337] N.F. Villeneuve, A. Lau, and D.D. Zhang. Regulation of the Nrf2-Keap1 antioxidant response by the ubiquitin proteasome system: An insight into Cullin-ring ubiquitin ligases. *Antioxidants & redox signaling*, 13(11):1699–1712, 2010.

[338] A.K. Jaiswal. Nrf2 signaling in coordinated activation of antioxidant gene expression. *Free Radical Biology and Medicine*, 36(10):1199–1207, 2004.

[339] T. Nguyen, P.J. Sherratt, H.C. Huang, C.S. Yang, and C.B. Pickett. Increased protein stability as a mechanism that enhances Nrf2-mediated transcriptional activation of the antioxidant response element degradation of Nrf2 by the 26 S proteasome. *Journal of Biological Chemistry*, 278(7):4536–4541, 2003.

[340] S.J. Chapple, R. Siowand, and G.E. Mann. Crosstalk between Nrf2 and the proteasome: Therapeutic potential of Nrf2 inducers in vascular disease and aging. *The International Journal of Biochemistry & Cell Biology*, 2012.

[341] K. Kitamura, M. Taki, N. Tanaka, and I. Yamashita. Fission yeast Ubr1 ubiquitin ligase influences the oxidative stress response via degradation of active Pap1 bZIP transcription factor in the nucleus. *Molecular microbiology*, 80(3):739–755, 2011.

[342] M. Shimanuki, Y. Saka, M. Yanagida, and T. Toda. A novel essential fission yeast gene *pad1+* positively regulates Pap1-dependent transcription and is implicated in the maintenance of chromosome structure. *Journal of cell science*, 108(2):569–579, 1995.

[343] V. Spataro, T. Toda, R. Craig, M. Seeger, W. Dubiel, A.L. Harris, and C. Norbury. Resistance to diverse drugs and ultraviolet light conferred by overexpression of a novel human 26 S proteasome subunit. *Journal of Biological Chemistry*, 272(48):30470–30475, 1997.

[344] K. Gulshan, B. Thommandru, and W.S. Moye-Rowley. Proteolytic degradation of the Yap1 transcription factor is regulated by subcellular localization and the E3 ubiquitin ligase Not4. *Journal of Biological Chemistry*, 287(32):26796–26805, 2012.

[345] L.I. Leichert and U. Jakob. Protein thiol modifications visualized *in vivo*. *PLoS biology*, 2(11):e333, 2004.

[346] Jason M Held and Bradford W Gibson. Regulatory control or oxidative damage? proteomic approaches to interrogate the role of cysteine oxidation status in biological processes. *Molecular & Cellular Proteomics*, 11(4), 2012.

[347] R.C. Cumming, N.L. Andon, P.A. Haynes, M. Park, W.H. Fischer, and D. Schubert. Protein disulfide bond formation in the cytoplasm during oxidative stress. *Journal of Biological Chemistry*, 279(21):21749–21758, 2004.

[348] Samie R Jaffrey, Hediye Erdjument-Bromage, Christopher D Ferris, Paul Tempst, Solomon H Snyder, et al. Protein S-nitrosylation: a physiological signal for neuronal nitric oxide. *Nature cell biology*, 3(2):193–197, 2001.

[349] Xunde Wang, Nicholas J Kettenhofen, Sruti Shiva, Neil Hogg, and Mark T Gladwin. Copper dependence of the biotin switch assay: modified assay for measuring cellular and blood nitrosated proteins. *Free Radical Biology and Medicine*, 44(7):1362–1372, 2008.

[350] Adrian T Saurin, Hendrik Neubert, Jonathan P Brennan, and Philip Eaton. Widespread sulfenic acid formation in tissues in response to hydrogen peroxide. *Proceedings of the National Academy of Sciences*, 101(52):17982–17987, 2004.

[351] Christina Lind, Robert Gerdes, Ylva Hamnell, Ina Schuppe-Koistinen, Helena Brockenhuus von Löwenhielm, Arne Holmgren, and Ian A Cotgreave. Identification of S-glutathionylated cellular proteins during oxidative stress and constitutive metabolism by affinity purification and proteomic analysis. *Archives of biochemistry and biophysics*, 406(2):229–240, 2002.

[352] N. Le Moan, G. Clement, S. Le Maout, F. Tacnet, and M.B. Toledano. The *Saccharomyces cerevisiae* proteome of oxidized protein thiols. *Journal of Biological Chemistry*, 281(15):10420–10430, 2006.

[353] J.W. Baty, M.B. Hampton, and C.C. Winterbourn. Proteomic detection of hydrogen peroxide-sensitive thiol proteins in Jurkat cells. *Biochemical Journal*, 389(Pt 3):785, 2005.

[354] S.P. Gygil, B. Rist, S.A. Gerber, F. Turecek, M.H. Gelb, and R. Aebersold. Quantitative analysis of complex protein mixtures using isotope-coded affinity tags. *Nature biotechnology*, 17(10):994–999, 1999.

[355] Mahadevan Sethuraman, Mark E McComb, Hua Huang, Sequin Huang, Tyler Heibeck, Catherine E Costello, and Richard A Cohen. Isotope-coded affinity tag (ICAT) approach to redox proteomics: identification and quantitation of oxidant-sensitive cysteine thiols in complex protein mixtures. *Journal of proteome research*, 3(6):1228–1233, 2004.

[356] Mahadevan Sethuraman, Nicolas Clavreul, Hua Huang, Mark E McComb, Catherine E Costello, and Richard A Cohen. Quantification of oxidative post-translational modifications of cysteine thiols of p21ras associated with redox modulation of activity using isotope-coded affinity tags (ICAT) and mass spectrometry. *Free radical biology & medicine*, 42(6):823, 2007.

[357] Lars I Leichert, Florian Gehrke, Harini V Gudiseva, Tom Blackwell, Marianne Ilbert, Angela K Walker, John R Strahler, Philip C Andrews, and Ursula Jakob. Quantifying changes in the thiol redox proteome upon oxidative stress *in vivo*. *Proceedings of the National Academy of Sciences*, 105(24):8197–8202, 2008.

[358] Cexiong Fu, Jun Hu, Tong Liu, Tetsuro Ago, Junichi Sadoshima, and Hong Li. Quantitative analysis of redox-sensitive proteome with DIGE and ICAT. *Journal of proteome research*, 7(9):3789–3802, 2008.

[359] N. Brandes, D. Reichmann, H. Tienson, L.I. Leichert, and U. Jakob. Using quantitative redox proteomics to dissect the yeast redoxome. *Journal of Biological Chemistry*, 286(48):41893–41903, 2011.

[360] Daniela Knoefler, Maike Thamsen, Martin Koniczek, Nicholas J Niemuth, Ann-Kristin Diederich, and Ursula Jakob. Quantitative *in vivo* redox sensors uncover oxidative stress as an early event in life. *Molecular Cell*, 2012.

[361] Caroline Kumsta, Maike Thamsen, and Ursula Jakob. Effects of oxidative stress on behavior, physiology, and the redox thiol proteome of *Caenorhabditis elegans*. *Antioxidants & redox signaling*, 14(6):1023–1037, 2011.

[362] Rosa E Hansen, Doris Roth, and Jakob R Winther. Quantifying the global cellular thiol–disulfide status. *Proceedings of the National Academy of Sciences*, 106(2):422–427, 2009.

[363] R.L. Levine, J.A. Williams, E.R. Stadtman, and E. Shacter. Carbonyl assays for determination of oxidatively modified proteins. *Methods in enzymology*, 233:346–357, 1994.

[364] Isabella Dalle-Donne, Marina Carini, Marica Orioli, Giulio Vistoli, Luca Regazzoni, Graziano Colombo, Ranieri Rossi, Aldo Milzani, and Giancarlo Aldini. Protein carbonylation: 2, 4-dinitrophenylhydrazine reacts with both aldehydes/ketones and sulfenic acids. *Free radical biology and medicine*, 46(10):1411–1419, 2009.

[365] Rukhsana Sultana, Shelley F Newman, Quanzhen Huang, D Allan Butterfield, et al. Detection of carbonylated proteins in two-dimensional sodium dodecyl sulfate polyacrylamide gel electrophoresis separations. *Methods Mol Biol*, 476:149–159, 2009.

[366] Joungil Choi, Christina A Malakowsky, John M Talent, Craig C Conrad, and Robert W Gracy. Identification of oxidized plasma proteins in Alzheimer's disease. *Biochemical and biophysical research communications*, 293(5):1566–1570, 2002.

[367] Craig C Conrad, Joungil Choi, Christina A Malakowsky, John M Talent, Rong Dai, Pam Marshall, and Robert W Gracy. Identification of protein carbonyls after two-dimensional electrophoresis. *Proteomics*, 1(7):829–834, 2001.

[368] H Fai Poon, Laila Abdullah, Jon Reed, Sarah M Doore, Cyndi Laird, Venkat Mathura, Michael Mullan, and Fiona Crawford. Improving image analysis in 2DGE-based redox proteomics by labeling protein carbonyl with fluorescent hydroxylamine. *Biological procedures online*, 9(1):65–72, 2007.

[369] Asish R Chaudhuri, Eric M de Waal, Anson Pierce, Holly Van Remmen, Walter F Ward, and Arlan Richardson. Detection of protein carbonyls in aging liver tissue: A fluorescence-based proteomic approach. *Mechanisms of ageing and development*, 127(11):849–861, 2006.

[370] Hamid Mirzaei and Fred Regnier. Affinity chromatographic selection of carbonylated proteins followed by identification of oxidation sites using tandem mass spectrometry. *Analytical chemistry*, 77(8):2386–2392, 2005.

[371] Hamid Mirzaei and Fred Regnier. Identification of yeast oxidized proteins: chromatographic top-down approach for identification of carbonylated, fragmented and cross-linked proteins in yeast. *Journal of Chromatography A*, 1141(1):22–31, 2007.

[372] Hamid Mirzaei, Beatriz Baena, Coral Barbas, and Fred Regnier. Identification of oxidized proteins in rat plasma using avidin chromatography and tandem mass spectrometry. *Proteomics*, 8(7):1516–1527, 2008.

[373] Ashraf G Madian and Fred E Regnier. Profiling carbonylated proteins in human plasma. *Journal of proteome research*, 9(3):1330–1343, 2010.

[374] Bingnan Han, Jan F Stevens, and Claudia S Maier. Design, synthesis, and application of a hydrazide-functionalized isotope-coded affinity tag for the quantification of oxylipid-protein conjugates. *Analytical chemistry*, 79(9):3342–3354, 2007.

[375] Jin-Hee Kim, Miroslav Sedlak, Qiang Gao, Catherine P Riley, Fred E Regnier, and Jiri Adamec. Dynamics of protein damage in yeast frataxin mutant exposed to oxidative stress. *OMICS: A Journal of Integrative Biology*, 14(6):689–699, 2010.

[376] Danni L Meany, Hongwei Xie, LaDora V Thompson, Edgar A Arriaga, and Timothy J Griffin. Identification of carbonylated proteins from enriched rat skeletal muscle mitochondria using affinity chromatography-stable isotope labeling and tandem mass spectrometry. *Proteomics*, 7(7):1150–1163, 2007.

[377] Mikel R Roe, Thomas F McGowan, LaDora V Thompson, and Timothy J Griffin. Targeted ^{18}O-labeling for improved proteomic analysis of carbonylated peptides by mass spectrometry. *Journal of the American Society for Mass Spectrometry*, 21(7):1190–1203, 2010.

[378] Hamid Mirzaei and Fred Regnier. Creation of allotypic active sites during oxidative stress. *Journal of proteome research*, 5(9):2159–2168, 2006.

[379] Ian M Møller, Adelina Rogowska-Wrzesinska, and RSP Rao. Protein carbonylation and metal-catalyzed protein oxidation in a cellular perspective. *Journal of proteomics*, 74(11):2228–2242, 2011.

[380] Lionel Tarrago, Edith Laugier, Mirko Zaffagnini, Christophe Marchand, Pierre Le Maréchal, Nicolas Rouhier, Stéphane D Lemaire, and Pascal Rey. Regeneration mechanisms of Arabidopsis thaliana methionine sulfoxide reductases B by glutaredoxins and thioredoxins. *Journal of Biological Chemistry*, 284(28):18963–18971, 2009.

[381] Etienne Maisonneuve, Adrien Ducret, Pierre Khoueiry, Sabrina Lignon, Sonia Longhi, Emmanuel Talla, and Sam Dukan. Rules governing selective protein carbonylation. *PloS one*, 4(10):e7269, 2009.

[382] Jesús R Requena, Chien-Chung Chao, Rodney L Levine, and Earl R Stadtman. Glutamic and aminoadipic semialdehydes are the main carbonyl products of metal-catalyzed oxidation of proteins. *Proceedings of the National Academy of Sciences*, 98(1):69–74, 2001.

[383] D.U. Kim, J. Hayles, D. Kim, V. Wood, H.O. Park, M. Won, H.S. Yoo, T. Duhig, M. Nam, G. Palmer, et al. Analysis of a genome-wide set of gene deletions in the fission yeast *Schizosaccharomyces pombe*. *Nature biotechnology*, 28(6):617–623, 2010.

[384] Nobuyasu Ikai and Mitsuhiro Yanagida. Cdc48 is required for the stability of Cut1/separase in mitotic anaphase. *Journal of structural biology*, 156(1):50–61, 2006.

[385] Hiroaki Seino, Tsutomu Kishi, Hideo Nishitani, and Fumiaki Yamao. Two ubiquitin-conjugating enzymes, UbcP1/Ubc4 and UbcP4/Ubc11, have distinct functions for ubiquitination of mitotic cyclin. *Molecular and cellular biology*, 23(10):3497–3505, 2003.

[386] Colin Gordon, Gordon McGurk, Patrick Dillon, Craig Rosen, and Nicholas D Hastie. Defective mitosis due to a mutation in the gene for a fission yeast 26S protease subunit. *Nature*, 366(6453):355–357, 1993.

[387] Colin Gordon, Gordon McGurk, Mairi Wallace, and Nicholas D Hastie. A conditional lethal mutant in the fission yeast 26 S protease subunit *mts3* is defective in metaphase to anaphase transition. *Journal of Biological Chemistry*, 271(10):5704–5711, 1996.

[388] Mary Penney, Caroline Wilkinson, Mairi Wallace, Jean-Paul Javerzat, Katherine Ferrell, Michael Seeger, Wolfgang Dubiel, Stuart McKay, Robin Allshire, and Colin Gordon. The *pad1+* gene encodes a subunit of the 26 S proteasome in fission yeast. *Journal of Biological Chemistry*, 273(37):23938–23945, 1998.

[389] Maria A Theodoraki, Nadinath B Nillegoda, Jagdeep Saini, and Avrom J Caplan. A network of ubiquitin ligases is important for the dynamics of misfolded protein aggregates in yeast. *Journal of Biological Chemistry*, 287(28):23911–23922, 2012.

[390] Katsuyuki K Tamai and Chikashi Shimoda. The novel HECT-type ubiquitin-protein ligase Pub2p shares partially overlapping function with Pub1p in *Schizosaccharomyces pombe*. *Journal of cell science*, 115(9):1847–1857, 2002.

[391] Bradley Nefsky and David Beach. Pub1 acts as an E6-AP-like protein ubiquitiin ligase in the degradation of cdc25. *The EMBO journal*, 15(6):1301, 1996.

[392] R Saleki, Z Jia, J Karagiannis, and PG Young. Tolerance of low pH in *Schizosaccharomyces pombe* requires a functioning Pub1 ubiquitin ligase. *Molecular and General Genetics MGG*, 254(5):520–528, 1997.

[393] Jim Karagiannis, Reza Saleki, and Paul G Young. The pub1 E3 ubiquitin ligase negatively regulates leucine uptake in response to NH4+ in fission yeast. *Current genetics*, 35(6):593–601, 1999.

[394] Leslie B Poole and Kimberly J Nelson. Discovering mechanisms of signaling-mediated cysteine oxidation. *Current opinion in chemical biology*, 12(1):18–24, 2008.

[395] Paul J Boersema, Reinout Raijmakers, Simone Lemeer, Shabaz Mohammed, and Albert JR Heck. Multiplex peptide stable isotope dimethyl labeling for quantitative proteomics. *Nature protocols*, 4(4):484–494, 2009.

[396] S. García-Santamarina, S. Boronat, G. Espadas, J. Ayté, H. Molina, and E. Hidalgo. The oxidized thiol proteome in fission yeast-optimization of an ICAT-based method to identify H2O2-oxidized proteins. *Journal of proteomics*, 74(11):2476–2486, 2011.

[397] Sarela García-Santamarina, Susanna Boronat, Isabel A Calvo, Miguel Rodríguez-Gabriel, José Ayté, Henrik Molina, and Elena Hidalgo. Is oxidized thioredoxin a major trigger for cysteine oxidation? clues from a redox proteomics approach. *Antioxidants & redox signaling*, 2012.

[398] Stephanie M Bozonet, Victoria J Findlay, Alison M Day, Jannine Cameron, Elizabeth A Veal, and Brian A Morgan. Oxidation of a eukaryotic 2-cys peroxiredoxin is a molecular switch controlling the transcriptional response to increasing levels of hydrogen peroxide. *Journal of Biological Chemistry*, 280(24):23319–23327, 2005.

[399] Elisa Cabiscol and Joaquim Ros. Oxidative damage to proteins: structural modifications and consequences in cell function. *Redox proteomics: from protein modification to cellular dysfunction and disease*, pages 399–471, 2006.

[400] Lionel Tarrago, Alaattin Kaya, Eranthie Weerapana, Stefano M Marino, and Vadim N Gladyshev. Methionine sulfoxide reductases preferentially reduce unfolded oxidized proteins and protect cells from oxidative protein unfolding. *Journal of Biological Chemistry*, 287(29):24448–24459, 2012.

[401] J. Moskovitz. Methionine sulfoxide reductases: ubiquitous enzymes involved in antioxidant defense, protein regulation, and prevention of aging-associated diseases. *Biochimica et Biophysica Acta (BBA)-Proteins & Proteomics*, 1703(2):213–219, 2005.

[402] S. Luo and R.L. Levine. Methionine in proteins defends against oxidative stress. *The FASEB Journal*, 23(2):464–472, 2009.

[403] Tammy M Bray. Antioxidants and oxidative stress in health and disease: introduction. In *Proceedings of the Society for Experimental Biology and Medicine.*

Society for Experimental Biology and Medicine (New York, NY), volume 222, pages 195–195. Royal Society of Medicine, 1999.

[404] Isabella Dalle-Donne, Andrea Scaloni, Daniela Giustarini, Eleonora Cavarra, Gianluca Tell, Giuseppe Lungarella, Roberto Colombo, Ranieri Rossi, and Aldo Milzani. Proteins as biomarkers of oxidative/nitrosative stress in diseases: the contribution of redox proteomics. *Mass spectrometry reviews*, 24(1):55–99, 2005.

[405] Caroline Alfa, Peter Fantes, Jeremy Hyams, Maureen McLeod, and Emma Warbrick. *Experiments with fission yeast: a laboratory course manual*. Cold Spring Harbor Laboratory Press Cold Spring Harbor, New York, 1993.

[406] Javier Benito, Cristina Martín-Castellanos, and Sergio Moreno. Regulation of the g1 phase of the cell cycle by periodic stabilization and degradation of the p25rum1 cdk inhibitor. *The EMBO journal*, 17(2):482–497, 1998.

[407] Jesper V Olsen, Lyris MF de Godoy, Guoqing Li, Boris Macek, Peter Mortensen, Reinhold Pesch, Alexander Makarov, Oliver Lange, Stevan Horning, and Matthias Mann. Parts per million mass accuracy on an orbitrap mass spectrometer via lock mass injection into a c-trap. *Molecular & Cellular Proteomics*, 4(12):2010–2021, 2005.

[408] Jürgen Cox and Matthias Mann. Maxquant enables high peptide identification rates, individualized ppb-range mass accuracies and proteome-wide protein quantification. *Nature biotechnology*, 26(12):1367–1372, 2008.

[409] Jue-Liang Hsu, Sheng-Yu Huang, Nan-Haw Chow, and Shu-Hui Chen. Stable-isotope dimethyl labeling for quantitative proteomics. *Analytical chemistry*, 75(24):6843–6852, 2003.

[410] Juri Rappsilber, Matthias Mann, and Yasushi Ishihama. Protocol for micro-purification, enrichment, pre-fractionation and storage of peptides for proteomics using stagetips. *Nature protocols*, 2(8):1896–1906, 2007.

[411] Jacek R WisÌniewski, Alexandre Zougman, and Matthias Mann. Combination of fasp and stagetip-based fractionation allows in-depth analysis of the hippocampal membrane proteome. *Journal of proteome research*, 8(12):5674–5678, 2009.

[412] Irfan Rahman, Aruna Kode, and Saibal K Biswas. Assay for quantitative determination of glutathione and glutathione disulfide levels using enzymatic recycling method. *Nature protocols*, 1(6):3159–3165, 2007.